Ex vivo imaging immune cell interactions in T cell vaccine-induced immunity and $CD8^+CD25^+$ T regulatory cell-mediated immune suppression

A Thesis Submitted to
College of Graduate Studies
and Research In Partial
Fulfillment of the
Requirements For the Degree
of Doctor of Philosophy
In School of Public Health
University of
Saskatchewan Saskatoon

by

LU WANG

PERMISSION TO USE

In presenting this thesis in partial fulfillment for a Ph.D. degree from the University of Saskatchewan, I agree that the libraries of this university may make it freely available for inspection. I further agree that permission for copying of this thesis in any manner, in whole or in part, for scholarly purposes may be granted by me or by Dr. Jim Xiang, or in his absence, by the Head of School of Public Health or the Dean of the College of Graduate Studies and Research. It is understood that any copying or publication or use of this thesis or parts thereof for financial gain shall not be allowed without my written permission. It is also understood that due recognition shall be given to me and to the University of Saskatchewan in any scholarly use which may be made of any material in my thesis.

Requests for permission to copy or to make other use of material in this thesis in whole or part should be addressed to:

School of Public Health
Health Sciences Building 107 Wiggins Road
University of Saskatchewan
Saskatoon, Saskatchewan S7N 5E5

ACKNOWLEDGEMENTS

I would like to offer my deepest gratitude to my supervisor, Dr. Jim Xiang, who has supported me throughout my Ph.D. studies with his patience and knowledge. Without his timely mentoring, this thesis would not have been completed. I would also like to express my sincerest appreciation to my co-supervisor Dr. Sean Mulligan, who has always inspired and encouraged me to step outside my comfort zone on both an academic and a personal level. One simply could not wish for a friendlier supervisor. Furthermore, I would like to thank my advisory committee members Dr. Qingyong Xu, Dr. Lixin Liu, Dr. Suresh Tikoo, Dr. John Krahn and Prof. A. Mabood Qureshi for their advices in this research. Special thank goes out to Dr. Sam Kung who kindly agreed to be the external examiner.

I would like to acknowledge with much appreciation to my co-worker, Dr. Yufeng Xie, whose contribution in stimulating suggestions and encouragement, helped me to fulfill my project. Many thanks to Dr. Xueshu Zhang, Dr. Khawaja Ashfaque Ahmed, Mark Boyd and Landon Baillie for helping and giving their best suggestions whenever I needed. A special gratitude to all the current and past members of Dr. Xiang's lab and all members in Saskatoon Cancer Centre research unit for their cooperation and kindness.

I appreciate the financial support from China Scholarship Council, Canadian Institutes of Health Research and Saskatchewan Cancer Agency for helping me to pursue my goals.

Most importantly, none of this would have been possible without the unconditional love and support from my parents Zhendong Liu and Ruixing Wang. Finally, I thank my husband Qian Wang, who has been there for me through my final endeavors.

ABSTRACT

The ultimate goal of antitumor vaccines is to develop memory $CD8^+$ cytotoxic T lymphocytes (CTLs), which are critical mediators of antitumor immunity. Previous work in our lab demonstrated that the ovalbumin (OVA)-specific $CD4^+$ T cell-based ($OVA\text{-}T_{EXO}$) vaccine generated using OVA-pulsed dendritic cell (DC_{OVA})-released exosomes (EXO_{OVA}) stimulates CTL responses via interleukin (IL)-2 and costimulatory CD80 signaling. To assess the potential involvement of other costimulatory pathways and to define the key constituent of costimulation for memory CTL development, we first immunized wild-type (WT) C57BL/6 and gene-knockout mice with WT $CD4^+$ $OVA\text{-}T_{EXO}$ cells or $OVA\text{-}T_{EXO}$ cells with various molecular deficiencies. We then assessed OVA-specific primary and recall CTL responses using PE-H-$2K^b/OVA_{257–264}$ tetramer and FITC-anti-CD8 antibody staining by flow cytometry. We also examined antitumor immunity against the OVA-expressing B16 melanoma cell line $BL6\text{-}10_{OVA}$. We demonstrate that $CD4^+$ $OVA\text{-}T_{EXO}$ cells form immunological synapses with cognate $CD8^+$ T cells *in vitro*. By assessment of the pattern of *ex vivo* interactions between OTI $CD8^+$ T cells and $OVA\text{-}T_{EXO}$ or $(K^{b-/-})T_{EXO}$ cells lacking peptide/major histocompatibitity complex (pMHC)-I expression, we provide the first visible evidence on the critical role of exosomal pMHC-I in targeting $OVA\text{-}T_{EXO}$ to cognate $CD8^+$ T cells using two-photon microscopy. By assessing primary and recall CTL responses in mice immunized with $OVA\text{-}T_{EXO}$ cells or with $OVA\text{-}T_{EXO}$ cells lacking the costimulatory molecules CD40L, 4-1BBL or OX40L, we demonstrated that these costimulatory signals are dispensable for CTL priming by $OVA\text{-}T_{EXO}$ cells. Interestingly, CD40L, but not 4-1BBL or OX40L, plays a crucial role in the development of functional memory CTLs against $BL6\text{-}10_{OVA}$ tumors. Overall, this work suggests that a novel $CD4^+$ T cell-based vaccine that is capable of stimulating long-term functional CTL memory via CD40L signaling may represent a novel, efficient approach to antitumor vaccination.

Breast cancer is the most common cancer among women in the western world. Approximately 20-30% of invasive breast carcinomas are proto-oncogene human epidermal growth factor receptor (HER)-2 positive and associated with increased metastatic potential and poor prognosis. The survival benefit of anti-HER2 driven therapies demonstrated in clinical trials indicates that

HER2 is one of the most promising molecules for targeted therapy to date. Above results prompt us to assess whether $CD4^+$ T-cell-based vaccine can stimulate efficient HER2-specific $CD8^+$ CTL responses and antitumor immunity in transgenic mice with HER2-specific self-immune tolerance. We prepared HER2-specific HER2-T_{EXO} using ConA-stimulated $CD4^+$ T cells with uptake of exosomes released from HER2-expressing AdV_{HER2}-transfected DCs. We found that HER2-T_{EXO} vaccine is capable of inducing HER2-specific CTL responses and protective immunity against transgene HLA-A2/HER2-expressing B16 melanoma BL6-$10_{HLA\text{-}A2/HER2}$ in 2/8 double transgenic HLA-A2/HER2 mice with HER2-specific self-immune tolerance. The remaining 6/8 mice had significantly prolonged survival. Therefore, the novel T cell-based HER2-T_{EXO} vaccine may provide a new therapeutic alternative for women with $HER2^+$ breast cancer.

In contrast to $CD4^+CD25^+$ regulatory T cells (Tregs), mechanisms of $CD8^+CD25^+$ Treg-mediated immunosuppression are not well understood. In this study, we purified polyclonal $CD8^+CD25^+$ Tregs from C57BL/6 mouse splenocytes and expanded them in culture medium containing CD3/CD28 microbeads. By using these amplified $CD8^+CD25^+$ Tregs, we demonstrated that $CD8^+CD25^+$ Tregs inhibit naive $CD4^+$ T-cell proliferation and induce naive T-cell anergy by up-regulating T-cell anergy-associated early growth response 2 (EGR2), and by decreasing T-cell proliferation and IL-2-secretion upon stimulation. They also impact the expression of perforin on effector CTLs and directly induce perforin-mediated CTL apoptosis. $CD8^+CD25^+$ Tregs, when pulsed with $OVA_{323\text{-}339}$ peptide, exert an enhanced inhibition. Interestingly, $CD8^+CD25^+$ Tregs, when pulsed with myelin oligodendrocyte glycoprotein $(MOG)_{35\text{-}55}$ peptide, become capable of inhibiting $MOG_{35\text{-}55}$-induced experimental autoimmune encephalomyelitis (EAE). Two-photon microscopic observations suggest that $OVA_{323\text{-}339}$-pulsed (armed) $CD8^+CD25^+$ Tregs reduce the interactions between DCs and cognate $CD4^+$ T cells *ex vivo* by increasing velocities of T cells in mouse lymph nodes. Therefore, redirecting antigen-specificity to nonspecific $CD8^+CD25^+$ Tregs can be achieved for enhanced immunosuppression through their arming with the antigen-specific pMHC-II complexes. This approach may have great impact on improvement of endogenous polyclonal Treg-mediated immunotherapy for autoimmune diseases.

Taken together, our studies demonstrate that nonspecific polyclonal $CD4^+$ T cells and $CD8^+CD25^+$ Tregs, when armed with HER2 and MOG antigen-specific pMHC-I and -II complexes, become capable of stimulating enhanced HER2-specific CTL responses and antitumor immunity in double transgenic HLA-A2/HER2 mice and inducing enhanced MOG-specific immunosuppression in MOG-induced EAE mice, respectively. Therefore, redirecting antigen specificity to nonspecific $CD4^+$ T and $CD8^+CD25^+$ Tregs by pMHC complex arming may have great impact in development of novel T cell-based vaccines for treatment of cancer and autoimmune diseases.

TABLE OF CONTENTS

LIST OF FIGURES

LIST OF TABLE

LIST OF ABBREVIATIONS

α-MEM	α-Minimal essential medium
aa	amino acid
Ab	Antibody
ADC	Antibody-drug conjugate
ADCC	Antibody-dependent cell-mediated cytotoxicity
Adv	Adenovirus
Ag	Antigen
AICD	Activation-induced cell death
APC	Antigen presenting cells
bp	Base pair
BAT3	HLA-B-associated transcript-3
Bcl6	B-cell lymphoma 6 protein
BM	Bone marrow
BM-DC(s)	Bone marrow-derived dendritic cell(s)
BSA	Bovine serum albumin
cDC	Classical dendritic cell
CCL	CC-chemokine ligand
CCR	CC-chemokine receptor
Cdc25	Cell division cyclin 25
CD	Cluster of differentiation
CDP	Common DC progenitor
CEA	Carcinoembryonic antigen
CFA	Complete Freund's Adjuvant
CFSE	Carboxyfluoroscein diacetate succinimidyl ester
CIA	Collagen-induced arthritis
Clec9A	C-type lectin domain family 9A
CMA	Cytomegalovirus
CMP	Common myeloid progenitors
CMV	Cytomegalovirus

CMTMR	5-(and-6)-(((4-Chloromethyl)Benzoyl)Amino)Tetramethylrhodamine
ConA	Concanavalin A
CPE	Cytopathic effects
CsCl	Cesium chloride
CTL(s)	Cytotoxic T lymphocyte(s)
CTLA-4	Cytotoxic T lymphocyte antigen 4
CXCL	C-X-C chemokine ligand
CXCR	C-X-C chemokine receptor
DC(s)	Dendritic cell(s)
DEX(s)	DC-derived exosome(s)
DFS	Disease free survival
DM	Diabetes mellitus
DMEM	Dulbecco's modified Eagle’s medium
DMSO	Dimethylsulfoxide
Ds	Double stranded
DT	Diphtheria toxin
EAE	Experimental autoimmune encephalomyelitis
EAU	Experimental autoimmune uveoretinitis
EBV	Epstein-Barr virus
ECD	Extracellular domain
EGFP	Enhanced green fluorescent protein
EGFR	Epidermal growth factor receptor
EGR2	Early growth response 2
ELISA	Enzyme linked immunosorbent assay
EMEM	Eagle's minimal essential medium
EXO(s)	Exosomes
FasL	Fas ligand
FCS	Fetal cattle serum
FDA	Food and drug administration

FDC(s)	Follicular dendritic cell(s)
FITC	Fluorescein isothiocyanate
Flt3	FMS-like tyrosine kinase 3
Foxp3	Fork-head/winged helix transcription factor
FRC(s)	Fibroblastic reticular cell(s)
GA	Glatiramer acetate
GAPDH	Glyceraldehyde-3-phosphate dehydrogenase
GITR	Glucocorticoid-induced tumor necrosis factor receptor
GM-CSF	Granulocyte macrophage-colony stimulating factor
HEK	Human embryonic kidney
HER2	Human epidermal growth factor receptor 2
HEV(s)	High endothelial venule(s)
HLA	Human leukocyte antigen
HSC70	Heat shock cognate protein 70
HSP	Heat-shock protein
i.d	intradermal
iTreg(s)	Adaptive/induced regulatory T cell(s)
i.v.	intravenous
ICAM-1	Intercellular adhesion molecule 1
ICD	Intracellular domain
IDO	Indoleamine 2,3-dioxygenase
IFN-γ	Interferon-gamma
Ig	Immunoglobulin
IL	Interleukin
ILT	Immunoglobulin-like transcript
IRF4	IFN regulatory factor 4
IS	Immunological synapse
Kb	Kilobase pair
kD	kilodalton
KO	Knockout
LAP	Latency-associated peptide

LB	Lysogeny broth
LC(s)	Langerhans cell(s)
LFA-1	Lymphocyte function-associated antigen 1
LN	Lymph node
LP	Lamina propria
LPS	Lipopolysaccharide
LTα	Lymphotoxin α
LYVE1	Lymphatic vessel endothelial receptor
mAb	Monoclonal antibody
miRNA	microRNAs
mtDNA	mitochondrial DNA
MAPK	Mitogen-activated protein kinase
MDP	Macrophage-DC progenitors
MDSC(s)	Myeloid-derived suppressor cell(s)
MG	Myasthenia gravis
MHC	Major histocompatibility complex
MLC(s)	Mixed lymphocyte culture(s)
M-MLV	Moloney murine leukemia virus
MOG	Myelin oligodendrocyte glycoprotein
MOI	Multiplicity of infection
MS	Multiple sclerosis
MT	Mycobacterium tuberculosis
MVBs	Multivesicular bodies
MVEs	Multivesicular endosomes
MyD88	Myeloid differentiation factor 88
nTreg(s)	Natural regulatory T cell(s)
NK	Natural killer
NOD	Non-obese diabetic
NPC	Nasopharyngeal carcinoma
OVA	Ovalbumin
pDC(s)	Plasmacytoid DC(s)

pMHC-I	peptide-MHC complex I
pre-DC(s)	precursor DC(s)
pre-cDC(s)	precursors of conventional DC(s)
PAMP(s)	Pathogen-associated molecular pattern(s)
PBMC(s)	Peripheral blood monouclear cell(s)
PBS	Phosphate buffered saline
PCR	Polymerase chain reaction
PD-1	Programmed cell death protein 1
PD-L1	Programmed death ligand 1
PE	R-Phycoerythrin
PFU	Plaque forming unit
PP	Peyer's patches
PI3K	Phosphatidylinositol 3-kinase
RA	Rheumatoid arthritis
RBC(s)	Red blood cell(s)
RGD	Arginine-Glycine-Aspartic acid
RORγt	Retinoic acid receptor-related orphan receptor gamma-T
RPMI	Roswell Park Memorial Institute medium
RT-PCR	Reverse transcription-polymerase chain reaction
s.c.	subcutaneous
S1P	Sphingosine-1-phosphate
S1PR1	Sphingosine-1-phosphate receptor 1
SAP	SLAM-associated protein
SHG	Second-harmonic generation
SLE	Systemic lupus erythematosus
SMAC	Supramolecular activation cluster
SNARE	Soluble *N*-ethylmaleimide-sensitive factor attachment protein receptor complex
STAT	Signal transduction and transcription
TAE	Tris-acetate EDTA
TCR	T cell receptor

T-DM1	Trastuzumab DM-1
TEX(s)	Tumor-derived exosome(s)
TfR	Transferring receptors
Tg	Transgenic
TGF-β	Transforming growth factor-beta
Th	T helper
TIL(s)	Tumor-infiltrating T lymphocyte(s)
TIM	T cell-immunoglobulin-mucin
TLR	Toll-like receptor
TNF-α	Tumor necrosis factor-alpha
TPM	Two-photon microscopy
Treg(s)	Regulatory T cell(s)
TRAIL	Tumor necrosis factor-related apoptosis-inducing ligand
ULBP	UL-16 binding protein
WT	Wild type
2-ME	2-mercaptoethanol

CHAPTER 1 LITERATURE REVIEWS

1.1 Cells of the Immune System

1.1.1 Overview of immune responses

Immunity results from a complex interplay between the antigen-nonspecific innate immune responses and antigen-specific adaptive immune responses. Innate immunity provides the early line of defense against microbes using non-clonal recognition receptors, including Toll-like receptors (TLRs), NOD-like receptors (NLRs), lectins and helicases. The principal effector cells of innate immunity are mononuclear phagocytes (monocytes, dendritic cells (DCs) and macrophages), neutrophils and natural killer (NK) cells. Among all those cells, DCs are considered as an essential bridge between the innate and adaptive immune responses, since they are linked to their environment through a serial of molecular sensors that allow them to capture invading microbes and to transmit the resulting information to lymphocytes. In contrast to innate immunity, adaptive immunity develops as a response to successive exposure to a particular microbe and adapts to this infection. There are two types of adaptive immune responses called humoral immunity and cellular immunity, which are mediated by different components of the immune system and function to eliminate different types of microbes. Humoral immunity is mediated by antibodies (Abs), which can bind to the microbes and toxin, and assist in their elimination. B lymphocytes are the only cells capable of producing Abs, thus functioning as the mediators of humoral immunity. Cellular immunity is mediated by T lymphocytes, which recognize the antigens of microbes and function to destroy these microbes or the infected cells. T lymphocytes have a restricted specificity for antigens that attach to host major histocompatibility complex (MHC) and express on the surfaces of other cells, thus only recognizing and responding to cell surface-associated but not soluble antigens. Antigen-presenting cells (APCs) are also required during the initiation and development of adaptive immune responses to capture and display antigens to specific lymphocytes, thus the elimination of antigens often requires the participation of various types of cells. Here, only a few immune cell types will be discussed.

1.1.2 DC subsets

DCs play important roles in coordinating innate and adaptive immune responses. They have long membranous projections and are related in lineage to mononuclear phagocytes. They also express pattern recognition receptors and respond to microbes by secreting cytokines. On the other hand, as professional APCs, DCs are critical for induction of adaptive immunity and tolerance. DCs comprise a heterogeneous population, which displays different surface markers, functions and origins across various organs in the body. DC subsets can be classified in several ways based on many criterions reviewed by Steinman and Idoyaga (1). Here, DCs are classified based on the precursor populations from which the various DC subsets originate. DCs derived from common DC progenitor (CDP) and precursor DC (pre-DC) populations are classified as conventional DCs, while monocyte-derived DCs and plasmacytoid DCs (pDCs) are classified as non-conventional DCs. Notably, although pDCs are derived from CDP, they are still be classified as non-conventional DCs due to their distinct function in secreting large amount of type I interferon.

1.1.2.1 Conventional steady-state DCs

Steady-state conventional DCs derived from CDP and pre-DCs can be further divided into migratory and lymphoid DCs. Migratory DCs, which have been found in the skin, lung, intestinal tract, liver and kidneys, migrate from peripheral tissues to lymphoid organs, whereas lymphoid DCs reside in the lymphoid organs without migratory function.

1.1.2.1.1 CDP and pre-DCs derived migratory DCs

Migratory DCs derived from CDP and pre-DCs have been characterized based on their different organ origin. Dermal langerin^{+} CD103^{+} DCs have been shown to play crucial role in cross-presentation of self and viral antigens (2). CD103^{+} CD11c^{high} CD11b^{-} DCs in the lung have been found to migrate to the draining lymph nodes, produce interleukin (IL)-12 and cross-present antigens to CD8^{+} T cells (3, 4). In the intestinal tract, CD103^{+} DCs have also been found in Peyer's patches (PP) and lamina propria (LP). CD103^{+} CX3CR1^{-} CD11b^{+} (CD103^{+} LP) DCs can

recognize pathogenic intestinal bacteria via TLR5 (5) and drive induction of gut homing $CD8^+$ T cells (6, 7), thus making it the major DC subset responsible for initiating adaptive immune responses in the intestinal tract. Additionally, they can also serve a regulatory role (8). Hepatic $CD103^+$ $CD11b^-$ DCs have been shown to highly express FMS-like tyrosine kinase 3 (Flt3), pointing to their pre-DCs origin (9). The pre-DC derived renal $CD103^+$ DCs have been shown to mediate tolerance to kidney allografts (10).

1.1.2.1.2 Lymphoid DCs

Lymphoid DCs have been found in lymphoid organs such as lymph nodes, spleen and thymus, and lack migratory properties. They have been further divided into $CD8^+$ $CD4^+$ DCs, $CD8^-$ $CD4^-$ DCs and $CD8^-$ $CD4^+$ DCs. Since $CD8^-$ $CD4^-$ DCs and $CD8^-$ $CD4^+$ DCs share a high degree of similarity, they will be referred to as $CD8^-$ DCs.

$CD8^+$ DCs

$CD8^+$ DCs were initially thought to express the complete CD8αβ heterodimer found on T cells, however, later it became apparent $CD8^+$ DCs express the CD8αα homodimer instead. $CD8^+$ DCs have been found to play a key role in viral immune responses to intracellular pathogens in the spleen and the lymph nodes (11). They are the most potent interferon (IFN)-α producers among lymphoid DCs, which contribute to viral immunity through increasing cytotoxicity of NK and T cells (12). The expression of CD36 and C-type lectin domain family 9A (Clec9A) has been found to give $CD8^+$ DCs the ability to phagocytose dead cells (13). The distinguishable feature of $CD8^+$ DCs is their ability to cross-present exogenous antigens through an MHC class I pathway (14) and this process has been found not only mediated by phagocytosis of dead cells, but also mediated by uptake of soluble antigens (15). Stimulation of $CD8^+$ DCs with a TLR ligand can induce CD40 expression, leading to an effector $CD8^+$ T-cell response (16). Moreover, the high expression of CD205 on $CD8^+$ DCs has been shown to mediate the efficient processing and presentation of antigens on MHC class II molecules (17), while neutralizing this $CD8^+$ $CD205^+$ DCs has been found to induce $CD8^+$ T-cell tolerance (18).

CD8$^-$ DCs

Compared to CD8$^+$ DCs, the understanding of CD8$^-$ DCs is fairly limited. One functional significant difference between CD4$^-$ CD8$^-$ and CD4$^+$ CD8$^-$ DCs is their ability to secrete IL-12p70 upon appropriate stimulation (19). The ability of CD8$^-$ CD4$^-$ DCs in driving T-cell response has been shown to depend on TLR9 signaling (20), whereas their ability in priming regulatory T cells (Tregs) has been found to relate to transforming growth factor (TGF)-β1 secretion (21). On the other hand, the secretion of IL-10 by CD8$^-$ CD4$^+$ DCs have been found to reduce the severity of experimental autoimmune encephalitis (EAE) in murine models through their tolerizing effects on T helper (Th) cells (22).

1.1.2.2 Non-conventional DCs

Non-conventional DCs are usually not seen in steady state but originated in response to inflammatory stimuli. Plasmacytoid DCs, which are unique in their ability to secrete high amounts of IFN despite of their CDP origin, and monocyte-derived DCs are classified as non-conventional DCs. However, the identification monocyte-derived DCs that arise under steady state conditions further complicates this classification.

1.1.2.2.1 Plasmacytoid DCs

Plasmacytoid DCs express TLR7 and TLR9, which recognize viral RNA and DNA, leading to the production of type I IFN production (23). In addition to serving as a source of IFN, they have also been shown to differentiate activated B cells into plasma cells via secretion of type I IFN and IL-6 (24). Moreover, MHC II synthesis did not down-regulate when pDCs undergo maturation and present antigens, thus providing pDCs with the ability to continuously present endogenous viral antigens in their activated state (25). Plasmacytoid DCs have also been associated with maintenance of peripheral tolerance by interacting with CD4$^+$ T cells via MHC II, which promotes the induction of Treg expansion (26). In contrast, they have been associated with autoimmune responses due to the production of IFN after their recognition of microbial TLR9

(27). The differential ability of pDCs in driving immunity versus tolerance might be attributed to different pDC subsets.

1.1.2.2.2 Monocyte-derived DCs

Monocytes are derived from common myeloid progenitors (CMPs) and macrophage-DC progenitors (MDPs), and can give rise to DCs under both inflammatory and steady state conditions. Monocyte-derived DCs, which are found in peripheral tissues such as the skin, intestine, lung and kidneys, have the ability to uptake antigen followed by migrating to draining lymph nodes. Langerhans cells (LCs) arise from skin-localized Ly-6C^{+} monocyte precursors during inflammation. They possess a unique cellular organelle Langerin (CD207)-containing Birbeck granule as their main component, which plays a role in antigen uptake (28). Activation-induced LCs have been shown to carry the antigen to the draining lymph nodes, where lymphoid CD8^{+} DCs take up the antigen followed by cross-presenting to CD4^{+} and CD8^{+} T cells (29, 30). E-cadherin^{+} intestinal DCs, which secret very high amounts of IL-23 and IL-12 upon stimulation (31), as well as CD103^{-} CX3CR1^{+} intestinal DCs, which mediate the initial innate immune response against pathogen (32), have also been shown their monocytic origin. In addition, pulmonary monocyte-derived CD103^{-} CD11c^{hi} CD11b^{+} DCs have been shown to play a critical role in airway inflammation by regulating Th2 (33) and Th17 (34) immune responses. Moreover, monocyte-derived CX3CR1^{+} CD11b^{+} DCs in kidney have been associated with the infiltration of T cells (35).

1.1.3 CD4^{+} T lymphocyte subsets

T lymphocytes, which mature in the thymus, are a type of lymphocytes that play a central role in cell-mediated immunity. They can be distinguished from other lymphocytes by the presence of a T-cell receptor (TCR) on the cell surface. CD4^{+} T cells, which possess TCR and CD4 molecules, help to eliminate microbes through secretion of cytokines and activation and through recruitment of other immune cells. Several subsets of CD4^{+} T cells have been identified based on their cytokine secretion and effector function.

1.1.3.1 Th1 and Th2 cells

Th1 and Th2 subsets develop from the same naive $CD4^+$ T lymphocytes precursors, and the pattern of differentiation is determined by stimuli present early during immune responses. Th1 differentiation occurs in response to intracellular bacteria and parasites (36), and involves the cooperation among signals from TCR, cytokines IFN-γ and IL-12, and transcription factor T-bet, signal transduction and transcription (STAT) 1 and STAT4 (37, 38). They evoke cell-mediated immunity and phagocyte-dependent inflammation mainly by secreting cytokine products such as IFN-γ, lymphotoxin α (LTα), and IL-2. IFN-γ is essential for the activation of macrophages, thus resulting in enhanced phagocytic activity (39). LTα has been shown to be responsible for some of the Th1-induced autoimmune diseases (40). IL-2, as T cell growth factor, promotes proliferation of $CD8^+$ T cells, as well as the development of $CD8^+$ memory cells after antigen priming, thereby participating in robust secondary immune response (41). Besides, it also essential for the survival and activation of thymus-derived natural Tregs (42).

Th2 differentiation occurs in response to some extracellular microbes, including helminthes and allergens (43), and involves the cooperation among signals from the TCR, the cytokine IL-4, and the transcription factor GATA-3 and STAT6 (44). They evoke strong Ab responses and eosinophil accumulation mainly by producing cytokines IL-4, IL-5, IL-9 and IL-13. IL-4 is a major cytokine involved in IgE switching and secretion by B cells, as well as in regulating other proinflammatory mediators (45, 46). IL-5 mainly targets eosinophils and their precursors, leading to their activation and release (47). Th1 and Th2 cells are considered terminally differentiated based on (i) lineage commitment of Th1 and Th2 require transcription factors T-bet and GATA-3, respectively; (ii) their abilities to mutually inhibit one another's activity through cytokine secretion. The concept of Th1/Th2 paradigm also provides an explanation of adaptive immunity against intracellular versus extracellular pathogens, and the pathogenesis of immune-mediated tissue damage in infection and allergy.

1.1.3.2 Th17 cells

Th1 cells have been associated with several autoimmune diseases through the production of inflammatory IFN-γ and IL-12, however, mice with selective blockade of IFN-γ and IL-12 function were still sensitive to some of the autoimmune diseases (48, 49), leading to discovery of a new $CD4^+$ T cell subset-Th17. Th17 differentiation occurs in response to extracellular bacteria and fungi, and involves the interplay of signals from cytokines IL-6, IL-21, IL-23 and TGF-β, and transcription factor retinoic acid receptor-related orphan receptor gamma-T (RORγt) (50) and STAT3. They are also involved in the generation of autoimmune diseases by producing effector cytokines IL-17A, IL-17F, IL-21, and IL-22. IL-17 leads to the induction of proinflammatory cytokines and chemokines to ensure the chemotaxis of inflammatory cells to the sites of inflammation (50, 51). In addition to facilitating Th17 development, IL-21 has also been shown to activate T and NK cells, as well as to induce B cell differentiation (52, 53). IL-22 is known to mediate inflammatory response in mucosal host defense against bacterial pathogens (54), and has been found its tissue protective property in limiting liver tissue damage (55).

1.1.3.3 Regulatory $CD4^+$ T cells

$CD4^+$ Tregs exist as natural thymus-derived and peripheral-induced subset. They play an important role in the maintenance of immunologic tolerance to self and foreign antigen after effector cell-mediated pathogens clearance, thereby protecting against immunopathology (56, 57). The $CD4^+$ Tregs differentiation involves the interplay of signals from cytokine TGF-β and transcription factor forkhead box P3 (Foxp3) and STAT5 (58, 59), while their main effector cytokines include IL-10, TGF-β, and IL-35. IL-10 is a potent inhibitory cytokine with the ability to suppress proinflammatory. TGF-β controls the differentiation of proinflammatory T cells. The combination effect of IL-10 and TGF-β has been shown to potently suppress IgE production, indicating their important roles in limiting tissue damage and attenuating allergic inflammation (58, 60).

1.1.3.4 Follicular helper (Tfh) T cells.

Tfh cells participate in the development of antigen-specific B-cell immunity in follicular areas of lymphoid tissue. Their differentiation involves the interplay of signals from cytokines IL-6 and IL-21, and transcription factor B-cell lymphoma 6 protein (Bcl6) and STAT3 (61, 62). Tfh cells express distinct surface marker C-X-C chemokine receptor-5 (CXCR5) after immunization and enter the pre-germinal centre for initial interactions with antigen-primed B cells (63). They later enter into the germinal area to further promote the development of long-live B memory cells.

1.1.3.5 More $CD4^+$ T-cell subsets: Th9 and Th22 cells

Th2-produced IL-9 has been reported to play an important role in the pathogenesis of asthma, IgE class switching and parasite clearance (64). However, a new IL-9 producing $CD4^+$ T-cell subset-Th9 was reported by two dependent group based on their studies of TCR stimulated naive $CD4^+$ T cells in the presence of TGF-β and IL-4 (65, 66). The transcription factor that involved in Th9 cells differentiation was later identified as the ETS family transcription factor PU.1 and IFN regulatory factor 4 (IRF4) (67, 68). Despite IL-22 can be produced by Th17 cells and a subset of NK cells, three dependent groups showed a new IL-22 secreting $CD4^+$ T subset-Th22, which can be generated by stimulating with pDCs in the presence of IL-6 and tumor necrosis factor-alpha (TNF-α) (69-71). Unlike other Th cells, no transcription factors have been identified for the development of Th22 cells yet. Only aryl hydrocarbon receptor was reported to play a role in IL-22 secreting by Th22 cells (69, 70).

1.1.4 $CD8^+$ T lymphocytes

$CD8^+$ cytotoxic T lymphocytes (CTLs), which can expand their number many thousand-fold at the peak of a primary immune response, are effector $CD8^+$ cells and able to eliminate intracellular microbes mainly by killing infected cells. They kill targets that express the MHC-I-associated antigen in a contact dependent way, and exert their cytolytic function mainly through perforin/granzyme-mediated or Fas ligand/Fas-mediated apoptosis (72). Following the elimination of the infected cells, effector $CD8^+$ T cells undergo a precipitous contraction phase.

Only ~5-10% pathogen-specific effector $CD8^+$ T cells will survive to further mature into memory $CD8^+$ T cells, while the majority will go apoptotic cell death. Notably, not all effector $CD8^+$ T cells have equal potential to form memory T cells, and their fates are based on the differences in gene and protein expression, effector functions and long-term proliferative capacity (73). Two broad phenotypes of memory T cells have been described, $CD62L^{high}CCR7^{high}$ (CC-chemokine receptor 7) central memory T cells and $CD62L^{low}CCR7^{low}$ effector memory T cells (74, 75). Other $CD8^+$ subpopulation, like $CD8^+$ T cells with regulatory activities, will be further discussed in Section 1.6.

1.1.5 Summary

Except for the above mentioned cells, B lymphocytes, monocytes, macrophages, granulocytes (eosinophils, neutrophils, basophils), mast cells and NK cells are all indispensable for making up the cellular components of the innate and adaptive immune systems, thus constituting a dynamic communication network to protect body from foreign organisms.

1.2 Exosome (EXO)-derived vaccines

1.2.1 EXO biogenesis and composition

EXOs, small membrane vesicles (40-100 nm), can be formed and secreted by the fusion of late endocytic compartments (multivesicular endosomes) (MVEs) containing intraluminal vesicles with plasma membrane via reverse-budding intracellular events (76). They were originally described as microvesicles containing ectoenzyme activity that were secreted by neoplastic cell lines (77). Their endocytic origin was reported a few years later (78, 79). Subsequent studies showed that EXOs can be constitutively or inductively secreted by a variety of cell types, including DCs, macrophages, mastocytes, T and B cells, epithelial cells (80), platelets, fibroblasts, schwann cells, adipocytes, neuronal cells and numoerous tumor cell lines (76, 81-84). In addition, EXOs can be purified without any mechanical dissociation from several biological fluids (84), such as human plasma, serum, bronchoalveolar fluid, urine, saliva, pleural

effusions of ascites, tumoral effusions, epididymal fluid, amniotic fluid and milk, indicating that EXOs can be released from several cell types and tissues *in vivo*.

The biogenesis of EXOs is regulated by multiple signaling molecules and can be triggered by many factors including extracellular stimuli and stresses. EXOs can be released into the extracellular environment by the fusion of multivesicular bodies (MVBs) with the cell surface. Briefly, plasma membrane first contracts and draws MVBs membranes together with the help of soluble *N*-ethylmaleimide-sensitive factor attachment protein receptor complex (SNARE complex) followed by cleaving the membrane connection and releasing the vesicles into the extracellular space (85) in a process dependent on the activity of Ras-related GTPase Rab27A and Rab27B (86).

EXOs have a lipid bilayer with a characteristic "saucer-like" morphology, which is consistent with the observed size and morphology of internal vesicles in MVEs (87), and float on sucrose gradients ranging from 1.13-1.19 g/mL. Based on the extensive proteomics and phosphoproteomics studies, EXOs are suggested to shuttle wide array of biologically relevant molecules, including proteins, lipids, carbohydrates and RNAs. In addition to the similarity of their morphology, EXOs are thought to be somewhat conservative in their protein and lipid composition. The ubiquitous proteins include cytoskeletal proteins, intracellular membrane fusion and transport proteins, signal transduction proteins, metabolic enzymes, heat-shock proteins (HSPs), tetraspanins, lipid-related proteins and phospholipases (88, 89). Certain raft-associated lipids are also enriched in EXOs, such as ceramide (90), cholesterol, sphingolipids and phospoglycerides with long and saturated fatty-acyl chains (91). The finding of nucleic acid contents of EXOs, such as messenger RNAs (mRNAs), small non-coding microRNAs (miRNAs) and mitochondrial DNA (mtDNA), has been considered as a major breakthrough in EXO research.

1.2.2 EXO biological functions

1.2.2.1 Elimination of obsolete proteins

For many years, EXOs have been considered as organelles to remove cell debris or obsolete proteins out of the cell. During the maturation of erythrocytes, EXOs are released to eliminate of obsolete transferring receptors (TfR) (78, 79, 92, 93). TfR's interaction with heat shock cognate protein 70 (HSC70) in secreted EXOs is required for the complete lost of TfR from the surface of the erythrocytes (94). Thus, EXOs was suggested as an effective alternative to lysosomal degradation, particularly in eliminating redundant plasma membrane proteins or other proteins that are resistant to degradation by lysosomal proteases. Therefore, the primary function of EXOs is postulated to clear away obsolete proteins during cell differentiation.

1.2.2.2 Intercellular communication

EXOs can affect the physiology of recipient cells in various ways via long-range membrane exchange. Recipient cells can induce intracellular signaling, as well as confer new functional properties after the acquisition of new receptors, enzymes or even genetic materials from the EXOs. Interactions between EXOs and recipient cells include (i) adhesion of EXOs to the surface of recipient cells via lipid or ligand-receptor conjunction followed by the direct fusion with recipient plasma membrane; (ii) internalization of EXOs into endocytic compartments followed by incorporation with endosomal membranes and further recycling to the recipient cell surface; (iii) degradation of endocytosed or phagocytosed EXOs followed by loading them onto the recipient MHC complex and further recycling to the recipient cell surface (84). Take DCs-released EXOs for example, it has been reported that mature DC-derived intercellular adhesion molecule (ICAM)-1 bearing EXOs can be captured by activated T cells (95) and $CD8^+$ DCs (96) via ICAM-1-LFA (lymphocyte function-associated antigen)-1 interaction. DC-derived EXOs have also be addressed specifically to both T cells and DCs through binding of exosomal $\alpha_M\beta_2$ integrin to ICAM-1 on T cells and DCs (76). In addition, DC-derived EXOs bearing MFG-E8 (lactadherin) can bind $\alpha_v\beta_{3/5}$ integrins expressed by DCs via Arginine-Glycine-Aspartic (RGD) domain (81, 97). Furthermore, tetraspanins on DC-derived EXOs have been shown related to

their capture by DCs (97). Of note, DC- or T cell-derived EXOs can be captured by T cells or DCs via antigen-specific TCR-pMHC-I/II interaction (98-100). Finally, DC-released EXOs exposing phosphatidylserine (PS) on their surface. Therefore, they can be captured by activated lymphocytes or phagocytes that express PS receptors such as T-cell immunoglobulin- and mucin-domain-containing molecules T cell-immunoglobulin-mucin 1 (TIM1) and TIM4 (101).

Besides targeting to recipient cells to exchange proteins and lipids or to trigger downstream signaling events, EXOs also deliver specific nucleic acid cargo to mediate intercellular communication (102-104) between widely separated locations in the body. Since miRNAs are short, non-coding RNAs that regulate the expression of complementary mRNAs, the shuttling of these molecules between cells aids in regulating the biology of target cells. The spread of oncogenes (105), mRNA, miRNA (106) and viruses (107, 108) has been reported.

1.2.3 Modulation of immune responses

1.2.3.1 Antigen presentation (Antigen-specific immune responses)

EXOs derived from culture cells or body fluids contain whole or partially processed antigenic materials and peptide-MHC (pMHC) complexes, thus playing a critical role in triggering immune responses via antigen presentation. EXOs derived from virtually any cell type bear MHC-I molecules that could potentially induce $CD8^+$ T-cell activation, in certain circumstances, could be directly presented to T cells via preformed peptide-MHC class I (pMHC-I) complex (109-111). Although preformed pMHC complexs on EXOs is functional, recipient DCs can also process MHC molecules and antigen from allogeneic DC-released EXOs to generate restriction peptides to reload onto their own MHC molecules, thus indirectly inducing antigen-specific $CD8^+$ (112-114) and/or $CD4^+$ (112, 115, 116) T-cell responses. In addition, tumor-released EXOs purified from cultured tumor cells (117) or from ascites of patients with tumors (118) have been shown to bear tumor antigens and pMHC-I complex, leading the activation of antigen-specific T cells *in vitro* in the presence of recipient DCs. The antigen-specific immune responses of tumor-derived EXOs are strictly dependent on recipient DCs, which may be due to the absence of costimulatory molecules on the surface of tumor cells and tumor cell-derived EXOs. Moreover,

intracellular pathogens infected macrophages-released EXOs have been shown to carry pathogen-derived antigens, which can be transferred to DCs leading to the activation of $CD4^+$ and $CD8^+$ T cells, as well as the generation of memory $CD4^+$ and $CD8^+$ T cells (119). Furthermore, EXOs derived from endothelial cells infected with cytomegalovirus (CMV) also transfer virus-derived antigens to DCs for activation of $CD4^+$ T cells, thus contributing to allograft rejection (120). Therefore, EXOs can directly or indirectly induce antigen-specific T-cell responses, representing a potential cell-free vaccine for cancer immunotherapy.

1.2.3.2 Antigen-independent roles in immune responses

In addition to MHC molecule-mediated antigen-specific immune responses, EXOs can promote or inhibit immune responses in various antigen-independent ways.

1.2.3.2.1 Antigen-independent immunostimulatory effects

Mycoplasma-contaminated EXOs released by infected DCs have been shown to induce the polycolonal activation of B cells and promote immunoglobulin (Ig) secretion (121). HLA-B-associated transcript-3 (BAT3) bearing EXOs derived from immature DCs can promote NK-cell activation and cytotoxicity (122). Furthermore, DC-derived EXOs containing both IL-15Rα and NKG2D ligands can contribute to NK-cell proliferation, activation and cytotoxicity in a IL-15Rα- and NKG2D-dependent fashion (123), which is different from the NKG2D ligand-bearing tumor-derived EXO-mediated immunosuppressive effect. Although many studies reported that tumor-derived EXOs containing FasL and NKG2D ligand exert immunosuppressive effects, there are still many reports showing that tumor-derived EXOs are immunogenic. The discrepancy may be due to differences in the types of EXOs produced and microenvironment such as immunological conditions. EXOs from heat-shocked (stressed) tumor cells have been found to promote NK-cell cytolytic activity, TNF-α production by macrophages and DC maturation, and more efficiently induce $CD4^+$ Th1-polarized and $CD8^+$ CTL responses in MHC-independent manner (124-127). EXOs released from macrophages infected with intracellular pathogens contain pathogen-associated molecular patterns (PAMPs) and can induce the secretion of proinflammatory cytokines such as TNF-α and IL-12 by recipient macrophages in a Toll-like

receptor (TLR)- and myeloid differentiation factor 88 (MyD88)-dependent manner (128, 129). Mast cell-derived EXOs harboring MHC-II, cell division cyclin 25 (Cdc25) and immunostimulatory molecules (such as CD86, LFA-1 and ICAM-1), can induce T cell activation, blast formation, cell proliferation and production of IL-2 and IFN-γ (130).

1.2.3.2.2 Antigen-independent immunosuppressive effects

Tumor-derived EXOs: EXOs derived from tumor cells such as melanoma and colorectal cancer cells can induce T-cell apoptosis via exosomal Fas ligand (FasL) (CD95L) and TNF-related apoptosis-inducing ligand (TRAIL)/APO2 ligand (APO2L) (131, 132), which is involved in tumor immune escape. Epstein-Barr virus (EBV)-associated nasopharyngeal carcinoma (NPC) cell- and NPC-bearing patient-derived EXOs contain high amounts of galectin-9, which can attenuate antitumor T-cell responses leading to immune evasion of tumor cells (133). In addition, mammary tumor-derived EXOs can inhibit IL-2-mediated activation, proliferation and cytotoxic activity of NK cells (134). Clayton et al. (135) reported that tumor-derived EXOs bearing membrane-bound TGF-β1 can impair IL-2-induced $CD8^+$ T-cell and NK-cell proliferation as well as their killing function by enhancing the function of $CD4^+CD25^+Foxp3^+$ Tregs via exosomal membrane-bound TGF-β1. The same group further reported that tumor-released EXOs can suppress the cytotoxic capacity of $CD8^+$ T cells and NK cells through exosomal NKG2D ligand MHC class I polypeptide-related sequence A (MICA)- and TGF-β1-mediated downregulation of activating receptor NKG2D (136). Moreover, tumor-derived EXOs can impair the differentiation of myeloid precursors into DCs and induce the generation of myeloid-derived suppressor cells (MDSCs) via TGF-β (137-139). Remarkably, several breast cancer cell lines released EXOs, which contain human epidermal growth factor receptor 2 (HER2), have been shown to bind the trastuzumab Ab *in vivo*, thus reducing its therapeutic availability and increasing tumor aggressiveness (140). Thus, tumor-derived EXOs can subvert antitumor immune responses via multiple pathways.

T cell-derived EXOs: Active T cells have been shown to release FasL and TRAIL/APO2L containing EXOs, which can rapidly induce apoptosis of bystander activated T cells via activation-induced cell death (AICD) (141, 142). The work in our lab further reported that DC-

activated T cell-secreted EXOs bear antigen-specific TCR and FasL, thus inhibiting T-cell immune responses through downregulation of pMHC complex on antigen-loaded DCs and FasL-mediated cytotoxicity (99, 100).

Placenta- and milk-derived EXOs: Placenta of pregnant women secreted EXOs have been shown to bear NKG2D ligand UL-16 binding proteins (ULBP), which can induce down-regulation of the NKG2D on NK and $CD8^+$ T cells, leading to reduction of their *in vitro* cytotoxicity (143, 144). In addition, EXOs derived from human colostrum and mature breast milk can increase number of $CD4^+$ $CD25^+$ $Foxp3^+$ Tregs and inhibit anti-CD3-induced production of IL-2 and IFN-γ from allogeneic and autologous peripheral blood mononuclear cells (PBMCs) (145).

1.2.4 EXO-based immunotherapy

It was initially reported in 1996 that B cell-derived EXOs could stimulate antigen- specific MHC II-dependent $CD4^+$ T cells *in vitro* (87). Subsequent report showed that tumor peptide-loaded autologous DC-derived EXOs expressing functional pMHC-I/II complexes and T-cell costimulatory molecules could elicit the eradication of established tumors *in vivo* via antigen-specific MHC class I-restricted $CD8^+$ CTL responses in a mouse tumor model (146). The pioneering studies prompted investigation into the application of DC-derived EXOs (DEX) in antitumor immunotherapy. Notably, DEX from mature DC and immature DC exhibit distinct bioactivities in line with their differential protein composition. Although immature DCs secreted much more EXOs than mature DCs (81, 116), extensive studies have shown that mature DC-derived EXOs (mDEX) bearing functional pMHC-I/II complexes and higher levels of costimulatory and adhesion molecules. Mature DEX can induce antigen-specific T-cell immune responses either directly by exposing exosomal pMHC complexes and costimulatory molecules to T cells (109-111, 147, 148) or indirectly by conveying pMHC complexes to recipient mature DCs (112-116). More recently, Qazi et al. (149) reported that OVA-pulsed DC-released EXOs could elicit OVA-specific Th1 cellular and immunoglobulin2a humoral immune responses via B cell-dependent mechanism. Importantly, DEX bearing can promote NK-cell proliferation, activation and cytotoxicity (122, 123), suggesting their modulating role in innate immune

responses. Injection of expression vector transfected targeted EXOs could possibly deliver siRNA to a mouse brain, thus postulating a potential therapeutic approach to Alzheimer's disease (150, 151). Let-7a miRNA loaded EXOs can be used to target epidermal growth factor receptor (EGFR)-expressing breast cancer cells, thus represent a vehicle for conveying drugs to tumors (152).

Preclinical studies in mouse models have shown that most of EXO-based vaccine can only induce a prophylactic (preventive) antitumor immunity but do not have significant therapeutic effect on established tumors. Some of factors that affect the bioactivity of EXOs have been addressed. Firstly, high dose level of EXOs and intradermal (i.d.) injection can induce more efficient $CD8^+$ CTL responses and stronger antitumor immunity (114, 153). Additionally, DEX can be directly loaded with antigen peptides (112, 149) or indirectly via DC pulsed with antigen peptides (146) or immunogens (149, 154, 155). Moreover, the roles of $CD4^+CD25^+$ Tregs in the inhibition of CTL-mediated antitumor immunity have been increasingly recognized (156-158). Tumor microenvironment can facilitate prompt recruitment and expansion of $CD4^+CD25^+$ Tregs leading to the delayed rejection of tumors (156, 159). Chemotherapy drug cyclophosphamide can enhance the magnitude of tumor antigen-specific secondary $CD8^+$ CTL responses induced by DEX via suppressing function of $CD4^+CD25^+$ Tregs (160). Furthermore, the immunogenicity of tumor-derived EXOs (TEX) can be improved via being exposed stress conditions and incorporating immunologic molecules. Heat-shocked or membrane-bound HSP70-engineered TEX can promote DC maturation, induce $CD8^+$ CTL responses and antitumor immunity, and activate NK cells and macrophages (124-127, 161). Heat-treated malignant ascites can improve the immunogenicity of TEXs, promote DC maturation and induce tumor-specific $CD8^+$ CTL responses (162). Oxidative stresses have also been shown to limit for solid tumor growth (163). Cytokine engineered TEX/IL-18 (164) or TEX/IL-12 (165) has been shown to more potentially induce $CD8^+$ CTL responses and antitumor immunity. The increasing knowledge about the biological effects of EXOs and enhancement of their immunogenicity will provide exciting prospects for EXO vaccine development in cancer immunotherapy.

Based on the knowledge that EXOs are well tolerated in humans and they have a long half-life in the blood, plus the established good manufacturing procedures in obtaining clinical-grade EXOs

(166), several clinical trials has been carried out with DEX- and TEX- based cancer immunotherapy. The DEX-based initial two Phase I clinical trials involved patients with advanced stage melanomas or non-small cell lung cancers (167). The clinical outcomes were encouraging, showing (i) the safety of treatment by DEX with minimal side effect; (ii) transient stabilization of the diseases; (iii) detectable immune responses, particularly enhanced NK cell cytotoxicity. A Phase I clinical trial in colorectal cancer showed that using ascites-derived EXOs in conjunction with granulocyte macrophage-colony stimulating factor (GM-CSF) induced more antigen-specific T cells (168), indicating a feasible and safe immunotherapy strategy. In addition, ovarian cancer ascites-derived EXOs combined with TLR3 agonist PolyI:C as a adjuvant is being planned to clinically treat advanced ovarian cancer patients after chemotherapy (169). These clinical trials suggested that EXO-based cancer immunotherapy might be better combined with several already established therapies that enhance immune responses. The relative stability of TEXs in body fluids makes them as the most reliable source of biomarkers for detecting and monitoring cancer (170). At present, two clinical trials investigate TEX for their prognostic and predictive biomarker in breast cancer (NCT01344109) and gastric cancer patients (NCT01779583), respectively. More EXO-based regimens tested in clinical trials can be found on ClinicalTrails.gov website.

1.2.5 Summary

Although DC represents a promising cell-based strategy to elicit or enhance antitumor immune responses, the percentage of live DCs after freeze-thaw and unknown behaviours or fates of DCs after injection such as short-lived, sensitive to CTL-mediated killing (111) and elusive modification of pMHC complexes displayed on their surface currently limit DC-based adoptive cancer immunotherapy. DEX, relatively stable secreted membrane vesicles, harboring high levels of functional pMHC-I/II complexes and costimulatory and adhension molecules, thus theoretically, could at least complement DC-based immunotherapy. In fact, EXOs has been emerging as major players in intercellular communications in the past few years. EXOs have been shown to contain diverse biological molecules including virions, miRNAs, proteins and their complexes. The presenting of contents to recipient cells could either invoke or suppress immune responses, indicating potential therapeutic roles of EXOs. A lipid bilayer membrane

confers a high degree of stability, which makes EXO even more attractive as diagnostic markers. Although much progress has been made where EXOs are considered good vehicles to shuttle nucleic acid contents for therapeutic approaches, the miRNA-based trials in the context of EXOs have not been initiated. Hopefully, the development of EXO-based strategies will help to overcome the most challenging issue in cancer therapy.

1.3 A new dynamic model of three cell interactions for CTL responses

1.3.1 Three-cell and sequential two-cell model

In the immune system, APCs such as DCs function by engulfing antigens, processing them, and subsequently presenting them to $CD4^+$ and $CD8^+$ T cells via MHC class II and MHC class I molecules, respectively, leading to $CD8^+$ CTL responses. However, how these three rare cell populations precisely interact and how $CD4^+$ T-helper cell signals are delivered to $CD8^+$ T cells *in vivo* remains controversial. Based on the observation that the antigen recognized by $CD4^+$ and $CD8^+$ T cells must be carried by the same DC, several distinct models have been proposed. A "three-cell interaction model" was originally proposed for $CD4^+$ T-cell dependent CTL responses (171), according to which antigen-specific $CD4^+$ and $CD8^+$ T-cell precursors must simultaneously interact with the same antigen-presenting DC (**Figure 1.1A**). However, as both antigen-specific $CD4^+$ and $CD8^+$ T-cell precursors are relatively rare, intuitively this three-cell interaction appears to be almost impossible. Later, Ridge et al. proposed a "dynamic model of sequential two-cell interactions by APCs" (172), according to which APCs must be first activated (licensed) by $CD4^+$ T cells via CD40/CD40L interaction and then the licensed DCs can directly stimulate memory CTL responses (**Figure 1.1B**). However, this model has been challenged by the observation that efficient memory CTL responses require CD40 expression on $CD8^+$ T cells but not on DCs (173), and as CD40L is mainly expressed by $CD4^+$ T cells, thus implicating direct $CD4^+$-$CD8^+$ T-cell interactions in the development of memory CTLs.

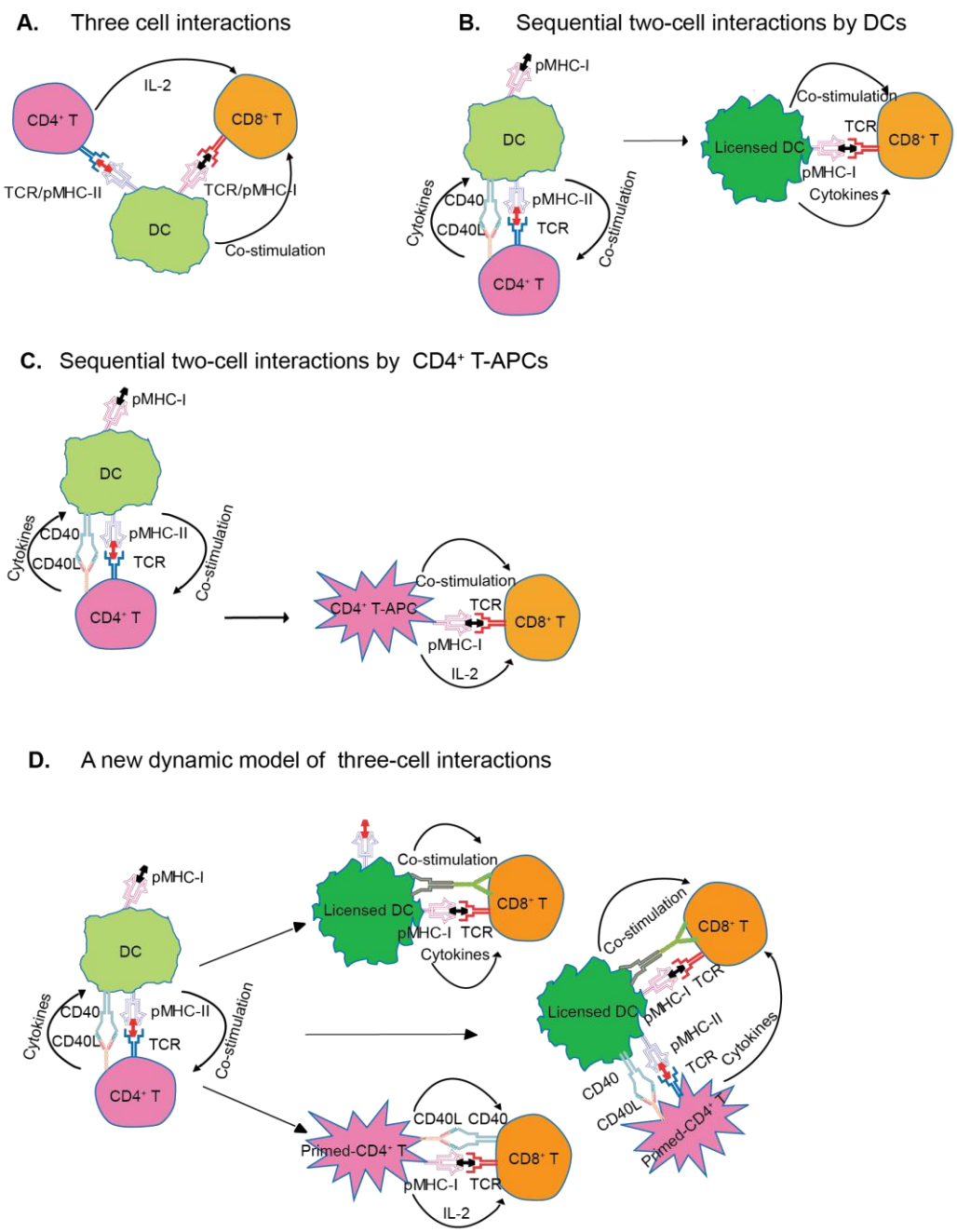
A. Three cell interactions
IL-2
CD4⁺ T
CD8⁺ T
TCR/pMHC-II
TCR/pMHC-I
DC
Co-stimulation
B. Sequential two-cell interactions by DCs
pMHC-I
DC
Cytokines
CD40
CD40L
pMHC-II
TCR
Co-stimulation
CD4⁺ T
Licensed DC
Co-stimulation
TCR
CD8⁺ T
pMHC-I
Cytokines
C. Sequential two-cell interactions by CD4⁺ T-APCs
pMHC-I
DC
Cytokines
CD40
CD40L
pMHC-II
TCR
Co-stimulation
CD4⁺ T
CD4⁺ T-APC
Co-stimulation
TCR
CD8⁺ T
pMHC-I
IL-2
D. A new dynamic model of three-cell interactions
pMHC-I
DC
Cytokines
CD40
CD40L
pMHC-II
TCR
Co-stimulation
CD4⁺ T
Licensed DC
Co-stimulation
CD8⁺ T
pMHC-I TCR
Cytokines
Primed-CD4⁺ T
CD40L CD40
CD8⁺ T
pMHC-I TCR
IL-2
Licensed DC
Co-stimulation
CD8⁺ T
pMHC-I TCR
pMHC-II
TCR
Cytokines
CD40
CD40L
Primed-CD4⁺ T
E. Exosome-targeted CD4⁺ T cell vaccine
mature DC
CD4⁺ T
CD40L CD40
CD4⁺ T EXO
CD8⁺ T
pMHC-I TCR
IL-2

Figure 1.1 A new, dynamic model of three-cell interactions. (**A**) The passive three-cell interaction model. A $CD4^+$ T helper activated by an APC delivers cytokine (IL-2) required for CTL activation to a $CD8^+$ T cell, which recognizes antigen on the same APC. (**B**) The dynamic model of sequential two-cell interactions by APCs. The cross-priming APC is activated (licensed) by an antigen-specific $CD4^+$ T cell through CD40-CD40L interactions, and then, the fully licensed APC gets the ability to prime CTL directly. (**C**) The dynamic model of sequential two-cell interactions by $CD4^+$ T-APCs. $CD4^+$ T cells can acquire molecules (particularly pMHC-I) from APCs by APC activation and thus, can stimulate CTL responses directly. (**D**) A new, dynamic model of three-cell interactions. The cross-priming DC first interacts with the antigen-specific $CD4^+$ T cell for the crucial first step in CTL responses, which are DC-$CD4^+$ T interaction, resulting in DC licensing and $CD4^+$ T cell activation (priming). Cognate $CD8^+$ CTLs can then receive helper or stimulatory signals, not only from DC-$CD4^+$ T clusters but also separately from fully licensed DCs and primed $CD4^+$ T cells, even after their dissociation from DC-$CD4^+$ T clusters. (**E**) A novel EXO-targeted $CD4^+$ T vaccine. EXO-loaded $CD4^+$ T cells stimulated $CD8^+$ T-cell priming via pMHC-I-mediated targeting.

1.3.2 Primed-$CD4^+$ T cell model

Trogocytosis (intercellular membrane protein transfer) is a ubiquitous phenomenon, when this involves immune cells, plays important roles in immune modulation (174). $CD8^+$ and $CD4^+$ T cells have been reported to acquire the immunological synapse (IS)-composed pMHC-I and pMHC-II complexes from activating DCs, respectively, via internalization and recycling of synapse components (175). As our lab was the first to discover that in addition to pMHC-II, $CD4^+$ T cells also acquire pMHC-I and CD80 molecules from DCs, and the acquired antigen presenting machinery remains functional that help $CD4^+$ T cells to directly stimulate cognate $CD8^+$ T cells. This led to the proposal of a "new dynamic model of sequential two-cell interactions by $CD4^+$ T cells" (**Figure 1.1C**), where primed-$CD4^+$ T cells that have acquired antigen presenting machinery from DCs function as APCs themselves (T-APC) (176). This model is also supported by recent evidence from another lab (177). Interestingly, our lab also showed that T-APCs preferentially stimulate $CD8^+CD44^+CD62L^{high}CD127^+$ central memory CTL responses (178). However, physiological significance of T-APC concept *in vivo* remains an open question. Thus, the original question, that is, the mechanisms for functional delivery of $CD4^+$ T-cell help, whether $CD8^+$ T cells receive helper signals by forming a three-cell cluster (DC-$CD4^+$-$CD8^+$), indirectly through licensed DCs, or directly from primed $CD4^+$ T cells, remains unresolved.

To gain a better insight into the mechanisms that regulate CTL responses, novel immunization protocols have been developed in our lab, wherein antigen-presenting DCs (CD11c-diphtheria toxin (DT) receptor transgenic DCs, presenting ovalbumin (OVA) as a model antigen), $CD4^+$ and $CD8^+$ T cells can be separately manipulated for dissecting their respective roles in the priming of CTL responses *in vivo* (179). In this experimental setup, $CD4^+$ T cells and antigen-presenting DCs were allowed to engage with one another *in vivo*, in the absence of cognate $CD8^+$ T cells ($CD8^+$ T cell-depleted host). Thereafter, either the previously engaged $CD4^+$ T cells (injecting the GK1.5 Ab) or DCs (injecting DT) can be selectively depleted before allowing the interaction of none, either or both of these populations with adoptively transferred naive $CD8^+$ T cells. This protocol allowed us not only to clearly document the importance of $CD4^+$ T cell-licensed DCs and DC-primed $CD4^+$ T cells in CTL responses, but also made possible the testing of previously proposed models in the same experimental setting. This study provided direct *in vivo* evidence that primed $CD4^+$ T cells or licensed DCs can stimulate CTL and memory responses, independent of DC-$CD4^+$ T-cell clusters. Remarkably, imaging study using intravital two-photon microscopy (TPM) provided first unequivocal *ex vivo* evidence for pMHC-I-dependent direct $CD4^+$-$CD8^+$ T-cell interactions in the absence of DC-$CD4^+$-$CD8^+$ T cell ternary clusters.

Thus, it provided for the first time physiologically relevant *in vivo* evidence that primed $CD4^+$ T cells can directly orchestrate efficient $CD8^+$ CTL responses, proposing a "new dynamic model of three-cell interactions for CTL responses" (**Figure 1.1D**) (179). According to such a dynamic model, CTL and memory responses do not depend on an antigen presenting DC simultaneously engaging cognate naive $CD4^+$ and $CD8^+$ T cells in an environment in which both of these latter cells are extremely rare. Directly attracting $CD8^+$ T-cell targets to primed $CD4^+$ T cells through acquired pMHC-I/TCR and CD40/CD40L engagement would also be expected to result in a more efficient delivery of IL-2 and hence a more efficient CTL memory induction. Altogether, this study revealed the coexistence of direct and indirect mechanisms of T cell help for CTL responses in non-inflammatory situations, thereby reconciling previous conflicting studies. In addition, the CTL programming derived from licensed DCs, primed $CD4^+$ T cells and DC-$CD4^+$ T-cell clusters reflects microenvironments differing in signal strength, co-stimulation and

cytokine levels. Such subtle differences could be one of the reasons of the T-cell heterogeneity during memory T-cell development (180).

1.3.3 A novel EXO-targeted $CD4^+$ T cell vaccine

Since immune cells also exchange various molecules through EXO release without any physical interaction, a variation on this theme has also been proposed in our lab. DCs process exogenous antigens in their endosomal compartments, which can later fuse with the plasma membrane, releasing antigen-presenting EXOs (146). Since the released EXOs can be captured by activated T cells (84), we propose that EXO-loaded activated T cells might be able to stimulate CTL responses similarly as DC-primed T cells. Interestingly, EXO-loaded $CD4^+$ T cells have been found to stimulate $CD8^+$ T-cell priming via pMHC-I-mediated targeting and via IL-2 and CD80 signaling (**Figure 1.1E**) (181). Further study elucidate that the principle of EXO primed $CD4^+$ T cell model can be applied as novel $CD4^+$ T cell-based vaccine capable of stimulating long-term functional CTL memory via CD40L (182). This immune priming process has also been confirmed *ex vivo* using TPM, where cognate $CD8^+$ T cells form stable contacts only when activated-T cells were loaded with antigen-specific DCs-released EXOs (183).

1.3.4 Summary

CTL immunity is orchestrated by dynamic interactions of antigen-presenting DCs, $CD4^+$ T and $CD8^+$ T cells, leading to the enhanced communications between rare antigen-specific immune precursors within a short window of time and to the efficient delivery of help signals. Although details remain to be explored, this concept may have a great impact for the design of vaccines and immunotherapy strategies against cancer and autoimmune diseases.

1.4 Two-photon microscopy

TPM has been introduced in immunology for almost a decade. The number of studies using this advanced technology has dramatically increased. The TPM allows long-term visualization of immune process hundreds of microns deep in the living tissue with minimal phototoxicity. From

imaging in explanted organs to performing the intravital studies in living animals, this technology reveals an elaborate cellular choreography of immune responses.

1.4.1 Principles of two-photon excitation

In traditional one-photon microscopy, such as confocal and fluorescent microscopy, one fluorochrome is excited by one high-energy photon. While in TPM, two lower-energy photons are absorbed nearly simultaneously by a single fluorochrome. As two photons excite one fluorochrome, each photon used in TPM harbors half of the energy used in one-photon microscopy. Therefore, the wavelength used in TPM is twice as long as in one-photon microscopy. The use of long wavelength excitation is particularly advantageous for imaging deep into highly scattering biological materials because scattering decreases with increasing wavelength (184), thus the infrared wavelengths used for two-photon imaging enable deeper tissue penetration (up to 1000 μm) than does one-photon imaging using visible wavelengths (185, 186). However, as the trade-off, the resolution for two-photon imaging is proportionally worse in comparison to one-photon methods. Since fluorescence excitation is limited only to the region where photon flux is the highest (focus point), photobleaching and damages outside the focus point are minimized, thereby highly benefiting long-term imaging. High power, pulsed laser must be used as the excitation source because fluorochrome is only energized to an excited state when a simultaneously absorption of two photons occurs. Despite the intensity of light, less damage is produced because the light is off most of the time in between laser pulses. Another merit of two-photon excitation is its nonlinear optical effects such as second-harmonic generation (SHG) (187). High-intensity lasers passing through a coordinated material can lead the generation of a second-harmonic emission at precisely half the wavelength of the original light. Many intrinsic biological structures, including collagen fibers, brain, muscle, cornea, and bone, can induce SHG, thus these structures can be visualized without exogenous fluorescent labeling. In brief, TPM is an ideal tool for long-term intravital imaging because of its low phototoxicity and superior penetration depth.

1.4.2 Lymph node cellular dynamics

1.4.2.1 Cellular dynamics within the lymph node

One of the earliest applications of intravital two-photon imaging was performed in an explanted lymph node (186). Membrane-permeable fluorescent dyes labeled lymphocytes such as T and B cells were visualized in lymph nodes, revealing the rapid migration of naive T and B cells under the basal conditions, which challenge the previous belief that T and B cells were immobile in the resting state. T cells are able to crawl more rapidly (10-12 μm/min (188) for 2-D velocities and 15 μm/min (189) for 3-D velocities) than any other cell type such as B cells (186), NK cells (190), neutrophils (191), and monocytes (192). All these cells have similar amoeboid actin-based motility. Therefore, they explore the environment using surface receptors and respond with altered dynamics when signals are transmitted. In contrast, APCs such as DCs (193, 194) and LCs (195) are generally sessile in tissue unless some microbial or inflammatory signals provided (196, 197).

It has been long appreciated that T cell responses require direct cell-cell contact. In order to perform effective molecular communication, random cellular movement must be overcome to prevent partner cells from moving outside the range, leading to the change of cell motility. It becomes clear that naive T cells migrate rapidly along a network of fibroblastic reticular cells (FRCs), making brief and frequent contacts with DCs. The independent migration of T and B cells is overcome when specific antigen shows up. After exposure to antigen, T cells are arrested by DCs, leading to the formation of T cell clusters around individual DC (194, 198). B cells that have acquired antigen become activated APCs. Most of them stop wandering and form stable conjugates with antigen-specific T cells in SLAM-associated protein (SAP)-dependent manner (199). Others do not get strong stop signal and continue to migrate, dragging the T cell behind (200).

1.4.2.2 Lymphocytes trafficking in lymph node

The process of lymphocyte homing and tissue localization have been extensively investigated using TPM, enlarging our current knowledge of how lymphocytes distribute from the blood to peripheral tissues and to lymphoid organs (201, 202). Lymph nodes, which are dispersed in the human body, are major sites for circulating naive lymphocytes to encounter with antigens and APCs. Recirculating of lymphocytes from the blood to lymphoid organs and back to the blood can be finished as quick as half day during homeostasis (203), allowing the extremely rare antigen specific lymphocytes to quickly survey the lymph for the presence of their target antigen. After homing from the blood into lymph nodes, lymphocytes spend several hours (T cells ~8-12 hrs) to a day (B cells ~24 hrs) in a given lymph node (204). During this time, they search around, and most of them leave the lymph node via efferent lymphatic vessels without finding antigens.

1.4.2.2.1 Entry of lymphocytes

High endothelial venules (HEVs) have been considered as the major sites for migration of lymphocytes from the blood into lymph nodes. The entry of naive T and B cells is mainly through rolling along HEV walls, based on the attraction between the expression of CC-chemokine ligand 21 (CCL21) on HEV endothelial cells and CCR7 expressed lymphocytes. Signaling through the CCR7, together with the shear force of blood flow, induce the activation of lymphocyte integrin LFA-1, leading the firm binding to ICAM-1 and ICAM-2 on the endothelium (205). After several minutes' crawling on the HEV surface, T cells enter the abluminal side of HEVs, where a sheath of FRCs are surrounded. Lymphocytes are transiently trapped in this perivascular space, where the accumulation of DCs are also shown, increasing the likelihood of T cell-DC encounters (194). After the transient retention around HEVs, T cells rapidly migrate along the FRCs-the major constituents of the backbone structure of the T cell zone (206). The production of CCL21 and C-X-C chemokine ligand 12 (CXCL12) by T cell zone FRCs thus attract CCR7 and CXCR4 expressed naive T cells entering into T cell zone. On the other hand, rather than rapidly heading to the follicles, B cells remain confined close to HEVs for 3-4 hrs and search for local DCs (207). CCR7 ligands are not involved in retaining B cells since CCR7-deficient B cells show a similar motility pattern around HEVs to that of wild-

type B cells (208). After leaving HEVs, B cells crawl on the FRC network in the T cell areas to reach the B cell follicles (206). The homing of naive B cells to the follicles depends on the expression of CXCR5 by B cells and CXCL13 by follicular dendritic cells (FDCs) (209). Notably, although the main function of HEVs is to recruit large numbers of naive B and T cells (also including central memory T cells and Tregs) into lymph nodes, they also mediate the entry of other important immune cell types during homeostasis such as pDCs (210) and the precursors of conventional DCs (pre-cDCs) (211).

DCs have been shown to enter lymph nodes via afferent lymphatic vessels rather than through HEVs. Under both steady state and inflammatory conditions, CCR7 expressed DCs sense local CCL21 gradients, which are provided by terminal lymphatics, and directionally migrate towards, and eventually into, lymphatic vessels (212). Following lymphatic entry, DCs crawl in the direction of lymph flow and migrate through FRC stromal networks into the lymph node paracortex under the guide of CCR7 and its ligand CCL21. Unlike the entry of lymphocytes through HEVs, this process seems to be independent of integrins (213). Over time, lymph-derived migratory DCs and HEV-derived pre-cDCs join and integrate into the network of resident DCs by internalization and/or desensitization of their CCR7, and start to continuously probe around.

1.4.2.2.2 Egress of lymphocytes

If naive lymphocytes do not encounter their target antigen after several hrs' exploring, they will leave the lymph node through efferent lymphatics. Sphingosine-1-phosphate (S1P) and its receptor S1PR1 have been shown to be required for the egress of both B and T cells (214) based on the fact that a agonist of S1P receptors (FTY720) inhibits the egress of lymphocytes into lymph by down-regulating S1PR1 expression on lymphocytes (215, 216). Recent TPM analyses indicate that the exit of B and T cells from lymph nodes is mainly through cortical sinuses. By overcoming retention signals from CCR7, migrating T cells contact and probe on lymphatic vessel endothelial receptor 1 $(LYVE1)^{+}$ cortical sinuses in the interfollicular areas. About one-third of T cells then cross the lymphatic endothelium and enter the lymph node sinus system in a S1P-dependent manner (217). Similarly, B cells desensitize their chemokine receptors (CXCR5

and CCR7) and sense the S1P-mediated egress signal followed by egression from the B cell follicle into adjacent cortical sinuses (208, 218).

1.4.3 Dynamics of DC-T cell interaction

1.4.3.1 Contacts in the absence of antigen

Because of the vigorous intranodal motility of naive T cells along stromal networks in lymph node T cell zone (206), roughly 500-5000 distinct T cells have been found to contact one DC per hour in the absence of antigen (193, 219). This process highly increases the change of initiating an immune response that rare antigen-presenting DCs encounter a low frequency of antigen-specific T cells. Without presenting cognate antigen, only a few-minute contact is established between DCs and T cells. Although those contacts fail to induce calcium signaling in T cells (220), they are likely to be functionally important. There are also some non-random chemokine-driven DC-T cell interactions in the absence of cognate antigen presentation. For example, CCL21 has been suggested to optimize the migration of CCR7-expressing T cells since this chemokine is bound to the surface of LN-resident DCs (221). CCL3 and CCL4 are produced at the site of DC-T conjugates, increasing the chance for CCR5-expressing $CD8^+$ T cells migrating to contact DCs (222, 223), thereby favoring the formation of three-cell clusters and promoting collaboration between DCs and T cells.

1.4.3.2 Contacts in the presence of antigen

DC-T cell interactions in LNs during the priming of both naive $CD8^+$ and $CD4^+$ T cells have been widely studied (186, 193, 194, 224-226). Few models have been proposed to explain how DC-T contacts shift from transient to stable over time. One model suggests the maturation state of the DCs determines the timing of T cell arrest (227). Another model believes that there is a threshold of signal receiving by T cells. Once reaching this threshold, T cells gain the "memory" to establish long-lasting interaction with DCs (228). Several studies agree on a three-phase model of DC-T cell interactions based on the order of occurrence during an immune response. Within the first few hrs following naive T cells' entry (phase 1), only brief contacts (< 10 min)

are established, which is hardly distinguishable from the situation that in the absence of antigen (194, 198). The second phase is characterized by a dramatic change in T cell behavior, including the decreased velocities and confined movements, resulting in stable DC-T cell interactions lasting 2-24 hrs depending on the different experiment settings. During this period, an increased in cytosolic calcium concentration has been found to associate with this stable DC-T cell interaction (220, 229). Finally, most clusters dissociate their stable interactions after 30 hrs (phase 3). T cells regain their velocities as well as their random movement pattern.

The molecular mechanisms that lead to variations in contact duration in the three-phase model have been described. The amount and the quality of peptide-MHC complexes largely contribute to determine the nature of these contacts (193, 229). During the first phase of transient interactions, T cells are likely to up-regulate the early activation marker CD69 after receiving an activation signal (194, 226, 229). Accumulated brief contacts may collect additional signals to sufficiently activate DCs, leading to stabilize the interactions between DCs and T cells. ICAM-1 is crucial for T-cell arrest on DCs following antigen recognition since ICAM-1 deficient DCs have been shown to establish only brief interactions with T cells (225). The expression of cytotoxic T lymphocyte antigen (CTLA)-4 on T cells, a receptor that normally down-regulates T-cell activation, can also override T-cell arrest following antigen recognition (230). However, in a pancreatic islet self-antigen tolerance model, the blockade of CTLA-4 neither altered T cell mobility nor favored the establishment of a stable contact with antigen presenting DCs (231). In fact, the blockade of programmed death ligand 1 (PD-L1) in the same study showed the impaired T cell motility and enhanced cell-cell interactions. T cells detach from DCs and become more dynamic after the phase of stable DC-T cell contacts. Signals that involve in the termination of long-lasting contacts are less clear. One possibility is the down-regulation of pMHC complexes on DCs (232). The injection of anti-MHC-II Abs has been reported to promote the dissociation of established DC-T cell conjugates (233), indicating that low amount of pMHC complexes may lead to the detaching of T cells. By contrast, reinjection of the antigen couldn't be able to prolong the phase of T cell arrests (226), suggesting that decreased antigen presentation by DC might not account for the phase three. The activation state of DCs might control the contact duration since encounter of DCs from phase three with T cells from phase two fails to restore stable DC-T cell interaction (226). The down-regulation of ICAM-1 has also been reported

during this late phase (225), suggesting that the variation in the expression of adhesion molecules by DCs could participate in the abrogation of long-lasting contacts.

1.4.3.3 Contacts in the presence of Tregs

Tregs modulate immune responses through mechanisms that may require direct contact between Tregs and DCs, T cells and/or bystander effects mediated by cytokines (234). Only few papers have applied imaging techniques to investigate these processes to date. Two *in vivo* imaging studies have provided direct evidence that Tregs interfere with the DC-T cell interaction. The reconstruction of naturally occurring antigen-specific Tregs has been shown to inhibit stable contacts between autoreactive myelin basic protein (MBP)-specific T cells and autoantigen loaded DCs in Treg-deficient mice (235). Similar suppressive effect of Tregs on the formation of stable clusters of diabetogenic T cells with DCs in isolated pancreatic LNs has also been reported (236). This paper has further demonstrated that Tregs are only detected to engage in long-lasting interactions with DCs rather than $CD4^+$ T cells. A somehow different report of Tregs' action has been obtained when imaging the interactions between $CD8^+$ CTLs and antigen-presenting target B cells (237). The presence of Tregs can't alter the recognition and stable interaction between CTL and target B cell, but profoundly inhibit the ability of $CD8^+$ CTLs in releasing cytolytic granules and lysing the targets. Notably, no direct interaction has been found between Tregs and $CD8^+$ CTLs in this study. All together, these results show that both initiation and effector phases of immune responses in lymph node may potentially be affected by Tregs. However, all the imaging experiments above performed with adoptive transferred, TCR-transgenic, high-affinity Tregs. In fact, more studies are focus on the endogenous polyclonal Tregs recently. One experiment has shown that the endogenous polyclonal Tregs could directly interact with DCs, and induce the death of DCs in tumor-draining lymph node through an antigen- and perforin-dependent mechanism (238). In another experiment setting, the depletion of endogenous polyclonal Tregs has been shown to stabilize the interactions between antigen-presenting DCs and low-avidity T cells (239). The presence of endogenous Tregs has actually been suggested to increase the avidity of primary $CD8^+$ T cell responses, thereby promoting effective memory.

1.4.4 Summary

Since 2002, the *in vivo* two-photon imaging has been applied to visualize of immune cell dynamics in real-time within various intact tissues, including lymph node, thymus, spleen, lung, gastrointestinal tract, pancreas, skin, bone marrow, blood vessels, spinal cord, brain and tumors (240-246). It provides a unique perspective to our current knowledge of the immune system in health and disease conditions. Although current imaging techniques have several limitations, the progress in the development of laser technologies and the improvement in equipment sensitivity would benefit the immunoimaging. A closer interplay with computational modeling should also profit further imaging analysis. Even though current studies have only scratched the surface, there is no doubt that immunoimaging has a bright future ahead in unveiling the choreography of immune responses.

1.5 The HER2 positive breast cancer

HER2, also known as c-ErbB-2/neu, is a transmembrane receptor with tyrosine kinase activity. Unlike other ErbB family members that require ligand binding for activation, HER2 can adopt a fixed conformation resembling a ligand-activated state, permitting it to dimerize in the absence of a ligand (247), which results in activation of a potent cell signaling cascade predominately though the phosphatidylinositide 3-kinase (PI3K) and mitogen-activated protein kinase (MAPK) pathway, leading to cell proliferation and survival. HER2 overexpression has been described in various human cancers, including ovary, prostate, gastric, lung, bladder, and kidney carcinomas (248, 249). Each year, breast cancer accounts for more than 400,000 new cancer cases and more than 130,000 cancer deaths in Europe. Approximately 20-30% of invasive breast carcinomas are HER2 positive and associated with increased metastatic potential and poor prognosis (250, 251). In the USA, approximately 5,000 patients with HER2-positive breast cancer die each year. In the last decades, several attempts have been made to develop strategies that could effectively recognize and eradicate cancer cells in HER2-positive breast cancer patients.

1.5.1 Passive immunotherapy

Different approaches fall into this catalog, including (i) the infusion of monoclonal antibodies (mAbs) specific for a given tumor antigen or inhibitors; (ii) adoptive transfer of antigen-specific T lymphocytes expanded *ex vivo*; (iii) the functional inhibition or depletion of Tregs-elements that are able to down-modulate antitumor T-cell responses.

1.5.1.1 mAbs specific for HER2 antigen or HER2 receptor inhibitors

Trastuzumab (Herceptin, Roche, Switzerland) is a humanized mAb directed against the extracellular domain (ECD) of HER2. It was approved by food and drug administration (FDA) in 1998 for metastatic HER2 over-expressing breast cancer combined with chemotherapy (252). The potential mechanisms for its antitumor action include antibody-dependent cell-mediated cytotoxicity (ADCC), blockade of HER2 ECD cleavage (253), inhibition of ligand-independent HER2 receptor dimerization, inhibition of downstream signal transduction pathways, induction of cell-cycle arrest, inhibition of angiogenesis, induction of apoptosis, and interference with DNA repair (254, 255). In early-stage disease, the addition of trastuzumab to adjuvant chemotherapy results in remarkably early and sustained improvement in disease-free survival and overall survival. However, drug resistance usually develops within one year from the beginning of the treatment in the metastatic setting (256, 257). Several mechanisms for inherent or acquired resistance have been proposed, including the loss of or increased HER2 expression; compensatory cross-talk with other ErbB receptors (eg. HER1 or HER3); increased TGF‑α expression (a ligand for EGFR/HER1); steric hindrance of HER2 Abs interaction by membrane-associated glycoproteins; inefficient trastuzumab binding by shedding of the HER2 ECD (258); and altered expression of downstream mediators of signaling pathways or constitutive activation of the PI3K/Akt signal pathway (259, 260). A better understanding of these mechanisms may help to design next-generation trastuzumab that can ameliorate or bypass tumor resistance.

Lapatinib is a reversible tyrosine kinase inhibitor that targets the intracellular domains (ICD) of both HER1 and HER2. FDA approved the use of Lapatinib in 2007 for use in combination with capecitabine to treat patients with advanced breast cancer or HER2 overexpressing metastatic

breast cancer. Lapatinib has been shown to retain activity in tumor that overexpresses the truncated form of HER2 (p95HER2), which has been associated with resistance to trastuzumab (258). Dual anti-HER2 regimen combined lapatinib and trastuzumab has been shown superior to the use of lapatinib alone on trastuzumab-based therapy in HER2-positive metastatic breast cancer patients (261).

Pertuzumab is a monoclonal Ab that blockades HER2:HER3 heterodimer formation and consequent downstream activation signals by binding to a distinct site on the HER2 ECD. It received FDA approval for the treatment of HER2-positive metastatic breast cancer in 2012. Similar to other HER2-targeted agents, pertuzumab demonstrates only modest activity as a single agent, while when administered with trastuzumab and chemotherapy, it is considered as the new standard of care for the first-line treatment of patients with HER2-positive metastatic breast cancer (262).

Trastuzumab DM-1 (T-DM1) or trastuzumab emtansine, is an antibody-drug conjugate (ADC) consisting of trastuzumab linked to the microtubule cytotoxic maytansine, which enters cells and destroys them by binding to tubulin (263). It received FDA approval for marketing on February 22, 2013. T-DM1 is often given as a single agent since this drug is more similar to combination treatment. It demonstrates the high efficacy against trastuzumab-sensitive and -resistant HER2-positive cell lines (264). The real benefit of T-DM1 lies in the potential to eliminate chemotherapy from therapeutic regimens. Therefore, it is becoming the new standard of care for refractory metastatic HER2-positive breast cancer after disease progression on trastuzumab.

Many other novel anti-HER2 agents also show promise in treating HER2-positive breast cancer, inculding Tanespimycin (265) (an intravenously administered inhibitor of HSP90), Ertumaxomab (266) (a trifunctional Ab that targets HER2, CD3 and activating FCγ receptors, leading to phagocytosis of tumor cells), Neratinib (267) (an irreversible tyrosine kinase inhibitor), XL147 (268) (pan-PI3K inhibitor), etc. They can either be directed at HER2 receptor itself or can target downstream effectors and interact with compensatory signaling pathways. Therefore, these new treatments are likely to enter the adjuvant setting in the near future.

1.5.1.2 HER2-specific CTLs

Increasing evidence shows that the presence of tumor-infiltrating T lymphocytes (TILs) is associated with a favorable prognosis of primary tumors. Non-responsive T cells may also be expanded due to the prevalence of antigen presentation and tolerance induction mediated by both the growing tumor and its surrounding stromal cells during tumor progression (269). Tumor-reactive T cells can be increased in the blood and within the tumor site by taking out potential tumor-reactive T cells from the tumor-bearing host and stimulating them *ex vivo* (270). A study adoptively transferred *ex vivo* expanded HER2-specific CTLs in HER2-overexpressing breast cancer patients revealed that the transferred T cells accumulated in the patient's bone marrow and migrated to the liver, but were unable to penetrate into the solid metastases (271).

1.5.1.3 Inhibition or depletion of Tregs

Another strategy in the context of passive immunotherapy is the functional inhibition or depletion of Tregs, leading to the up-regulation of T-cell responses. This can be achieved directly by using recombinant IL-2-DT fusion protein (also called ONTAK) to specifically target $CD25^+$ Tregs (272, 273). It also can be achieved indirectly by negative regulation of T-cell activation and function. CTLA-4 is physiologically expressed on both activated $CD8^+$ T cell and Tregs, the blockade of CTLA-4 may enhance the activity of the former and down-regulate the inhibitory function of the latter, suggesting a particularly promising approach in this context. Clinical trials using anti-CTLA4 Abs (Tremelimumab) have shown promising results in cancer patients previously vaccinated with GM-CSF-expressing tumor vaccines (274, 275). Notably, since Tregs depletion could exacerbate autoimmunity, close monitoring is needed during immunotherapy trials.

1.5.2 Active immunotherapy

Active immunotherapy aims at activating patients' own immune system through the administration of a therapeutic vaccine. Vaccine can elicit immune responses directed against antigens selectively expressed by tumor cells, sparing normal tissues with consequent low toxic

effect. HER2 over-expression has been linked to aggressive disease and poorer prognosis in node-positive breast cancer. Several investigations show that some patients develop spontaneous anti-HER2-specific immunity with high levels of both cellular and humoral responses (276, 277), suggesting that HER2 is a suitable target for active immunization. On the other hand, most patients only develop low or even a lack of immune response, strongly suggesting that immune tolerance to HER2 has been developed probably related to the oncofetal origin of HER2. Thus, the effective vaccine design should be able to circumvent tolerance and induce an integrated immune responses composed of CTLs, Abs and $CD4^+$ T cells to overcome HER2-induced tumor resistance.

1.5.2.1 Peptide-based vaccines

Peptide-based vaccines are designed to induce immune responses using antigenic epitopes derived from tumor-associated antigens. Computer modeling programs are effective in predicting potential immunogenic epitopes of self-protein HER2. MHC class I-binding epitopes can be identified, and corresponding synthetic peptides have been tested for their capacity to induce tumor-specific CTLs (278). E75 (HER2 amino acid (aa) 369-377) derived from the ECD of HER2 and characterized by HLA-A2 restriction (279), is HLA class-I peptide that stimulates CTLs. Clinical studies using E75 as an anti-HER2 vaccine in combination with GM-CSF have shown that vaccination can induce a specific anti-peptide immune response with no associated toxicity (280). Patients expressing low levels of HER2 have more robust immunologic responses (281), and the disease free survival (DFS) rate is improved at 24-month follow-up (282). GP2 is HLA-A2-restricted peptide derived from the transmembrane domain of HER2 (aa 654-662). Preclinical evaluation of GP2 has confirmed its immunogenicity despite it is a subdominant HER2 epitope with lower affinity than E75 (283). A phase I clinical study using GP2 in combination with GM-CSF have shown that the vaccine is tolerable and able to effectively induce immunological responses in high-risk, lymph node-negative breast cancer patients (284).

The design of multiple or long multivalent peptides is aiming at eliciting stronger and more complete responses, including HLA class-II restricted T-helper cells (285). AE37, constructed by fusing MHC-II peptide of HER2 (aa 776-779) (AE36) with a LRMK (li-Key) sequence to make

easier antigenic epitope presentation of the peptide with HLA class II molecules, has been found to augment the $CD4^+$ T-cell response (286). Vaccination with AE37, with or without GM-CSF, has been shown to induce a dose-dependent cellular immune response specific to AE37. This is also the first study demonstrating the effectiveness of a peptide vaccine in the absence of an adjuvant according to the authors (287).

Their easy manufacturing and capability of eliciting evaluable antigen-specific immune response entitle peptide-based vaccines a promising future. However, peptide vaccinations also present some potential limitations. For example, although epitope spreading has been found in some clinical settings (288), which could be correlated with clinical benefit, immune response is still mostly restricted to one or few epitopes, limiting the magnitude of response and effectiveness in fighting tumor cells. Besides, in order to generate a strong and sustained immunological memory, continued antigen exposure and stimulation by APCs are needed, whereas most peptide vaccines only stimulate a single $CD8^+$ T-cell response.

1.5.2.2 Protein-based vaccines

In order to stimulate more complete immunological responses, including extending responses to different epitopes of HER2, protein-based vaccines has been developed consisting of the entire or truncated forms of HER2. A phase I clinical trial has been conducted in patients with HER2 over-expressing breast or ovarian cancer using HER2 ICD (aa 676-1255) in combination with GM-CSF (289). HER2 ICD specific T-cell response, anti-HER2 IgG and maintained cellular immunity have been observed. Another clinical study using HER2 ECD and a portion of ICD fused protein vaccine has shown the development of HER2 ECD and ICD specific Abs after multiple immunizations (290). A protein-based vaccine by inserting a truncated HER2 protein (aa 1-146) into a delivery system consisting of cholesteryl pullulan nanogels (CHP) has also been designed. Induced $CD4^+$ and/or $CD8^+$ T-cell responses have been observed (291), as well as the production of truncated HER2-specific IgG (292). Protein-based vaccine has the theoretical advantage in including both HLA class I and II epitopes, however, exogenous soluble protein antigens stimulated APCs are in general efficient in sensitizing $CD4^+$ T cells than in sensitizing

$CD8^+$ T cells. Moreover, with this type of vaccines, it is more difficult to monitor the responses of patients.

1.5.2.3 DNA-bases vaccines

DNA vaccines have the advantage of being simple to construct, produce and administer. Besides, co-delivery of cytokine genes can increase their efficacy (293, 294). The goal of DNA vaccine is target gene being transferred into target cells, translated into protein and processed for presentation. As a result, antigen-specific T-cell response and Ab production will be generated. DNA is usually delivered in the form of expression plasmid, such as DNA coding for HER2 ICD cloned into pNGVL3 plasmid (NCT00363012, NCT00436254). Viral adenovirus vector (NCT00307229) has also been used in clinical trials. A modified vaccinia Ankara-based recombinant vaccine vector MVA-BN®-HER2, which encodes HER2 ECD and two promiscuous T helper cell epitopes from tetanus toxin, has shown improved immunogenicity in a tolerant environment (295). The administration of this modified vaccine has also been associated with HER2-specific Abs and T-cell responses in clinical trial (296).

1.5.2.4 Tumor cell vaccines

Tumor cell vaccine has the theoretical advantage of providing a pool of tumor antigens to develop effective and complete $CD4^+$ and $CD8^+$ T-cell responses. Non-specific co-stimulatory signals are needed to induce an antigen-specific immune response, however, most solid tumors do not express these co-stimulatory molecules. Therefore, they are unable to provide all the signals necessary for T-cell activation. Genetically modified tumor cells, which express co-stimulatory molecules or immune-activating cytokines, may help to amplify immunological stimulation. Patients can be immunized with their own PBMCs (autologous) (297), which are activated *in vitro* by recombinant fusion protein (composed of HER2 ICD and ECD, as well as GM-CSF). They also can be immunized with HER2 overexpressing SKBR1 or SKBR3 cell-line (allogeneic) (298), which is genetically modified to secrete GM-CSF. Efficient immune response has been induced, and the results can be enhanced with Tregs depletion.

1.5.2.5 DC vaccines

DC vaccine strategy has the theoretical advantage of promoting the presentation of the vaccine antigens to other cell types since DCs express high levels of both class I/II and co-stimulatory molecules, and produce cytokines that are necessary for T-cell activation. A preclinical study using HER2/neu modified DCs has shown the prevented or delayed onset of mammary carcinomas in a transgenic mouse model of breast cancer (299). Administration of DCs transfected with an adenovirus encoding both HER2/neu and IL-12 (300) or TNF-α (301) has been shown to induce tumor protection in FVB mice challenged with syngeneic HER2/neu over-expressing tumor cells in other preclinical studies. DCs transfected with an adenovirus encoding HER2/neu has been found more efficient than the plasmid DNA vaccine (302). Later, a recombinant adenovirus was constructed, which encoded the HER2/neu protein and RGD motif. The addition of the RGD motif in the construct has been observed with increased expression of HER2/neu. DCs transfected with RGD motif modified HER2/neu adenovirus showed higher CTL and humoral responses and better anti-tumor protection than the ones only transfected with regular HER2/neu adenovirus (303).

Mature DCs pulsed with HLA-A2-restricted HER2 peptide have been applied to patients with advanced ovarian and breast carcinoma in a clinical trial. Tumor-specific CTLs has been found in some patients with the ability to efficiently inhibit HER2 overexpressing cancer cell lines *in vitro* (304). More recently, patients with HER2 over-expressing ductal carcinoma *in situ* have been found to develop peptide specific immune responses and present high levels of $CD4^+$ and $CD8^+$ T cells after the injection of DCs, which are loaded with a mixture of HLA class I- and II-restricted HER2 peptides (305). Another clinical trial used vaccine that consisted of both mature and immature autologous DCs loaded with HER2 ICD peptide in HER2-positive breast cancer patients who were disease free after surgery or adjuvant therapy. Most of the patients have been reported to develop immunological T-cell response against HER2 ICD and secret specific Abs (306). In addition, patients treated with Lapuleucel-T, a vaccine that used autologous PBMCs loaded *ex vivo* with a recombinant fusion antigen consisting of extensive HER2 sequence linked to GM-CSF domain, have also shown antigen-specific immune responses (307).

Although the use of DC vaccines seems promising, several things are still need to be further studied. *Ex vivo* expansion and activation of DCs are still technically challenging, which is crucial for optimal antigen presentation and T cell stimulation. The route of administration is also something that needs to be optimized in the future.

1.5.3 Passive and active immunotherapy

Although vaccines in HER2-positive breast cancer show an excellent safety profile and result in significant effectiveness, antigen variability and mechanisms of tumor cell immune escaping can impair effectiveness of active immunization. Combining tumor vaccines with passive immunotherapy is likely to increase the effectiveness of each approach. Different combination strategies have been used in clinical trials such as trastuzumab combined with HER2 peptide (308, 309), DNA (310) or allogeneic tumor cell vaccine (311), lapatinib concomitant with recombinant protein vaccine (312).

1.5.4 Summary

The survival benefit of anti-HER2 driven therapies demonstrated in clinical trials indicates that HER2 is one of the most promising molecules for targeted therapy to date. The recombinant humanized monoclonal Ab trastuzumab represents one of the most successful adjuvant treatments for patients with HER2-positive early stage breast cancer. Many new agents are in clinical development, including those directing at the HER2 receptor itself, and those targeting downstream effectors and interacting compensatory signaling pathways. Since the HER2 blockade of tumor cell growth by trastuzumab can be circumvented through alternative growth signaling pathways, the antibody-drug conjugate (T-DM1) starts to represent a promising tool in the treatment of HER2-positive breast carcinoma. Although combining various chemotherapeutic drugs with anti-HER2 Ab is more efficient in clinical trials, it has limited efficacy over time and leads to significant increase in toxic effects.

Several mechanisms have been proposed to explain the low clinical effectiveness. The main barrier is probably due to immune escaping mechanisms developed by cancer cells. The

depletion of Tregs or blockage of immune-checkpoints (e.g. CTLA-4, PD-1/PD-L1) may unleash the immune response. On the other hand, the paucity of specific T-cell precursors makes it difficult to efficiently elicit both humoral and cellular responses against tumor antigens. An increased presentation of HER2 peptides exceeding a critical threshold may break tolerance by efficiently stimulating low-avidity T-cell clones, which have escaped negative selection in the thymus. Moreover, deleterious impact of chemotherapy and radiotherapy might be another obstacle to translate the immunological responses into satisfactory clinical responses. Efforts should be made to conduct clinical trials in patients with low tumor burden, not heavily pretreated, and most likely to benefit from the vaccines. In conclusion, with the better understanding of the complexity of tumor progression, the improvement in technology and identification of the optimal clinical setting, defeating HER2-positive breast cancer would be challenging yet still plausible in the near future.

1.6 $CD8^+$ regulatory T cells

The existence of T cells being capable of suppressing immune responses was first proposed in the 1970s (313), when Gershon et al. observed thymic lymphocytes mediating the adoptive transfer of tolerance in mice. Most of these cells with suppressive activities resided in $CD8^+$ compartment (314-316), but subsequent studies failed to identify the molecular basis of suppression due to technical limitations. Then it was neglected for many years and finally revived by the identification of natural $CD4^+CD25^+$ T cells as potent suppressors of autoimmunity (317). In the past decade, $CD4^+$ Tregs have been extensively studied in various disease models. The key issue is finding specific marker to identify Tregs. Although many markers associated with Tregs have been reported, some of them are also activation markers and are not specific for Tregs. For example, CD25 has been widely used as a marker of Tregs, but its expression is not necessarily associated with Treg function. Similarly, the tumor necrosis factor family molecule glucocorticoid-induced tumor necrosis factor receptor (GITR) and CTLA-4 have been reported as makers for Tregs (157), but they are also expressed on activated effector T cells. Foxp3 is the best marker identified to date for $CD4^+$ Tregs (318). The elimination of $Foxp3^+$ Tregs in healthy mice can lead to death resulting from multi-organ autoimmunity within 10 days (319), and the mutation of Foxp3 gene can cause fatal autoimmune disease

immunodysregulation polyendocrinopathy enteropathy X-linked syndrome (IPEX) in human (320, 321). In addition, the reduction of Foxp3 amount can impair their suppressive function (322). A growing list of mechanisms is attributed to the suppressive action of $CD4^+Foxp3^+$ Tregs (318), but the mechanisms of immune regulation elaborated by regulatory $CD8^+$ subsets remain less clear despite the fact that $CD8^+$ T cells are the initial targets of work in this area. It is now widely accepted Tregs exist within both $CD4^+$ and $CD8^+$ compartments and constitute a heterogeneous class of cells with diverse mechanisms of action. Tregs that originate in the thymus through interactions between classical MHC molecules and the TCR (323-325) are often referred to as natural Tregs (nTregs), while those that arise in the periphery in response to antigenic stimulation (326-330) are termed adaptive/induced Tregs (iTregs). Although, in principle, functional and phenotypic similarities could be drawn from subsets of $CD4^+$ and $CD8^+$ Tregs, no clear definition of mechanisms of action or phenotypes of $CD8^+$ Tregs can be easily fitting into such categorization without potentially over-simplifying.

1.6.1 Subsets of $CD8^+$ Tregs and related autoimmune diseases

Multiple subsets of thymus derived or peripherally induced $CD8^+$ Tregs have been described in both humans and mice autoimmune diseases. No universal phenotypic marker has been defined based on the diverse origins from which they may have arisen *in vivo* or different experimental conditions to which they have been subjected prior to characterization. Each of these regulatory cells is known to possess distinct but sometimes overlapping phenotypes.

1.6.1.1 Qa-1/HLA-E restricted $CD8^+$ Tregs

Mouse Qa-1 and its human homolog HLA-E belong to nonclassical MHC class I molecules (331). Qa-1 is preferentially expressed on activated but not resting T cells and thymocytes, thereby protecting unstimulated T cells from the effects of Qa-1-restricted $CD8^+$-dependent suppression. Studies with Qa-1-restricted $CD8^+$ Tregs showed that these cells suppress intermediate-avidity $CD4^+$ T cell responses by sensing their self-peptides that are displayed by Qa-1, but enrich high or low avidity $CD4^+$ T cell responses against foreign antigens (332). It has been shown that the protective effects of Qa-1-restricted $CD8^+$ Tregs require perforin and the

presence of IFN-γ (333). Qa-1-restricted Tregs cloned from TCR peptide-vaccinated mice have also been characterized, revealing the expression of IL-7R, CD25, CD122, CD28, and NKG2/CD94 (334).

Using the murine EAE model, several groups reported the involvement of Qa-1-restricted $CD8^+$ Tregs in the regulation of pathogenic self-reactive $CD4^+$ T cells (335, 336). Vaccination of mice with activated MBP-specific $CD4^+$ T cells (337) or anti-TCR mAbs (338) resulted in protection from the subsequent induction of EAE and the induction of Qa-1-restricted $CD8^+$ Tregs. HLA-E-restricted $CD8^+$ Tregs have also been found in patients with multiple sclerosis (MS) treated with glatiramer acetate (GA), suggesting that treatment with GA might induce upregulation of HLA-E-restricted $CD8^+$ T cells, which in turn exert a regulatory/suppressor function and are capable of modulating *in vivo* immune responses by directly killing pathogenic $CD4^+$ T cells (339-341). Therapeutic effect of GA-induced $CD8^+$ Tregs has also been found in experimental inflammatory bowel diseases (IBDs) in mice (342). In addition to EAE/MS, beneficial effects of autoreactive T-cell induced Qa-1-restricted $CD8^+$ Tregs have been observed in non-obese diabetic (NOD) mice (343) and collagen-induced arthritis (CIA) mice (344). Qa-1-restricted $CD8^+$ T cells have also been shown to specifically suppress Qa-1 expressing follicular T-helper cells based on the fact that the genetic disruption of this inhibitory interaction promotes systemic lupus erythematosus (SLE)-like autoimmune disease in mice (345).

1.6.1.2 $CD8^+CD25^+$ Tregs

Human $CD8^+CD25^+$ (CD25: IL-2 receptor α chain) thymocytes sharing phenotype, functional features and mechanism of action with $CD4^+CD25^+$ Tregs have been shown to suppress autologous T cell responses in a cell contact-dependent manner (346). These cells constitutively express cytoplasmic CTLA-4, surface tumor necrosis factor receptor 2 (TNFR2), CCR8 as well as high levels of Foxp3 mRNA. When activated with long-term anti-CD3/CD28 treatment *in vitro*, they up-regulate surface expression of CTLA-4 and TGF-β1. Several reports documented the generation of $CD8^+CD25^+$ Tregs by culturing human peripheral blood *in vitro* (347-350). The $CD25^-$ precursor cells up-regulated the expression of CD25, Foxp3, GITR, CD28 and CTLA-4 after continuous antigen stimulation, thereby possessing the ability to inhibit $CD4^+$ and $CD8^+$ T-

cell proliferation and cytokine production (349). A similar experiment further showed that continuous *in vitro* antigenic stimulated $CD8^+CD25^+Foxp3^+LAG\text{-}3^+$ Tregs suppress T cell responses via a CCL4 partially dependent mechanism (348). Co-culturing human PBMCs with autologous LPS-activated DCs can also generate $CD8^+CD25^+Foxp3^+$ T cells with regulatory activity in a cell-cell contact and CTLA-4 dependent manner (350). In mice, a similar subset has been found in the thymus and periphery of MHC class II-deficient animals (351). CD44, GITR, LFA-1 and intracellular CTLA-4 expressing $CD8^+CD25^+$ T cells have been shown to suppress anti-CD3-stimulated $CD25^-$ T cell responses *in vitro* in a contact-dependent, IL-10-independent manner. Notably, although both naturally occurring and induced $CD8^+Foxp3^+$ T cells have been demonstrated to express *bona fide* Treg markers including CD25, GITR, CTLA4 and CD103, induced $CD8^+Foxp3^+$ T cells have been shown to mildly suppress T-cell proliferation and IFN-γ production in mice (352).

Treatment of diabetes mellitus (DM) patients with a modified anti-CD3 mAbs have been shown improved insulin secretion, an effect associated with an increase of $CD8^+CD25^+Foxp3^+CTLA\text{-}4^+$ Tregs (353). Similarly, in NOD mice, glutamate decarboxylate 65 (GAD)-IgG-transduced splenocytes have been found to induce an antigen-specific $CD8^+CD25^+Foxp3^+$ T cells with suppressive activity (354).

1.6.1.3 $CD8^+CD122^+$ Tregs

$CD8^+CD122^+$ (CD122: IL-2 receptor β chain) T cells are another type of naturally occurring Tregs found in the periphery of naive, unmanipulated mice. Mice genetically deficient for CD122 gene spontaneously develop severe hyperimmunity by abnormal expansion of activated T cells and differentiation of B cells into antibody-secreting plasma cells (355). This abnormal phenotype can be reversed by transfer of purified $CD8^+CD122^+$ T cells into CD122-deficient neonates, indicating that the $CD8^+CD122^+$ population includes naturally occurring $CD8^+$ Tregs that control potentially dangerous T cells (356). Interestingly, the mechanism of suppressive function of $CD8^+CD122^+$ Tregs has been shown independent of APC or cell-cell contact, but at least in part dependent on the secreting of regulatory cytokine IL-10 (357). A later study confirmed the important role of IL-10 in this suppression (358). Moreover, it has also been

shown that the costimulatory signals of both CD28 and PD-1 are required for their optimal IL-10 production. The blockage of PD-1 inhibited the suppressive function of $CD8^+CD122^+PD\text{-}1^+$ T cells, suggesting that the suppressive activity of this Treg subset resides within its PD-1 fraction. Like CD25 (which is also expressed in activated T cells) is not an exclusive marker for $CD4^+$ Tregs, CD122 cannot be an ideal marker for $CD8^+$ Tregs either since it is also a marker of $CD8^+$ T memory cells.

$CD8^+CD122^+$ Tregs have been identified in multiple autoimmune scenarios in murine models, including Graves' disease (359), EAE (360) and $CD4^+$ T cell-induced colitis (361). In the absence of $CD8^+CD122^+$ Tregs, the activation of autoreactive T cells in these models becomes aggressive, suggesting their importance in maintaining immune homeostasis. In addition, IL-10 neutralization can largely reverse disease protection in all of these cases. Human $CD8^+CXCR3^+$ T cells have been considered as the functional counterpart of the murine $CD8^+CD122^+$ T cells (362) as they demonstrate their regulatory activities of producing IL-10 and suppressing IFN-γ *in vitro* in a similar way. Moreover, treatment of NOD mice with disease-relevant peptide MHC nanoparticle complexes has been shown to mediate effective expansion of cognate low-avidity, memory-like $CD8^+CD122^+CXCR3^+$ T cells *in vivo*, which abrogate disease by suppressing local presentation of autoantigens via IFN-γ, indoleamine 2,3-dioxygenase (IDO) and perforin-dependent mechanisms (363).

1.6.1.4 $CD8^+CD28^-$ Tregs

A series of studies on $CD8^+CD28^-$ T cells showed that they are able to suppress antigen specific $CD4^+$ T cell responses *in vitro* (364-367). In the literature, this $CD8^+CD28^-$ T cell subset is commonly referred to as T suppressor (Ts). Some reports indicated that Foxp3 is a reliable marker for identification of $CD8^+CD28^-$ Ts (368), which express similar markers as $CD4^+CD25^+$ Tregs, including Foxp3, GITR, CTLA-4, CD25, CD103, CD62L and 4-1BB (369), while others failed to identify the expression of Foxp3. Mechanistically, $CD8^+CD28^-$ Ts target DCs and other nonprofessional APCs either by down-regulating co-stimulatory molecules on APCs (364) or by up-regulating expression of the inhibitory receptors immunoglobulin-like transcript 3 (ILT3) and

ILT4 on APCs (370) or endothelial cells (371), thereby rendering these APCs tolerogenic, which in turn, conferring regulatory activity upon $CD4^+$ T cells.

The deficit of $CD8^+CD28^-$ T-cell population has been observed in numerous animal and human autoimmune diseases. $CD8^{-/-}CD28^{-/-}$ double knockout (KO) mice has been found susceptible to EAE, and adoptive transfer of *in vitro*-activated $CD8^+CD28^-$ T cells into MOG peptide-immunized $CD8^{-/-}$ mice can significant decrease the severity of EAE (372). The suppressive mechanism of $CD8^+CD28^-$ T cells is MHC class I-restricted and cell-cell contact dependent. A recent study using CD28 conditional KO mice, in which CD28 is deleted under the control of Foxp3 promoter, has shown that these animals accumulate large numbers of activated T cells, develop severe autoimmunity and fail to appropriately resolve induced EAE by dampening the expression of CTLA-4, PD-1 and CCR6 (373). In an experimental model of myasthenia gravis (MG), treatment with a dual-altered peptide ligand has been suggested to prevent disease through the expansion of $CD8^+CD28^-Foxp3^+$ Tregs, which produce immunosuppressive cytokines such as IL-10 and TGF-β, thereby transferring the protection into MG-prone animals (374, 375). *In vitro* expanded $CD8^+CD28^-CD56^+$ T cells have been shown to blunt synovitis in NOD-SCID (severe combined immunodeficiency) mice engrafted with synovial tissues from patients with rheumatoid arthritis (RA) (376). The suppressive activity of $CD8^+CD28^-$ T cells has also been demonstrated in patients with Hashimoto thyroiditis, Grave's disease (377) and systemic sclerosis (378), but not in healthy individuals. Notably, the frequency and function of $CD8^+CD28^-$ Tregs has been shown to correlate with diseased states in type 1 DM (379), MS (379-381) and SLE patients (382).

1.6.1.5 $CD8^+CD11c^+$ Tregs

$CD8^+$ T cells co-expressing CD11c are a new addition to the growing list of Tregs. $CD8^+CD11c^+$ T cells exist in naive mice less than 3%, but they neither present appreciable suppressive activity *in vitro* nor substantially develop into mature $CD8^+CD11c^+$ T cells (383). Instead, $CD11c^-CD8^+$ T cells when stimulate with antigen and anti-4-1BB Ab can develop into $CD11c^+CD8^+$ T cells in an antigen-specific manner. 4-1BB signaling other than CD3, CD28 or cytokines has been shown to effective support $CD8^+CD11c^+$ T cells expansion. The anti-4-1BB-expanded $CD8^+CD11c^+$ T

cells are characterized by strong expression of IFN-γ, which in turn primed DCs/macrophages to generate immunosuppressive IDO (384, 385). Such IDO^+ APCs when collaborate with autoreactive $CD4^+$ T cells can cause the suppression of $CD4^+$ T cells (383-385). Notably, activated $CD8^+CD11c^+$ T cells have also been shown to function as immune effectors in viral infection models (386, 387). Therefore, it would be interested to explore the mechanism that switches between their proposed effector and regulatory roles in the future.

Inducible expansion of $CD8^+CD11c^+$ T cells has been associated with the suppression of antigen-specific $CD4^+$ T-cell activity in autoimmune disease like CIA (385), experimental autoimmune uveoretinitis (EAU) (384) and IBD (388). A study in an animal model of CIA showed that the protective effect of $CD8^+CD11c^+$ T cells is linked to the production of IFN-γ and the activity of IDO, but failed to demonstrate whether it is a direct result of $CD8^+CD11c^+$ Tregs or not. The protective function of $CD8^+CD11c^+$ T cells has also been observed in EAU since the depletion of $CD8\alpha^+$ cells can partially neutralize the anti-4-1BB-mediated protective effects.

1.6.1.6 $CD8^+CD103^+$ Tregs

CD103 is the alpha chain of the integrin $\alpha_E\beta_7$ and provides tissue retention at sites enriched in E cadherin. Animal studies pointed that although the integrin CD103 is not necessary for the migration of T cells to sites of inflammation, it favored prolonged retention of Tregs at these sites (389, 390). Murine Tregs significantly differ with human Tregs in regard to CD103 expression (391). In naive mice, up to 30% of $CD25^+Foxp3^+$ lymphocytes in fact express CD103. In contrast, cells with this marker are virtually absent among human $CD25^{high}Foxp3^+$ Tregs. However, CD103 expression is dramatically upregulated on alloreactive $CD8^+$ T cells upon entry into a renal graft site or on $CD8^+$ T cells within the gut epithelium (392) in a TGF-β1 and IL-2-dependent manner (393). Although alloantigen induced $CD8^+CD103^+$ T cells were initially identified as an effector subset, these cells have also been addressed possessing regulatory activity (394). The increased CD103 expression on alloreactive $CD8^+$ T cells has been shown in the presence of TGF-β, IL-4 and IL-10, but not in the presence of IL-12 in mixed lymphocyte cultures (MLCs). Their suppressive activity is antigen nonspecific and depends on cell-cell contact. In addition, TGF-β-based suppression has been suggested to depend completely upon

the $CD8^+$ Tregs being capable of binding IFN-γ (395). $CD8^+CD103^+$ TGF-β-secreting T cells have also shown their protective function in a model of TNF-driven chronic ileitis (396) and in a liver allograft setting (397). However, the relationship between $CD8^+CD103^+$ Tregs and autoimmune disease remains to be determined.

1.6.1.7 Other $CD8^+$ Tregs

$CD8^+HLA\text{-}G^+$ Tregs: HLA-G, a non-classical HLA class Ib molecule with immune-suppressive function (398-401), is mainly expressed on placental trophoblasts, ectopic expressed on small populations of peripheral blood $CD4^+$ and $CD8^+$ T cells and at sites of inflammation (402). $CD8^+HLA\text{-}G^+$ $Foxp3^-$ T cells are detectable in the human thymus and constitute on average 3.3% of the total $CD8^+$ T cell population within human PBMCs. This $HLA\text{-}G^+$ subset presents with an anergic phenotype in response to allogeneic and polyclonal stimuli, and has been shown to suppress both $CD4^+$ and $CD8^+$ T cell proliferation *in vitro*. Infiltrating or invading $CD8^+HLA\text{-}G^+$ T cells has been found elevated in muscle biopsies from patients with inflammatory myopathies, and the frequencies of this population has been shown associated with the degree of cellular infiltrate in the muscle (402), suggesting their modulation role in inflamed tissue.

$CD8^+LAP^+$ Tregs: Latency-associated peptide (LAP), a membrane bound form of TGF-β, has been reported expressed on approximately 3.3% of the splenic $CD8^+$ T cell population in unmanipulated mice (403). Only a small fraction of $CD8^+LAP^+$ cells have been shown to express Foxp3 or CD25, although the expression level of Foxp3 for these cells are higher than their LAP^- counterparts. $CD8^+LAP^+$ cells have been found to suppress EAE in an IFN-γ and TGF-β-dependent manner based on the facts (i) *In vivo* neutralization of TGF-β significantly reverses the suppression of EAE mediated by $CD8^+LAP^+$ cells; (ii) The suppressive function of $CD8^+LAP^+$ cells is markedly diminished when these cells are purified from IFN-$\gamma^{-/-}$ mice. Whether a counterpart of suppressive $CD8^+LAP^+$ cells, which play the suppressive role in human, remains to be determined.

$CD8^+CD45RO^+$ Tregs: A subset of $CD8^+$ T cells, which has been identified in patients that receive HLA-matched, minor histocompatibility antigen (HA-1)-mismatched renal transplants,

has shown suppressive ability on both cognate delayed-type hypersensitivity responses and responses towards a third party antigen via IL-10, TGF-β and CTLA-4-dependent mechanisms (404). These $CD8^+$ cells consist mainly of $CD45RO^+CD62L^-CCR7^-$ T cells of the memory effector type. Another subset of $CD8^+$ T cells with the expression of CD45RO and CCR7 have also been found in patients with ovarian carcinoma. These tumor ascites pDCs induced cells have been observed to suppress tumor-antigen driven T cell responses *in vitro* by secreting IL-10 (405).

pCons-induced $CD8^+$ Tregs: A nucleosomal histone peptide has been documented to treat lupus-prone animals by induction of regulatory $CD8^+$ T cells. $CD8^+$ Tregs, which produce and require TGF-β for immunosuppression, suppressed antigen-driven T cell responses in a contact-independent manner (406). Similar subsets have been described in a model of murine systemic lupus, where treatment with a pConsensus (pCons) either by i.v. (407) or oral (408) administration induced a population of $CD8^+$ T cells that suppress autoimmune responses. pCons-induced $CD8^+$ Tregs have been shown to exert protective effects in lupus mice by differentially modulating the activity of different T cell subsets (409) along with increased cytotoxic activity against B cells, thereby exerting their influences by both suppressing helper T cells and killing pathogenic B cells (410).

$CD8^+CD39^+$ Tregs: CD39, an ectonucleotidase, presents at the surface of different immune cells and catalyzes conversion of extracellular ATP or ADP to AMP (411). ATP is a potent activator of immune cells and inflammation, thus the presence of CD39 deprives cells of an important energy source and favors the formation of a potent inhibitor of effector function. CD39 has been found on $CD4^+CD25^+$ Tregs and involves in their regulatory activity (412, 413). A recent study has shown that it also participates in mediating the suppressive activity of $CD8^+$ Tregs (414). Besides, intratumoral $CD8^+$ Treg-mediated suppression has been associated with CD39 expression, suggesting that CD39-mediated inhibition constitutes a prevalent hallmark of their function.

$CD8^+CD38^+$ Tregs: CD38, similar as CD39, is another ectonucleotidases that strongly influences the adaptive immunity (415). In the absence of CD38, NOD mice developed

accelerated autoimmune diabetes, and $CD38^{-/-}$ mice showed an impaired regulatory T cell development (416). In human, the detection of anti-CD38 autoantibodies has been associated with chronic autoimmune thyroiditis, Graves' disease and Type I diabetes (417, 418). Previous study showed that high expression of CD38 on $CD4^{+}Foxp3^{+}$ T cell subpopulation correlated with strongest regulatory properties of $CD4^{+}$ Tregs (419). Moreover, regulatory $CD8^{+}$ T cells with the memory-like phenotype of $CD8^{+}CD38^{high}CD44^{+}CD122^{+}CD62L^{high}$ also showed suppressive function on $CD4^{+}$ effector T-cell proliferation in a cell-cell contact dependent, TGF-β and granzyme B independent manner (420). $CD8^{+}CD38^{high}$ T cell-treated MOG-induced EAE mice showed reduced clinical score and disease severity compared to mice that received $CD8^{+}CD38^{-}$ T cells, suggesting the potential role of $CD8^{+}CD38^{high}$ T cells in inhibiting excessive immune responses.

1.6.2 Summary

Although $CD4^{+}$ Treg subsets have been more extensively studied in the last decade, growing interest is presently devoted to $CD8^{+}$ Treg subsets. A wide array of $CD8^{+}$ Treg subpopulation has been characterized both in mice and human. These cells are involved in physiological mechanisms that guarantee immune homeostasis and protect immune system from autoimmune reactions. Notably, Tregs have both positive and negative functions in the immune system. Other than the positive aspects of Tregs, including suppression of autoimmune responses, maintenance immune homeostasis, as well as tolerance in xenotransplantation, negative aspects of Tregs have also been widely studied. For example, some infectious agents can manipulate Tregs to avoid the host's immune responses; or in cancer scenario, Tregs can provide help to suppress the body's cytotoxic immune response to neoplastic cells. Therefore, immune homeostasis, which results from the controlled balance between effector and regulatory immune responses, determines the fate of an immune response.

CHAPTER 2 HYPOTHESIS

Hypothesis I. With the targeting role of exosomal pMHC-I complexes, HER2-specific exosome-targeted $CD4^+$ T cell-based vaccine (HER2-T_{EXO}) can stimulate efficient HER2-specific $CD8^+$ CTL responses and antitumor immunity in double transgenic HER2/HLA-A2 mice with HER2-specific self-immune tolerance.

Hypothesis II. Similar to natural $CD4^+CD25^+$ Tregs, *in vitro* activated polyclonal $CD8^+CD25^+$ Tregs may have immunosuppressive effect. With the targeting role of pMHC-II complexes, redirecting antigen specificity to non-specific polyclonal $CD8^+CD25^+$ Tregs by $OVA_{323-339}$ and MOG_{35-55} peptide pulsing can enhance the suppressive effects on OVA-specific tumor model and MOG-induced EAE model.

CHAPTER 3 OBJECTIVES

For testing hypothesis I, objectives are:

i. Generation of OVA-T_{EXO} vaccine as well as OVA-($K^{b-/-}$)T_{EXO}, (4-1BBL$^{-/-}$)T_{EXO}, (OX40L$^{-/-}$)T_{EXO} and (CD40L$^{-/-}$)T_{EXO}, lacking pMHC-I, 4-1BBL, OX40L and CD40L, respectively.

ii. Assessment of the role of pMHC-I and costimulatory 4-1BBL, OX40L and CD40L in OVA-T_{EXO}-stimulated CTL response and memory development.

iii. Assessment of critical role of exosomal pMHC-I complexes in targeting OVA-T_{EXO} cells to cognate $CD8^+$ T cells *ex vivo* in mouse lymph nodes by two-photon microscopy.

iv. Generation of HER2-T_{EXO} vaccine using ConA-stimulated $CD4^+$ T cells with uptake of HER2-expressing DC-released exosomes.

v. Assessment of HER2-T_{EXO}-stimulated HER2-specific CTL responses and antitumor immunity against HLA-A2/HER2-expressing B16 melanoma in double transgenic HLA-A2/HER2 mice with HER2-specific self-immune tolerance.

For testing hypothesis II, objectives are:

i. Purification and expansion of polyclonal $CD8^+CD25^+$ Tregs in culture using CD3/CD28 microbeads.

ii. Phenotypic characterization of $CD8^+CD25^+$ Tregs.

iii. Functional characterization of $CD8^+CD25^+$ Treg-mediated suppression *in vitro*.

iv. Functional characterization of $CD8^+CD25^+$ Treg-mediated suppression *in vivo* in OVA-specific animal tumor model.

v. Comparison of $OVA_{323-339}$- and MOG_{35-55}-pulsed $CD8^+CD25^+$ Treg-mediated suppression to $CD8^+CD25^+$ Treg-mediated suppression *in vivo* in OVA-specific animal tumor model and in MOG-induced EAE model.

vi. Assessment of critical role of exosomal pMHC-II complexes in targeting OVA-T_{EXO} cells to cognate $CD4^+$ T cells *ex vivo* in mouse lymph nodes by two-photon microscopy.

CHAPTER 4 MATERIALS AND METHODS

4.1 Materials

4.1.1 Reagents

Table 4.1 lists the chemicals used in this dissertation. All of the reagents are molecular biology or research grade. **Table 4.2** lists Abs labeled with fluorescein isothiocyanate (FITC), phycoerythrin (PE), PE-Cy5 or biotin. **Table 4.3** lists the commercially available kits used in this dissertation.

Table 4.1 List of chemicals and reagents

Reagents	Suppliers
α-MEM	Gibco
λ *HindIII* DNA Ladder	New England Biolabs
Agar	Invitrogen
Agarose	Invitrogen
AIM-V medium	Gibco
Ammonium Chloride	EM Sciences
Ampicillin	Sigma
Anti-biotin MicroBeads	Miltenyi Biotec
Bacto-tryptone	BD Biosciences
BSA	Sigma
Calcium chloride	Sigma
Cesium chloride	Sigma
CFA	Sigma
CFSE	Invitrogen
CMTMR	Invitrogen
Collagenase	Worthington Biochemical
dNTP mix (dATP, dCTP, dGTP, dTTP)	Invitrogen

Reagents	**Suppliers**
DMEM	Gibco
Dynabeads® Mouse T-Activator CD3/CD28	Invitrogen
G418	Invitrogen
Gentamicin	Gibco
Glycerol	BDH Inc
GM-CSF	R&D Systems
$HER2_{369-377}$ (KIFGSLAFL)	Synthesized by New England Peptide
HindIII Restriction Enzyme	New England Biolabs
Hygromycin	Invitrogen
IL-2	Peprotech
IL-4	R & D Systems
Kanamycin	EM Sciences
Lipofectamine2000	Invitrogen
LS column	Miltenyi Biotec
Mouse anti-biotin MicroBeads	Miltenyi Biotec
Mouse CD4 (L3T4) MicroBeads	Miltenyi Biotec
Mouse CD8 (Ly-2) MicroBeads	Miltenyi Biotec
MOG_{35-55} (MEVGWYRSPFSRVVHLYRNGK)	Anaspec
Mut1 (FEQNTAQP)	Anaspec
NEBuffer 2.1	New England Biolabs
OVAI ($OVA_{257-264}$, SIINFEKL)	Anaspec
OVAII ($OVA_{323-339}$, ISQAVHAAHAEINEAGR)	Anaspec
pcDNA3.1(+)neo plasmids	Invitrogen
PacI Restriction Enzyme	New England Biolabs
PmeI Restriction Enzyme	New England Biolabs
Poly-D-Lysine/Laminin coated culture slides	BD Biosciences
ProLong Gold antifade reagent	Invitrogen
RPMI-1640	Gibco
Quick-Seal tube (12.5 mL)	Beckman Coulter
Slide-A-lyzer dialysis cassettes	Thermo Fisher Scientific Inc.

Reagents	Suppliers
SYBR® Safe DNA Gel Stain	Invitrogen
T4 DNA ligase	New England Biolabs
Taq DNA polymerase	Qiagen
ThiolTracker™ Violet	Invitrogen
XbaI Restriction Enzyme	New England Biolabs
100 bp Plus Opti-DNA Marker	Applied Biological Materials Inc.
2-ME	Bio-Rad
3.8 μm diameter aldehyde/sulfate latex beads	Interfacial Dynamics

Table 4.2 List of antibodies

Antibodies	Clone	Suppliers
Anti-H2-K^b/OVAI (pMHC-I)	25-D1.16	eBioscience
Anti-human HER2	24D2	Biolegend
Anti-human HLA-A2	BB7.2	Santa Cruz Biotechnology
Anti-mouse CD103	M290	BD Biosciences
Anti-mouse CD11c	HL3	BD Biosciences
Anti-mouse CD20	AISB12	eBioscience
Anti-mouse CD25	7D4	BD Biosciences
Anti-mouse CD28	37.51	BD Biosciences
Anti-mouse CD317 (BST-2)	120G8.04	Dendritics
Anti-mouse CD4	GK1.5	BD Biosciences
Anti-mouse CD40	HM40-3	BD Biosciences
Anti-mouse CD40L	MR1	Biolegend
Anti-mouse CD44	IM7	BD Biosciences
Anti-mouse CD45R/B220	RA3-6B2	BD Biosciences
Anti-mouse CD8	53-6.7	eBioscience
Anti-mouse CD80	16-10A1	BD Biosciences
Anti-mouse CTLA-4	UC10-4F10-11	BD Biosciences

Antibodies	Clone	Suppliers
Anti-mouse GITR	DTA-1	BD Biosciences
Anti-mouse Granzyme B	NGZB	eBioscience
Anti-mouse OX40L	RM134L	Biolegend
Anti-mouse perforin	eBioOMAK-D	eBioscience
Anti-mouse PKCθ	C-19	Santa Cruz Biotechnology
Anti-mouse I-A^b	AF6-120.1	BD Biosciences
Anti-mouse IgG		Jackson Immunoresearch
Anti-mouse talin	8D4	Sigma
Anti-mouse 4-1BBL	TKS-1	eBioscience
Anti-goat IgG		Jackson Immunoresearch
Streptavidin-FITC		BD Biosciences
Streptavidin-PE		BD Biosciences
Streptavidin-PE-Cy5		BD Biosciences

Table 4.3 List of kits

Commercial kits	Suppliers
EasySep™ Mouse $CD4^+$ T Cell Isolation Kit	Stemcell
EasySep™ Mouse $CD8^+$ T Cell Isolation Kit	Stemcell
ELISA Kits for IL-2	BD Biosciences
Fixation and Permeabilization Solution Kit with BD GolgiStop™	BD Biosciences
Mouse Regulatory T Cell Staining Kit #3	eBioscience
GranToxiLux	OncoImmunin, Inc.
QIAprep Spin Miniprep Kit	Qiagen
QIAquick Gel Extraction Kit	Qiagen
QIAquick PCR purification Kit	Qiagen
RNeasy Plus Mini Kit	Qiagen
RT^2 First Strand Kit	Qiagen
RT^2 SYBR Green qPCR Mastermixes	Qiagen

4.1.2 Cell lines

The highly metastatic B16 mouse melanoma BL6-10 and BL6-10_{OVA} tumor cells were cultured in alpha-minimum essential medium (α-MEM). BL6-10_{HER2} tumor cells were cultured in α-MEM plus 1 mg/mL G418. BL6-$10_{HLA\text{-}A2/HER2}$ tumor cells were cultured in α-MEM plus 1 mg/ mL G418 and 0.5 mg/mL hygromycin. Human embryonic kidney cells (HEK293) express early region-1 (E1) of adenovirus (AdV), which helps the growth and amplification of replication deficient AdV. These cells were purchased from the Microbix, and cultured in Eagle's minimal essential medium (EMEM).

All culture media were supplemented with 10% (v/v) fetal calf serum (FCS) and 30 µg/mL gentamicin reagent. c-PEG solution and 1× citric saline solution were used for BL6-10 and HEK293 cell passage, respectively. Cells were cultured in a humidified incubator at 37 ºC with 5% CO_2 saturation. Viable cells were counted using Trypan blue stain using a haemocytometer.

4.1.3 Bacterial cells

Escherichia coli (*E. coli*), DH5α strain (New England Biolabs), was routinely used for expression-vector propagation. *E. coli*, BJ5183 strain (Stratagene), was used for the homologous recombination in AdV vector construction. Both cells were grown in Lysogeny broth (LB) at 37 ºC on a shaker. Medium was supplemented with selective antibiotic, ampicillin (100 µg/mL) or kanamycin (50 µg/mL), depending on the expression vector's resistance gene. After transformation, transformed bacterial cells were selected by plating them on selective LB-agar plates containing appropriate selective antibiotics. Plates were incubated overnight at 37 ºC.

4.1.4 Animals

Wild-type (C57BL/6) female mice with H2-K^b background, OVA-specific TCR-transgenic OTI (transgenic for αβTCR specific for OVA-peptide 257-264 in the context of H-$2K^b$) and OTII (transgenic for αβTCR specific for 323-339 OVA-peptide in the context of I-A^b) mice, CD11c-DTR mice, various gene KO mice (H-$2K^{b\text{-}/\text{-}}$, I-$A^{b\text{-}/\text{-}}$, $CD40L^{-/-}$, $CD40^{-/-}$, 4-$1BB^{-/-}$, $OX40L^{-/-}$ and

OX40$^{-/-}$) and transgenic HLA-A2 mice were obtained from the Jackson Laboratory. 4-1BBL$^{-/-}$ mice were obtained from Amgen. Homozygous OTII/H-2K$^{b-/-}$, OTII/CD40L$^{-/-}$, OTII/4-1BBL$^{-/-}$ and OTII/OX40L$^{-/-}$ mice were generated by backcrossing the designated gene KO mice onto the OTII background. The transgenic (Tg) HER2 (H-2K^{b}) mice (421) with HER2-specific self-immune tolerance were obtained from Dr. Wei-Zen Wei (Wayne State University). The double transgenic HLA-A2/HER2 mice were generated by backcrossing male HER2 mice with female HLA-A2 mice. All mice used in the experiments were 6-8 weeks old and were treated according to the animal care committee guidelines of the University of Saskatchewan.

4.2 Methods

4.2.1 Molecular biology experiments

4.2.1.1 General molecular biology techniques

General molecular biology techniques used in this dissertation were based on the protocols described in Molecular Cloning, a Laboratory Manual by Sambrook et al. (422) and Sambrook and Russel (423) with few modifications.

4.2.1.1.1 Restriction enzyme digestion

The restriction enzymes *HindIII* and *XbaI* were purchased from New England Biolabs. DNA digestions were performed according to the manufacturer's guidelines. Briefly, around 1 µg of DNA was digested using 1 unit of specific restriction enzyme in 1× recommended NEBuffer 2.1 for 1 hour at 37 ºC.

4.2.1.1.2 Agarose gel electrophoresis

Agarose gels were prepared in varying concentration, from 0.7% (w/v) to 2% (w/v), in Tris-acetate EDTA (TAE) buffer, depending on the size of the DNA band to be visualized. 10,000× dilution of SYBR® Safe DNA Gel Stain was used in the gel to stain DNA. Samples were mixed

with loading buffer and loaded on the gel along with DNA markers. For optimal resolution, gels were run between 90 to 110 volts in TAE buffer for varying times. Bands were visualized under UV trans-illuminator gel documentation system (Bio-Rad).

4.2.1.1.3 Purification of linear DNA fragments

For further downstream applications, PCR products were purified using QIAquick PCR purification Kit. DNA fragments from agarose gel were purified using QIAquick Gel Extraction Kit. The method was followed as per the procedure provided by manufacturer. Typically, DNA was eluted in 20 µL of sterile water to facilitate the subsequent ligation or transfection procedures.

4.2.1.1.4 DNA ligation

DNA ligation was performed using T4 DNA ligase in supplied ligation buffer. Typically, a 20 µL ligation reaction consists of 50 ng of vector DNA, at least 150 ng of purified insert DNA with 1-5 units of T4 DNA ligase in 1× ligation buffer. Ligation reactions were performed overnight at 4 ºC.

4.2.1.1.5 Heat shock transformation

100 µL competent cells (DH5α or BJ5183) were mixed with plasmid DNA or DNA ligation products and kept on ice for 30 min. The sample was heat shocked at 42 ºC for 90 sec by quickly placing the sample into a water bath. The sample was then placed on ice for at least 2 min. Transformed bacteria cells were then cultured in 500 µL LB medium at 37 ºC for 45 min. Cells were then added onto selective LB-agar plates to get individual bacteria clone, and cultured at 37 ºC for 12-16 hrs.

4.2.1.1.6 Plasmid DNA purification

To screen positive recombinant colonies after transformation, single isolated colonies were selected. For recombinant BJ5183 colonies, a tiny single colony was selected. The colonies were further cultured to amplify copies of recombinant plasmid DNA in LB broth with selective antibiotic overnight. Cells were pelleted the next day, plasmids were isolated using QIAprep Spin Miniprep Kit according to the manufacturer's protocol. Finally, purified plasmid DNA was quantified using Nanodrop (Thermo-Scientific).

4.2.1.1.7 DNA sequencing

Automated sequencing was performed at the sequencing facilities located in Plant Biotechnology Institute of the National Research Council of Canada in Saskatoon, Canada. Sequences were then analyzed through Blast on NCBI.

4.2.1.2 Construction of pcDNA3.1/HER2 vectors

The human $HER2_{690aa}$ cDNA fragments coding for the extracellular and transmembrane domains of human HER2 were amplified by PCR using PCR2.1/HER2 plasmids carrying full length human HER2 3768 bp cDNA (GenBank accession no. NM_004448) as templates, and $HER2_{690aa}$-F (5'-CTT AAG CTT GCC ACC ATG GAG CTG GCG GCC TTG TG-3') and $HER2_{690aa}$-R (5'-GAG TCT AGA GTC TCC GCA TCG TGT ACT TC-3') as primers under conditions [1 cycle at 94 ºC (2 min) and then 72 ºC (7 min) followed by 30 cycles at 94 ºC (50 sec), 58 ºC (50 sec) and 72 ºC (2 min)]. The PCR reaction products were analyzed on 1% agarose gel electrophoresis with SYBR® Safe DNA Gel staining. Then the about 2070 bp $HER2_{690aa}$ cDNA fragments were inserted into pcDNA3.1(+)neo plasmids containing neomycin (G418) resistance gene at *HindIII* and *XbaI* sites. The recombinant eukaryotic expression vector pcDNA3.1(+)neo/$HER2_{690aa}$ (termed pcDNA3.1/HER2 hereafter) were further identified by PCR, double enzyme digestion and DNA sequencing analysis, respectively.

4.2.1.3 AdV_{HER2} construction

The overall method for construction of recombinant replication-incompetent Ad5E1- and E3-deleted adenovirus expressing human $HER2_{690aa}$ as reported by He et al. in 1998 (424). To develop a more efficient gene delivery system, we used RGD-modified pAdEasy-1 (425) as an adenoviral backbone plasmid, which contains an integrin-binding motif RGD sequence in the HI loop of adenoviral fiber, in the construction of human $HER2_{690aa}$-expressing recombinant adenovirus. In brief, the 2070 bp $HER2_{690aa}$ fragments released from recombinant eukaryotic expression plasmids pcDNA3.1/HER2 by double enzyme digestion with *HindIII* and *XbaI* were inserted into pShuttle-CMV transfer (shuttle) plasmid at *HindIII* and *XbaI* sites to form recombinant transfer vector pShuttle-CMV/$HER2_{690aa}$. After homologous recombination of pShuttle-CMV/$HER2_{690aa}$ or control pShuttle-CMV and pAdEasy-1 (RGD) in *E.coli* BJ5183 bacteria, the recombinant pAdEasy-$HER2_{690aa}$ (termed AdV_{HER2} hereafter) or control blank adenovirus were subsequently linearized by *PacI* digestion and transfected into HEK293 cells for replication-deficient AdV_{HER2} production (**Figure 4.1**).

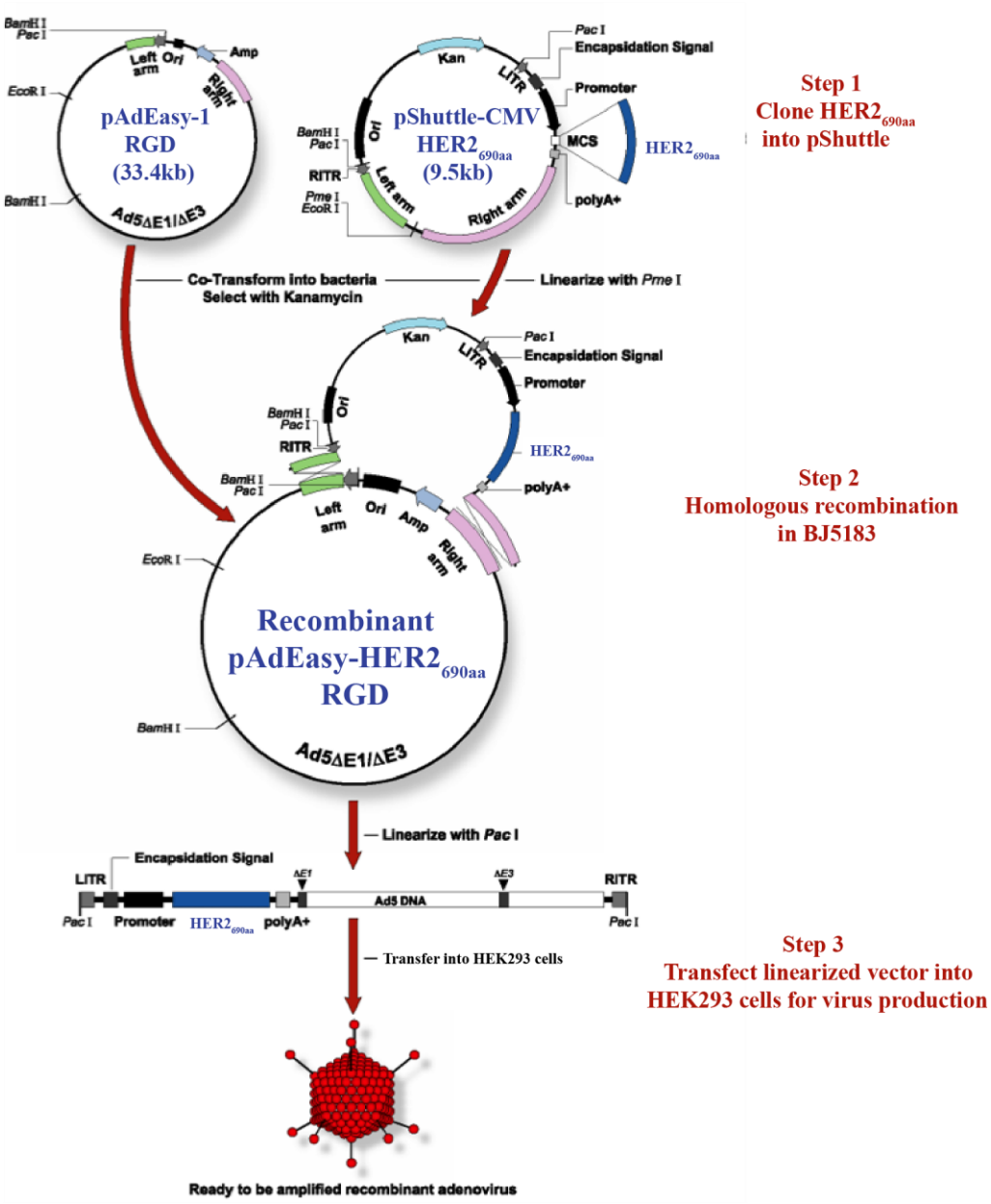

Figure 4.1 Schematic representation of AdEasy system and AdV production (adapted from Qbiogene, Inc) $HER2_{690aa}$ gene was cloned into pShuttle-CMV vector before homologous recombination with the Ad5 backbone gene. pShuttle-CMV-$HER2_{690aa}$ was linearized by *PmeI* restriction enzyme, and then transformed into *E. coli* BJ5183 containing the backbone vector, pAdEasy-1. Homologous recombination between the two vectors in *E. coli* BJ5183 cells resulted in adenoviral vector pAdEasy-$HER2_{690aa}$. Resulting recombinant vector was linearized by *PacI* digestion and transfected into HEK293 cells for replication-deficient AdV_{HER2} production.

4.2.1.4 Production of AdV_{HER2}

To produce AdV_{HER2}, *PacI* linearized recombinant adenoviral DNA vector (4 μg) was added into 500 μL EMEM. Lipofectamine2000 (16 μL) was added into another 500 μL EMEM medium. Each mixture was incubated at room temperature for 5 min. These two mixtures were then further mixed and kept at room temperature for 20 min. The DNA : liposome mixture solution was added to HEK293 cells plated at a cell density of $1x10^6$ cells per well in 6-well plate. Cells were incubated in 2 mL EMEM medium at 37 ºC in a CO_2 incubator. Medium was replaced by EMEM with 10% FCS after 4 hrs. Cells were continually monitored for 7-10 days for formation of plaques. Cell culture medium was refreshed as required. When cytopathic effects (CPE) were apparent and extensive, cells with medium were subjected five rounds of freeze/thaw cycles performed at -80 ºC and 37 ºC, respectively, resulting in generation of the initial crude viral lysates. Crude viral lysates were used to infect more HEK293 cells in T75 flasks. Infected cells went through further freeze/thaw cycles. The supernatants were collected and used as the source of the virus for further infection of HEK293 cells in T175 flasks.

4.2.1.5 Purification of AdV_{HER2}

When more than 50% CPE was observed in the last step of amplification, entire cells were harvested in phosphate-buffered saline (PBS) or serum-free EMEM and subjected to five rounds of freeze and thaw cycles as mentioned above. Subsequently, samples were centrifuged at 300 *g* for 10 min followed by 10,000 g for 30 min twice at 4 ºC to remove as much cell debris as possible, which otherwise may interfere with virus purification. After centrifugation, supernatants were collected for discontinuous cesium chloride (CsCl) density-gradient ultracentrifugation. It was performed using Quick-Seal centrifuge tubes layered with 1.25 g/mL CsCl and 1.40 g/mL CsCl gradient solutions. Viral lysate was layered slowly above the density gradient solutions and subjected to ultracentrifugation at 235,000 g at 20 ºC for 2 hrs. The lower viral band was collected and layered on a 1.34 g/mL CsCl gradient solution and centrifuged again at 235,000 g for about 18 hrs at 20 ºC. After centrifugation, the opalescent band was collected. Salts presented in the purified AdV samples were removed by dialysis using slide-A-lyzer dialysis cassettes following the manufacturer's instructions. Finally, the concentration of

the AdV was determined by spectrophotometry at A260 as described by Xiang and Wu et al. (426). Optical density of 1 is equivalent to 1×10^{10} plaque forming unit (PFU)/mL. The virus was stored in sterile 10% (v/v) glycerol at -80 ºC until use.

4.2.1.6 Reverse transcriptase (RT)-PCR

The expression of adenovirus-mediated human $HER2_{690aa}$ transgene in HEK293 cells or bone marrow-derived dendritic cells (BM-DCs) was determined by RT-PCR. The ratio of adenovirus to target cells is called multiplicity of infection (MOI) in the following experiments. Briefly, HEK293 cells or BM-DCs were infected with AdV_{HER2} or control AdV at the MOI of 10 (HEK293) or 100 (BM-DCs). The medium containing PBS without adenovirus was used as a cell control (PBS control). After 48 hrs of infection, the AdV_{HER2}-, AdV-infected or uninfected HEK293 cells or BM-DCs were harvested, washed in PBS, and then subjected to RT-PCR. Total cellular RNAs were extracted using RNeasy Plus Mini Kit following the manufacturer's guidelines. Sample concentration and purity was determined using Nanodrop (Thermo scientific). cDNA was synthesized immediately using RT² First Strand Kit. The PCR reactions were performed using cDNA as template and primers specific for human $HER2_{690aa}$, human housekeep gene β-actin (F, 5'-TGC GTG ACA TTA AGG AGA AG-3'; and R, 5'-CTG CAT CCT GTC GGC AAT G-3') or mouse housekeep gene GAPDH (F: 5'-TGC ACC ACC AAC TGC TTA-3'; and R: 5'-GGA TGC AGG GAT GAT GTT C-3') under conditions [1 cycle at 94 ºC (2 min) and then 72 ºC (7 min) followed by 30 cycles at 94 ºC (50 sec), 58 ºC (50 sec) and 72 ºC (2 min)].

4.2.1.7 Preparation of transgenic tumor cell lines

The BL6-10 melanoma cells were dispensed into 24-well culture plates at 2×10^4 cells/mL of growth medium per well. After 24 hrs of incubation, cells could usually be 70% confluent at the time of transfection. The BL6-10 tumor cells were then transfected with eukaryotic expression plasmids pcDNA3.1/HER2 expressing human $HER2_{690aa}$ or control plasmids pcDNA3.1(+)neo using Lipofectamine2000 transfection reagent according to manufacturer's instructions. Briefly, 1 μg of pcDNA3.1/HER2 or pcDNA3.1(+)neo plasmid DNA and 2 μL of Lipofectamine2000

were diluted in 50 μL serum-free α-MEM medium without antibiotics, respectively. The diluted DNA solution was then mixed gently with diluted Lipofectamine2000 solution, and incubated at room temperature. After 30 min of incubation, the DNA-Lipofectamine complex (100 μL) plus 200 μL of serum-free α-MEM medium was added into each well containing BL6-10 tumor cells which has been washed with serum-free α-MEM medium 2 times. After another 6 hrs of incubation, the 300 μL of fresh growth medium were then supplemented into each well. 24 or 48 hrs after transfection, cells were plated at a ration of 1:6 into selection medium (α-MEM medium with 10% FBS and 1 mg/mL G418). The transfectants were selected for 2-3 weeks in the selection medium. Then the G418-resistant polyclonal cells were plated at a density of 1 cell/well in a 96-well tissue culture plate in selection medium. After a few days of growth, only wells with single colony per well were selected. The selected monoclone was further determined by RT-PCR and flow cytometric analysis. BL6-$10_{HLA\text{-}A2/HER2}$ double transgenic tumor cells were constructed by transfecting pcDNA3.1/HLA-A2 or control pcDNA3.1(+)hygro plasmids containing hygromycin resistance gene into BL6-10_{HER2} tumor cells using Lipofectamine2000 as described above. The hygromycin and G418 double-resistant clones were selected and maintained in growth medium with 0.5 mg/mL hygromycin and 1 mg/mL G418. To screen the BL6-$10_{HLA\text{-}A2/HER2}$ double transgenic tumor cells, HLA-A2 and $HER2_{690aa}$ transgene expression in resulting hygromycin and G418 double-resistant clones were further determined by RT-PCR and flow cytometric analysis.

4.2.1.8 Real-time PCR

The preparation of $CD8^+CD25^+$ Tregs and naive $CD4^+$ T cells will be described in Section 4.2.2. $CD8^+CD25^+$ Tregs were cultured with naive $CD4^+$ T cells at 1:1 ratio in culture medium containing IL-4 (10 ng/mL) for 16 hrs since IL-4 can promote T-cell survival (427). $CD8^+CD25^+$ Tregs-treated $CD4^+$ T cells were then purified by CD4-microbeads. Total cellular RNAs were extracted from naive $CD4^+$ or $CD8^+CD25^+$ Treg-treated $CD4^+$ T cells (428) using RNeasy Plus Mini Kit according to manufacturer's guidelines. Sample concentration was determined using Nanodrop (Thermo scientific). cDNA was synthesized immediately using RT² First Strand Kit. Real-time PCR was carried out with RT² SYBR Green qPCR Mastermix using a StepOnePlus Real-time PCR system (Applied Biosystems). A panel of primers specific for T-cell anergy-

associated genes were synthesized (429). Expression of each gene was normalized to β-actin. The primers were as follows: β-actin: F-GTGAC GTTGA CATCC GTAAA GA; R-GCCGG ACTCA TCGTA CTCC; Grail: F-GCGCA GTCAG CAAAT GAA; R-TGTCA ACATG GGGAA CAACA; Ikaros: F-GCTGG CTCTC GGAGG AG; R-CGCAC TTGTA CACCT TCAGC; Casp3: F-ACGCG CACAA GCTAG AATTT; R-CTTTG CGTGG AAAGT GGAGT; EGR2: F-TCAGT GGTTT TATGC ACCAG C; R-GAAGC TACTC GGATA CGGGA G; Grg4 F-TCACT CAAGT TTGCC CACTG; R-CACAG CTAAG CACCG ATGAG; Itch: F-GTGTG GAGTC ACCAG ACCCT; R-GCTTC TACTT GCAGC CCATC. The fold induction represents the ratio of mRNA expression in $CD8^+CD25^+$ Treg-treated $CD4^+$ T cells to that in naive $CD4^+$ T cells.

4.2.2 Cell generation

4.2.2.1 Generation of BM-DCs

BM-DCs were generated from C57BL/6 as described previously (430). Bone marrow cells from the femorae and tibiae of normal C57BL/6 mice were depleted of red blood cells (RBCs) with 0.85% (w/v) Tris-NH_4Cl buffer on day 1 and plated in Dulbecco's modified Eagle's medium (DMEM) plus 10% FCS, GM-CSF (20 ng/mL) and IL-4 (20 ng/mL). On day 3, the nonadherent granulocytes, T and B cells were gently removed. Old medium was replaced with fresh medium. On day 5, proliferating aggregates of DCs were observed. Fresh medium was added if necessary. On day 6, cells slightly adherent to the plate were observed and these cells were pulsed with 0.4 mg/mL OVA in FCS-free AIM-V medium plus lipopolysaccharide (LPS) (1μg/mL) overnight. The resultant DCs were referred to as DC_{OVA}. The DC_{OVA} from H-$2K^{b-/-}$, 4-$1BBL^{-/-}$, $OX40L^{-/-}$ and $CD40L^{-/-}$ KO mice were termed ($K^{b-/-}$)DC_{OVA}, (4-$1BBL^{-/-}$)DC_{OVA}, ($OX40L^{-/-}$)DC_{OVA}, and ($CD40L^{-/-}$)DC_{OVA}, respectively. HLA-A2/HER2 mouse BM-DCs were transfected with AdV_{HER2} for 1 hour at 37 ºC in DC culture medium at a MOI of 100 (302), then the medium was replaced. DCs were cultured for another 24 hrs to achieve optimal transgene expression. These DCs were termed DC_{HER2}.

4.2.2.2 Generation of spleen derived DCs (sDCs)

Briefly, spleens were digested in DMEM containing 1 mg/mL collagenase for 45-60 min at 37 ºC. After removing the RBCs using 0.85% (w/v) Tris-NH_4Cl buffer, cells were re-suspended in AIM-V® medium plus OVA protein (0.4 mg/mL), GM-CSF (20 ng/mL) and 2-mercaptoethanol (2-ME) (50 μM), and incubated at 37 ºC for 90 min. Nonadherent cells were then removed by gently washing three times with pre-warmed PBS, used medium was kept for culturing adherent cells overnight. Adherent cells were further purified by incubating them with the biotin-conjugated anti-CD11c Ab followed by anti-biotin microbeads according to the company's instruction (21), and termed sDC_{OVA}.

4.2.2.3 Purification of EXOs

EXOs were isolated as described previously (431). Briefly, supernatants from BM-DCs cultured overnight in FCS-free AIM-V medium containing OVA (0.4 mg/mL) were subjected to four successive centrifugations at 300 g for 10 min to remove cells, 10,000 g for 30 min twice to remove cellular debris and 136,000 g for one hour to pellet the EXOs. The pellets were washed twice in a large volume of PBS and recovered by centrifugation at 136,000 g for another one hour. The amount of exosomal protein recovered was measured using Nanodrop (Thermo scientific). EXOs derived from DC_{OVA}, ($K^{b-/-}$)DC_{OVA}, (4-1$BBL^{-/-}$)DC_{OVA}, ($OX40L^{-/-}$)DC_{OVA}, and ($CD40L^{-/-}$)DC_{OVA} were referred to as EXO_{OVA}, ($K^{b-/-}$)EXO_{OVA}, (4-1$BBL^{-/-}$)EXO_{OVA}, ($OX40L^{-/-}$)EXO_{OVA}, and ($CD40L^{-/-}$)EXO_{OVA}, respectively. EXOs purified from culture supernatants of DC_{HER2} were termed EXO_{HER2}.

4.2.2.4 $CD4^+$ T_{EXO} vaccine preparation

Transgenic OTII mice spleens were collected aseptically and single cell suspensions were prepared. RBCs were depleted using 0.85% (w/v) Tris-NH_4Cl buffer, and splenocytes were cultured in Roswell Park Memorial Institute medium (RPMI)-1640 containing 10% FCS, IL-2 (20 U/mL) and ConA (1 mg/mL) for 3 days. ConA-activated $CD4^+$ T cells were purified using Mouse CD4 (L3T4) microbeads according to the manufacture's instructions. ConA-T cells

derived from OTII/H-2K$^{b-/-}$, OTII/4-1BBL$^{-/-}$, OTII/OX40L$^{-/-}$ and OTII/CD40L$^{-/-}$ mice were termed (K$^{b-/-}$)T, (4-1BBL$^{-/-}$)T, (OX40L$^{-/-}$)T and (CD40L$^{-/-}$)T cells, respectively. ConA-T cells were incubated with EXO_{OVA} and EXO_{HER2} (15 μg/1×10^6 T cells) at 37 ºC for 3 hrs and were termed OVA-T_{EXO} and HER2-T_{EXO}, respectively. (K$^{b-/-}$)T, (4-1BBL$^{-/-}$)T, (OX40L$^{-/-}$)T and (CD40L$^{-/-}$)T cells that had internalized (K$^{b-/-}$)EXO_{OVA}, (4-1BBL$^{-/-}$)EXO_{OVA}, (OX40L$^{-/-}$)EXO_{OVA}, and (CD40L$^{-/-}$)EXO_{OVA} were termed (K$^{b-/-}$)T_{EXO}, (4-1BBL$^{-/-}$)T_{EXO}, (OX40L$^{-/-}$)T_{EXO} and (CD40L$^{-/-}$)T_{EXO} , respectively.

4.2.2.5 Naive T cell preparation

The naive polyclonal CD8$^+$ or OTI CD8$^+$ T cells were prepared from splenocytes of C57BL/6 or transgenic OTI mice using EasySep^{TM} Mouse CD8$^+$ T cell isolation kits according to manufacturer's protocol. Naive CD4$^+$ T cells were prepared from splenocytes of C57BL/6 mice using EasySep^{TM} Mouse CD4$^+$ T cell isolation kits according to manufacturer's protocol.

4.2.2.6 Preparation of CD8$^+$CD25$^+$ Tregs

Naive CD8$^+$CD25$^+$ Tregs were purified from C57BL/6 mouse splenocytes by using EasySep^{TM} Mouse CD8$^+$ T-cell isolation kits, followed by biotin-labeled anti-CD25 Ab and anti-biotin microbeads. Those cells were further amplified in culture using Dynabeads® Mouse T-Activator CD3/CD28 at a ratio of 1:1 for 4-6 days in the presence of IL-2 (100 U/mL) and 2-ME (50 μM). The amplified CD8$^+$CD25$^+$ Tregs were incubated in medium containing OVAI-, OVAII- and MOG-peptide (12 μM) for 3 hrs, and termed $Tr_{/OVAI}$-, $Tr_{/OVAII}$- and $Tr_{/MOG}$-cells, respectively. CD8$^+$CD25$^+$ (perforin$^{-/-}$)Tregs were purified from perforin KO mouse splenocytes as described above.

4.2.3 *In vitro* T-cell proliferation assay

Naive CD4$^+$ and CD8$^+$CD25$^+$ Treg-treated CD4$^+$ T cells (1×10^5 cells/well) were incubated in anti-CD3 and anti-CD28 Ab-coated plate, respectively. One day subsequently, the supernatants were assayed for IL-2 secretion using ELISA kits (178). In another experiment, sDCs (1×10^5

cells/well) and their 2-fold dilutions were cultured with a constant number of naive $CD4^+$ or $CD8^+CD25^+$ Treg-treated $CD4^+$ T cells (1×10^5 cells/well) in culture medium containing anti-CD3 Ab (2 μg/mL) and IL-2 (100 U/mL) (351). After 48 hrs, ^{3}H-thymidine incorporation was determined by liquid scintillation counting.

4.2.4 Flow cytometry staining

4.2.4.1 EXO staining

FITC conjugated Abs were used for the EXOs staining. About 1 μL of 1:50 diluted FITC-conjugated Abs were added to the 20-40 μg EXOs re-suspended in 100 μL PBS, and incubated for 30 min on ice. The samples were further diluted with PBS (final volume 300-400 μL) and analyzed by flow cytometry. Expression profiles are presented in histograms of fluorescence intensity (*Log*10) of FITC on X-axis (analyzed for CD11c, CD40, CD80, 4-1BBL, OX40L and pMHC-I expression) and the number of EXOs on the Y-axis. A total of 30,000 events were analyzed by flow cytometry for each marker.

4.2.4.2 Tetramer staining assay

C57BL/6 or various gene KO mice (6 mice/group) were injected intravenously (i.v.) with DC_{OVA}, OVA-T_{EXO} or OVA-T_{EXO} with a specific molecular deficiency (3×10^6 cells/mouse). To assess recall responses, immunized mice were boosted i.v. with DC_{OVA} (0.5×10^6 cells/mouse) on day 30 after the primary immunization. Six or four days after the primary immunization or the boost, peripheral blood samples were incubated with PE-H-$2K^b$/$OVA_{257–264}$ and FITC-anti-CD8 Ab for 30 min at room temperature, and analyzed by flow cytometry.

C57BL/6 mice (8 mice/group) were i.v. immunized with sDC_{OVA} (2×10^6 cells/mouse), sDC_{OVA} plus $CD8^+CD25^+$ Tregs, $Tr_{/OVAI}$-cells or $Tr_{/OVAII}$-cells (3×10^6 cells/mouse), respectively. Six days after immunization, mice tail blood samples were analysis as described above.

4.2.4.3 Assessment of CTL responses by CD44 expression and IFN-γ secretion

HLA-A2/HER2 mice (6 mice/group) were i.v. injected with HER2-T_{EXO} (3×10^6 cells/mouse). Six days after the immunization, HLA-A2/HER2 mouse blood samples were collected for staining of FITC-anti-CD8 and PE-anti-CD44 (T-cell activation marker) Abs.

Intracellular IFN-γ secretion was also analyzed using fixation and permeabilization solution kit with BD GolgiStop (432). Briefly, blood samples were collected and diluted 1:1 using RPMI-1640 with 10% FCS. Cells were further stimulated with 10 μM of $HER2_{369-377}$ peptide (KIFGSLAFL) for 5 hrs in the presence of 0.7 μL GolgiStop/mL diluted blood in U-bottom culture plates. RBCs were then depleted using 0.85% (w/v) Tris-NH_4Cl lysis buffer. Stimulated cells were washed with PBS, stained with anti-CD8-FITC Abs at room temperature for 20 min followed by washing with PBS twice. Each sample was then fixed and permeabilized with 500μL cytofix/cytoperm solution at room temperature for 20 min. Samples were washed twice in 1× wash buffer and stained with PE-anti-IFN-γ Ab on ice for 30 min. Finally, samples were washed twice and analyzed by flow cytometry. Flow cytometry profiles are presented as dot-scatter plots. In each dot-scatter plot, X-axis represents fluorescence intensity of FITC (CD8 molecule expression) and Y-axis represents fluorescence intensity of PE (IFN-γ^+ lymphocytes). The value in each plot represents percentage of IFN-γ^+ $CD8^+$ T cells in total $CD8^+$ population.

4.2.4.4 Assessment the impact of $CD8^+CD25^+$ Tregs on effector $CD8^+$ T cells

Effector $CD8^+$ T cells (also referred to as target CTLs) were prepared from OTI transgenic mice. Splenocytes were cultured in RPMI-1640 medium containing IL-2 (20 U/mL) and ConA (1 mg/mL) for 3 days. The ConA-activated effector OTI T cells were then purified using Mouse CD8 (Ly-2) microbeads. To assess the impact of $CD8^+CD25^+$ Tregs on effector $CD8^+$ CTLs, purified $CD8^+$ OTI CTLs were co-cultured with or without $CD8^+CD25^+$ Tregs at 1:1 ratio for 16 hrs. Cell mixtures were then stained with PE-Cy5-anti-CD8 and PE-Tetramer Abs followed by FITC-anti-perforin or FITC-anti-Granzyme B staining after cell membrane permeabilized with Cytofix/Cytoperm solutions. $CD8^+$ and Tetramer double-positive population was gated for analysis of perforin and granzyme B expression by flow cytometry.

4.2.5 Cytotoxicity assays

C57BL/6 mouse splenocytes were labeled with either high (3.0 µM) or low (0.6 µM) concentrations of Carboxyfluorescein succinimidyl ester (CFSE). $CFSE^{high}$ and $CFSE^{low}$ cells were then pulsed with OVAI ($OVA_{257-264}$, SIINFEKL) and irrelevant Mut1 (FEQNTAQP) peptides, and served as internal OVA-specific target and control cells, respectively. These peptide-pulsed target cells were i.v. co-injected at 1:1 ratio into mice immunized with OVA-T_{EXO} or OVA-T_{EXO} with various molecule deficiency (3×10^6 cells/mouse) six days after the immunization. Sixteen hrs later, the residual antigen-specific $CFSE^{high}$ and control $CFSE^{low}$ target cells remaining in the recipients' spleens were analyzed by flow cytometry (176). This *in vivo* cytotoxicity assay was also performed in sDC_{OVA} (2×10^6 cells/mouse) with or without $CD8^+CD25^+$ Treg, $Tr_{/OVAI}$ and $Tr_{/OVAII}$ Tregs (3×10^6 cells/mouse) injected C57BL/6 mice six days after immunization.

In another cytotoxicity assay, the potential killing effect of $CD8^+CD25^+$ Tregs on ConA-stimulated target CTLs was assessed. Target CTLs were labeled with TFL2 (cell dye) using GranToxiLux Plus kit, and then incubated with $CD8^+CD25^+$ Tregs or ($perforin^{-/-}$)Tregs for 45 min. Cell permeable fluorogenic granzyme-B substrate was subsequently added to the cell mixture followed by flow cytometry to detect cell apoptosis by assessment of granzyme-B substrate cleavage.

4.2.6 Imaging analysis

4.2.6.1 Electron microscopic analysis of EXOs

Purified EXOs were fixed in 4% (w/v) para-formaldehyde. They were loaded on carbon-coated formvar grids and incubated for 20 min in a moist chamber. Later, the samples were washed twice with PBS and fixed in 1% (w/v) glutaraldehyde for 5 min. The samples were then washed three times with PBS and stained with aqueous uranyl for 10 min. EXOs were finally examined with a JEOL 1200EX electron microscope at 60 KV.

4.2.6.2 Confocal microscopic analysis of IS formation

OVA-T_{EXO} cells were loaded with 5 μM ThiolTracker™ Violet for 30 min at 37 ºC. Cells were allowed to adhere to the Poly-D-Lysine/Laminin coated culture slide for 30 min in RPMI-1640 containing 10% FCS. Naive OTI $CD8^+$ T cells (1:1 ratio) were added to the culture slides and co-cultured with OVA-T_{EXO} cells for another 3 hrs. Cells were fixed and permeabilized at 4 ºC for 12 hrs in the dark and stained with goat anti-PKCθ Ab followed by Cy5-conjugated anti-goat IgG. Finally, slide was mounted with ProLong Gold antifade reagent and analyzed using a Carl Zeiss LSM 510 confocal microscope with a 25× objective. Similarly, OVA-T_{EXO} cells were labeled with 5 μM 5-(and-6)-(((4-Chloromethyl)Benzoyl)Amino)Tetramethylrhodamine (CMTMR) to assess the expression of talin. Fixed and permeabilized cell conjugates were stained with mouse anti-talin Ab followed by FITC-conjugated anti-mouse IgG.

4.2.6.3 Two-photon imaging and data analysis

C57BL/6 mice were i.v. injected with CFSE-labeled (5 μM, 30 min, 37 ºC) OVA-T_{EXO} (10-15×10^6 cells) or OVA-($K^{b-/-}$)T_{EXO} cells. 24 hrs later, equal amounts of CMTMR-labeled (5 μM, 30 min, 37 ºC) naive OTI $CD8^+$ T cells were transferred into the same recipient mouse. To compare the dynamics of antigen-specific OTI with polyclonal $CD8^+$ T cells, 10-15×10^6 unlabeled OVA-T_{EXO} were injected into the C57BL/6 mouse. 24 hrs later, CFSE-labeled naive OTI $CD8^+$ T cells and CMTMR-labeled naive polyclonal $CD8^+$ T cells were co-injected into the same mouse. In order to rule out the effect of host APCs, CD11c-DTR mice (express DT receptor under CD11c promoter) were also used as recipient mice. $CD11c^+$ APCs were deleted by injection of DT (100 ng/mouse, i.p.). Neutralization Abs anti-CD20 (AISB12) and anti-CD317 (120G8) (300 μg/mouse) were i.p. injected to delete B cells and pDCs. 24 hrs later, unlabeled OVA-T_{EXO} were injected followed by CFSE-labeled naive OTI $CD8^+$ T cells and CMTMR-labeled naive polyclonal $CD8^+$ T cells as described above. Inguinal lymph nodes were collected 3 hrs later and then immobilized in an imaging chamber continuously perfused with RPMI-1640 bubbled with 95% O_2 and 5% CO_2 at 37 ºC. Imaging was performed with a two-photon laser-scanning microscope (Olympus BX51WIF fitted with a LUMPLFL/IR 40× W/0.8

NA Olympus objective lens). Samples were excited with a MaiTai Ti-Saphire laser tuned to a wavelength of 800 nm so as to equally excite both fluorophors. CFSE and CMTMR fluorescence emissions were acquired with the use of selective emission bandpass 535 nm (50 nm bandpass) and 610 nm (75 nm bandpass) filters.

To visualize DC-T cellular interactions, 5×10^6 DsRed-expressing sDC_{OVA} derived from transgenic DsRed mice were injected into footpads of C57BL/6 recipient mouse followed by i.v. injection of 5×10^6 CFSE-labeled OTII $CD4^+$ T cells one day later. To assess the influence of Tregs, 5×10^6 $CD8^+CD25^+$ Tregs or $Tr_{/OVAII}$ cells were i.v. injected one day before the injection of sDC_{OVA}. Mouse popliteal lymph node imaging was performed in an imaging chamber 6 hrs subsequent to adoptive transfer of $CD4^+$ T cells by TPM (179). Samples were excited with a MaiTai Ti-Saphire laser tuned to a wavelength of 850 nm. CFSE and DsRed fluorescence emissions were acquired with the use of selective emission bandpass 535 nm (50 nm bandpass) and 610 nm (75 nm bandpass) filters.

Images were collected with typical voxel size of 0.587 × 0.587 × 3-5 μm and volume dimension varied in each case. Imaris ×64 (Bitplane, Zurich, Switzerland) was used for four-dimensional image analysis and automated tracking of cells. The confinement ratio corresponded to the ratio of the distance between the initial and final positions of each cell to the total distance covered by the same cell. The duration of individual new contact formed during the imaging session was quantitated by individual inspection of each time slice at each z-slice level in the 4D imaging data set.

4.2.7 Tumor protection study

To examine antitumor protective immunity, C57BL/6 mice (6 mice/group) were i.v. injected with OVA-T_{EXO} or OVA-T_{EXO} with a specific molecular deficiency (3×10^6 cells/mouse). Thirty days after the immunization, mice were i.v. challenged with 0.5×10^6 OVA-expressing BL6-10_{OVA} melanoma cells. The mice were euthanized three weeks after tumor cell challenge, and the lung metastatic tumor colonies were counted in a blind fashion. Metastase on freshly isolated

lungs appeared as discrete, black-pigmented foci in BL6-10_{OVA} tumors. Metastatic foci that were too numerous to count were assigned an arbitrary value of > 300 (176).

To examine the protective antitumor immunity, transgenic HLA-A2 and HLA-A2/HER2 mice (8 mice/group) were i.v. injected with HER2-T_{EXO} (3×10^6 cells/mouse), respectively. ConA-T cells were used as a control. Six days after immunization, mice were s.c. challenged with 0.2×10^6 BL6-$10_{HLA\text{-}A2/HER2}$ tumor cells. Mice were monitored for tumor growth. For ethical reason, mice bearing tumor with 1 cm in diameter were sacrificed.

C57BL/6 mice (8 mice/group) were injected i.v. with sDC_{OVA} (2×10^6 cells/mouse) with or without co-injection of $CD8^+CD25^+$ Treg, $Tr_{/OVAI}$ or $Tr_{/OVAII}$ (3×10^6 cells/mouse). To assess the antitumor immunity, immunized mice were s.c. challenged with 0.1×10^6 BL6-10_{OVA} cells 7 days subsequent to the immunization. Mice were monitored for tumor growth. For ethical reason, mice bearing tumor with 1 cm in diameter were sacrificed.

4.2.8 EAE Induction

EAE was induced in C57BL/6 mice (10 mice/group) by s.c. injection over 4 sites in the flank with $MOG_{35\text{-}55}$ peptide (200 μg/mouse) emulsified in complete freund's adjuvant (CFA) containing 0.6 mg mycobacterium tuberculosis (MT) (433). To assess the suppressive effect, 5×10^6 $CD8^+CD25^+$ Tregs or $Tr_{/MOG}$-cells were i.v. injected into each mouse one day before and two days after MOG peptide immunization. Mice were examined daily for clinical signs. Mice were scored on scale of 0 to 5: 0, no clinical sign; 0.5, partially limp tail; 1, limp/flaccid tail; 2, moderate hind limb weakness; 2.5, one hind limb paralyzed; 3, both hind limbs paralyzed; 3.5, hind limbs paralyzed and weakness in forelimbs; 4, forelimbs paralyzed; 5, moribund/death (433).

4.2.9 Statistical analyses

Statistical analyses were carried out using Prism software (GraphPad Software Inc.) to perform *Log* rank test to compare mouse survival between groups (302). Student *t* test was performed to

determine the significance of differences between groups. A value of $p < 0.05$ was considered statistically significant.

CHAPTER 5 RESULTS

5.1 A novel T cell-based vaccine capable of stimulating long-term functional CTL memory against B16 melanoma via CD40L signaling

Our previous work have shown that ConA-stimulated $CD4^+$ T cells derived from OVA-specific TCR transgenic OTII mice can internalize OVA-pulsed, DC-released EXO (EXO_{OVA}) via TCR/MHC and LFA-1/CD54 interactions. EXO_{OVA}-loaded $CD4^+$ T cells can be used as OVA-T_{EXO}-cell vaccines capable of stimulating $CD8^+$ T-cell priming via IL-2 and CD80 costimulatory signaling. In this section, we further assessed (i) the formation of immunological synapses between $CD4^+$ T_{EXO} and cognate $CD8^+$ T cells; (ii) the critical role of exosomal pMHC-I complexes in interaction of $CD4^+$ T_{EXO} cells with cognate $CD8^+$ T cells *ex vivo* by two-photon microscopy. Furthermore, we assessed the potential role of other costimulatory molecules such as CD40L, 4-1BBL and OX40L in OVA-specific EXO-targeted T cell-based vaccine-induced $CD8^+$ CTL responses and antitumor immunity against OVA-expressing B16 melanoma cell line.

5.1.1 OVA-T_{EXO} cell form immunological synapse (IS) with $CD8^+$ T cells leading to efficient CTL responses via exosomal pMHC-I targeting

C57BL/6 BM-DCs were *in vitro* pulsed with OVA protein overnight. OVA-pulsed DCs (DC_{OVA})-released exosomes (EXO_{OVA}) were purified from DC_{OVA} culture supernatants by differential ultracentrifugation and subjected to electron microscopic analysis. As shown in **Figure 5.1A**, EXO_{OVA} showed a typical exosomal characteristic of "saucer" or round shape with a diameter 40-100 nm. DC_{OVA} and EXO_{OVA} were then stained with a panel of Abs and analyzed by flow cytometry. The relative size of EXO_{OVA} to 3.8 μm diameter aldehyde/sulfate latex beads was shown in **Figure 5.1B**. DC_{OVA} expressed CD11c (DC marker), costimulatory molecules CD40 and CD80, and pMHC-I complexes, whereas EXO_{OVA} also displayed these molecules, but in a much less extent (**Figure 5.1C**). OVA-T_{EXO} cells derived from ConA-stimulated OTII $CD4^+$ T lymphocytes (ConA-T) upon uptaking of EXO_{OVA}, expressed CD11c, CD40, CD80 and pMHC-I (**Figure 5.1D**), however, they did not express pMHC-I if using ($K^{b-/-}$)EXO_{OVA} (released from OVA protein pulsed K^b knockout BM-DCs) (**Figure 5.1E**).

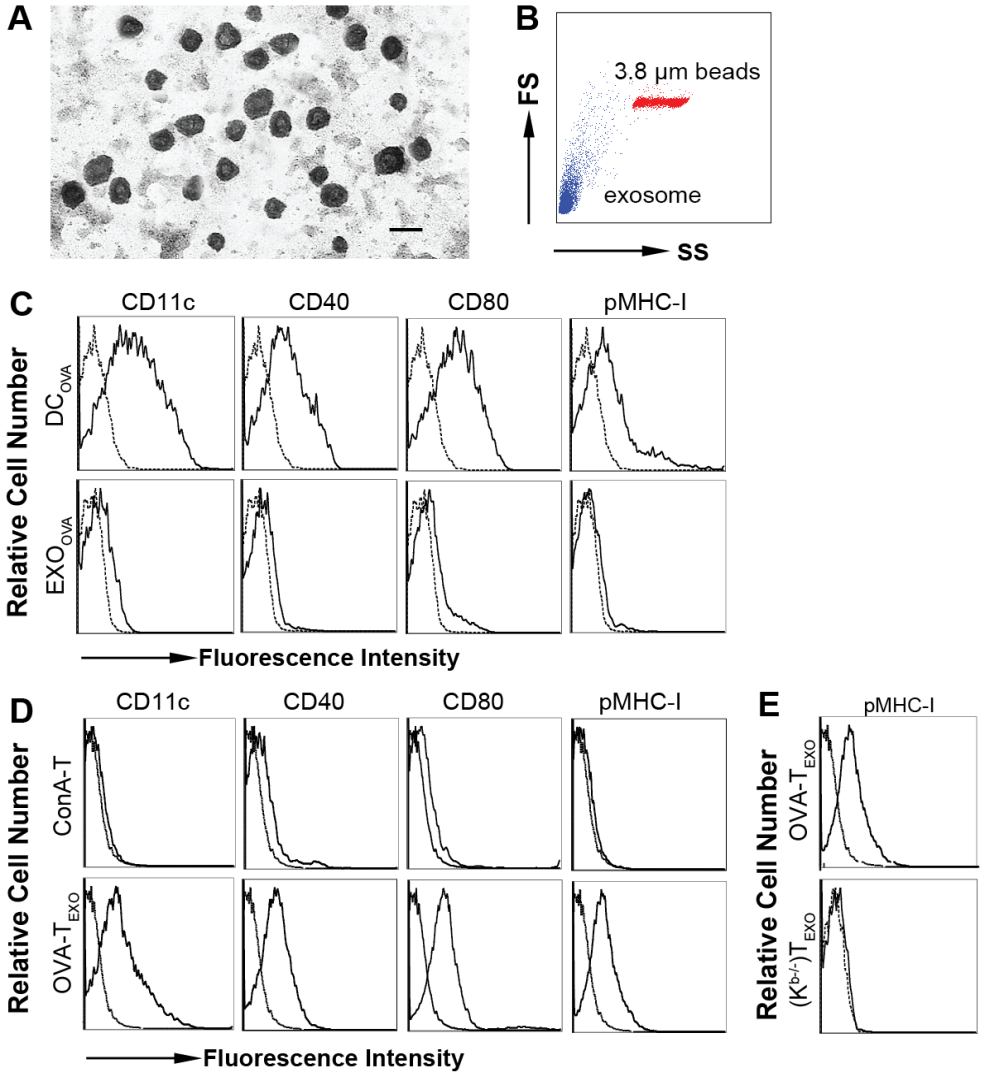

Figure 5.1 Flow cytometric analysis. (**A**) Electron micrograph of BM-DCs released EXOs. Bar, 100 nm. (**B**) Relative distribution of EXO_{OVA} in the presence of 3.8 μm diameter beads. SS: side scatter; FS: forward scatter. Flow cytometric analysis of various molecules expressed on (**C**) $DC_{OVA,}$ EXO_{OVA}, (**D**) OVA-T_{EXO} and (**E**) pMHC-I expression on OVA-($K^{b-/-}$)T_{EXO}. Samples were stained with a panel of Abs (solid lines) or isotype-matched irrelevant Abs (dotted lines). One representative experiment of two is shown.

Since EXOs harbor many immune molecules including pMHC complexes and costimulatory molecules, OVA-T_{EXO} with acquired exosomal molecules may have a potent effect in stimulating T cell responses. To examine the stimulatory effect, C57BL/6 or I-$A^{b-/-}$ mice were immunized with OVA-T_{EXO} or DC_{OVA} (used as a positive control). $CD8^+$ T-cell response was assessed using

FITC-anti-CD8 Ab and PE-H-2K^{b}/OVA$_{257-264}$ tetramer staining by flow cytometry on day 6 after the immunization. Both OVA-T$_{EXO}$ and DC$_{OVA}$ vaccinations induced *in vivo* OVA-specific CD8^{+} T cell responses in C57BL/6 mice (**Figure 5.2A**). However, OVA-T$_{EXO}$ cells but not DC$_{OVA}$ were also capable of inducing CD8^{+} T cell responses in I-A$^{b-/-}$ mice lacking classical MHC II (**Figure 5.2B**), indicating that OVA-T$_{EXO}$ could directly stimulate CD8^{+} T cell responses independent of CD4^{+} T-cell help. Since OVA-specific TCRs of the cognate CD8^{+} T cells are recognized by OVA-specific pMHC-I complex, we assumed that it is the exosomal pMHC-I that targets OVA-T$_{EXO}$ to cognate naive CD8^{+} T cells *in vivo*, leading to direct stimulation of cognate CD8^{+} T cells. To assess this assumption, C57BL/6 mice were immunized with OVA-(K$^{b-/-}$)T$_{EXO}$ lacking pMHC-I expression. We demonstrated that OVA-(K$^{b-/-}$)T$_{EXO}$ lacking pMHC-I expression completely lost the ability to stimulate OVA-specific CTL responses (**Figure 5.2A**), indicating that OVA-T$_{EXO}$ cells directly stimulate CD8^{+} T-cell responses via exosomal pMHC-I targeting.

When the TCR complex recognizes MHC-associated peptide on an APC, several T cell surface proteins and intracellular signaling molecules are rapidly mobilized to the site of T cell-APC contact. This region of physical contact between T cell and APC forms a bull's-eye-like structure that is called an IS or a supramolecular activation cluster (SMAC). Since the formation of IS between APCs and T cells is a critical event for controlling T cell activation (434), we sought to determine whether, similar to DCs, CD4^{+} OVA-T$_{EXO}$ cells form IS with cognate CD8^{+} T cells. OVA-T$_{EXO}$ cells (stained with ThiolTracker™ Violet or CMTMR) were co-cultured with naive OTI CD8^{+} T cells for 3 hrs. Cell mixtures were fixed, permeabilized and stained with either PKCθ (435, 436) (hallmark of a mature IS) or talin (435, 436) (located in the peripheral SMAC) Ab. Using confocal microscopy, we found a polarized and condensed contact region of PKCθ (red; **Figure 5.2C**) and talin (green; **Figure 5.2D**) molecules formed between OVA-T$_{EXO}$ and cognate CD8^{+} T cell, indicating the formation of mature IS.

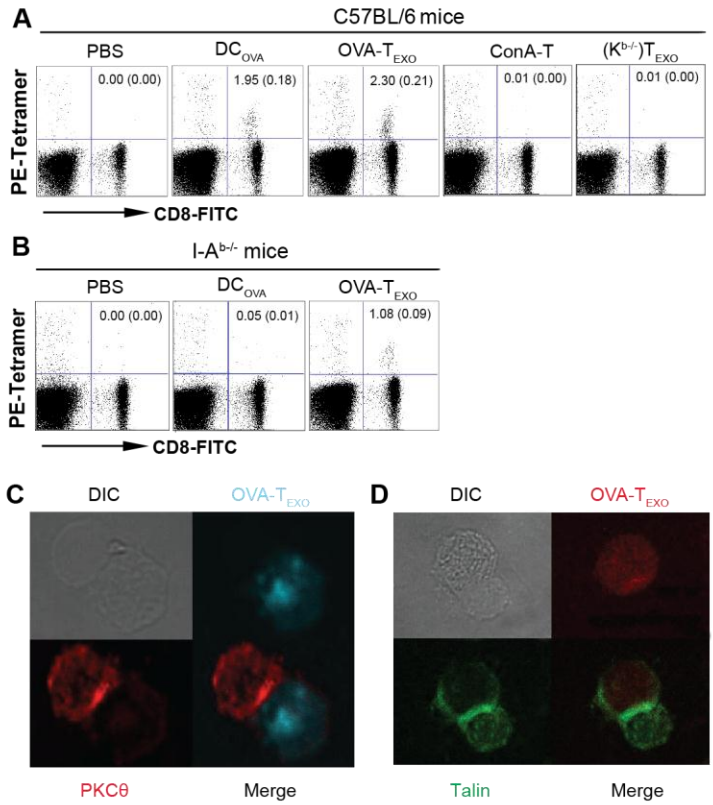

Figure 5.2 OVA-T_{EXO} cells form IS with cognate $CD8^+$ T cells leading to efficient CTL responses via exosomal pMHC-I targeting. On day 6 after immunization of (**A**) C57BL/6 mice or (**B**) I-$A^{b-/-}$ mice with OVA-T_{EXO} or OVA-($K^{b-/-}$)T_{EXO}, tail-blood samples were stained with PE-H-2K^b/$OVA_{257-264}$ tetramer and FITC-anti-CD8 Ab, and then analyzed by flow cytometry. Values in each panel represent the percentage of OVA-specific $CD8^+$ T cells to the total $CD8^+$ T-cell population with standard deviation in parenthesis. One representative experiment of two is shown. OVA-T_{EXO} stained with (**C**) ThiolTracker™ Violet (blue) or (**D**) CMTMR (red) were co-cultured with unlabeled OTI $CD8^+$ T cells for 3 hrs. Cell mixtures were fixed and stained with (C) PKCθ Abs (red) or (D) talin Abs (green). Images were obtained with a 25× objective.

5.1.2 Visualization of interactions between $CD4^+$ OVA-T_{EXO} and cognate $CD8^+$ T cells *ex vivo*

To investigate the $CD4^+$ OVA-T_{EXO}/$CD8^+$ T ($CD4^+$ T-$CD8^+$ T) cell interactio, C57BL/6 mice were i.v. injected with CFSE-labeled OVA-T_{EXO} followed by the injection of CMTMR-labeled OTI $CD8^+$ T cells. Upon exposure to OVA-T_{EXO} cells (green), naive OTI $CD8^+$ T cells (red) quickly formed tight conjugates with both stationary and motile OVA-T_{EXO} assessed by TPM (**Figure 5.3B**; **sMovie 5.1**). To those low motility clusters, cognate $CD8^+$ T cells stayed in a close proximity to stationary $CD4^+$ OVA-T_{EXO} cells. While in highly motile conjugates, OVA-T_{EXO} cells always moved in front of $CD8^+$ T cells and made turns first, suggesting that the conjugated pair is led by OVA-T_{EXO} cells. The pathways of an OVA-T_{EXO} and a $CD8^+$ T cell remained interconnected during the recording period (**Figure 5.3C**; **sMovie 5.2**), indicating that $CD4^+$ OVA-T_{EXO} cells directly interact with the cognate $CD8^+$ T cells *ex vivo*. Although motile conjugates were largely monogamous, polygamous conjugates consisting of one OVA-T_{EXO} cell sandwiched by two $CD8^+$ T cells were also observed (**Figure 5.3D**; **sMovie 5.3**).

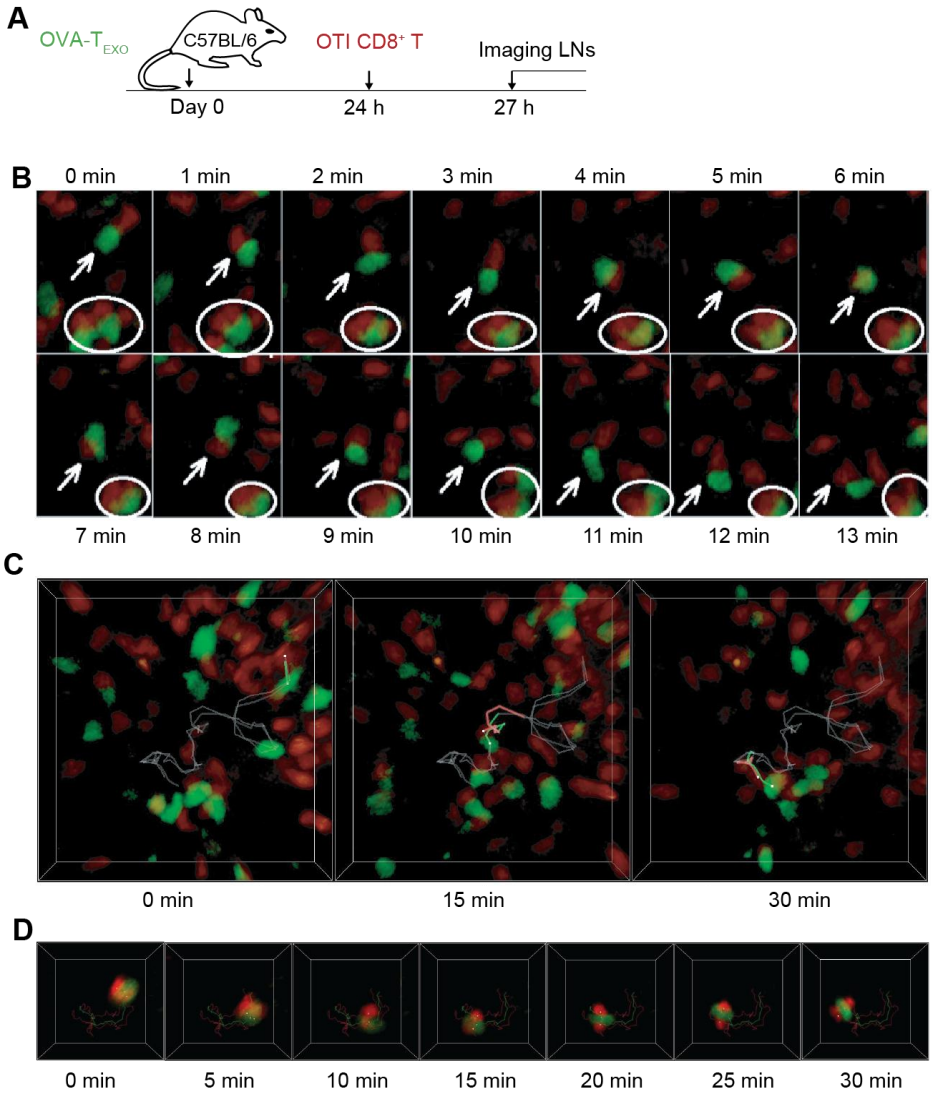

Figure 5.3 Dynamics of OVA-T_{EXO}/$CD8^+$ T-cell interactions in intact lymph nodes. (**A**) Experimental protocol. C57BL/6 mice received i.v. injection of CFSE-labeled OVA-T_{EXO}, followed by the injection of CMTMR-labeled OTI $CD8^+$ T cells 24 hrs later. Inguinal lymph nodes were imaged in T-zone region by TPM 3 hrs later. (**B**) Cognate $CD8^+$ T cells (red) formed tight conjugates with both stationary (circle) and motile (arrow) OVA-T_{EXO} cells (green). (**C**) Cognate $CD8^+$ T cells (red) followed OVA-T_{EXO} cells (green) in their migration. The pathways of an OVA-T_{EXO} (green/grey line) and a $CD8^+$ T cell (red/grey line) remaining interlocked for 30 min are shown. (**D**) Time-lapse images of one OVA-T_{EXO} (green) sandwiched by two $CD8^+$ T cells (red). White points represent the center of cells. The pathways of one OVA-T_{EXO} (green line) and two $CD8^+$ T cells (red line) remaining interlocked for 30 min are shown.

5.1.3 Visualization of the targeting role of OVA-T_{EXO} exosomal pMHC-I

Previous results showed that OVA-T_{EXO}'s pMHC-I complexes are critical in targeting their stimulatory effect to cognate $CD8^+$ T cells *in vivo*. To visually monitor the critical effect of exosomal pMHC-I, we also used OVA-($K^{b-/-}$)T_{EXO} cells lacking pMHC-I expression in TPM study. We didn't observe long lasting interactions between $CD4^+$ OVA-($K^{b-/-}$)T_{EXO} and $CD8^+$ T cells (**Figure 5.4B**, left panel; **sMovie 5.4**). The mean velocity of OTI $CD8^+$ T cells increased from 5.28 μm/min to 11.38 μm/min (**Figure 5.4C**) and the confinement ratio increased from 0.40 to 0.50 ($p < 0.01$) (**Figure 5.4D**), indicating that OVA-specific pMHC-I complexes control the motile behavior and assure the ability of OVA-T_{EXO} cells in forming stable conjugates with $CD8^+$ T cells. Interactions between OVA-($K^{b-/-}$)T_{EXO} and OTI $CD8^+$ T cells were only intermittent (most of contacts lasted less than 5 min), while OVA-T_{EXO} cells established long-lasting contacts with $CD8^+$ T cells (70% of contacts lasted more than 5 min) (**Figure 5.4E**), further confirming the important role of pMHC-I in targeting OVA-T_{EXO} cells to cognate $CD8^+$ T cells *ex vivo*.

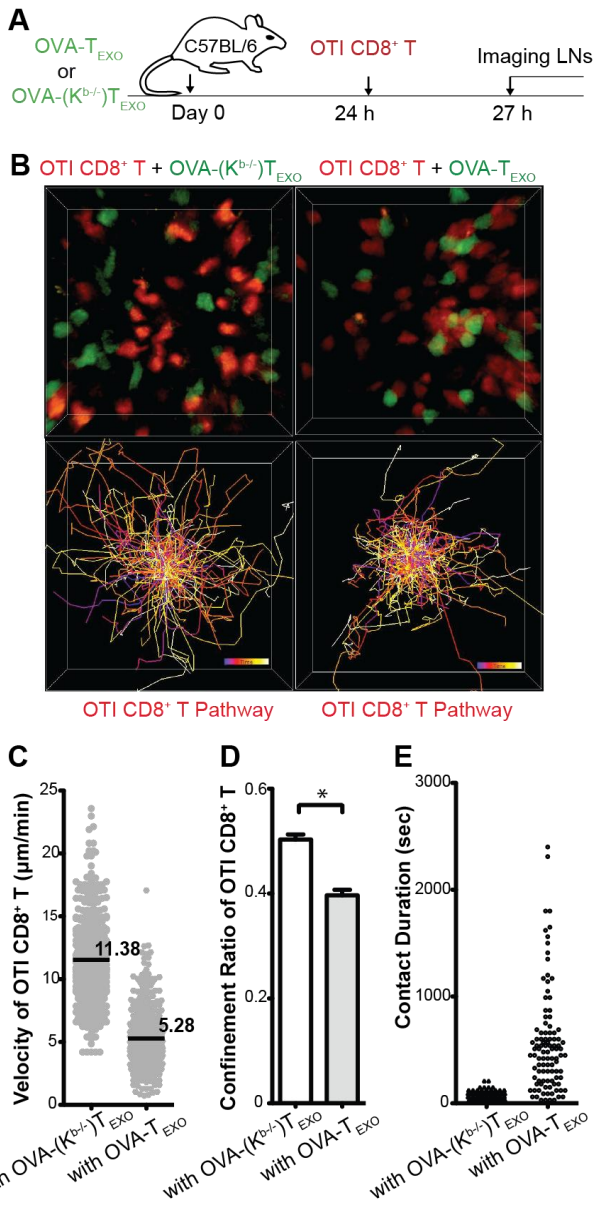

Figure 5.4 Migration dynamics of naive OTI CD8$^+$ T cells in the presence of OVA-T$_{EXO}$ or OVA-(K$^{b-/-}$)T$_{EXO}$ cells. (**A**) Experimental protocol. CFSE-labeled OVA-T$_{EXO}$ and OVA-(K$^{b-/-}$)T$_{EXO}$ were injected into the C57BL/6 recipient mice, respectively. 24 hrs later, equal amounts of CMTMR-labeled naive OTI CD8$^+$ T cells were injected, respectively. Inguinal lymph nodes were imaged in T-zone region by TPM 3 hrs later. (**B**) Tracks of OTI CD8$^+$ T cells in the present of OVA-T$_{EXO}$ (right panel) or OVA-(K$^{b-/-}$)T$_{EXO}$ (left panel). Individual cells are displayed as color-coded tracks to represent increasing time from blue (start of imaging) to yellow (end of imaging). Tracks are overlaid after normalizing their starting coordinates. (**C**) Velocity measurements of naive OTI CD8$^+$ T cells. (**D**) Confinement ratio: corresponded to the ratio of the distance between the initial and final positions of each cell to the total distance covered by the same cell. (**E**) Contact times: durations of contact between OVA-T$_{EXO}$ or OVA-(K$^{b-/-}$)T$_{EXO}$ and OTI CD8$^+$ T cells. Data were pooled from five independent experiments. *, $p < 0.01$.

To determine whether the formation of stable conjugates was due to antigen specificity, unlabeled OVA-T_{EXO} cells were injected into the C57BL/6 mouse. 24 hrs later, equal amounts of CMTMR-labeled polyclonal $CD8^+$ T cells (red) and CFSE-labeled OTI $CD8^+$ T cells (green) were co-injected into the same mouse. The intranodal migration behavior of the antigen specific or non-specific naive $CD8^+$ T cells in the presence of OVA-T_{EXO} was highly different (**sMovie 5.5**). To rule out the involvement of host APCs in affecting the different behaviors of two types of T cells, CD11c-DTR/EGFP mice were used as the recipient mice. In addition to DT treatment that depleted CD11c-DTR macrophages/myeloid DCs (437), neutralization Abs AISB12 and 120G8 were also administered to deplete B cells and pDCs (438) one day before adoptive transfer of unlabeled OVA-T_{EXO} cells. As shown in **Figure 5.5B**, DT treatment deleted $CD11c^{high}GFP^+$ DTR-DCs completely, as well as a complete depletion (> 99%) of $B220^+$ cells in AISB12- and 120G8 Ab treatment (B220 expressed on both B cells and pDCs) (**Figure 5.5C**). Similar results were obtained with all treatments, resembling initial observations in untreated animals. Polyclonal $CD8^+$ T cells (red) exhibited a highly motile migration (8.87 μm/min) covering large areas, whereas OVA-specific OTI $CD8^+$ T cells (green) showed a slower (5.15 μm/min) and much more confined movement ($p < 0.01$) (**Figure 5.5D-F**; **sMovie 5.6**). Using CD11c-DTR/EGFP mice without DT and neutralization Abs treatment as the recipient mice showed that there were no direct interactions between local CD11c-positive cells and naive OTI $CD8^+$ T cells (data not shown), indicating that OVA-T_{EXO} is the reason behind different migration behaviors of $CD8^+$ T cells.

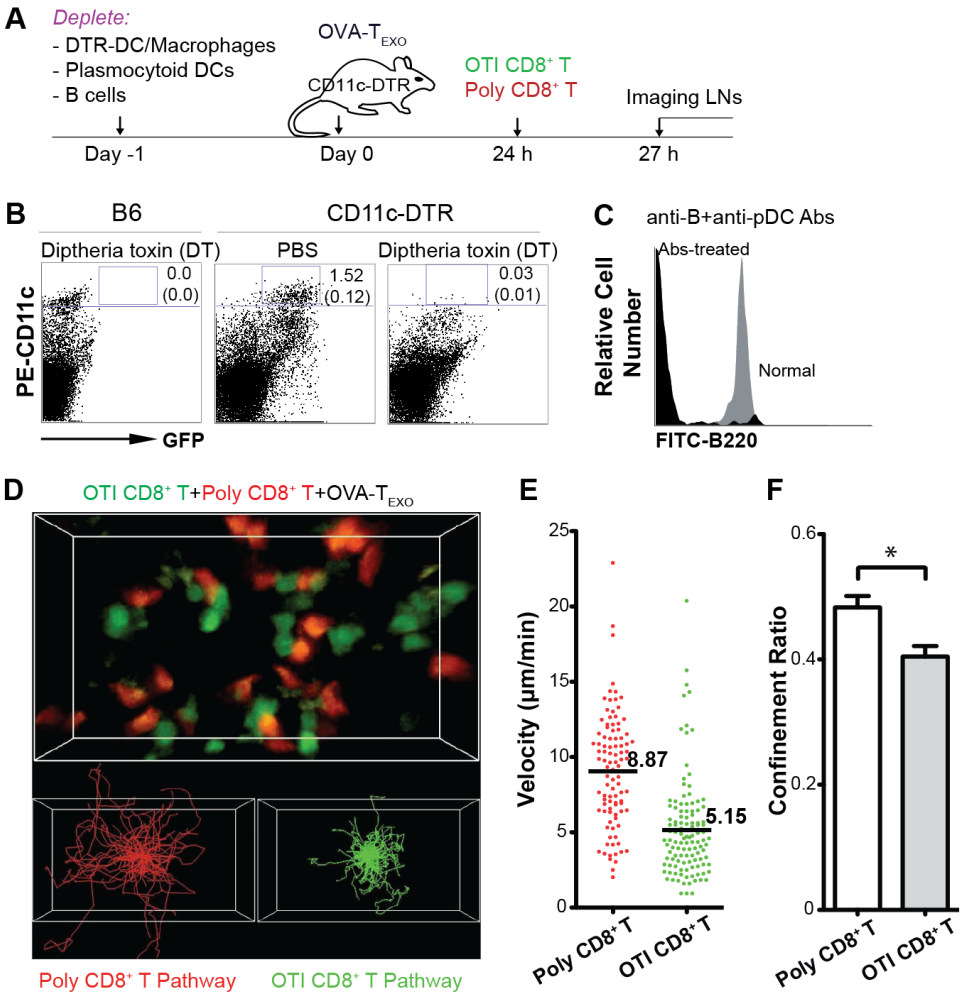

Figure 5.5 Dynamics of OTI CD8$^+$ and polyclonal CD8$^+$ T cells in the presence of OVA-T$_{EXO}$ cells. (**A**) Experimental protocol. DT, anti-CD20 Ab and anti-CD317 Ab were administered to deplete CD11c-positive cells, B cells and pDCs one day before adoptive transfer of unlabeled OVA-T$_{EXO}$ cells. 24 hrs later, equal amounts of CMTMR-labeled polyclonal CD8$^+$ T cells (red) and CFSE-labeled OTI CD8$^+$ T cells (green) were co-injected into the treated CD11c-DTR/EGFP recipient mouse. Inguinal lymph nodes were imaged in T-zone region by TPM 3 hrs later. (**B**) C57BL/6 or CD11c-DTR/EGFP mouse was i.p.-treated with DT. Splenocytes were stained with PE-CD11c Ab and analyzed by flow cytometry one day post treatment. Panel represents the mean percentage of GFP$^+$CD11c^{high} DCs in the total cell population assessed, and values in parentheses represent the standard deviation. (**C**) Histograms demonstrate depletion of B220$^+$ cells in mice with treatment of anti-CD20 and anti-CD317 Abs (black) compared with treatment of isotype control Abs (grey). (**D**) Automated tracking polyclonal CD8$^+$ T (lower left) and OTI CD8$^+$ T cells' (lower right) migration. Tracks are overlaid after normalizing their starting coordinates. (**E**) Velocity measurements of polyclonal or OTI CD8$^+$ T cells in the presence of OVA-T$_{EXO}$ cells. (**F**) The confinement ratio corresponded to the ratio of the distance between the initial and final positions of each cell to the total distance covered by the same cell. Data were pooled from five independent experiments. *, $p < 0.01$.

5.1.4 CD40L, 4-1BBL and OX40L signaling are dispensable in priming of effector $CD8^+$ CTL responses

Other costimulatory molecules, such as 4-1BBL and OX40L, have also been found to express on DC_{OVA}. Similarly, they displayed in a much less extend on EXO_{OVA} as expected (**Figure 5.6A**). As shown in **Figure 5.6B**, $(CD40L^{-/-})T_{EXO}$, $(4\text{-}1BBL^{-/-})T_{EXO}$ or $(OX40L^{-/-})T_{EXO}$ cells lacked expression of the respective molecule compared with OVA-T_{EXO} cells. We previously demonstrated that the CD80 costimulation played an important role in OVA-T_{EXO}-initiated $CD8^+$ T-cell responses (181). To assess the potential role of other costimulators such as CD40L, 4-1BBL and OX40L, C57BL/6 mice were immunized with $(CD40L^{-/-})T_{EXO}$, $(4\text{-}1BBL^{-/-})T_{EXO}$ or $(OX40L^{-/-})T_{EXO}$ cells. We found that $(CD40L^{-/-})T_{EXO}$, $(4\text{-}1BBL^{-/-})T_{EXO}$ and $(OX40L^{-/-})T_{EXO}$-stimulated OVA-specific $CD8^+$ T-cell responses assessed 6 days after the immunization were similar to responses observed in mice immunized with OVA-T_{EXO} cells (2.30%) (**Figure 5.6C**), indicating that CD40L, 4-1BBL and OX40L signaling are not involved in OVA-T_{EXO}-induced $CD8^+$ T-cell priming. This was further confirmed by our assessment of CTL priming in C57BL/6 or gene KO mice immunized with OVA-T_{EXO} cells, showing that there was also no significant difference between C57BL/6 and gene KO groups (**Figure 5.6D**). To assess the effector function of primed $CD8^+$ T cells, we performed the *in vivo* cytotoxicity assay. In the assay, OVAI peptide-pulsed/$CFSE^{high}$ and irrelevant Mut1 peptide-pulsed/$CFSE^{low}$ mouse splenocytes (which served as OVA-specific and control target cells, respectively) were i.v. co-injected at 1:1 ratio into C57BL/6 mice immunized with OVA-T_{EXO} or OVA-T_{EXO} with various molecule deficiency 6 days after the immunization. 16 hrs later, the residual OVA-specific $CFSE^{high}$ and control $CFSE^{low}$ target cells remaining in the recipients' spleens were analyzed by flow cytometry. We found that 88% of the OVA-specific $CFSE^{high}$ target cells, but none of the irrelevant control Mut1 peptide-pulsed ($CFSE^{low}$) target cells were killed in 16 hrs following target cells' transfer in OVA-T_{EXO}-immunized mice (**Figure 5.6E**), indicating that OVA-T_{EXO} can efficiently stimulate $CD8^+$ T-cell differentiation into CTL effectors, further confirming that CD40L, 4-1BBL and OX40L signaling by $CD4^+$ OVA-T_{EXO} cells is dispensable for priming effector $CD8^+$ CTL responses.

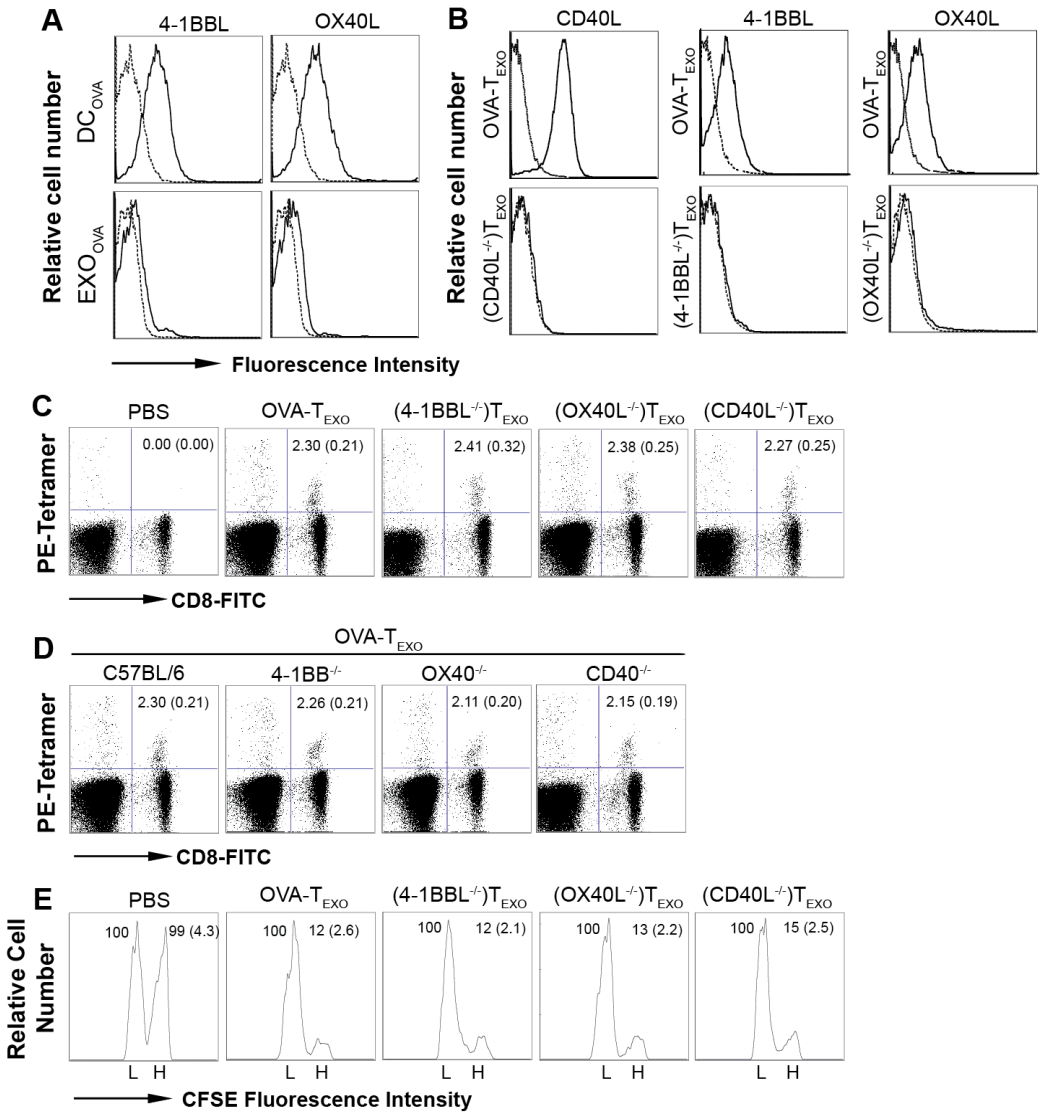

Figure 5.6 CD40L, 4-1BBL and OX40L signaling by OVA-T_{EXO} are not involved in effector $CD8^+$ T-cell priming. (**A**) Flow cytometric analysis of 4-1BBL and OX40L expression on DC_{OVA} and EXO_{OVA}. (**B**) OVA-T_{EXO} or OVA-T_{EXO} with various molecule deficiency were stained with a panel of Abs (solid lines) or isotype-matched irrelevant Abs (dotted lines) and analyzed by flow cytometry. One representative experiment of two is shown. (**C**) C57BL/6 or (**D**) gene KO mice were immunized with DC_{OVA}, OVA-T_{EXO} or OVA-T_{EXO} with indicated molecular deficiencies. Six days after the immunization, tail-blood samples were stained with PE-H-$2K^b$/OVAI peptide tetramer and FITC-anti-CD8 Ab, and analyzed by flow cytometry. Values in each panel represent the percentage of OVA-specific $CD8^+$ T cells to the total $CD8^+$ T-cell population with standard deviation in parenthesis. (**E**) *In vivo* $CD8^+$ T cell cytotoxicity assay. OVA-specific $CFSE^{high}$ and irrelevant $CFSE^{low}$ splenocytes were i.v. injected into OVA-T_{EXO} or gene KO OVA-T_{EXO}-immunized C57BL/6 mice 6 days after immunization. 16 hrs later, the percentage of residual $CFSE^{high}$ (H) and $CFSE^{low}$ (L) target cells remaining in the recipients' spleens was analyzed by flow cytometry. One representative experiment of two is shown.

5.1.5 CD40L-, but not 4-1BBL- or OX40L-induced signaling is required for functional CTL memory development

To assess whether $CD8^+$ CTLs are functional memory cells, mice were further boosted with DC_{OVA} 30 days after the immunization, when OVA-T_{EXO}-stimulated effector $CD8^+$ CTLs became memory T cells. We found over 20-fold increase in boosted $CD8^+$ T cells 4 days after the boost in mice previously immunized with OVA-specific OVA-T_{EXO}, ($OX40L^{-/-}$)T_{EXO} and (4-$1BBL^{-/-}$)T_{EXO} cells ($p > 0.05$) (**Figure 5.7B**). Interestingly, there was no increase in boosted $CD8^+$ T cells in mice previously immunized with ($CD40L^{-/-}$)T_{EXO} cells ($p < 0.05$) (**Figure 5.7B**), suggesting that CD40L-, but not 4-1BBL- and OX40L-signaling by OVA-T_{EXO} cells is required for functional $CD8^+$ T-cell memory development. This was further confirmed by our finding that $CD40^{-/-}$ CTLs in $CD40^{-/-}$ mice, which were primed by OVA-T_{EXO} also had defect in recall responses (**Figure 5.7D**). To assess the antitumor immunity, the immunized mice were further challenged with OVA-expressing B16 melanoma cell line BL6-10_{OVA} 30 days after the primary immunization. OVA-T_{EXO}, ($OX40L^{-/-}$)T_{EXO} and (4-$1BBL^{-/-}$)T_{EXO}-immunized mice were significantly more protected against BL6-10_{OVA} tumor challenge than ($CD40L^{-/-}$)T_{EXO}-immunized ones ($p < 0.01$) (**Figure 5.7E**), confirming the loss of functional CTL memory is derived from ($CD40L^{-/-}$)T_{EXO} immunization.

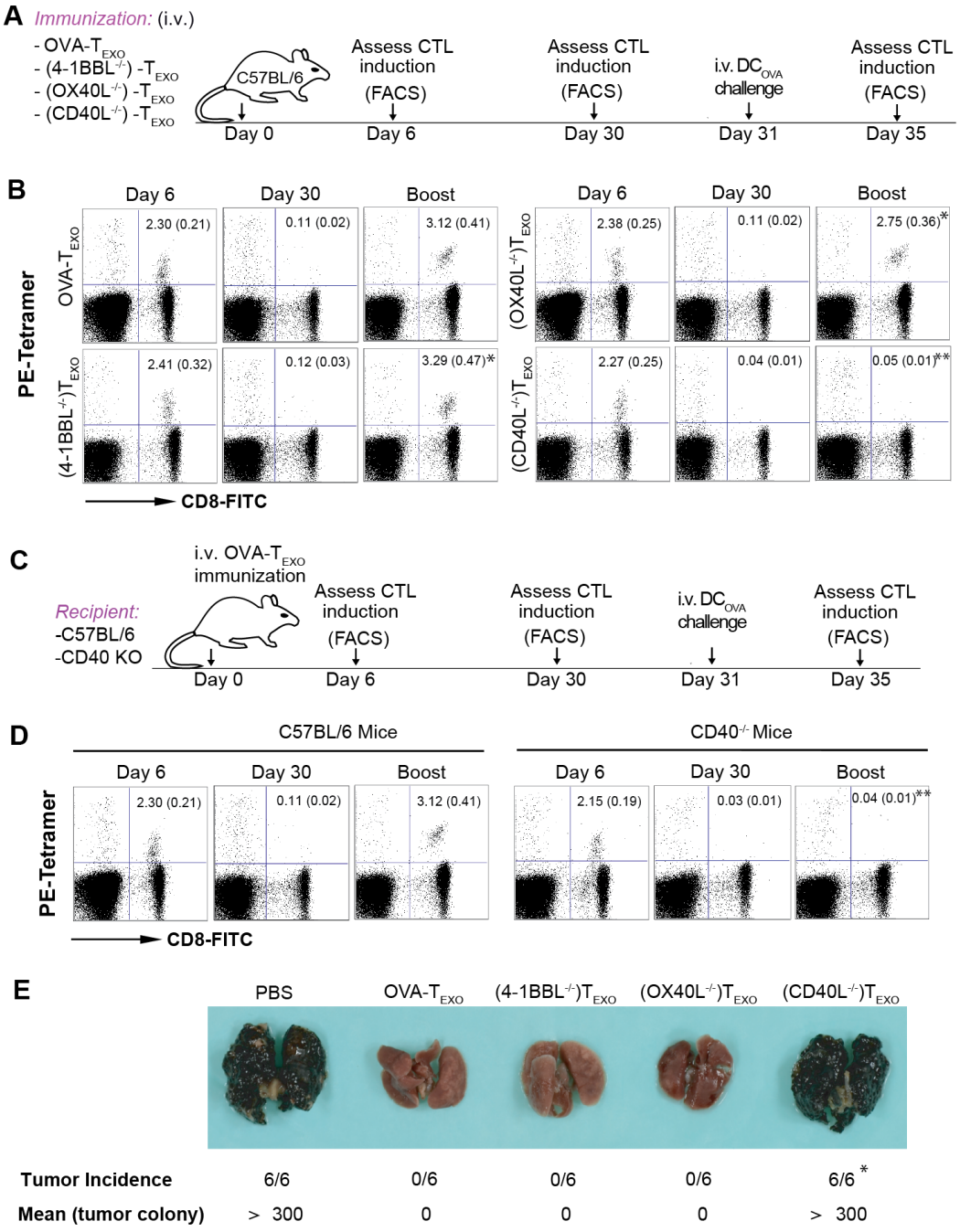

Figure 5.7 CD40L signaling by OVA-T_{EXO} is involved in $CD8^+$ T-cell memory development. (A) Experimental protocol. C57BL/6 mice were immunized with OVA-T_{EXO} or OVA-T_{EXO} with indicated molecular deficiencies. Tail-blood samples were analyzed on Day 6 and Day 30 for OVA-specific memory CTLs by flow cytometry. All above immunized mice were further boosted with DC_{OVA}. Four days after the boost, tail-blood samples of immunized mice were analyzed for OVA-specific memory CTL recall responses by flow cytometry. (**B**) Values in each panel represent the percentage of OVA-specific $CD8^+$ T cells to total $CD8^+$ T-cell population with standard deviation in parenthesis. *, $p > 0.05$ and **, $p < 0.05$ vs cohorts of OVA-T_{EXO} group (Student *t* test). (**C**) Experimental protocol. C57BL/6 or CD40 KO mice were

immunized with OVA-T_{EXO}. Tail-blood samples were analyzed at day 6 and day 30 for OVA-specific memory CTLs by flow cytometry. All above immunized mice were further boosted with DC_{OVA}. Four days after the boost, tail-blood samples of immunized mice were analyzed for OVA-specific memory CTL recall responses by flow cytometry. (**D**) Values in each panel represent the percentage of OVA-specific $CD8^+$ T cells to total $CD8^+$ T-cell population with standard deviation in parenthesis. **, $p < 0.05$ vs cohorts of C57BL/6 mice (Student *t* test). (**E**) Lung metastatic BL6-10_{OVA} melanoma in immunized mice. The OVA-$T_{EXO,}$ ($CD40L^{-/-}$)T_{EXO}, (4-$1BBL^{-/-}$)T_{EXO} or ($OX40L^{-/-}$)T_{EXO} cells immunized mice were challenged with BL6-10_{OVA} tumor cells at day 30 following the primary immunization, and mice were sacrificed three weeks subsequent to challenge. Lungs with black tumor nodules are displayed. *, $p < 0.01$ vs cohorts of OVA-T_{EXO} group (Mann-Whilney-U test). One representative experiment of two is shown.

5.2 HER2-specific $CD4^+$ T cell-based vaccination stimulating CTL responses leading to antitumor immunity in HLA-A2/HER2 mice

Since the success of DC-released exosome-targeted T cell-based vaccines in OVA-specific antitumor immunity, we applied this vaccine strategy to HER2 tumor antigen. In this section, we first constructed a recombinant human HER2-expressing adenovirus and established a HER2 transgenic B16 melanoma cell line. We then examined HER2-specific $CD8^+$ CTL responses and antitumor immunity by HER2-specific EXO-targeted T cell-based vaccine in double transgenic HLA-A2/HER2 mice with HER2-specific self-immune tolerance.

5.2.1 AdV_{HER2} construction

To construct recombinant adenovirus-expressing human HER2 690aa, we firstly obtained the human $HER2_{690aa}$ 2070 bp cDNA fragments (**Figure 5.8B**, *lane 1*) from pcDNA3.1/HER2 plasmids by *HindIII* and *XbaI* digestion. The released fragments were subcloned into pShuttle-CMV transfer plasmid at *HindIII* and *XbaI* sites, and identified by PCR (**Figure 5.8C**, *lane 2*) and double enzyme digestion (**Figure 5.8D**, *lane 4*). The recombinant transfer plasmid pShuttle-CMV/$HER2_{690aa}$ or control pShuttle-CMV was then transformed into BJ5183 bacteria containing backbone plasmids RGD-pAdEasy-1 for homologous recombination. The RGD-pAdEasy-1-pShuttle-CMV/$HER2_{690aa}$ or control RGD-pAdEasy-1-pShuttle-CMV (termed RGD-pAd/$HER2_{690aa}$ and RGD-pAd hereafter) homologous recombinant adenoviral plasmids were screened by comparison of plasmid size with pShuttle-CMV/$HER2_{690aa}$ (pShuttle-CMV) and RGD-pAdEasy-1. RGD-pAd/$HER2_{690aa}$ (**Figure 5.8E,** right panel, clone #6) and RGD-pAd (**Figure 5.8E,** left panel, clone #5) plasmids were then abundantly amplified in *E.coli* DH5α bacteria and purified by QIAprep Spin Miniprep Kit. To confirming $HER2_{690aa}$ fragments in the RGD-pAd/$HER2_{690aa}$ homologous recombinant adenoviral plasmids, PCR analysis was further performed (**Figure 5.8F**, *lane 2*). Both of *PacI*-digested RGD-pAd/$HER2_{690aa}$ and RGD-pAd released 4.5 kb fragment of ori and kanamycin (Kana) resistance gene (**Figure 5.8G**, *lane 1 and 2*), suggesting the homologous recombination happened at replication origin sites between transfer plasmid pShuttle-CMV/$HER2_{690aa}$ or pShuttle-CMV and adenoviral backbone plasmid RGD-pAdEasy-1.

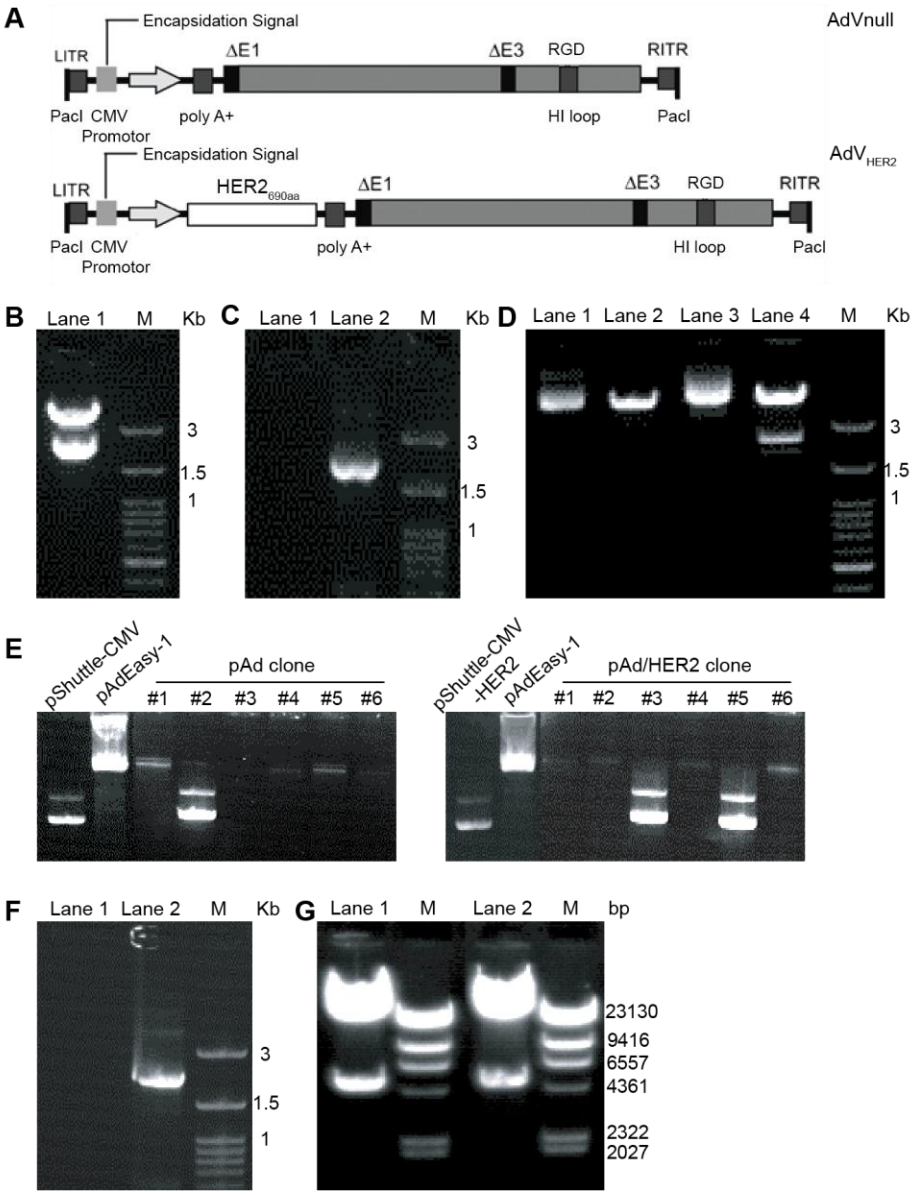

Figure 5.8 Construction of AdV_{HER2} adenoviral vector. (**A**) Schematic representation of AdV vectors. The E1/E3-deleted replication-deficient AdV vectors are under the regulation of the cytomegalovirus (CMV) early/immediate promoter/enhancer. The AdV vectors include AdVnull without any transgene expression and AdV_{HER2} expressing transgene human $HER2_{690aa}$. ITR, inverted terminal repeat (**B**) The 2070 bp human $HER2_{690aa}$ cDNA fragments (lane 1) were released from pcDNA3.1neo/$HER2_{690aa}$ plasmids by double digestion with *HindIII* and *XbaI*. (**C**) The human $HER2_{690aa}$ cDNA fragments were amplified by PCR using recombinant pShuttle-CMV/$HER2_{690aa}$ (lane 2) or pShuttle-CMV control plasmids (lane 1) as templates and primer sets specific for human $HER2_{690aa}$. (**D**) The recombinant plasmids pShuttle-CMV/$HER2_{690aa}$ (lane 4) or pShuttle-CMV control plasmids (lane 2) were digested with *HindIII* and *XbaI* or not (lane 3 and lane 1). (**E**) Identification of RGD-pAd/$HER2_{690aa}$ by molecular weight. Kana-resistant clone derived plasmids from pShuttle-CMV/$HER2_{690aa}$ (right, clone # 1-6) or pShuttle-

CMV transformed in BJ5183 containing RGD-pAdEasy-1 (left, clone # 1-6) were resolved in 0.7% TAE-agarose gel electrophoresis with SYBR® Safe DNA Gel staining. (**F**) $HER2_{690aa}$ cDNA fragments were amplified by PCR using RGD-pAd/$HER2_{690aa}$ (lane 2) or RGD-pAd control plasmids (lane 1) as templates and primer sets specific for human $HER2_{690aa}$. The reaction products in (B-D, F) were resolved in 1% TAE-agarose gel electrophoresis with SYBR® Safe DNA Gel staining. M, 100 bp Plus Opti-DNA Marker. (**G**) Identification of RGD-pAd/$HER2_{690aa}$ by *PacI* digestion. The RGD-pAd/$HER2_{690aa}$ (lane 2) or RGD-pAd control plasmids (lane 1) were digested with *PacI*. The reaction products were resolved in 0.7% TAE-agarose gel electrophoresis with SYBR® Safe DNA Gel staining. M, *λ HindIII* DNA marker.

5.2.2 Adenovirus-mediated human $HER2_{690aa}$ transgene expression

After homologous recombination of pShuttle-CMV/$HER2_{690aa}$ or control pShuttle-CMV with RGD-pAdEasy-1 in *E.coli* BJ5183 bacteria, recombinant adenoviruses $AdV_{HER2/690aa}$ (termed AdV_{HER2} hereafter) and control AdV blank adenovirus were subsequently abundantly amplified in HEK293 cells, and purified by CsCl density-gradient ultracentrifugation. HLA-A2/HER2 mouse BM-DCs transfected with AdV_{HER2} at MOI of 100 (302) were termed DC_{HER2}. 24 hrs after infection, total cellular RNAs derived from AdV_{HER2}- or AdV-infected HEK293 and BM-DCs, as well as uninfected HEK293 and BM-DCs were analyzed by RT-PCR, respectively. As shown in **Figure 5.9A**, abundant amounts of human $HER2_{690aa}$ transcriptional expression were found in AdV_{HER2}-infected HEK293 and BM-DCs but not in AdV-infected or uninfected control cells. Flow cytometric analysis (**Figure 5.9B**) showed the translational expression of adenovirus-mediated human $HER2_{690aa}$ on the surfaces of AdV_{HER2}-infected HEK293 and DC_{HER2} cells. Above data indicate that the constructed AdV_{HER2} harboring human $HER2_{690aa}$ gene can functionally direct human $HER2_{690aa}$ transgene expression in mammalian cells such as HEK293 cells and BM-DCs.

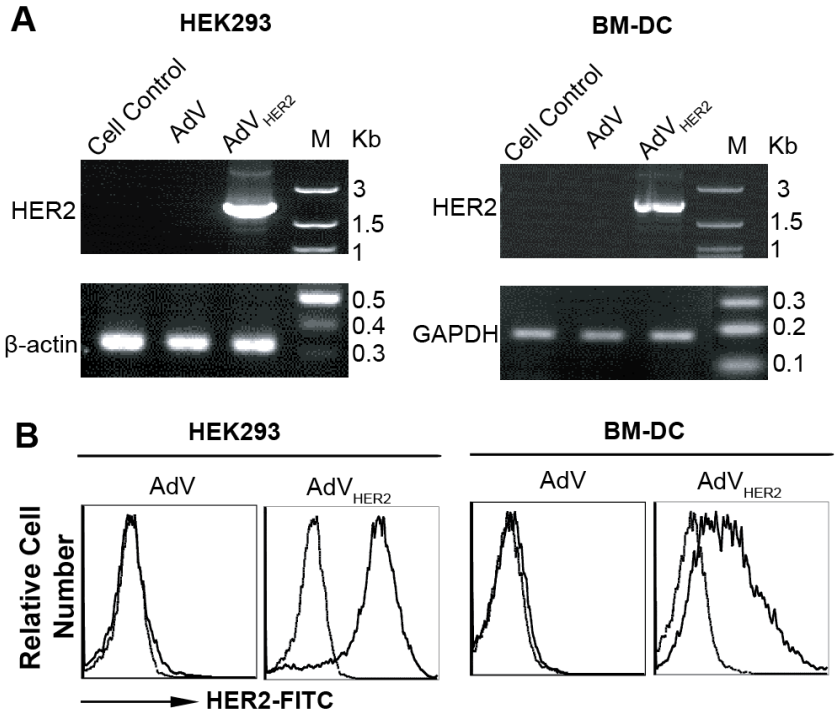

Figure 5.9 Adenovirus-mediated human $HER2_{690aa}$ transgene expression. The HEK293 cells and BM-DCs were infected with AdV_{HER2} or AdV blank adenovirus at the MOI of 10 (HEK293) or 100 (BM-DCs). The adenovirus-mediated human $HER2_{690aa}$ transgene expression was then determined by RT-PCR and flow cytometry, respectively. (**A**) Total cellular RNAs were extracted using RNeasy Plus Mini Kit. cDNA was synthesized immediately using RT² First Strand Kit. PCRs were conducted using primer sets specific for human $HER2_{690aa}$ and internal control human housekeep gene β-actin or mouse housekeep gene GAPDH, respectively. (**B**) The AdV_{HER2}- or AdV-infected HEK293 and BM-DC cells (solid lines) and uninfected HEK293 and BM-DC control cells (dotted lines) were stained with mouse anti-human CD340 (ErbB2/HER2) monoclonal Ab (clone 24D2) followed by FITC-conjugated anti-mouse IgG secondary Ab, and analyzed by flow cytometry.

5.2.3 Establishment of transgenic tumor cell lines

To select an optimal BL6-10_{HER2} transgenic tumor cell line stably and highly expressing human $HER2_{690aa}$, total 10 G418-resistant monoclones derived from G418-resistant BL6-10-pcDNA3.1/HER2 or mock BL6-10-pcDNA3.1(+)neo transfectants were employed to expanded and then subjected to RT-PCR and flow cytometric analysis. As shown in **Figure 5.10A**, significant transcriptional amount of transgene $HER2_{690aa}$ were found in 9 G418-resistant BL6-10-pcDNA3.1/HER2 clones (clone #1, 2, 4, 5, 6, 7, 8, 9 and 10) but not in clone #3, suggesting that clone #3 derived from the resistance to G418 of BL6-10 tumor cells themselves. Furthermore, flow cytometric analysis (**Figure 5.10B**) showed that only clone #1, 4 and 10 among above 9 clones stably expressed high translational levels of transgene $HER2_{690aa}$ on the surface of BL6-10 tumor cells, whereas others expressed either moderate or undetectable levels of $HER2_{690aa}$. In addition, no detectable amount of $HER2_{690aa}$ at both transcriptional and translational levels was found in BL6-10-pcDNA3.1 (+)neo or BL6-10 control tumor cells (**Figure 5.10**). The data indicated that a human $HER2_{690aa}$-transgenic BL6-10 tumor cell line (BL6-10_{HER2}) with stable and high expression of human $HER2_{690aa}$ was successfully established. BL6-$10_{HLA-A2/HER2}$ double transgenic tumor cells were constructed by transfecting pcDNA3.1/HLA-A2 or control pcDNA3.1 (+) hygro plasmids containing hygromycin resistance gene into BL6-10_{HER-2} tumor cells. Flow cytometric analysis (**Figure 5.10C**) revealed the Hygro and G418 double-resistant clone stably exhibited high levels of human $HER2_{690aa}$ and moderate levels of HLA-A2 on the surface of BL6-$10_{HLA-A2/HER2}$ transgenic cells. No detectable amount of HLA-A2 or HER2 was found in BL6-10 control tumor cells. Above data indicate the successful establishment of a human $HER2_{690aa}$ and HLA-A2 double-transgenic BL6-10 (BL6-$10_{HLA-A2/HER2}$) tumor cell line with stable and high expression of both human $HER2_{690aa}$ and HLA-A2.

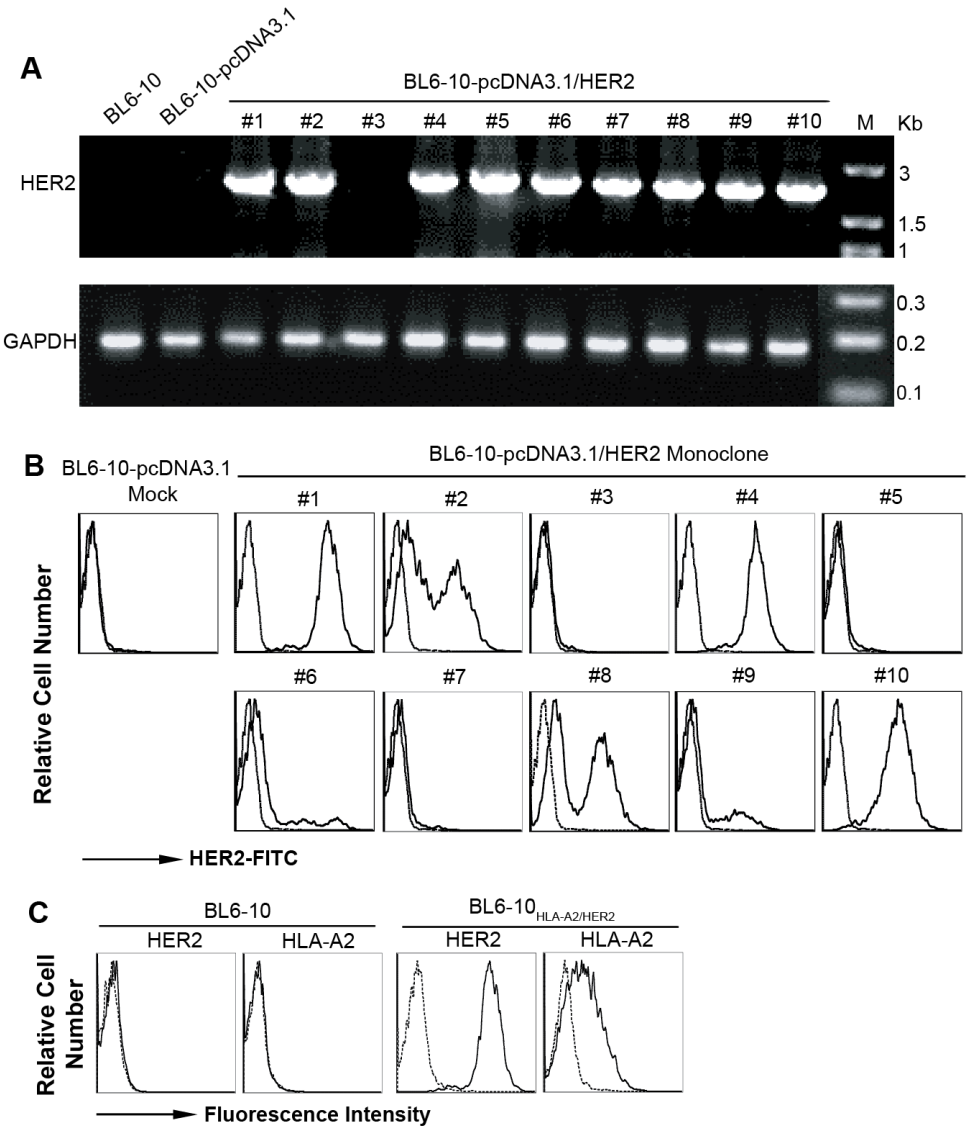

Figure 5.10 Establishment of BL6-10$_{HLA-A2/HER2}$ transgenic cell line. (**A**) RT-PCR analysis of human HER-2$_{690aa}$ transgene transcriptional expression in BL6-10$_{HER2}$ tumor cells. Total cellular RNAs were obtained from G418-resistant pcDNA3.1neo/HER2- or pcDNA3.1neo-transfected BL6-10 monoclones and untransfected BL6-10 control cells. PCRs were conducted using primer sets specific for HER2$_{690aa}$ and internal control housekeep gene GAPDH, respectively. (**B**) The G418-resistant pcDNA3.1neo/HER2- and pcDNA3.1neo-transfected BL6-10 monoclone cells (solid lines) or untransfected BL6-10 control cells (dotted lines) were stained with anti-HER2 Abs, and analyzed by flow cytometry. (**C**) BL6-10$_{HLA-A2/HER2}$ tumor cells were stained with anti-HER2, anti-HLA-A2 Ab (solid lines) or irrelevant isotype-matched control Ab (dotted lines), and analyzed by flow cytometry. One representative experiment of two is shown.

5.2.4 HER2-T_{EXO} vaccine stimulates CTL responses leading to antitumor immunity in double transgenic HLA-A2/HER2 mice

AdV_{HER2} transfected BM-DCs can express DC-derived molecules, such as CD11c, CD40 and CD80, as well as HER2. Whereas EXO_{HER2} derived from the culture supernatants of BM-DC_{HER2} can only express them in a less extent (**Figure 5.11A**). ConA-T cells generated from double transgenic mice were incubated with EXO_{HER2} and termed HER2-T_{EXO}, which also expressed CD11c, CD40, CD80 and HER2. The stimulatory effect of HER2-T_{EXO} was evaluated in double transgenic mouse HLA-A2/HER2 generated by crossing male HER2 with homozygous female HLA-A2 mice. After HLA-A2/HER2 mice were immunized, $CD8^+$ CTL responses were assessed by using nonspecific FITC-anti-CD8 and PE-anti-CD44 Abs staining by flow cytometry. HER2-T_{EXO} more efficiently stimulated the upregulated expression of T-cell activation marker CD44 on $CD8^+$ T cells than ConA-T cells ($p < 0.05$) (**Figure 5.11B** upper panel). HER2-specific $CD8^+$ T cell responses were further quantified by intracellular IFN-γ staining assay. 4.16% $CD8^+$ T cells in HER2-T_{EXO}-immunized mice produced IFN-γ after $HER2_{369-377}$ peptide stimulation, which is significantly more than that in ConA-T-immunized mice (0.42%) ($p < 0.05$) (**Figure 5.11B** lower panel), indicating that HER2-T_{EXO} vaccine stimulates HER2-specific CTL responses.

In animal studies, HLA-A2 and HLA-A2/HER2 mice were immunized with HER2-T_{EXO} and ConA-T, respectively, followed by BL6-$10_{HLA\text{-}A2/HER2}$ tumor cell challenge. All 8/8 (100%) mice immunized with HER2-T_{EXO} had complete antitumor immune protection in transgenic HLA-A2 mice (**Figure 5.11E**). Furthermore, HER2-T_{EXO} vaccine was capable of protecting 2/8 (25%) mice from BL6-$10_{HLA\text{-}A2/HER2}$ tumor challenge, and the remaining 6/8 (75%) mice immunized with HER2-T_{EXO} had significantly prolonged survival than mice immunized with the control ConA-T ($p < 0.05$) (**Figure 5.11F**), indicating that HER2-T_{EXO} can stimulate CTL responses, leading to partially protective immunity against HLA-A2/HER2-expressing BL6-$10_{HLA\text{-}A2/HER2}$ tumor challenge in double transgenic HLA-A2/HER2 mice with HER2-specific self immune tolerance.

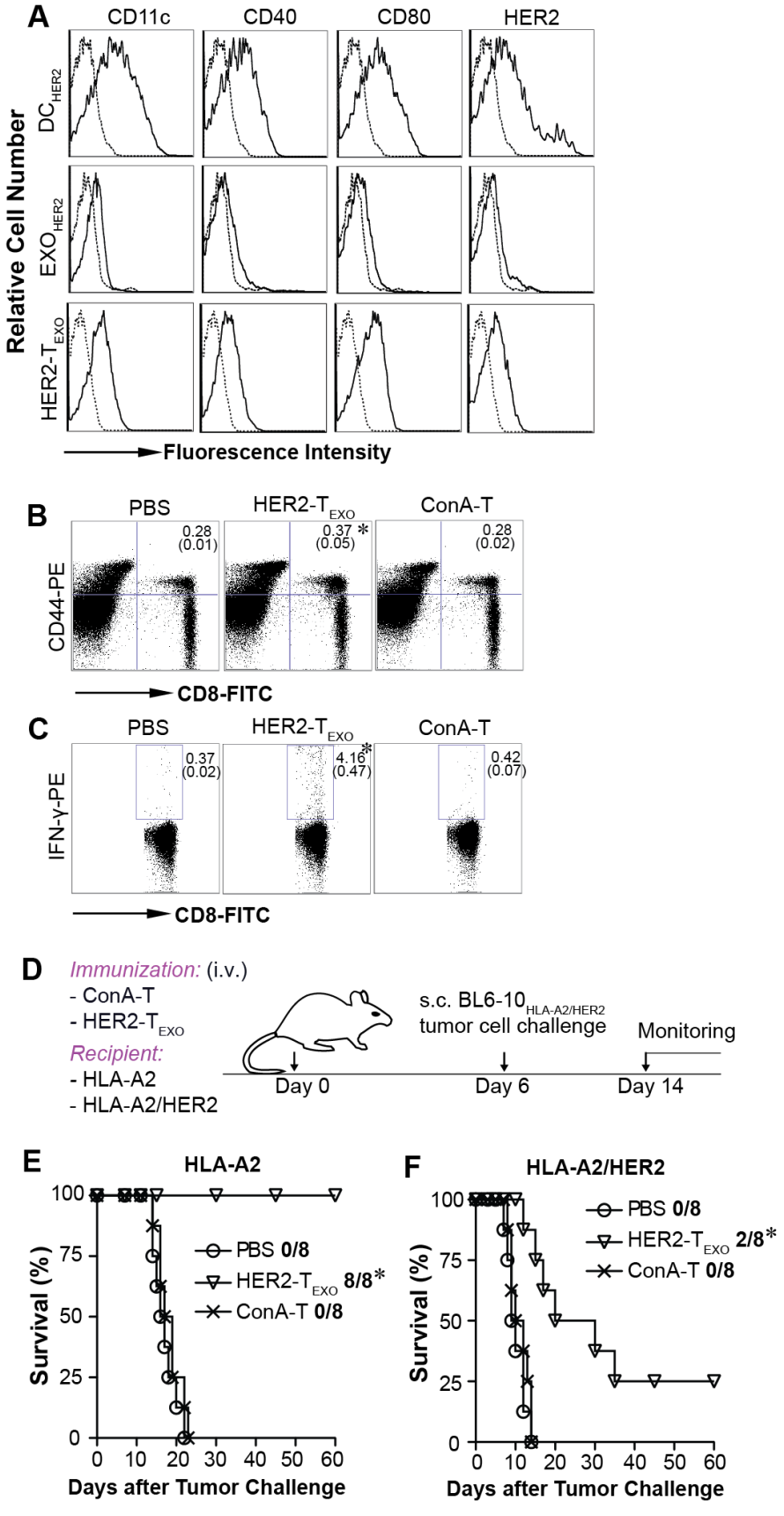
A
CD11c
CD40
CD80
HER2
DC HER2
EXO HER2
HER2-T EXO
Relative Cell Number
Fluorescence Intensity
B
PBS
HER2-T EXO
ConA-T
0.28 (0.01)
0.37 * (0.05)
0.28 (0.02)
CD44-PE
CD8-FITC
C
PBS
HER2-T EXO
ConA-T
0.37 (0.02)
4.16 * (0.47)
0.42 (0.07)
IFN-γ-PE
CD8-FITC
D
Immunization: (i.v.)
- ConA-T
- HER2-T EXO
Recipient:
- HLA-A2
- HLA-A2/HER2
s.c. BL6-10 HLA-A2/HER2 tumor cell challenge
Monitoring
Day 0
Day 6
Day 14
E
HLA-A2
PBS 0/8
HER2-T EXO 8/8*
ConA-T 0/8
Survival (%)
Days after Tumor Challenge
F
HLA-A2/HER2
PBS 0/8
HER2-T EXO 2/8*
ConA-T 0/8
Survival (%)
Days after Tumor Challenge

Figure 5.11 HER2-T_{EXO} vaccine stimulates CTL responses and antitumor immunity in HLA-A2/HER2 mice. (**A**) Flow cytometric analysis of various molecules expressed on DC_{HER2}, EXO_{HER2} and HER2-T_{EXO}. Samples were stained with a panel of Abs (solid lines) or isotype-matched irrelevant Abs (dotted lines). One representative experiment of two is shown. Six days after HER2-T_{EXO} immunization, tail-blood samples were stained with FITC-anti-CD8 and (**B**) PE-anti-CD44 or (**C**) PE-anti-IFN-γ Abs, and then analyzed by flow cytometry. Values represent the percentage of HER2-specific $CD8^+$ T cells to total $CD8^+$ T-cell population with standard deviation in parenthesis. *, $p < 0.05$ vs cohorts of ConA-T cells (Student *t* test). (**D**) Experimental protocol. (**E**) HLA-A2 and (**F**) HLA-A2/HER2 mice were immunized with HER2-T_{EXO} or control ConA-T cells, respectively. Six days after immunization, mice were s.c. challenged with BL6-$10_{HLA-A2/HER2}$ tumor cells. Tumor growth was monitored daily and mice were sacrificed when tumors grew to 1 cm in diameter. *, $p < 0.05$ vs cohorts of ConA-T cells (*Log* rank test). One representative experiment of two is shown.

5.3 Redirecting antigen-specificity by peptide/MHC-II arming to nonspecific $CD8^+CD25^+$ Tregs for enhanced immunosuppression

Unlike $CD4^+CD25^+$ Tregs, the critical cellular and molecular mechanisms responsible for $CD8^+CD25^+$ Treg-mediated suppression remain largely unknown. In this section, we assessed immunosuppressive effects and potential mechanisms of *in vitro* expended $CD8^+CD25^+$ Tregs. In addition, antigen-specific pMHC complex-armed $CD8^+CD25^+$ Tregs were further assessed their enhanced inhibitory effects in both OVA-specific tumor model and MOG-induced EAE model.

5.3.1 $CD8^+CD25^+$ T cells express some of Tregs' markers

$CD4^+CD25^+$ and $CD8^+CD25^+$ T cells were first analyzed using regulatory T cell staining kit. As shown in **Figure 5.12A**, $CD4^+CD25^+$ and $CD8^+CD25^+$ T cells accounted for 7.12% and 0.43% of total $CD4^+$ T cell and $CD8^+$ T cell population in mouse splenocytes, respectively, which is consistent with previous reports (351, 439). Both $CD4^+CD25^+$ and $CD8^+CD25^+$ T cells expressed Foxp3. Purified $CD8^+CD25^+$ double positive T cells were then expanded *in vitro* using CD3/CD28 beads for 4-6 days, and analyzed by flow cytometry. $CD8^+CD25^+$ Tregs expressed Treg markers such as cell-surface CD25, CD103, GITR, CTLA-4, as well as intracellular perforin and granzyme B (**Figure 5.12B**). In addition, they also expressed cell surface CD28.

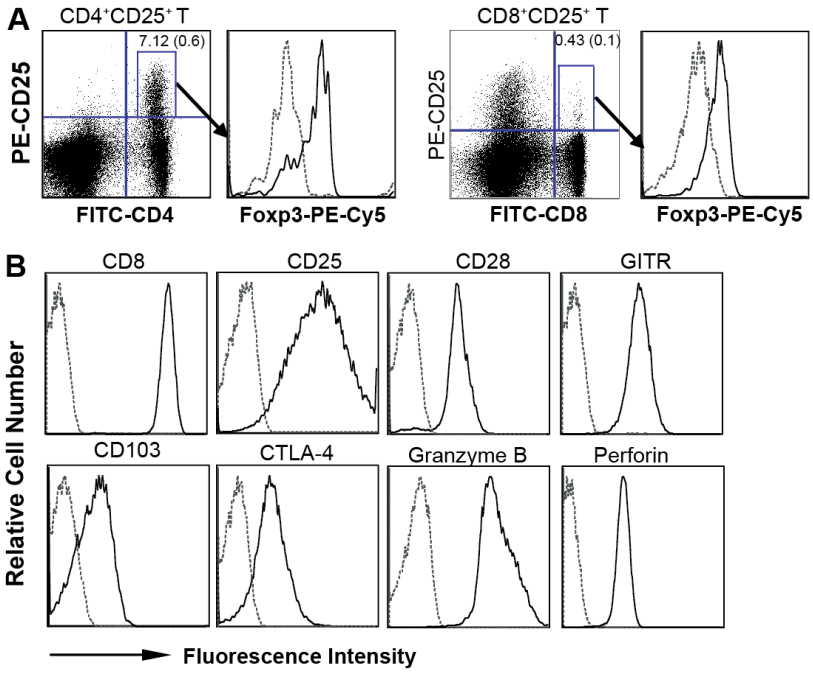

Figure 5.12 Phenotypic characterization of $CD8^+CD25^+$ Tregs. (**A**) Flow cytometric analysis of Foxp3 expression on $CD4^+CD25^+$ and $CD8^+CD25^+$ T cells. C57BL/6 mouse splenocytes were stained with PE-anti-CD25 and FITC-anti-CD4 or -CD8 Abs, and then stained with PE-Cy5-anti-Foxp3 Ab after cell membrane permeabilized with Cytofix/Cytoperm solutions. The stained cells were analyzed by flow cytometry. Naive $CD4^+CD25^+$ and $CD8^+CD25^+$ T cells in boxes were gated for analysis of Foxp3 expression. (**B**) *In vitro* expanded $CD8^+CD25^+$ Tregs were stained with FITC Abs for different molecules (solid lines) or FITC-conjugated isotype-matched irrelevant Abs (dotted lines), and analyzed by flow cytometry.

5.3.2 Immune suppression of $CD8^+CD25^+$ Tregs

To assess the immune suppression of $CD8^+CD25^+$ Tregs, C57BL/6 mice were i.v. immunized with sDC_{OVA} with co-injection of $CD8^+CD25^+$ Tregs. CTL responses were examined using mouse blood samples by flow cytometry. sDC_{OVA} stimulated PE-H-$2K^b$/OVAI tetramer-positive $CD8^+$ T cell responses, accounting for 1.82% in total $CD8^+$ T-cell population in C57BL/6 mice. However, PE-H-$2K^b$/OVAI tetramer-positive $CD8^+$ T-cell responses in mice with co-injection of $CD8^+CD25^+$ Tregs significantly dropped from 1.82% to 1.17% in the total $CD8^+$ T-cell population ($p < 0.05$) (**Figure 5.13B**), indicating that $CD8^+CD25^+$ Tregs are capable of suppressing *in vivo* sDC_{OVA}-stimulated OVA-specific $CD8^+$ T-cell responses. Next, *in vivo* cytotoxicity assay was performed to assess whether $CD8^+CD25^+$ Tregs suppress $CD8^+$ T-cell differentiation into effector $CD8^+$ CTLs. As shown in **Figure 5.13C**, 82.7% of the OVA-specific $CFSE^{high}$ target cells, but none of the irrelevant control Mut1 peptide-pulsed $CFSE^{low}$ target cells were killed over 16 hrs after transfer of target cells into mice immunized with sDC_{OVA}, while the injection of $CD8^+CD25^+$ Tregs significantly reduced the loss of $CFSE^{high}$ target cells to 57.9% (**Figure 5.13C**), indicating that $CD8^+CD25^+$ Tregs efficiently inhibit *in vivo* effector CTL responses. To assess whether $CD8^+CD25^+$ Tregs suppress antitumor immunity, animal studies was performed. As shown in **Figure 5.13D**, all PBS control mice died of tumor within 25 days after s.c. inoculation of BL6-10_{OVA} tumor cells, whereas 8/8 of sDC_{OVA}-immunized mice (100%) were protected from BL6-10_{OVA} cell challenge. However, the administration of $CD8^+CD25^+$ Tregs significantly reduced sDC_{OVA}-induced antitumor immunity and 4/8 (50%) of mice died of tumor ($p < 0.05$), indicating that $CD8^+CD25^+$ Tregs also suppress *in vivo* CTL-mediated antitumor immunity.

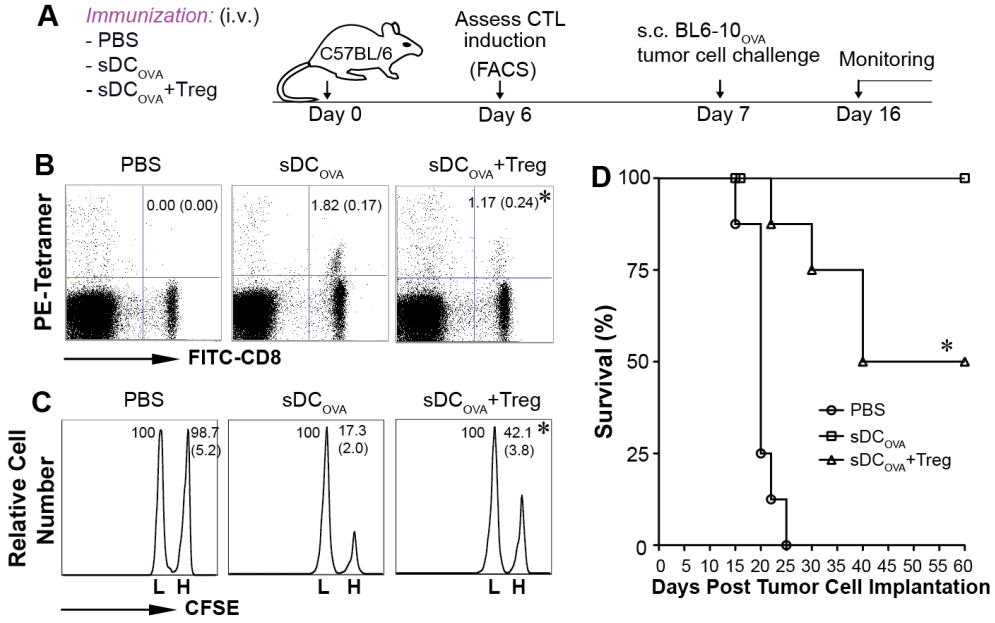

Figure 5.13 Immune suppression of CD8$^+$CD25$^+$ Tregs. (**A**) Experimental protocol. C57BL/6 mice were i.v. immunized with sDC$_{OVA}$ with or without CD8$^+$CD25$^+$ Tregs. (**B**) Blood samples were assessed for OVA-specific CTL responses using PE-tetramer and FITC-CD8 staining by flow cytometry. Values in each panel represent the percentage of OVA-specific CD8$^+$ T cells to total CD8$^+$ T-cell population with standard deviation in parenthesis. *, $p < 0.05$ vs cohorts of sDC$_{OVA}$ group (Student's *t* test). (**C**) *In vivo* cytotoxicity assay. 16 hrs after target cell delivery, the residual OVAI peptide-pulsed CFSE^{high}- and the control Mut1 peptide-pulsed CFSE^{low}-target cells remaining in the spleens of above immunized mice were sorted and analyzed by flow cytometry. The value in each panel represents the percentage of OVA-specific CFSE^{high} and control CFSE^{low} target cells remaining in the spleens. *, $p < 0.05$ vs cohorts of sDC$_{OVA}$ group (Student's *t* test). One representative experiment of two is shown. (**D**) In animal studies, 7 days after immunization, mice were s.c. challenged with BL6-10$_{OVA}$ tumor cells. Tumor growth was monitored daily for 60 days. *, $p < 0.05$ vs cohorts of sDC$_{OVA}$ group (*Log* rank test).

5.3.3 $CD8^+CD25^+$ Tregs induce naive $CD4^+$ T-cell anergy

$CD4^+CD25^+$ Tregs have been reported to play inhibitory role via rendering naive T cells functional anergic (440). However, the molecular phenotype of these anergic T cells is not well characterized. To assess the effect of $CD8^+CD25^+$ Tregs on naive T cells, naive $CD4^+$ T cells were incubated with $CD8^+CD25^+$ Tregs and phenotypically characterized. $CD8^+CD25^+$ Treg-treated $CD4^+$ T cells showed similar level of Grail, Grg4, Caspase 3, Itch and Ikaros, but 4-fold higher of anergic early growth response 2 (EGR2) compared with naive $CD4^+$ T cells (**Figure 5.14A**) by real time-PCR analysis using DNA primers specific for a panel of T cell anergy-associated genes (429). In addition, $CD8^+CD25^+$ Treg-treated $CD4^+$ T cells were stimulated in anti-CD3 and anti-CD28 Ab-coated wells. As shown in **Figure 5.14B**, $CD8^+CD25^+$ Treg-treated $CD4^+$ T cells secreted significantly lower level of IL-2 (0.07 ng/mL) than control naive $CD4^+$ T cells (0.53 ng/mL). ^{3}H-thymidine incorporation assay was also performed to determine the extent of cell division that occurred in response to $CD8^+CD25^+$ Tregs treatment. As shown in **Figure 5.14C**, the primary naive $CD4^+$ T cells proliferated upon DC stimulation in a dose-dependent manner. However, $CD8^+CD25^+$ Treg-treated $CD4^+$ T cells completely lost their capacity for cellular proliferation, consistent with the hyporesponsive state of T-cell anergy.

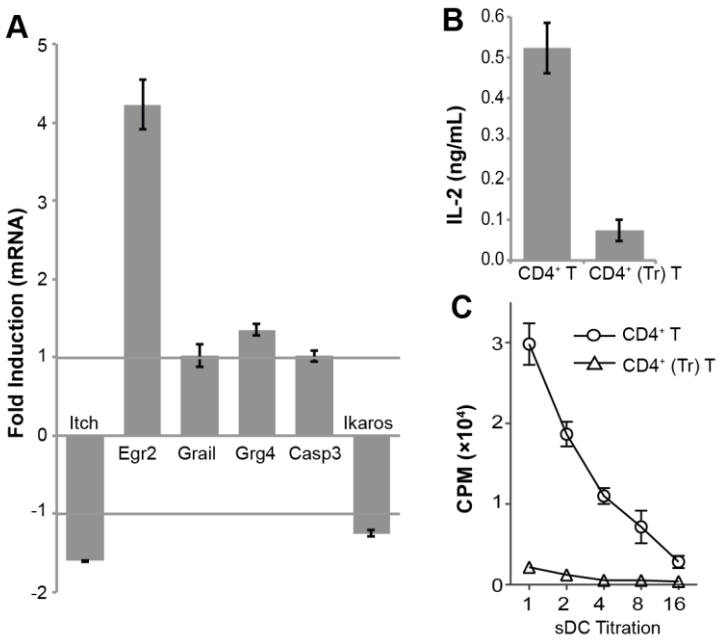

Figure 5.14 CD8$^+$CD25$^+$ Tregs anergize naive CD4$^+$ T cells. (**A**) cDNA was synthesized from total cellular RNAs isolated from naive CD4$^+$ T cells or CD8$^+$CD25$^+$ Treg-treated CD4$^+$ T cells. Real time-PCR was carried out using a panel of primers specific for β-actin, Grail, Ikaros, Casp3, EGR2, Grg4 and Itch. Values of fold induction (the ratio of mRNA expression in CD8$^+$CD25$^+$ Treg-treated CD4$^+$ T cells to that in naive CD4$^+$ T cells) were the mean ± SD (standard deviation) of three independent experiments. (**B**) Naive CD4$^+$ or CD8$^+$CD25$^+$ Treg-treated CD4$^+$ T cells were incubated in anti-CD3 and anti-CD28 Ab-coated wells. Supernatants were collected and analyzed for IL-2 secretion by ELISA. (**C**) Naive CD4$^+$ or CD8$^+$CD25$^+$ Treg-treated CD4$^+$ T cells were incubated with sDCs in the presence of anti-CD3 Ab and IL-2 in an *in vitro* ^{3}H-thymidin incorporation assay. The levels of ^{3}H-thymidine incorporation into the cellular DNA were determined by liquid scintillation counting. Each point represents the mean of triplicates. One representative experiment of two in the above different experiments is shown.

5.3.4 $CD8^+CD25^+$ Tregs downregulate CTL perforin expression and induce perforin-mediated CTL apoptosis

Since $CD4^+CD25^+$ Tregs were reported to inhibit CTL killing effect (237) and involved in cytolytic effect on target cells (441), we assume that the above *in vitro* $CD8^+CD25^+$ Treg-induced inhibition could be a result of either modulation of CTL killing activity or killing-activity to target cells. To assess our assumption, $CD8^+CD25^+$ Tregs were incubated with CTLs followed by assessment of intracellular perforin and granzyme B expression on target CTLs. $CD8^+CD25^+$ Treg-treated CTLs were found to decrease perforin (not granzyme B) expression (**Figure 5.15A**) when compared with untreated CTLs. $CD8^+CD25^+$ Tregs were also incubated with TFL2-labeled CTLs followed by assessment of target cell apoptosis. $CD8^+CD25^+$ Tregs induced apoptosis in 17.2% Treg-treated CTLs (**Figure 5.15B**), while spontaneous apoptosis was seen in only 3.7% untreated CTLs. However, ($perforin^{-/-}$)Tregs lacking perforin expression lost their killing effect on CTLs (**Figure 5.15B**), indicating that $CD8^+CD25^+$ Tregs kill target CTLs via perforin-mediated apoptosis.

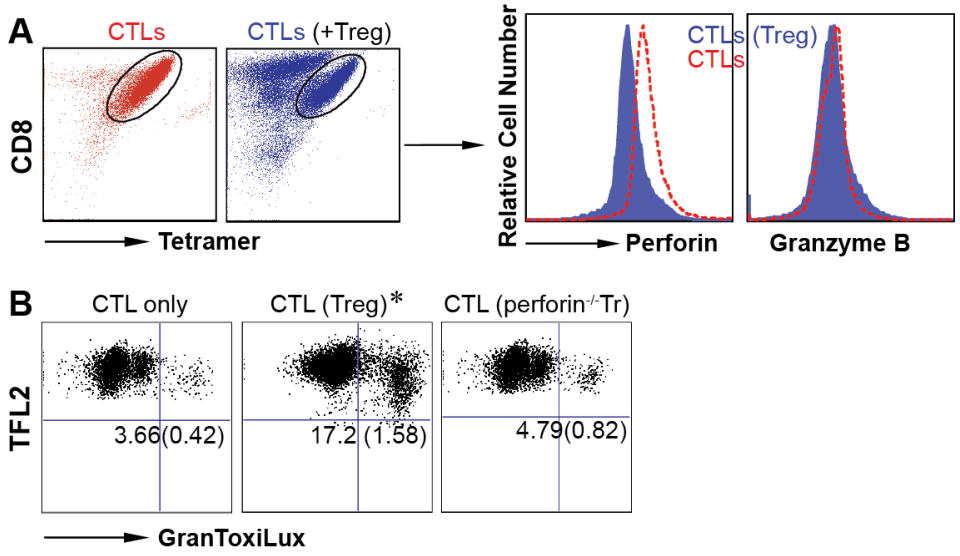

Figure 5.15 Effect of $CD8^+CD25^+$ Tregs on CTLs. (**A**) ConA-stimulated OTI $CD8^+$ CTLs were co-cultured with or without $CD8^+CD25^+$ Tregs overnight. Cell mixtures were stained with PE-Cy5-anti-CD8 and PE-Tetramer Abs, and then stained with FITC-anti-perforin or granzyme B Ab after cell membrane permeabilized with Cytofix/Cytoperm solutions. The stained cells were analyzed by flow cytometry. CTLs in boxes were gated for analysis of perforin or granzyme B expression. (**B**) $CD8^+CD25^+$ Tregs or $CD8^+CD25^+$ (perforin$^{-/-}$)Tregs were incubated with TFL2 (cell dye)-labeled CTLs for 45 min. Cell permeable fluorogenic granzyme-B substrate was subsequently added followed by flow cytometric analysis. $CD8^+CD25^+$ Tregs' killing effect was assessed by the ability of target CTLs cleaving granzyme-B substrate using flow cytometry. *, $p < 0.05$ vs cohorts of CTL only group (Student's *t* test). One representative experiment of two is shown.

5.3.5 $CD8^+CD25^+$ Tregs with OVA-specific pMHC-II arming enhance their inhibition of CTL responses and antitumor immunity

Previous work demonstrated that polyclonal $CD4^+$ T cells, after uptake of DC_{OVA}-released exosomes, became capable of stimulation of OVA-specific CTL responses via exosomal pMHC-I targeting (431). To assess whether pMHC-I or the pMHC-II complexes are involved in enhanced suppression, we pulsed $CD8^+CD25^+$ Tregs with OVAI- and OVAII-peptide to form functional pMHC-I-expressing $CD8^+CD25^+$ $Tr_{/OVAI}$- and pMHC-II-expressing $CD8^+CD25^+$ $Tr_{/OVAII}$-cells, respectively. Interestingly, only $CD8^+CD25^+$ $Tr_{/OVAII}$, but not $CD8^+CD25^+$ $Tr_{/OVAI}$ cells (**Figure 5.16B**) showed significantly enhanced suppression to sDC_{OVA}-induced CTL responses ($p < 0.05$) compared with $CD8^+CD25^+$ Tregs, indicating that $CD8^+CD25^+$ Tregs with OVA-specific pMHC-II arming enhance their inhibition of CTL responses. Similarly, $CD8^+CD25^+$ $Tr_{/OVAII}$, but not $CD8^+CD25^+$ $Tr_{/OVAI}$ cells, also demonstrated an enhanced effect on suppressing $CD8^+$ T cells differentiation into effector CTLs response (**Figure 5.16C**), and antitumor immunity in C57BL/6 mice (**Figure 5.16D**) compared with $CD8^+CD25^+$ Tregs ($p < 0.05$).

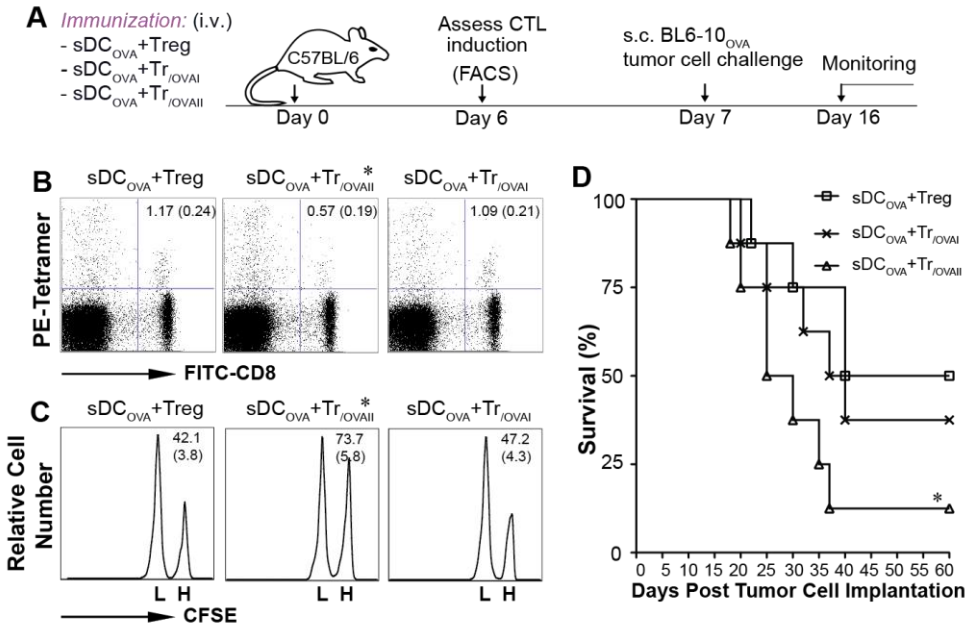

Figure 5.16 CD8$^+$CD25$^+$ Tregs with OVA-specific pMHC-II arming enhance their antitumor immunity. (**A**) Experimental protocol. C57BL/6 mice were immunized with sDC$_{OVA}$ plus CD8$^+$CD25$^+$ Tregs, CD8$^+$CD25$^+$ Tr$_{/OVAI}$ or CD8$^+$CD25$^+$ Tr$_{/OVAII}$ cells. (**B**) Blood samples were assessed for OVA-specific CTL responses using PE-tetramer and FITC-CD8 staining by flow cytometry. Values in each panel represent the percentage of OVA-specific CD8$^+$ T cells to total CD8$^+$ T-cell population with standard deviation in parenthesis. *, $p < 0.05$ vs cohorts of sDC$_{OVA}$ plus Treg group (Student's *t* test) (**C**) *In vivo* cytotoxicity assay. 16 hrs after target cell delivery, the residual OVAI peptide-pulsed CFSE^{high}- and the control Mut1 peptide-pulsed CFSE^{low}-target cells remaining in the spleens of the above immunized mice were sorted and analyzed by flow cytometry. The value in each panel represents the percentage of OVA-specific CFSE^{high} and control CFSE^{low} target cells remaining in the spleens. *, $p < 0.05$ vs cohorts of sDC$_{OVA}$ plus Treg group (Student's *t* test). (**D**) In animal studies, 7 days after immunization, mice were s.c. challenged with BL6-10$_{OVA}$ tumor cells. Tumor growth was monitored daily for 60 days. *, $p < 0.05$ vs cohorts of sDC$_{OVA}$ plus Treg group (*Log* rank test). One representative experiment of two is shown.

5.3.6 $CD8^+CD25^+$ Tregs with OVA-specific pMHC-II arming reduce cognate $CD4^+$ T-cell interaction with sDC *ex vivo*

Tregs have previously been shown to regulate DC-$CD4^+$ T cell interaction during priming (235, 236), we therefore hypothesized that armed $CD8^+CD25^+$ Tregs destabilized sDC-$CD4^+$ T cell interaction more efficiently than regular $CD8^+CD25^+$ Tregs. To investigate this possibility, recipient mice were adoptively transferred with $CD8^+CD25^+$ Tregs and $CD8^+CD25^+$ $Tr_{/OVAII}$ cells, respectively. One day later, mice were i.v. injected with DsRed fluorescent protein-expressing sDC_{OVA} (red) derived from transgenic DsRed mice followed by i.v. injection of CFSE-labeled $CD4^+$ T cells (green). Recipient mice that did not receive Tregs were considered as positive control. Imaging assay was then performed in mouse popliteal lymph nodes to analyze $CD4^+$ T-cell motility by TPM. No significant change of $CD4^+$ T-cell dynamics was found in mice with or without co-injection of $CD8^+CD25^+$ Tregs (data not shown). In contrast, the presence of $CD8^+CD25^+$ $Tr_{/OVAII}$ cells resulted in a less confined migration pattern (**Figure 5.17B**; **sMovie 5.7-5.8**), and a slight but statistically significant increase of $CD4^+$ T cell velocities (4.47 μm/min versus 5.25 μm/min) ($p < 0.05$) (**Figure 5.17C**). The quality of T-DC interaction was also measured by the contact duration. Contacts detectable throughout a complete 40-min imaging period were defined as stable ones. All other interactions were considered as transient contacts. The analysis of the duration of individual transient T-DC interaction showed that transient contacts lasted shorter in the presence of pMHC-II-armed Tregs (median contact duration 7.5 min versus 14.7 min; **Figure 5.17D**). Therefore, our data indicate that $CD8^+CD25^+$ Tregs with OVA-specific pMHC-II arming reduce cognate $CD4^+$ T-cell interactions with sDCs *ex vivo*.

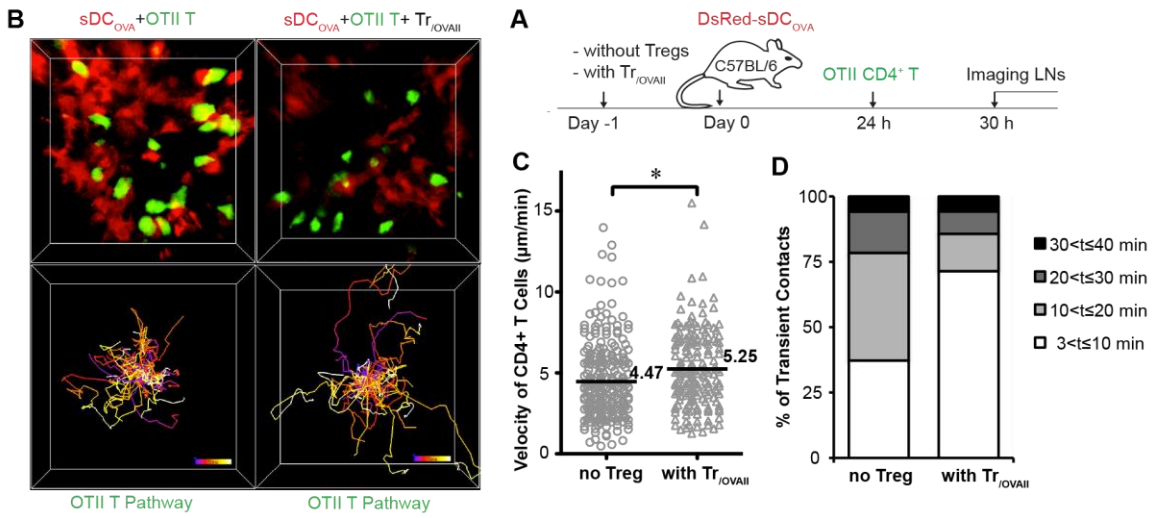

Figure 5.17 CD4$^+$ T-cell dynamics in the presence pMHC-II armed Tregs. (**A**) Experimental protocol. Unlabeled CD8$^+$CD25$^+$ Tr$_{/OVAII}$-cells were adoptively transferred into recipient mice one day before. The mice were injected in footpad with DsRed-sDC$_{OVA}$ (red) followed by i.v. injection of CFSE-CD4$^+$ T cells (green) one day later. Popliteal lymph nodes were imaged in T-zone region by TPM 6 hrs later. (**B**) Migration behavior of CFSE-labeled OTII CD4$^+$ T cells (green) in the absence of unlabeled CD8$^+$CD25$^+$ Tregs (left) or in the presence of CD8$^+$CD25$^+$ Tr$_{/OVAII}$ (right) cells. Individual cells are displayed as color-coded tracks to represent increasing time from blue (start of imaging) to yellow (end of imaging). Tracks are overlaid after normalizing their starting coordinates (lower panel). (**C**) Average velocities of OTII CD4$^+$ T cells. Each dot represents an individual cell; bars indicate median values. *, $p < 0.05$ between cohorts of no Tregs and Tr$_{/OVAII}$ group (Student's *t* test). (**D**) Duration of transient contacts between OTII CD4$^+$ T cells and sDC$_{OVA}$ in the absence of CD8$^+$CD25$^+$ Tregs or in the presence of pMHC-II-armed Tr$_{/OVAII}$ cells. Transient contacts of individual T cells were grouped into four categories with regard to the contact duration. Data shown are representative from one of at least three independent experiments.

5.3.7 Providing $CD8^+CD25^+$ Tregs with pMHC-II complexes enhance their EAE-inhibiting capacity

To induce mild EAE, we only administered MOG_{35-55} peptide plus CFA/MT, but not pertussis toxin (442). Treated-mice developed EAE with clinical scores (**Figure 5.18**). To assess the potential immunosuppressive effect, $CD8^+CD25^+$ Tregs were applied to the MOG peptide-injected EAE mice. Tregs only slightly, but not statistically significantly inhibited MOG peptide-induced EAE. When MOG-specific pMHC-II-armed $CD8^+CD25^+$ $Tr_{/MOG}$ cells were applied to EAE mice, the immunosuppression was significantly stronger in regards to clinical scores assessed in EAE mice with injection of $Tr_{/MOG}$ cells than that in EAE mice with injection of Tregs ($p < 0.05$), indicating that arming $CD8^+CD25^+$ Tregs with MOG-specific pMHC-II complexes enhance their inhibition of EAE.

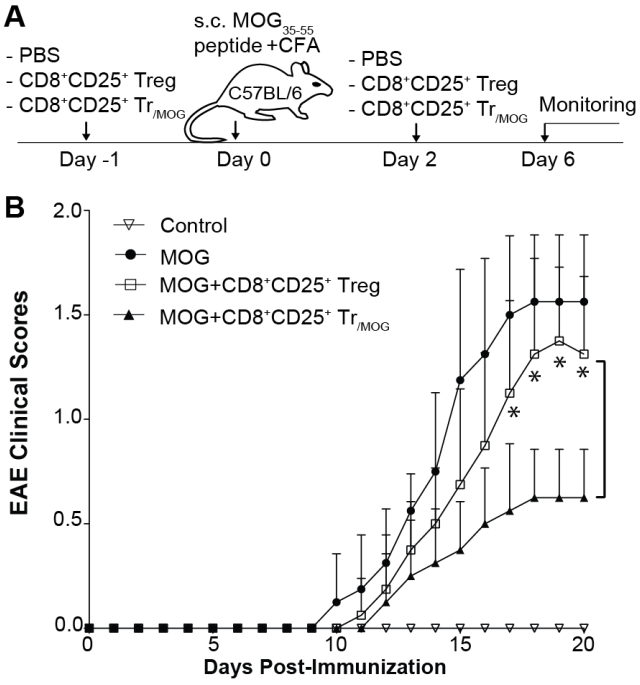

Figure 5.18 $CD8^+CD25^+$ $Tr_{/MOG}$ cells in MOG peptide induced EAE. (**A**) Experimental protocol. Wild-type C57BL/6 mice were immunized with MOG_{35-55}. $CD8^+CD25^+$ Tregs or MOG-specific pMHC-II-armed $CD8^+CD25^+$ $Tr_{/MOG}$ cells were applied to the MOG peptide-induced EAE mice one day pre- and two days-post the immunization. (**B**) C57BL/6 mice immunized with CFA only were used as control. The analysis was performed on the raw data that included all clinical scores for each mouse at each time point in each group. *, $p < 0.05$ vs cohorts of MOG $CD8^+CD25^+$ Treg group (Student's *t* test).

CHAPTER 6 DISCUSSIONS

Vaccines that are capable of stimulating effector and memory $CD8^+$ CTL responses have been extensively studied in an effort to control pathogen-induced diseases and tumor development. Stimulation of T-cell responses by APCs involves at least two signaling events: one elicited by TCRs recognizing pMHC complexes and another triggered by costimulatory molecular signaling such as CD40, CD80, 4-1BBL and OX40L (443). To achieve T cell activation, the formation of IS composed of TCR-pMHC complexes, CD28-CD80 and LFA-1-CD54 engagements at the interface between an APC and a T cell must occur after initial engagement of TCR molecules (434). Monks et al. further showed that, instead of uniform distribution, these proteins clustered into segregated three-dimensional domains within the cell contacts (435). The condensed central distribution and essential role in TCR-triggered T-cell activation (444) make PKC-θ a perfect marker for IS formation. APCs also provide an additional polarization signal (signal 3), such as IL-12 (445), which selectively drives the development of type I or type II immunity, each characterized by a distinct microenvironment promoting a particular set of effector mechanisms (446, 447). Following the recognition of foreign antigen, $CD8^+$ T cells undergo three distinct developmental phases: (i) a proliferation (primary) phase, in which naive $CD8^+$ T cells undergo autonomous clonal expansion and develop into effector CTLs; (ii) a contraction phase, in which approximately 95% of the effector CTLs undergo AICD through apoptosis, allowing the remaining approximately 5%-10% of the CTLs to develop into memory CTLs; and (iii) a maintenance phase, in which memory CTLs survive for a prolonged duration. Unlike their naive counterparts, memory CTLs display enhanced responses to subsequent antigen encounters, undergo rapid proliferation and have heightened effector functions during recall responses.

Hao et al. (181) showed that ConA-stimulated $CD4^+$ T cells derived from OVA-specific TCR transgenic OTII mice can internalize OVA-pulsed DC-released EXO (EXO_{OVA}) via TCR/MHC and LFA-1/CD54 interactions. EXO_{OVA}-loaded $CD4^+$ T cells can be used as OVA-T_{EXO} vaccines capable of stimulating $CD8^+$ T-cell priming via pMHC-I-mediated targeting and via IL-2 and CD80 costimulatory signaling. This mechanism has been further unveiled in this dissertation by the finding that OVA-T_{EXO} cells are capable of inducing $CD8^+$ T cell responses in I-$A^{b-/-}$ mice, indicating that OVA-T_{EXO} could directly stimulate $CD8^+$ T cell responses independent of $CD4^+$

T-cell help. The confocal imaging data in this dissertation also demonstrate the direct evidence that, similarly to APCs, OVA-T_{EXO} can also form PKC-θ-composed IS with cognate $CD8^+$ T cells, which is consistent with previous work by Sumoza-Toledo et al (448), thereby leading to the induction of CTL responses.

$CD4^+$ T cell's CD40L signaling has been found to be important in licensing DCs to induce CTL responses via DC's CD40/$CD4^+$ T cell's CD40L interactions (449). In addition, Munroe et al. demonstrated a functional costimulation of T cell's CD40 via induction of kinase and transcription factor activities (450). Furthermore, Bourgeois et al. reported that CD40 deficiency had a major impact on the CTL memory responses when re-challenged with the same antigen, suggesting that the help of $CD4^+$ T-cell to $CD8^+$ T-cell involves $CD4^+$-$CD8^+$ T cell interactions by forming DC-$CD4^+$-$CD8^+$ T cell clusters (173). However, they did not provide any direct *in vivo* evidence for role of $CD4^+$ T cell's CD40L in CTL memory development. In this study, we demonstrate that although CD40L signaling of $CD4^+$ OVA-T_{EXO} is not involved in $CD8^+$ T cell priming, it does play an important role in functional $CD8^+$ T cell memory development since $CD4^+$ ($CD40L^{-/-}$)T_{EXO}-stimulated $CD8^+$ T memory cells lose their functional recall responses, thereby clearly indicating the critical role of $CD4^+$ T cell's CD40L signaling in CTL memory development.

TPM has been widely used in assessment of immune cell interactions *in vivo* (188), specially the interactions between DC-T cells. It has been shown in many cases that $CD4^+$ helper T cells promote the quality of $CD8^+$ T cell responses (451, 452). Using intravital imaging, Beuneu et al. (453) showed that recruiting $CD8^+$ T cells to DCs was enhanced by the presence of $CD4^+$ T cells that recognize their cognate peptide on the same DC, thereby suggesting ternary clusters with both $CD4^+$ and $CD8^+$ T cells in direct contact with antigen-bearing DCs. Similarly, Castellino et al. (222) demonstrated that the up-regulated expression of CCR5 on naive $CD8^+$ T cells permitted these cells to be attracted to sites of antigen-specific DC-$CD4^+$ T cell interaction where the chemokines CCL3 and CCL4 were produced. A variation of this theme was shown by Ahmed et al. (179) that DC-primed $CD4^+$ T cells were able to directly interact with $CD8^+$ T cells to prime CTL responses in the absence of DCs. Trogocytosis, a process whereby lymphocytes conjugated to APCs extract surface molecules from these cells and express them on their own

surface, could be partially explain this $CD4^+$-$CD8^+$ interaction theme. In this dissertation, interactions between OVA-T_{EXO} and OTI $CD8^+$ T cells have also been shown *ex vivo* by two-photon imaging. Upon exposure to OVA-T_{EXO}, naive OTI $CD8^+$ T cells show significantly lower velocity (5.15 μm/min) and confined movement compared with those OTI $CD8^+$ T cells exposed to OVA-($K^{b-/-}$)T_{EXO} (11.38 μm/min). Therefore, we provide the first *ex vivo* evidence on the important role of exosomal pMHC-I in targeting OVA-T_{EXO} cells to cognate $CD8^+$ T cells. Interestingly, we also find that the velocity of polyclonal $CD8^+$ T cells (8.87 μm/min) in the presence of OVA-T_{EXO}-OTI $CD8^+$ T cells conjugates is lower than the velocity of polyclonal $CD8^+$ T cells (11.38 μm/min) in the presence of OVA-T_{EXO} alone, indicating that help to polyclonal $CD8^+$ T cells can be provided by antigen specific $CD8^+$ T cells responding to OVA-T_{EXO} cells. In fact, our result is consistent with a previous observation by Hugues et al. (223), showing that the nonspecific interactions between polyclonal $CD8^+$ T cells and DCs, which occurred in the presence of an ongoing antigen-specific $CD8^+$ T-cell responses, though much shorter than the antigen-specific interactions, were longer than the nonspecific interactions with DCs alone.

The transgenic HER2 mice express human HER2 under the whey acidic protein promoter and have HER2-specific self-immune tolerance (421). Since there is ~10% difference between rat and human ErbB-2 proteins (454), these mice have become a useful model for evaluation of various human HER2-specific antitumor vaccines (455, 456). The double transgenic HLA-A2/CEA (carcinoembryonic antigen) mice expressing both HLA-A2 and CEA molecules have been constructed and extensively used to assess CEA-specific antitumor vaccines (126, 457, 458). Similarly, we establish, for the first time, the double transgenic HLA-A2/HER2 mice by cross-breeding of transgenic HLA-A2 female mice with transgenic HER2 male mice, to assess CTL responses and antitumor immunity derived from HER2-T_{EXO} vaccination. We demonstrate that HER2-T_{EXO} vaccine is capable of stimulating efficient HER2-specific CTL responses and inducing protective immunity against BL6-$10_{HLA\text{-}A2/HER2}$ tumor *in vivo* in 2/8 double transgenic HLA-A2/HER2 mice with HER2-specific self-immune tolerance. In addition, the remaining 6/8 mice have significantly prolonged survival.

Several reports from experimental models and clinical studies have shown that HER2 is an immunogenic molecule since it generates antibody responses and activation of HER2-specific $CD4^+$ helper T cell and $CD8^+$ CTL responses (459-462). Vaccines against HER2 have been tested in mouse models and in human clinical trials, showing that significant levels of HER2-specific CTL responses can be generated with active immunization (462, 463). An issue of whether tumor antigen-specific vaccines induce autoimmunity since most tumor antigens are self-antigens in nature is still controversial. In some animal models, no tumor antigen-specific vaccine-induced autoimmunity was demonstrated (464, 465). However, vaccine-induced autoimmunity was reported in other melanoma/melanocyte-associated antigen models (466, 467). These discrepant results may derive from differences of distinct tumor antigens in nature, which are targeted in these animal models. Moreover, although some strategies using Tregs' inhibitor in previously vaccinated cancer patients have shown promising results (274, 275), autoimmunity is prone to occur due to the inhibition or depletion of Tregs. Thus, the balance between antitumor efficacy and autoimmunity pathology should be considered when designing vaccines (468). So far, signs of autoimmunity directed against normal tissues have not been encountered by various HER2-specific vaccinations (469). In fact, we did not find any clinical signs related to autoimmunity six months after HER2-T_{EXO} vaccination administration (data not shown). Most probably, it is because the vaccine itself is not strong enough to completely break HER2-specific self-immune tolerance. Besides, no Treg inhibitors have been added in this vaccine strategy to increase the occurrence of systematic autoimmunity. Therefore, the risk of induction of autoimmunity by using HER2-T_{EXO} vaccine is, at present, negligible.

Compared with $CD4^+CD25^+$ Tregs, mechanisms for $CD8^+CD25^+$ Tregs suppression are less studied. Cosmi et al. (346) identified a subset of human $CD8^+CD25^+$ thymocytes that shared phenotype, functional features, and mechanism of action with $CD4^+CD25^+$ Tregs. Mahic et al. (349) found that $CD8^+CD25^-$ T cells up-regulated CD25, Foxp3, GITR, CD28 and CTLA-4 after continuous antigen stimulation, and inhibited $CD4^+$ and $CD8^+$ T cell proliferation and cytokine production via a contact-dependent mechanism. A similar subset has also been found in the thymus and periphery of MHC class II-deficient mice by Bienvenu et al. (351), showing that CD44, GITR, LFA-1 and intracellular CTLA-4 expressing $CD8^+CD25^+$ T cells suppressed anti-CD3-stimulated $CD25^-$ T cell responses *in vitro* in a contact-dependent, IL-10-independent

manner. However, one study by Mayer et al. pointed out that although both naturally occurring and induced $CD8^+Foxp3^+$ T cells expressed *bona fide* Treg markers including CD25, GITR, CTLA-4 and CD103, induced $CD8^+Foxp3^+$ T cells only mildly suppressed T-cell proliferation and IFN-γ production (352). In this dissertation, we use natural $CD8^+CD25^+$ Tregs expanded *in vitro* with CD3/CD28 microbeads as previously described (470, 471) to study cellular and molecular mechanisms of $CD8^+CD25^+$ Treg-mediated immunosuppression. We demonstrate that $CD8^+CD25^+$ Tregs express *bona fide* Treg markers (CD25, CD103, GITR and CTLA-4) and CD28, which is partially consistent with recently reported data by Mayer et al.(352). Therefore, these $CD8^+CD25^+$ Tregs are phenotypically distinct from some of other $CD8^+$ Treg subsets, such as $CD8^+CD25^+CD103^-$ and $CD8^+CD25^+CD28^-$ Tregs (472). The work conducted by other peoples in our lab show that these induced $CD8^+CD25^+$ Tregs inhibit DC-stimulated $CD4^+$ and $CD8^+$ T-cell proliferation in a cell-cell contact-dependent manner, but the inhibitory effect is not mediated by the secretion of IL-10, TGF-β or by the expression of CTLA-4, which is consistent with previous reported characteristics of $CD8^+CD25^+$ Tregs (351, 473).

The presence of activated Tregs has been reported to affect CTL killing function. Chen et al. (474) showed that co-transfer of antigen-specific Tregs with antigen-specific $CD8^+$ T cells followed by implantation of tumor cells resulted in the failure of CTL-induced tumor rejection. Similarly, Mempel et al. (237) showed that the ability of $CD4^+CD25^+$ Tregs regulated CTLs in inducing target cell lysis was greatly impaired, which is correlated with impaired release of lytic granules. Tregs have also been shown with the expression of perforin and granzyme B, and the ability in killing target cells in different experimental settings (441, 475-477). Boissonnas et al. (238) further demonstrated $Foxp3^+$ Tregs induced the death of DCs through a perforin-dependent mechanism, involving direct contacts between Tregs and DCs. In this dissertation, we find that $CD8^+CD25^+$ Treg-treated CTLs down-regulate the expression of perforin, which could affect CTL function in lysing target cells. On the other hand, since granzyme B only becomes active when effector cells are induced in the presence of target cells, measurement of granzyme B activity inside target cells provides an extremely early quantitative assessment of cell-mediated cellular cytotoxicity. Thus, through the measurement of granzyme B activity in target CTLs, $CD8^+CD25^+$ Tregs show direct killing effect to target CTLs via the release of cytolytic granzyme B, while the perforin KO $CD8^+CD25^+$ Tregs fail to do so. $CD8^+CD25^+$ Tregs efficiently suppress

splenic DC_{OVA}-stimulated CTL responses and antitumor immunity against OVA-expressing BL6-10_{OVA} melanoma, while $CD8^+CD25^+$ Tregs lacking perforin only induced weaker inhibitory effects (data not shown). Thus $CD8^+CD25^+$ Tregs' inhibitory effect may be derived from a combined actions of modulation of CTLs' killing activity and direct killing target cells, and the impaired killing ability in perforin KO $CD8^+CD25^+$ Tregs is probably because of the poor pore formation by perforin in controlling the entry of cytolytic granzyme B.

Adaptive antigen-specific $CD4^+$ Tregs such as type 1 T regulatory (Tr1)- and Th3-cells secreting IL-10 and expressing antigen-specific TCRs are generated in the periphery by the stimulation of TGF-β- or IL-10-producing DCs through the recognition of antigen-specific TCRs by matching antigen-specific pMHC-II complexes (478, 479). Those T cells execute the immunosuppression in either cell-cell contact dependent or independent fashion (480). In comparison, polyclonal $CD4^+CD25^+$ and $CD8^+CD25^+$ Tregs, which express a pool of self-reactive (autoantigen-specific) TCRs, are nonspecific. Autoantigen-directed $CD4^+CD25^+$ Treg derived from TCR-transgenic mice have been shown to be more efficient at preventing autoimmunity than polyclonal $CD4^+CD25^+$ Tregs (481-483), indicating that the augmentation of Treg function in an autoantigen-specific manner is likely to be beneficial for treating autoimmunity. Reprogramming the specificity of polyclonal $CD4^+CD25^+$ Tregs achieved by introducing antigen-specific TCRs (484-486) would thus enhance $CD4^+CD25^+$ Treg-mediated immune suppression. However, some critical disadvantages associated with this approach may still limit its clinical use. In addition to the complexity of TCR cloning and transduction, the optimal TCR affinity suitable for each therapeutic application is difficult to define (487, 488). Sometimes, the excessive TCR-affinity could also be detrimental (489, 490). Tregs may also target pathogenic T cells via their expression of class II molecules. LaGuern et al. (491) found enhanced Treg function in allogeneic transplantation studies using murine class II transfected Tregs. Engineered Tregs that coexpressing Foxp3 and class II autoantigen-peptide complexes, have been shown to efficient inhibit of autoimmune T cell function and prevent the development of autoimmune arthritis (492).

Alternatively, redirecting antigen specificity to non-specific polyclonal T cells can be achieved via the acquisition of pMHC complexes. Previous work in our lab demonstrated that polyclonal

$CD4^+$ and $CD8^+$ T cells, when acquiring antigen-specific pMHC-I-expressing EXOs, became capable of stimulating antigen-specific CTL responses as these exosomal pMHC-I complexes targeted them to cognate $CD8^+$ T cells *in vivo* (431, 493). In this thesis, $CD8^+CD25^+$ Tregs weakly express $I\text{-}A^b$ (data not shown), which is still quite controversial (494), and exert an enhanced inhibition of CTL responses and antitumor immunity when pulsed with OVAII-peptide for pMHC-II arming (but not OVAI-peptide for pMHC-I arming). This indicates that $CD8^+CD25^+$ $Tr_{/OVAII}$ cells expressing pMHC-II enhance their immunosuppressive action because of pMHC-II arming, which potentially redirects them in an antigen-specific manner towards matching cognate $CD4^+$ T cells *in vivo*.

TPM provides a unique perspective to examine the cellular mechanisms of Treg-mediated suppression *in vivo.* Two imaging studies demonstrated by Tang et al. (236) and Tadokoro et al. (235) have provided direct evidence that Tregs interfere with the interactions between antigen-loaded DCs and their cognate T cells, and the long-lasting interactions between $CD4^+CD25^+$ Tregs and DCs have also been visualized. To address the potential suppressive role of $CD8^+CD25^+$ Tregs, interactions between antigen-loaded DCs (DC_{OVA}) and cognate OTII $CD4^+$ T cells have been carefully studied in the presence or absence of $CD8^+CD25^+$ Tregs. $CD8^+CD25^+$ Tregs are unable to alter the $CD4^+$ T-DC interaction, which contradicts with previous reports (235, 236). This apparent contradiction could be due to the lower potency of polyclonal $CD8^+CD25^+$ Tregs (472) used in this dissertation. However, Mempel et al. (237) also demonstrated that the presence of Tregs didn't alter $CD8^+$ CTL recognition and stable interactions with antigen presenting B cells, but profoundly inhibited the ability of $CD8^+$ CTLs in releasing cytolytic granules and lysing the targets. Interestingly, decreased contact duration has been observed after the administration of pMHC-II armed $CD8^+CD25^+$ Treg, suggesting $CD8^+CD25^+$ $Tr_{/OVAII}$ cells participate in inhibiting T-DC interactions. Our data thus confirm an alternative way to constitute antigen specificity to polyclonal Tregs by pMHC-II arming that can direct nonspecific $CD8^+CD25^+$ Tregs towards antigen-specific $CD4^+$ T cells, possibly leading to the inhibition of priming cognate $CD4^+$ T cells by DCs. Unfortunately, we fail to detect the interaction between $CD8^+CD25^+$ $Tr_{/OVAII}$ cells and cognate $CD4^+$ T cells. Moreover, no direct $CD8^+CD25^+$ $Tr_{/OVAII}$-DCs interaction has been observed in our experiment setting, although both

antigen-specific (236) and endogenous polyclonal Tregs (238) have been found to directly interact with DCs.

EAE is a rodent model that has been valuable for characterization of the immunopathogenic processes of human MS. The pathologic correlate of the multifocal neurologic deficit is the invasion of immune cells, predominantly T cells and macrophages in the CNS, which attack the myelin sheath and lead to disseminated plaque-like demyelination. Both encephalitogenic $CD4^+$ Th1 and Th17 cells have been found to play an important role in EAE (495, 496). In a therapeutic context, natural $CD4^+CD25^+$ Treg populations expanded *in vitro* can be used for preventing autoimmune diseases (497, 498). Polyclonal $CD4^+CD25^+$ Tregs, Qa-1/HLA-E restricted $CD8^+$ Tregs and some $CD8^+CD25^-$ Tregs such as $CD8^+CD122^+$ and $CD8^+LAP^+$ Tregs have also been reported to suppress EAE (335, 360, 403, 499). Moreover, Tregs expressing TCR specific for either MBP- or MOG antigen have been shown to be very effective in inhibiting primary EAE as well treating relapsing disease (500, 501). In this thesis, we demonstrate that $CD8^+CD25^+$ Tregs with pMHC-II arming can significantly suppress EAE, possibly via induction of both cell anergy and effector apoptosis.

CHAPTER 7 CONCLUSIONS AND FUTURE DIRECTIONS

In summary, our studies demonstrate that nonspecific polyclonal $CD4^+$ T cells, when armed with HER2 antigen-specific pMHC-I complexes, become capable of stimulating HER2-specific CTL responses and antitumor immunity in double transgenic HLA-A2/HER2 mice. Therefore, redirecting antigen specificity to nonspecific $CD4^+$ T by pMHC complex arming may have great impact on development of novel T cell-based vaccines for treatment of HER2-positive breast cancer. Since HER2 has also been found to be overexpressed in many other human malignancies including ovary, prostate, gastric, lung, bladder and kidney carcinomas (248), our novel HER2-T_{EXO} vaccine may be useful in treatment of these human cancers.

In addition, our studies also demonstrate that nonspecific polyclonal $CD8^+CD25^+$ Tregs, when armed with MOG antigen-specific pMHC-II complexes, become capable of inducing enhanced MOG-specific immunosuppression in MOG-induced EAE mice. Many autoantigens, including insulin, MBP and collagen type II targeted in autoimmune diseases such as type-I diabetes, MS and rheumatoid arthritis, have been defined (502), which makes the generation of pMHC-II-armed Tregs possible. Since $CD4^+CD25^+$ Tregs demonstrate more potent immunosuppression (352) than $CD8^+CD25^+$ Tregs, the principle of this study can thus be more likely applied to $CD8^+CD25^+$ Treg-mediated immunotherapy. Therefore, redirecting antigen specificity to nonspecific $CD8^+CD25^+$ Tregs by pMHC complex arming may have great impact on development of novel immunotherapeutics for treatment of autoimmune diseases, such as MS.

CHAPTER 8 REFERENCES

1. Steinman, R. M., and J. Idoyaga. 2010. Features of the dendritic cell lineage. *Immunol. Rev.* 234: 5-17.
2. Bedoui, S., P. G. Whitney, J. Waithman, L. Eidsmo, L. Wakim, I. Caminschi, R. S. Allan, M. Wojtasiak, K. Shortman, F. R. Carbone, A. G. Brooks, and W. R. Heath. 2009. Cross-presentation of viral and self antigens by skin-derived CD103+ dendritic cells. *Nat. Immunol.* 10: 488-495.
3. del Rio, M. L., J. I. Rodriguez-Barbosa, E. Kremmer, and R. Forster. 2007. CD103- and CD103+ bronchial lymph node dendritic cells are specialized in presenting and cross-presenting innocuous antigen to CD4+ and CD8+ T cells. *J. Immunol.* 178: 6861-6866.
4. Sung, S. S., S. M. Fu, C. E. Rose, Jr., F. Gaskin, S. T. Ju, and S. R. Beaty. 2006. A major lung CD103 (alphaE)-beta7 integrin-positive epithelial dendritic cell population expressing Langerin and tight junction proteins. *J. Immunol.* 176: 2161-2172.
5. Uematsu, S., M. H. Jang, N. Chevrier, Z. Guo, Y. Kumagai, M. Yamamoto, H. Kato, N. Sougawa, H. Matsui, H. Kuwata, H. Hemmi, C. Coban, T. Kawai, K. J. Ishii, O. Takeuchi, M. Miyasaka, K. Takeda, and S. Akira. 2006. Detection of pathogenic intestinal bacteria by Toll-like receptor 5 on intestinal CD11c+ lamina propria cells. *Nat. Immunol.* 7: 868-874.
6. Johansson-Lindbom, B., M. Svensson, O. Pabst, C. Palmqvist, G. Marquez, R. Forster, and W. W. Agace. 2005. Functional specialization of gut CD103+ dendritic cells in the regulation of tissue-selective T cell homing. *J. Exp. Med.* 202: 1063-1073.
7. Annacker, O., J. L. Coombes, V. Malmstrom, H. H. Uhlig, T. Bourne, B. Johansson-Lindbom, W. W. Agace, C. M. Parker, and F. Powrie. 2005. Essential role for CD103 in the T cell-mediated regulation of experimental colitis. *J. Exp. Med.* 202: 1051-1061.
8. Varol, C., A. Vallon-Eberhard, E. Elinav, T. Aychek, Y. Shapira, H. Luche, H. J. Fehling, W. D. Hardt, G. Shakhar, and S. Jung. 2009. Intestinal lamina propria dendritic cell subsets have different origin and functions. *Immunity* 31: 502-512.
9. Ginhoux, F., K. Liu, J. Helft, M. Bogunovic, M. Greter, D. Hashimoto, J. Price, N. Yin, J. Bromberg, S. A. Lira, E. R. Stanley, M. Nussenzweig, and M. Merad. 2009. The origin and development of nonlymphoid tissue CD103+ DCs. *J. Exp. Med.* 206: 3115-3130.
10. Degauque, N., D. Lair, A. Dupont, A. Moreau, G. Roussey, F. Moizant, F. X. Hubert, C. Louvet, M. Hill, F. Haspot, R. Josien, C. Usal, B. Vanhove, J. P. Soulillou, and S. Brouard. 2006. Dominant tolerance to kidney allografts induced by anti-donor MHC class II antibodies: cooperation between T and non-T CD103+ cells. *J. Immunol.* 176: 3915-3922.
11. Shortman, K., and W. R. Heath. 2010. The CD8+ dendritic cell subset. *Immunol. Rev.* 234: 18-31.
12. Hochrein, H., K. Shortman, D. Vremec, B. Scott, P. Hertzog, and M. O'Keeffe. 2001. Differential production of IL-12, IFN-alpha, and IFN-gamma by mouse dendritic cell subsets. *J. Immunol.* 166: 5448-5455.
13. Iyoda, T., S. Shimoyama, K. Liu, Y. Omatsu, Y. Akiyama, Y. Maeda, K. Takahara, R. M. Steinman, and K. Inaba. 2002. The CD8+ dendritic cell subset selectively endocytoses dying cells in culture and in vivo. *J. Exp. Med.* 195: 1289-1302.

14. den Haan, J. M., S. M. Lehar, and M. J. Bevan. 2000. CD8(+) but not CD8(-) dendritic cells cross-prime cytotoxic T cells in vivo. *J. Exp. Med.* 192: 1685-1696.
15. Schnorrer, P., G. M. Behrens, N. S. Wilson, J. L. Pooley, C. M. Smith, D. El-Sukkari, G. Davey, F. Kupresanin, M. Li, E. Maraskovsky, G. T. Belz, F. R. Carbone, K. Shortman, W. R. Heath, and J. A. Villadangos. 2006. The dominant role of CD8+ dendritic cells in cross-presentation is not dictated by antigen capture. *Proc. Natl. Acad. Sci. U. S. A.* 103: 10729-10734.
16. Schulz, O., A. D. Edwards, M. Schito, J. Aliberti, S. Manickasingham, A. Sher, and C. Reis e Sousa. 2000. CD40 triggering of heterodimeric IL-12 p70 production by dendritic cells in vivo requires a microbial priming signal. *Immunity* 13: 453-462.
17. Shrimpton, R. E., M. Butler, A. S. Morel, E. Eren, S. S. Hue, and M. A. Ritter. 2009. CD205 (DEC-205): a recognition receptor for apoptotic and necrotic self. *Mol. Immunol.* 46: 1229-1239.
18. Bonifaz, L., D. Bonnyay, K. Mahnke, M. Rivera, M. C. Nussenzweig, and R. M. Steinman. 2002. Efficient targeting of protein antigen to the dendritic cell receptor DEC-205 in the steady state leads to antigen presentation on major histocompatibility complex class I products and peripheral CD8+ T cell tolerance. *J. Exp. Med.* 196: 1627-1638.
19. Edwards, A. D., D. Chaussabel, S. Tomlinson, O. Schulz, A. Sher, and C. Reis e Sousa. 2003. Relationships among murine CD11c(high) dendritic cell subsets as revealed by baseline gene expression patterns. *J. Immunol.* 171: 47-60.
20. Zhang, X., M. A. Munegowda, J. Yuan, Y. Wei, and J. Xiang. 2010. Optimal TLR9 signal converts tolerogenic CD4-8- DCs into immunogenic ones capable of stimulating antitumor immunity via activating CD4+ Th1/Th17 and NK cell responses. *J. Leukoc. Biol.* 88: 393-403.
21. Zhang, X., H. Huang, J. Yuan, D. Sun, W. S. Hou, J. Gordon, and J. Xiang. 2005. CD4-8- dendritic cells prime CD4+ T regulatory 1 cells to suppress antitumor immunity. *J. Immunol.* 175: 2931-2937.
22. Legge, K. L., R. K. Gregg, R. Maldonado-Lopez, L. Li, J. C. Caprio, M. Moser, and H. Zaghouani. 2002. On the role of dendritic cells in peripheral T cell tolerance and modulation of autoimmunity. *J. Exp. Med.* 196: 217-227.
23. Guiducci, C., C. Ghirelli, M. A. Marloie-Provost, T. Matray, R. L. Coffman, Y. J. Liu, F. J. Barrat, and V. Soumelis. 2008. PI3K is critical for the nuclear translocation of IRF-7 and type I IFN production by human plasmacytoid predendritic cells in response to TLR activation. *J. Exp. Med.* 205: 315-322.
24. Jego, G., A. K. Palucka, J. P. Blanck, C. Chalouni, V. Pascual, and J. Banchereau. 2003. Plasmacytoid dendritic cells induce plasma cell differentiation through type I interferon and interleukin 6. *Immunity* 19: 225-234.
25. Young, L. J., N. S. Wilson, P. Schnorrer, A. Proietto, T. ten Broeke, Y. Matsuki, A. M. Mount, G. T. Belz, M. O'Keeffe, M. Ohmura-Hoshino, S. Ishido, W. Stoorvogel, W. R. Heath, K. Shortman, and J. A. Villadangos. 2008. Differential MHC class II synthesis and ubiquitination confers distinct antigen-presenting properties on conventional and plasmacytoid dendritic cells. *Nat. Immunol.* 9: 1244-1252.
26. Irla, M., N. Kupfer, T. Suter, R. Lissilaa, M. Benkhoucha, J. Skupsky, P. H. Lalive, A. Fontana, W. Reith, and S. Hugues. 2010. MHC class II-restricted antigen presentation by plasmacytoid dendritic cells inhibits T cell-mediated autoimmunity. *J. Exp. Med.* 207: 1891-1905.

27. Lande, R., J. Gregorio, V. Facchinetti, B. Chatterjee, Y. H. Wang, B. Homey, W. Cao, Y. H. Wang, B. Su, F. O. Nestle, T. Zal, I. Mellman, J. M. Schroder, Y. J. Liu, and M. Gilliet. 2007. Plasmacytoid dendritic cells sense self-DNA coupled with antimicrobial peptide. *Nature* 449: 564-569.
28. Romani, N., B. E. Clausen, and P. Stoitzner. 2010. Langerhans cells and more: langerin-expressing dendritic cell subsets in the skin. *Immunol. Rev.* 234: 120-141.
29. Carbone, F. R., G. T. Belz, and W. R. Heath. 2004. Transfer of antigen between migrating and lymph node-resident DCs in peripheral T-cell tolerance and immunity. *Trends Immunol.* 25: 655-658.
30. Allan, R. S., J. Waithman, S. Bedoui, C. M. Jones, J. A. Villadangos, Y. Zhan, A. M. Lew, K. Shortman, W. R. Heath, and F. R. Carbone. 2006. Migratory dendritic cells transfer antigen to a lymph node-resident dendritic cell population for efficient CTL priming. *Immunity* 25: 153-162.
31. Siddiqui, K. R., S. Laffont, and F. Powrie. 2010. E-cadherin marks a subset of inflammatory dendritic cells that promote T cell-mediated colitis. *Immunity* 32: 557-567.
32. Schulz, O., E. Jaensson, E. K. Persson, X. Liu, T. Worbs, W. W. Agace, and O. Pabst. 2009. Intestinal CD103+, but not CX3CR1+, antigen sampling cells migrate in lymph and serve classical dendritic cell functions. *J. Exp. Med.* 206: 3101-3114.
33. Medoff, B. D., E. Seung, S. Hong, S. Y. Thomas, B. P. Sandall, J. S. Duffield, D. A. Kuperman, D. J. Erle, and A. D. Luster. 2009. CD11b+ myeloid cells are the key mediators of Th2 cell homing into the airway in allergic inflammation. *J. Immunol.* 182: 623-635.
34. Lewkowich, I. P., S. Lajoie, J. R. Clark, N. S. Herman, A. A. Sproles, and M. Wills-Karp. 2008. Allergen uptake, activation, and IL-23 production by pulmonary myeloid DCs drives airway hyperresponsiveness in asthma-susceptible mice. *PLoS One* 3: e3879.
35. Heymann, F., C. Meyer-Schwesinger, E. E. Hamilton-Williams, L. Hammerich, U. Panzer, S. Kaden, S. E. Quaggin, J. Floege, H. J. Grone, and C. Kurts. 2009. Kidney dendritic cell activation is required for progression of renal disease in a mouse model of glomerular injury. *J. Clin. Invest.* 119: 1286-1297.
36. Paul, W. E., and R. A. Seder. 1994. Lymphocyte responses and cytokines. *Cell* 76: 241-251.
37. Lighvani, A. A., D. M. Frucht, D. Jankovic, H. Yamane, J. Aliberti, B. D. Hissong, B. V. Nguyen, M. Gadina, A. Sher, W. E. Paul, and J. J. O'Shea. 2001. T-bet is rapidly induced by interferon-gamma in lymphoid and myeloid cells. *Proc. Natl. Acad. Sci. U. S. A.* 98: 15137-15142.
38. Kaplan, M. H., Y. L. Sun, T. Hoey, and M. J. Grusby. 1996. Impaired IL-12 responses and enhanced development of Th2 cells in Stat4-deficient mice. *Nature* 382: 174-177.
39. Suzuki, Y., M. A. Orellana, R. D. Schreiber, and J. S. Remington. 1988. Interferon-gamma: the major mediator of resistance against Toxoplasma gondii. *Science* 240: 516-518.
40. Chiang, E. Y., G. A. Kolumam, X. Yu, M. Francesco, S. Ivelja, I. Peng, P. Gribling, J. Shu, W. P. Lee, C. J. Refino, M. Balazs, A. Paler-Martinez, A. Nguyen, J. Young, K. H. Barck, R. A. Carano, R. Ferrando, L. Diehl, D. Chatterjea, and J. L. Grogan. 2009. Targeted depletion of lymphotoxin-alpha-expressing TH1 and TH17 cells inhibits autoimmune disease. *Nat. Med.* 15: 766-773.

41. Williams, M. A., A. J. Tyznik, and M. J. Bevan. 2006. Interleukin-2 signals during priming are required for secondary expansion of CD8+ memory T cells. *Nature* 441: 890-893.
42. Wuest, T. Y., J. Willette-Brown, S. K. Durum, and A. A. Hurwitz. 2008. The influence of IL-2 family cytokines on activation and function of naturally occurring regulatory T cells. *J. Leukoc. Biol.* 84: 973-980.
43. Sokol, C. L., N. Q. Chu, S. Yu, S. A. Nish, T. M. Laufer, and R. Medzhitov. 2009. Basophils function as antigen-presenting cells for an allergen-induced T helper type 2 response. *Nat. Immunol.* 10: 713-720.
44. Kaplan, M. H., U. Schindler, S. T. Smiley, and M. J. Grusby. 1996. Stat6 is required for mediating responses to IL-4 and for development of Th2 cells. *Immunity* 4: 313-319.
45. Steinke, J. W., and L. Borish. 2001. Th2 cytokines and asthma. Interleukin-4: its role in the pathogenesis of asthma, and targeting it for asthma treatment with interleukin-4 receptor antagonists. *Respir. Res.* 2: 66-70.
46. Doucet, C., D. Brouty-Boye, C. Pottin-Clemenceau, C. Jasmin, G. W. Canonica, and B. Azzarone. 1998. IL-4 and IL-13 specifically increase adhesion molecule and inflammatory cytokine expression in human lung fibroblasts. *Int. Immunol.* 10: 1421-1433.
47. Martinez-Moczygemba, M., and D. P. Huston. 2003. Biology of common beta receptor-signaling cytokines: IL-3, IL-5, and GM-CSF. *J. Allergy Clin. Immunol.* 112: 653-665; quiz 666.
48. Ferber, I. A., S. Brocke, C. Taylor-Edwards, W. Ridgway, C. Dinisco, L. Steinman, D. Dalton, and C. G. Fathman. 1996. Mice with a disrupted IFN-gamma gene are susceptible to the induction of experimental autoimmune encephalomyelitis (EAE). *J. Immunol.* 156: 5-7.
49. Becher, B., B. G. Durell, and R. J. Noelle. 2002. Experimental autoimmune encephalitis and inflammation in the absence of interleukin-12. *J. Clin. Invest.* 110: 493-497.
50. Ivanov, II, B. S. McKenzie, L. Zhou, C. E. Tadokoro, A. Lepelley, J. J. Lafaille, D. J. Cua, and D. R. Littman. 2006. The orphan nuclear receptor RORgammat directs the differentiation program of proinflammatory IL-17+ T helper cells. *Cell* 126: 1121-1133.
51. Moseley, T. A., D. R. Haudenschild, L. Rose, and A. H. Reddi. 2003. Interleukin-17 family and IL-17 receptors. *Cytokine Growth Factor Rev.* 14: 155-174.
52. Korn, T., E. Bettelli, W. Gao, A. Awasthi, A. Jager, T. B. Strom, M. Oukka, and V. K. Kuchroo. 2007. IL-21 initiates an alternative pathway to induce proinflammatory T(H)17 cells. *Nature* 448: 484-487.
53. Leonard, W. J., and R. Spolski. 2005. Interleukin-21: a modulator of lymphoid proliferation, apoptosis and differentiation. *Nat. Rev. Immunol.* 5: 688-698.
54. Aujla, S. J., Y. R. Chan, M. Zheng, M. Fei, D. J. Askew, D. A. Pociask, T. A. Reinhart, F. McAllister, J. Edeal, K. Gaus, S. Husain, J. L. Kreindler, P. J. Dubin, J. M. Pilewski, M. M. Myerburg, C. A. Mason, Y. Iwakura, and J. K. Kolls. 2008. IL-22 mediates mucosal host defense against Gram-negative bacterial pneumonia. *Nat. Med.* 14: 275-281.
55. Zenewicz, L. A., G. D. Yancopoulos, D. M. Valenzuela, A. J. Murphy, M. Karow, and R. A. Flavell. 2007. Interleukin-22 but not interleukin-17 provides protection to hepatocytes during acute liver inflammation. *Immunity* 27: 647-659.

56. Fujio, K., T. Okamura, and K. Yamamoto. 2010. The Family of IL-10-secreting CD4+ T cells. *Adv. Immunol.* 105: 99-130.
57. Sakaguchi, S., M. Ono, R. Setoguchi, H. Yagi, S. Hori, Z. Fehervari, J. Shimizu, T. Takahashi, and T. Nomura. 2006. Foxp3+ CD25+ CD4+ natural regulatory T cells in dominant self-tolerance and autoimmune disease. *Immunol. Rev.* 212: 8-27.
58. Li, M. O., Y. Y. Wan, and R. A. Flavell. 2007. T cell-produced transforming growth factor-beta1 controls T cell tolerance and regulates Th1- and Th17-cell differentiation. *Immunity* 26: 579-591.
59. Fontenot, J. D., M. A. Gavin, and A. Y. Rudensky. 2003. Foxp3 programs the development and function of CD4+CD25+ regulatory T cells. *Nat. Immunol.* 4: 330-336.
60. Ouyang, W., S. Rutz, N. K. Crellin, P. A. Valdez, and S. G. Hymowitz. 2011. Regulation and functions of the IL-10 family of cytokines in inflammation and disease. *Annu. Rev. Immunol.* 29: 71-109.
61. Vogelzang, A., H. M. McGuire, D. Yu, J. Sprent, C. R. Mackay, and C. King. 2008. A fundamental role for interleukin-21 in the generation of T follicular helper cells. *Immunity* 29: 127-137.
62. Nurieva, R. I., Y. Chung, G. J. Martinez, X. O. Yang, S. Tanaka, T. D. Matskevitch, Y. H. Wang, and C. Dong. 2009. Bcl6 mediates the development of T follicular helper cells. *Science* 325: 1001-1005.
63. Schaerli, P., K. Willimann, A. B. Lang, M. Lipp, P. Loetscher, and B. Moser. 2000. CXC chemokine receptor 5 expression defines follicular homing T cells with B cell helper function. *J. Exp. Med.* 192: 1553-1562.
64. Kovanen, P. E., and W. J. Leonard. 2004. Cytokines and immunodeficiency diseases: critical roles of the gamma(c)-dependent cytokines interleukins 2, 4, 7, 9, 15, and 21, and their signaling pathways. *Immunol. Rev.* 202: 67-83.
65. Veldhoen, M., C. Uyttenhove, J. van Snick, H. Helmby, A. Westendorf, J. Buer, B. Martin, C. Wilhelm, and B. Stockinger. 2008. Transforming growth factor-beta 'reprograms' the differentiation of T helper 2 cells and promotes an interleukin 9-producing subset. *Nat. Immunol.* 9: 1341-1346.
66. Dardalhon, V., A. Awasthi, H. Kwon, G. Galileos, W. Gao, R. A. Sobel, M. Mitsdoerffer, T. B. Strom, W. Elyaman, I. C. Ho, S. Khoury, M. Oukka, and V. K. Kuchroo. 2008. IL-4 inhibits TGF-beta-induced Foxp3+ T cells and, together with TGF-beta, generates IL-9+ IL-10+ Foxp3(-) effector T cells. *Nat. Immunol.* 9: 1347-1355.
67. Chang, H. C., S. Sehra, R. Goswami, W. Yao, Q. Yu, G. L. Stritesky, R. Jabeen, C. McKinley, A. N. Ahyi, L. Han, E. T. Nguyen, M. J. Robertson, N. B. Perumal, R. S. Tepper, S. L. Nutt, and M. H. Kaplan. 2010. The transcription factor PU.1 is required for the development of IL-9-producing T cells and allergic inflammation. *Nat. Immunol.* 11: 527-534.
68. Staudt, V., E. Bothur, M. Klein, K. Lingnau, S. Reuter, N. Grebe, B. Gerlitzki, M. Hoffmann, A. Ulges, C. Taube, N. Dehzad, M. Becker, M. Stassen, A. Steinborn, M. Lohoff, H. Schild, E. Schmitt, and T. Bopp. 2010. Interferon-regulatory factor 4 is essential for the developmental program of T helper 9 cells. *Immunity* 33: 192-202.
69. Duhen, T., R. Geiger, D. Jarrossay, A. Lanzavecchia, and F. Sallusto. 2009. Production of interleukin 22 but not interleukin 17 by a subset of human skin-homing memory T cells. *Nat. Immunol.* 10: 857-863.

70. Trifari, S., C. D. Kaplan, E. H. Tran, N. K. Crellin, and H. Spits. 2009. Identification of a human helper T cell population that has abundant production of interleukin 22 and is distinct from T(H)-17, T(H)1 and T(H)2 cells. *Nat. Immunol.* 10: 864-871.
71. Eyerich, S., K. Eyerich, D. Pennino, T. Carbone, F. Nasorri, S. Pallotta, F. Cianfarani, T. Odorisio, C. Traidl-Hoffmann, H. Behrendt, S. R. Durham, C. B. Schmidt-Weber, and A. Cavani. 2009. Th22 cells represent a distinct human T cell subset involved in epidermal immunity and remodeling. *J. Clin. Invest.* 119: 3573-3585.
72. Russell, J. H., and T. J. Ley. 2002. Lymphocyte-mediated cytotoxicity. *Annu. Rev. Immunol.* 20: 323-370.
73. Kaech, S. M., and W. Cui. 2012. Transcriptional control of effector and memory CD8+ T cell differentiation. *Nat. Rev. Immunol.* 12: 749-761.
74. Sallusto, F., D. Lenig, R. Forster, M. Lipp, and A. Lanzavecchia. 1999. Two subsets of memory T lymphocytes with distinct homing potentials and effector functions. *Nature* 401: 708-712.
75. Ahmed, R., M. J. Bevan, S. L. Reiner, and D. T. Fearon. 2009. The precursors of memory: models and controversies. *Nat. Rev. Immunol.* 9: 662-668.
76. Thery, C., L. Zitvogel, and S. Amigorena. 2002. Exosomes: composition, biogenesis and function. *Nat. Rev. Immunol.* 2: 569-579.
77. Trams, E. G., C. J. Lauter, N. Salem, Jr., and U. Heine. 1981. Exfoliation of membrane ecto-enzymes in the form of micro-vesicles. *Biochim. Biophys. Acta* 645: 63-70.
78. Harding, C., J. Heuser, and P. Stahl. 1983. Receptor-mediated endocytosis of transferrin and recycling of the transferrin receptor in rat reticulocytes. *J. Cell Biol.* 97: 329-339.
79. Pan, B. T., K. Teng, C. Wu, M. Adam, and R. M. Johnstone. 1985. Electron microscopic evidence for externalization of the transferrin receptor in vesicular form in sheep reticulocytes. *J. Cell Biol.* 101: 942-948.
80. Kapsogeorgou, E. K., R. F. Abu-Helu, H. M. Moutsopoulos, and M. N. Manoussakis. 2005. Salivary gland epithelial cell exosomes: A source of autoantigenic ribonucleoproteins. *Arthritis Rheum.* 52: 1517-1521.
81. Thery, C., A. Regnault, J. Garin, J. Wolfers, L. Zitvogel, P. Ricciardi-Castagnoli, G. Raposo, and S. Amigorena. 1999. Molecular characterization of dendritic cell-derived exosomes. Selective accumulation of the heat shock protein hsc73. *J. Cell Biol.* 147: 599-610.
82. Zech, D., S. Rana, M. W. Buchler, and M. Zoller. 2012. Tumor-exosomes and leukocyte activation: an ambivalent crosstalk. *Cell Commun. Signal* 10: 37.
83. Wang, G., M. Dinkins, Q. He, G. Zhu, C. Poirier, A. Campbell, M. Mayer-Proschel, and E. Bieberich. 2012. Astrocytes secrete exosomes enriched with proapoptotic ceramide and prostate apoptosis response 4 (PAR-4): potential mechanism of apoptosis induction in Alzheimer disease (AD). *J. Biol. Chem.* 287: 21384-21395.
84. Thery, C., M. Ostrowski, and E. Segura. 2009. Membrane vesicles as conveyors of immune responses. *Nat. Rev. Immunol.* 9: 581-593.
85. Cocucci, E., G. Racchetti, and J. Meldolesi. 2009. Shedding microvesicles: artefacts no more. *Trends Cell Biol.* 19: 43-51.
86. Ostrowski, M., N. B. Carmo, S. Krumeich, I. Fanget, G. Raposo, A. Savina, C. F. Moita, K. Schauer, A. N. Hume, R. P. Freitas, B. Goud, P. Benaroch, N. Hacohen, M. Fukuda, C. Desnos, M. C. Seabra, F. Darchen, S. Amigorena, L. F. Moita, and C. Thery. 2010.

Rab27a and Rab27b control different steps of the exosome secretion pathway. *Nat. Cell Biol.* 12: 19-30; sup pp 11-13.

87. Raposo, G., H. W. Nijman, W. Stoorvogel, R. Liejendekker, C. V. Harding, C. J. Melief, and H. J. Geuze. 1996. B lymphocytes secrete antigen-presenting vesicles. *J. Exp. Med.* 183: 1161-1172.
88. Conde-Vancells, J., E. Rodriguez-Suarez, N. Embade, D. Gil, R. Matthiesen, M. Valle, F. Elortza, S. C. Lu, J. M. Mato, and J. M. Falcon-Perez. 2008. Characterization and comprehensive proteome profiling of exosomes secreted by hepatocytes. *J. Proteome Res.* 7: 5157-5166.
89. Subra, C., D. Grand, K. Laulagnier, A. Stella, G. Lambeau, M. Paillasse, P. De Medina, B. Monsarrat, B. Perret, S. Silvente-Poirot, M. Poirot, and M. Record. 2010. Exosomes account for vesicle-mediated transcellular transport of activatable phospholipases and prostaglandins. *J. Lipid Res.* 51: 2105-2120.
90. Trajkovic, K., C. Hsu, S. Chiantia, L. Rajendran, D. Wenzel, F. Wieland, P. Schwille, B. Brugger, and M. Simons. 2008. Ceramide triggers budding of exosome vesicles into multivesicular endosomes. *Science* 319: 1244-1247.
91. Subra, C., K. Laulagnier, B. Perret, and M. Record. 2007. Exosome lipidomics unravels lipid sorting at the level of multivesicular bodies. *Biochimie* 89: 205-212.
92. Pan, B. T., and R. M. Johnstone. 1983. Fate of the transferrin receptor during maturation of sheep reticulocytes in vitro: selective externalization of the receptor. *Cell* 33: 967-978.
93. Johnstone, R. M., M. Adam, J. R. Hammond, L. Orr, and C. Turbide. 1987. Vesicle formation during reticulocyte maturation. Association of plasma membrane activities with released vesicles (exosomes). *J. Biol. Chem.* 262: 9412-9420.
94. Geminard, C., A. De Gassart, L. Blanc, and M. Vidal. 2004. Degradation of AP2 during reticulocyte maturation enhances binding of hsc70 and Alix to a common site on TFR for sorting into exosomes. *Traffic* 5: 181-193.
95. Nolte-'t Hoen, E. N., S. I. Buschow, S. M. Anderton, W. Stoorvogel, and M. H. Wauben. 2009. Activated T cells recruit exosomes secreted by dendritic cells via LFA-1. *Blood* 113: 1977-1981.
96. Segura, E., C. Guerin, N. Hogg, S. Amigorena, and C. Thery. 2007. CD8+ dendritic cells use LFA-1 to capture MHC-peptide complexes from exosomes in vivo. *J. Immunol.* 179: 1489-1496.
97. Morelli, A. E., A. T. Larregina, W. J. Shufesky, M. L. Sullivan, D. B. Stolz, G. D. Papworth, A. F. Zahorchak, A. J. Logar, Z. Wang, S. C. Watkins, L. D. Falo, Jr., and A. W. Thomson. 2004. Endocytosis, intracellular sorting, and processing of exosomes by dendritic cells. *Blood* 104: 3257-3266.
98. Arnold, P. Y., and M. D. Mannie. 1999. Vesicles bearing MHC class II molecules mediate transfer of antigen from antigen-presenting cells to CD4+ T cells. *Eur. J. Immunol.* 29: 1363-1373.
99. Xie, Y., H. Zhang, W. Li, Y. Deng, M. A. Munegowda, R. Chibbar, M. Qureshi, and J. Xiang. Dendritic cells recruit T cell exosomes via exosomal LFA-1 leading to inhibition of CD8+ CTL responses through downregulation of peptide/MHC class I and Fas ligand-mediated cytotoxicity. *J. Immunol.* 185: 5268-5278.
100. Zhang, H., Y. Xie, W. Li, R. Chibbar, S. Xiong, and J. Xiang. CD4(+) T cell-released exosomes inhibit CD8(+) cytotoxic T-lymphocyte responses and antitumor immunity. *Cell. Mol. Immunol.* 8: 23-30.

101. Miyanishi, M., K. Tada, M. Koike, Y. Uchiyama, T. Kitamura, and S. Nagata. 2007. Identification of Tim4 as a phosphatidylserine receptor. *Nature* 450: 435-439.
102. Valadi, H., K. Ekstrom, A. Bossios, M. Sjostrand, J. J. Lee, and J. O. Lotvall. 2007. Exosome-mediated transfer of mRNAs and microRNAs is a novel mechanism of genetic exchange between cells. *Nat. Cell Biol.* 9: 654-659.
103. Luo, S. S., O. Ishibashi, G. Ishikawa, T. Ishikawa, A. Katayama, T. Mishima, T. Takizawa, T. Shigihara, T. Goto, A. Izumi, A. Ohkuchi, S. Matsubara, T. Takeshita, and T. Takizawa. 2009. Human villous trophoblasts express and secrete placenta-specific microRNAs into maternal circulation via exosomes. *Biol. Reprod.* 81: 717-729.
104. Pegtel, D. M., M. D. van de Garde, and J. M. Middeldorp. 2011. Viral miRNAs exploiting the endosomal-exosomal pathway for intercellular cross-talk and immune evasion. *Biochim. Biophys. Acta* 1809: 715-721.
105. Al-Nedawi, K., B. Meehan, J. Micallef, V. Lhotak, L. May, A. Guha, and J. Rak. 2008. Intercellular transfer of the oncogenic receptor EGFRvIII by microvesicles derived from tumour cells. *Nat. Cell Biol.* 10: 619-624.
106. Skog, J., T. Wurdinger, S. van Rijn, D. H. Meijer, L. Gainche, M. Sena-Esteves, W. T. Curry, Jr., B. S. Carter, A. M. Krichevsky, and X. O. Breakefield. 2008. Glioblastoma microvesicles transport RNA and proteins that promote tumour growth and provide diagnostic biomarkers. *Nat. Cell Biol.* 10: 1470-1476.
107. Pegtel, D. M., K. Cosmopoulos, D. A. Thorley-Lawson, M. A. van Eijndhoven, E. S. Hopmans, J. L. Lindenberg, T. D. de Gruijl, T. Wurdinger, and J. M. Middeldorp. 2010. Functional delivery of viral miRNAs via exosomes. *Proc. Natl. Acad. Sci. U. S. A.* 107: 6328-6333.
108. Chertova, E., O. Chertov, L. V. Coren, J. D. Roser, C. M. Trubey, J. W. Bess, Jr., R. C. Sowder, 2nd, E. Barsov, B. L. Hood, R. J. Fisher, K. Nagashima, T. P. Conrads, T. D. Veenstra, J. D. Lifson, and D. E. Ott. 2006. Proteomic and biochemical analysis of purified human immunodeficiency virus type 1 produced from infected monocyte-derived macrophages. *J. Virol.* 80: 9039-9052.
109. Hwang, I., X. Shen, and J. Sprent. 2003. Direct stimulation of naive T cells by membrane vesicles from antigen-presenting cells: distinct roles for CD54 and B7 molecules. *Proc. Natl. Acad. Sci. U. S. A.* 100: 6670-6675.
110. Admyre, C., S. M. Johansson, S. Paulie, and S. Gabrielsson. 2006. Direct exosome stimulation of peripheral human T cells detected by ELISPOT. *Eur. J. Immunol.* 36: 1772-1781.
111. Luketic, L., J. Delanghe, P. T. Sobol, P. Yang, E. Frotten, K. L. Mossman, J. Gauldie, J. Bramson, and Y. Wan. 2007. Antigen presentation by exosomes released from peptide-pulsed dendritic cells is not suppressed by the presence of active CTL. *J. Immunol.* 179: 5024-5032.
112. Hsu, D. H., P. Paz, G. Villaflor, A. Rivas, A. Mehta-Damani, E. Angevin, L. Zitvogel, and J. B. Le Pecq. 2003. Exosomes as a tumor vaccine: enhancing potency through direct loading of antigenic peptides. *J. Immunother.* 26: 440-450.
113. Andre, F., N. Chaput, N. E. Schartz, C. Flament, N. Aubert, J. Bernard, F. Lemonnier, G. Raposo, B. Escudier, D. H. Hsu, T. Tursz, S. Amigorena, E. Angevin, and L. Zitvogel. 2004. Exosomes as potent cell-free peptide-based vaccine. I. Dendritic cell-derived exosomes transfer functional MHC class I/peptide complexes to dendritic cells. *J. Immunol.* 172: 2126-2136.

114. Chaput, N., N. E. Schartz, F. Andre, J. Taieb, S. Novault, P. Bonnaventure, N. Aubert, J. Bernard, F. Lemonnier, M. Merad, G. Adema, M. Adams, M. Ferrantini, A. F. Carpentier, B. Escudier, T. Tursz, E. Angevin, and L. Zitvogel. 2004. Exosomes as potent cell-free peptide-based vaccine. II. Exosomes in CpG adjuvants efficiently prime naive Tc1 lymphocytes leading to tumor rejection. *J. Immunol.* 172: 2137-2146.
115. Thery, C., L. Duban, E. Segura, P. Veron, O. Lantz, and S. Amigorena. 2002. Indirect activation of naive CD4+ T cells by dendritic cell-derived exosomes. *Nat. Immunol.* 3: 1156-1162.
116. Segura, E., C. Nicco, B. Lombard, P. Veron, G. Raposo, F. Batteux, S. Amigorena, and C. Thery. 2005. ICAM-1 on exosomes from mature dendritic cells is critical for efficient naive T-cell priming. *Blood* 106: 216-223.
117. Wolfers, J., A. Lozier, G. Raposo, A. Regnault, C. Thery, C. Masurier, C. Flament, S. Pouzieux, F. Faure, T. Tursz, E. Angevin, S. Amigorena, and L. Zitvogel. 2001. Tumor-derived exosomes are a source of shared tumor rejection antigens for CTL cross-priming. *Nat. Med.* 7: 297-303.
118. Andre, F., N. E. Schartz, M. Movassagh, C. Flament, P. Pautier, P. Morice, C. Pomel, C. Lhomme, B. Escudier, T. Le Chevalier, T. Tursz, S. Amigorena, G. Raposo, E. Angevin, and L. Zitvogel. 2002. Malignant effusions and immunogenic tumour-derived exosomes. *Lancet* 360: 295-305.
119. Giri, P. K., and J. S. Schorey. 2008. Exosomes derived from M. Bovis BCG infected macrophages activate antigen-specific CD4+ and CD8+ T cells in vitro and in vivo. *PLoS One* 3: e2461.
120. Walker, J. D., C. L. Maier, and J. S. Pober. 2009. Cytomegalovirus-infected human endothelial cells can stimulate allogeneic CD4+ memory T cells by releasing antigenic exosomes. *J. Immunol.* 182: 1548-1559.
121. Quah, B. J., and H. C. O'Neill. 2007. Mycoplasma contaminants present in exosome preparations induce polyclonal B cell responses. *J. Leukoc. Biol.* 82: 1070-1082.
122. Simhadri, V. R., K. S. Reiners, H. P. Hansen, D. Topolar, V. L. Simhadri, K. Nohroudi, T. A. Kufer, A. Engert, and E. Pogge von Strandmann. 2008. Dendritic cells release HLA-B-associated transcript-3 positive exosomes to regulate natural killer function. *PLoS One* 3: e3377.
123. Viaud, S., M. Terme, C. Flament, J. Taieb, F. Andre, S. Novault, B. Escudier, C. Robert, S. Caillat-Zucman, T. Tursz, L. Zitvogel, and N. Chaput. 2009. Dendritic cell-derived exosomes promote natural killer cell activation and proliferation: a role for NKG2D ligands and IL-15Ralpha. *PLoS One* 4: e4942.
124. Gastpar, R., M. Gehrmann, M. A. Bausero, A. Asea, C. Gross, J. A. Schroeder, and G. Multhoff. 2005. Heat shock protein 70 surface-positive tumor exosomes stimulate migratory and cytolytic activity of natural killer cells. *Cancer Res.* 65: 5238-5247.
125. Vega, V. L., M. Rodriguez-Silva, T. Frey, M. Gehrmann, J. C. Diaz, C. Steinem, G. Multhoff, N. Arispe, and A. De Maio. 2008. Hsp70 translocates into the plasma membrane after stress and is released into the extracellular environment in a membrane-associated form that activates macrophages. *J. Immunol.* 180: 4299-4307.
126. Dai, S., T. Wan, B. Wang, X. Zhou, F. Xiu, T. Chen, Y. Wu, and X. Cao. 2005. More efficient induction of HLA-A*0201-restricted and carcinoembryonic antigen (CEA)-specific CTL response by immunization with exosomes prepared from heat-stressed CEA-positive tumor cells. *Clin Cancer Res* 11: 7554-7563.

127. Cho, J. A., Y. S. Lee, S. H. Kim, J. K. Ko, and C. W. Kim. 2009. MHC independent anti-tumor immune responses induced by Hsp70-enriched exosomes generate tumor regression in murine models. *Cancer Lett.* 275: 256-265.
128. Bhatnagar, S., K. Shinagawa, F. J. Castellino, and J. S. Schorey. 2007. Exosomes released from macrophages infected with intracellular pathogens stimulate a proinflammatory response in vitro and in vivo. *Blood* 110: 3234-3244.
129. Bhatnagar, S., and J. S. Schorey. 2007. Exosomes released from infected macrophages contain Mycobacterium avium glycopeptidolipids and are proinflammatory. *J. Biol. Chem.* 282: 25779-25789.
130. Skokos, D., S. Le Panse, I. Villa, J. C. Rousselle, R. Peronet, B. David, A. Namane, and S. Mecheri. 2001. Mast cell-dependent B and T lymphocyte activation is mediated by the secretion of immunologically active exosomes. *J. Immunol.* 166: 868-876.
131. Andreola, G., L. Rivoltini, C. Castelli, V. Huber, P. Perego, P. Deho, P. Squarcina, P. Accornero, F. Lozupone, L. Lugini, A. Stringaro, A. Molinari, G. Arancia, M. Gentile, G. Parmiani, and S. Fais. 2002. Induction of lymphocyte apoptosis by tumor cell secretion of FasL-bearing microvesicles. *J. Exp. Med.* 195: 1303-1316.
132. Huber, V., S. Fais, M. Iero, L. Lugini, P. Canese, P. Squarcina, A. Zaccheddu, M. Colone, G. Arancia, M. Gentile, E. Seregni, R. Valenti, G. Ballabio, F. Belli, E. Leo, G. Parmiani, and L. Rivoltini. 2005. Human colorectal cancer cells induce T-cell death through release of proapoptotic microvesicles: role in immune escape. *Gastroenterology* 128: 1796-1804.
133. Klibi, J., T. Niki, A. Riedel, C. Pioche-Durieu, S. Souquere, E. Rubinstein, S. Le Moulec, J. Guigay, M. Hirashima, F. Guemira, D. Adhikary, J. Mautner, and P. Busson. 2009. Blood diffusion and Th1-suppressive effects of galectin-9-containing exosomes released by Epstein-Barr virus-infected nasopharyngeal carcinoma cells. *Blood* 113: 1957-1966.
134. Liu, C., S. Yu, K. Zinn, J. Wang, L. Zhang, Y. Jia, J. C. Kappes, S. Barnes, R. P. Kimberly, W. E. Grizzle, and H. G. Zhang. 2006. Murine mammary carcinoma exosomes promote tumor growth by suppression of NK cell function. *J. Immunol.* 176: 1375-1385.
135. Clayton, A., J. P. Mitchell, J. Court, M. D. Mason, and Z. Tabi. 2007. Human tumor-derived exosomes selectively impair lymphocyte responses to interleukin-2. *Cancer Res.* 67: 7458-7466.
136. Clayton, A., J. P. Mitchell, J. Court, S. Linnane, M. D. Mason, and Z. Tabi. 2008. Human tumor-derived exosomes down-modulate NKG2D expression. *J. Immunol.* 180: 7249-7258.
137. Yu, S., C. Liu, K. Su, J. Wang, Y. Liu, L. Zhang, C. Li, Y. Cong, R. Kimberly, W. E. Grizzle, C. Falkson, and H. G. Zhang. 2007. Tumor exosomes inhibit differentiation of bone marrow dendritic cells. *J. Immunol.* 178: 6867-6875.
138. Valenti, R., V. Huber, P. Filipazzi, L. Pilla, G. Sovena, A. Villa, A. Corbelli, S. Fais, G. Parmiani, and L. Rivoltini. 2006. Human tumor-released microvesicles promote the differentiation of myeloid cells with transforming growth factor-beta-mediated suppressive activity on T lymphocytes. *Cancer Res.* 66: 9290-9298.
139. Xiang, X., A. Poliakov, C. Liu, Y. Liu, Z. B. Deng, J. Wang, Z. Cheng, S. V. Shah, G. J. Wang, L. Zhang, W. E. Grizzle, J. Mobley, and H. G. Zhang. 2009. Induction of myeloid-derived suppressor cells by tumor exosomes. *Int. J. Cancer* 124: 2621-2633.
140. Ciravolo, V., V. Huber, G. C. Ghedini, E. Venturelli, F. Bianchi, M. Campiglio, D. Morelli, A. Villa, P. Della Mina, S. Menard, P. Filipazzi, L. Rivoltini, E. Tagliabue, and

S. M. Pupa. 2012. Potential role of HER2-overexpressing exosomes in countering trastuzumab-based therapy. *J. Cell. Physiol.* 227: 658-667.
141. Martinez-Lorenzo, M. J., A. Anel, S. Gamen, I. Monle n, P. Lasierra, L. Larrad, A. Pineiro, M. A. Alava, and J. Naval. 1999. Activated human T cells release bioactive Fas ligand and APO2 ligand in microvesicles. *J. Immunol.* 163: 1274-1281.
142. Monleon, I., M. J. Martinez-Lorenzo, L. Monteagudo, P. Lasierra, M. Taules, M. Iturralde, A. Pineiro, L. Larrad, M. A. Alava, J. Naval, and A. Anel. 2001. Differential secretion of Fas ligand- or APO2 ligand/TNF-related apoptosis-inducing ligand-carrying microvesicles during activation-induced death of human T cells. *J. Immunol.* 167: 6736-6744.
143. Taylor, D. D., S. Akyol, and C. Gercel-Taylor. 2006. Pregnancy-associated exosomes and their modulation of T cell signaling. *J. Immunol.* 176: 1534-1542.
144. Hedlund, M., A. C. Stenqvist, O. Nagaeva, L. Kjellberg, M. Wulff, V. Baranov, and L. Mincheva-Nilsson. 2009. Human placenta expresses and secretes NKG2D ligands via exosomes that down-modulate the cognate receptor expression: evidence for immunosuppressive function. *J. Immunol.* 183: 340-351.
145. Admyre, C., S. M. Johansson, K. R. Qazi, J. J. Filen, R. Lahesmaa, M. Norman, E. P. Neve, A. Scheynius, and S. Gabrielsson. 2007. Exosomes with immune modulatory features are present in human breast milk. *J. Immunol.* 179: 1969-1978.
146. Zitvogel, L., A. Regnault, A. Lozier, J. Wolfers, C. Flament, D. Tenza, P. Ricciardi-Castagnoli, G. Raposo, and S. Amigorena. 1998. Eradication of established murine tumors using a novel cell-free vaccine: dendritic cell-derived exosomes. *Nat. Med.* 4: 594-600.
147. Sprent, J. 2005. Direct stimulation of naive T cells by antigen-presenting cell vesicles. *Blood Cells Mol. Dis.* 35: 17-20.
148. Kovar, M., O. Boyman, X. Shen, I. Hwang, R. Kohler, and J. Sprent. 2006. Direct stimulation of T cells by membrane vesicles from antigen-presenting cells. *Proc. Natl. Acad. Sci. U. S. A.* 103: 11671-11676.
149. Qazi, K. R., U. Gehrmann, E. Domange Jordo, M. C. Karlsson, and S. Gabrielsson. 2009. Antigen-loaded exosomes alone induce Th1-type memory through a B-cell-dependent mechanism. *Blood* 113: 2673-2683.
150. Alvarez-Erviti, L., Y. Seow, H. Yin, C. Betts, S. Lakhal, and M. J. Wood. 2011. Delivery of siRNA to the mouse brain by systemic injection of targeted exosomes. *Nat. Biotechnol.* 29: 341-345.
151. El-Andaloussi, S., Y. Lee, S. Lakhal-Littleton, J. Li, Y. Seow, C. Gardiner, L. Alvarez-Erviti, I. L. Sargent, and M. J. Wood. 2012. Exosome-mediated delivery of siRNA in vitro and in vivo. *Nat. Protoc.* 7: 2112-2126.
152. Ohno, S., M. Takanashi, K. Sudo, S. Ueda, A. Ishikawa, N. Matsuyama, K. Fujita, T. Mizutani, T. Ohgi, T. Ochiya, N. Gotoh, and M. Kuroda. 2013. Systemically injected exosomes targeted to EGFR deliver antitumor microRNA to breast cancer cells. *Mol. Ther.* 21: 185-191.
153. Hao, S., Z. Ye, J. Yang, O. Bai, and J. Xiang. 2006. Intradermal vaccination of dendritic cell-derived exosomes is superior to a subcutaneous one in the induction of antitumor immunity. *Cancer Biother. Radiopharm.* 21: 146-154.

154. Aline, F., D. Bout, S. Amigorena, P. Roingeard, and I. Dimier-Poisson. 2004. Toxoplasma gondii antigen-pulsed-dendritic cell-derived exosomes induce a protective immune response against T. gondii infection. *Infect. Immun.* 72: 4127-4137.
155. Colino, J., and C. M. Snapper. 2006. Exosomes from bone marrow dendritic cells pulsed with diphtheria toxoid preferentially induce type 1 antigen-specific IgG responses in naive recipients in the absence of free antigen. *J. Immunol.* 177: 3757-3762.
156. Curiel, T. J., G. Coukos, L. Zou, X. Alvarez, P. Cheng, P. Mottram, M. Evdemon-Hogan, J. R. Conejo-Garcia, L. Zhang, M. Burow, Y. Zhu, S. Wei, I. Kryczek, B. Daniel, A. Gordon, L. Myers, A. Lackner, M. L. Disis, K. L. Knutson, L. Chen, and W. Zou. 2004. Specific recruitment of regulatory T cells in ovarian carcinoma fosters immune privilege and predicts reduced survival. *Nat. Med.* 10: 942-949.
157. Sakaguchi, S. 2004. Naturally arising CD4+ regulatory t cells for immunologic self-tolerance and negative control of immune responses. *Annu. Rev. Immunol.* 22: 531-562.
158. Viguier, M., F. Lemaitre, O. Verola, M. S. Cho, G. Gorochov, L. Dubertret, H. Bachelez, P. Kourilsky, and L. Ferradini. 2004. Foxp3 expressing CD4+CD25(high) regulatory T cells are overrepresented in human metastatic melanoma lymph nodes and inhibit the function of infiltrating T cells. *J. Immunol.* 173: 1444-1453.
159. Ghiringhelli, F., N. Larmonier, E. Schmitt, A. Parcellier, D. Cathelin, C. Garrido, B. Chauffert, E. Solary, B. Bonnotte, and F. Martin. 2004. CD4+CD25+ regulatory T cells suppress tumor immunity but are sensitive to cyclophosphamide which allows immunotherapy of established tumors to be curative. *Eur. J. Immunol.* 34: 336-344.
160. Taieb, J., N. Chaput, N. Schartz, S. Roux, S. Novault, C. Menard, F. Ghiringhelli, M. Terme, A. F. Carpentier, G. Darrasse-Jeze, F. Lemonnier, and L. Zitvogel. 2006. Chemoimmunotherapy of tumors: cyclophosphamide synergizes with exosome based vaccines. *J. Immunol.* 176: 2722-2729.
161. Xie, Y., O. Bai, H. Zhang, J. Yuan, S. Zong, R. Chibbar, K. Slattery, M. Qureshi, Y. Wei, Y. Deng, and J. Xiang. Membrane-bound HSP70-engineered myeloma cell-derived exosomes stimulate more efficient CD8(+) CTL- and NK-mediated antitumour immunity than exosomes released from heat-shocked tumour cells expressing cytoplasmic HSP70. *J. Cell. Mol. Med.* 14: 2655-2666.
162. Zhong, H., Y. Yang, S. Ma, F. Xiu, Z. Cai, H. Zhao, and L. Du. Induction of a tumour-specific CTL response by exosomes isolated from heat-treated malignant ascites of gastric cancer patients. *Int. J. Hyperthermia* 27: 604-611.
163. Park, J. E., H. S. Tan, A. Datta, R. C. Lai, H. Zhang, W. Meng, S. K. Lim, and S. K. Sze. 2010. Hypoxic tumor cell modulates its microenvironment to enhance angiogenic and metastatic potential by secretion of proteins and exosomes. *Mol. Cell. Proteomics* 9: 1085-1099.
164. Dai, S., X. Zhou, B. Wang, Q. Wang, Y. Fu, T. Chen, T. Wan, Y. Yu, and X. Cao. 2006. Enhanced induction of dendritic cell maturation and HLA-A*0201-restricted CEA-specific CD8(+) CTL response by exosomes derived from IL-18 gene-modified CEA-positive tumor cells. *J Mol Med (Berl)* 84: 1067-1076.
165. Yang, Y., F. Xiu, Z. Cai, J. Wang, Q. Wang, Y. Fu, and X. Cao. 2007. Increased induction of antitumor response by exosomes derived from interleukin-2 gene-modified tumor cells. *J. Cancer Res. Clin. Oncol.* 133: 389-399.

166. Lamparski, H. G., A. Metha-Damani, J. Y. Yao, S. Patel, D. H. Hsu, C. Ruegg, and J. B. Le Pecq. 2002. Production and characterization of clinical grade exosomes derived from dendritic cells. *J. Immunol. Methods* 270: 211-226.
167. Morse, M. A., J. Garst, T. Osada, S. Khan, A. Hobeika, T. M. Clay, N. Valente, R. Shreeniwas, M. A. Sutton, A. Delcayre, D. H. Hsu, J. B. Le Pecq, and H. K. Lyerly. 2005. A phase I study of dexosome immunotherapy in patients with advanced non-small cell lung cancer. *J. Transl. Med.* 3: 9.
168. Dai, S., D. Wei, Z. Wu, X. Zhou, X. Wei, H. Huang, and G. Li. 2008. Phase I clinical trial of autologous ascites-derived exosomes combined with GM-CSF for colorectal cancer. *Mol. Ther.* 16: 782-790.
169. Adams, M., H. Navabi, D. Croston, S. Coleman, Z. Tabi, A. Clayton, B. Jasani, and M. D. Mason. 2005. The rationale for combined chemo/immunotherapy using a Toll-like receptor 3 (TLR3) agonist and tumour-derived exosomes in advanced ovarian cancer. *Vaccine* 23: 2374-2378.
170. D'Souza-Schorey, C., and J. W. Clancy. 2012. Tumor-derived microvesicles: shedding light on novel microenvironment modulators and prospective cancer biomarkers. *Genes Dev.* 26: 1287-1299.
171. Mitchison, N. A., and C. O'Malley. 1987. Three-cell-type clusters of T cells with antigen-presenting cells best explain the epitope linkage and noncognate requirements of the in vivo cytolytic response. *Eur. J. Immunol.* 17: 1579-1583.
172. Ridge, J. P., F. Di Rosa, and P. Matzinger. 1998. A conditioned dendritic cell can be a temporal bridge between a CD4+ T-helper and a T-killer cell. *Nature* 393: 474-478.
173. Bourgeois, C., B. Rocha, and C. Tanchot. 2002. A role for CD40 expression on CD8+ T cells in the generation of CD8+ T cell memory. *Science* 297: 2060-2063.
174. Ahmed, K. A., and J. Xiang. 2011. Mechanisms of cellular communication through intercellular protein transfer. *J. Cell. Mol. Med.* 15: 1458-1473.
175. Huang, J. F., Y. Yang, H. Sepulveda, W. Shi, I. Hwang, P. A. Peterson, M. R. Jackson, J. Sprent, and Z. Cai. 1999. TCR-Mediated internalization of peptide-MHC complexes acquired by T cells. *Science* 286: 952-954.
176. Xiang, J., H. Huang, and Y. Liu. 2005. A new dynamic model of CD8+ T effector cell responses via CD4+ T helper-antigen-presenting cells. *J. Immunol.* 174: 7497-7505.
177. Rosenits, K., S. J. Keppler, S. Vucikuja, and P. Aichele. 2010. T cells acquire cell surface determinants of APC via in vivo trogocytosis during viral infections. *Eur. J. Immunol.* 40: 3450-3457.
178. Umeshappa, C. S., H. Huang, Y. Xie, Y. Wei, S. J. Mulligan, Y. Deng, and J. Xiang. 2009. CD4+ Th-APC with acquired peptide/MHC class I and II complexes stimulate type 1 helper CD4+ and central memory CD8+ T cell responses. *J. Immunol.* 182: 193-206.
179. Ahmed, K. A., L. Wang, M. A. Munegowda, S. J. Mulligan, J. R. Gordon, P. Griebel, and J. Xiang. 2012. Direct in vivo evidence of CD4+ T cell requirement for CTL response and memory via pMHC-I targeting and CD40L signaling. *J. Leukoc. Biol.* 92: 289-300.
180. Jameson, S. C., and D. Masopust. 2009. Diversity in T cell memory: an embarrassment of riches. *Immunity* 31: 859-871.
181. Hao, S., Y. Liu, J. Yuan, X. Zhang, T. He, X. Wu, Y. Wei, D. Sun, and J. Xiang. 2007. Novel exosome-targeted CD4+ T cell vaccine counteracting CD4+25+ regulatory T cell-mediated immune suppression and stimulating efficient central memory CD8+ CTL responses. *J. Immunol.* 179: 2731-2740.

182. Xie, Y., L. Wang, A. Freywald, M. Qureshi, Y. Chen, and J. Xiang. 2013. A novel T cell-based vaccine capable of stimulating long-term functional CTL memory against B16 melanoma via CD40L signaling. *Cell. Mol. Immunol.* 10: 72-77.
183. Wang, L., Y. Xie, K. A. Ahmed, S. Ahmed, A. Sami, R. Chibbar, Q. Xu, S. E. Kane, S. Hao, S. J. Mulligan, and J. Xiang. 2013. Exosomal pMHC-I complex targets T cell-based vaccine to directly stimulate CTL responses leading to antitumor immunity in transgenic FVBneuN and HLA-A2/HER2 mice and eradicating trastuzumab-resistant tumor in athymic nude mice. *Breast Cancer Res. Treat.*
184. Oheim, M., E. Beaurepaire, E. Chaigneau, J. Mertz, and S. Charpak. 2001. Two-photon microscopy in brain tissue: parameters influencing the imaging depth. *J. Neurosci. Methods* 111: 29-37.
185. Germain, R. N., M. J. Miller, M. L. Dustin, and M. C. Nussenzweig. 2006. Dynamic imaging of the immune system: progress, pitfalls and promise. *Nat. Rev. Immunol.* 6: 497-507.
186. Miller, M. J., S. H. Wei, I. Parker, and M. D. Cahalan. 2002. Two-photon imaging of lymphocyte motility and antigen response in intact lymph node. *Science* 296: 1869-1873.
187. Campagnola, P. J., and L. M. Loew. 2003. Second-harmonic imaging microscopy for visualizing biomolecular arrays in cells, tissues and organisms. *Nat. Biotechnol.* 21: 1356-1360.
188. Cahalan, M. D., and I. Parker. 2008. Choreography of cell motility and interaction dynamics imaged by two-photon microscopy in lymphoid organs. *Annu. Rev. Immunol.* 26: 585-626.
189. Worbs, T., T. R. Mempel, J. Bolter, U. H. von Andrian, and R. Forster. 2007. CCR7 ligands stimulate the intranodal motility of T lymphocytes in vivo. *J. Exp. Med.* 204: 489-495.
190. Garrod, K. R., S. H. Wei, I. Parker, and M. D. Cahalan. 2007. Natural killer cells actively patrol peripheral lymph nodes forming stable conjugates to eliminate MHC-mismatched targets. *Proc. Natl. Acad. Sci. U. S. A.* 104: 12081-12086.
191. Chtanova, T., M. Schaeffer, S. J. Han, G. G. van Dooren, M. Nollmann, P. Herzmark, S. W. Chan, H. Satija, K. Camfield, H. Aaron, B. Striepen, and E. A. Robey. 2008. Dynamics of neutrophil migration in lymph nodes during infection. *Immunity* 29: 487-496.
192. Auffray, C., D. Fogg, M. Garfa, G. Elain, O. Join-Lambert, S. Kayal, S. Sarnacki, A. Cumano, G. Lauvau, and F. Geissmann. 2007. Monitoring of blood vessels and tissues by a population of monocytes with patrolling behavior. *Science* 317: 666-670.
193. Bousso, P., and E. Robey. 2003. Dynamics of CD8+ T cell priming by dendritic cells in intact lymph nodes. *Nat. Immunol.* 4: 579-585.
194. Mempel, T. R., S. E. Henrickson, and U. H. Von Andrian. 2004. T-cell priming by dendritic cells in lymph nodes occurs in three distinct phases. *Nature* 427: 154-159.
195. Kissenpfennig, A., S. Henri, B. Dubois, C. Laplace-Builhe, P. Perrin, N. Romani, C. H. Tripp, P. Douillard, L. Leserman, D. Kaiserlian, S. Saeland, J. Davoust, and B. Malissen. 2005. Dynamics and function of Langerhans cells in vivo: dermal dendritic cells colonize lymph node areas distinct from slower migrating Langerhans cells. *Immunity* 22: 643-654.

196. Lindquist, R. L., G. Shakhar, D. Dudziak, H. Wardemann, T. Eisenreich, M. L. Dustin, and M. C. Nussenzweig. 2004. Visualizing dendritic cell networks in vivo. *Nat. Immunol.* 5: 1243-1250.
197. Sen, D., L. Forrest, T. B. Kepler, I. Parker, and M. D. Cahalan. 2010. Selective and site-specific mobilization of dermal dendritic cells and Langerhans cells by Th1- and Th2-polarizing adjuvants. *Proc. Natl. Acad. Sci. U. S. A.* 107: 8334-8339.
198. Miller, M. J., O. Safrina, I. Parker, and M. D. Cahalan. 2004. Imaging the single cell dynamics of CD4+ T cell activation by dendritic cells in lymph nodes. *J. Exp. Med.* 200: 847-856.
199. Qi, H., J. L. Cannons, F. Klauschen, P. L. Schwartzberg, and R. N. Germain. 2008. SAP-controlled T-B cell interactions underlie germinal centre formation. *Nature* 455: 764-769.
200. Okada, T., M. J. Miller, I. Parker, M. F. Krummel, M. Neighbors, S. B. Hartley, A. O'Garra, M. D. Cahalan, and J. G. Cyster. 2005. Antigen-engaged B cells undergo chemotaxis toward the T zone and form motile conjugates with helper T cells. *PLoS Biol.* 3: e150.
201. Campbell, D. J., C. H. Kim, and E. C. Butcher. 2003. Chemokines in the systemic organization of immunity. *Immunol. Rev.* 195: 58-71.
202. von Andrian, U. H., and T. R. Mempel. 2003. Homing and cellular traffic in lymph nodes. *Nat. Rev. Immunol.* 3: 867-878.
203. Gowans, J. L. 1959. The recirculation of lymphocytes from blood to lymph in the rat. *J. Physiol.* 146: 54-69.
204. Tomura, M., N. Yoshida, J. Tanaka, S. Karasawa, Y. Miwa, A. Miyawaki, and O. Kanagawa. 2008. Monitoring cellular movement in vivo with photoconvertible fluorescence protein "Kaede" transgenic mice. *Proc. Natl. Acad. Sci. U. S. A.* 105: 10871-10876.
205. Shamri, R., V. Grabovsky, J. M. Gauguet, S. Feigelson, E. Manevich, W. Kolanus, M. K. Robinson, D. E. Staunton, U. H. von Andrian, and R. Alon. 2005. Lymphocyte arrest requires instantaneous induction of an extended LFA-1 conformation mediated by endothelium-bound chemokines. *Nat. Immunol.* 6: 497-506.
206. Bajenoff, M., J. G. Egen, L. Y. Koo, J. P. Laugier, F. Brau, N. Glaichenhaus, and R. N. Germain. 2006. Stromal cell networks regulate lymphocyte entry, migration, and territoriality in lymph nodes. *Immunity* 25: 989-1001.
207. Qi, H., J. G. Egen, A. Y. Huang, and R. N. Germain. 2006. Extrafollicular activation of lymph node B cells by antigen-bearing dendritic cells. *Science* 312: 1672-1676.
208. Park, C., I. Y. Hwang, R. K. Sinha, O. Kamenyeva, M. D. Davis, and J. H. Kehrl. 2012. Lymph node B lymphocyte trafficking is constrained by anatomy and highly dependent upon chemoattractant desensitization. *Blood* 119: 978-989.
209. Ansel, K. M., V. N. Ngo, P. L. Hyman, S. A. Luther, R. Forster, J. D. Sedgwick, J. L. Browning, M. Lipp, and J. G. Cyster. 2000. A chemokine-driven positive feedback loop organizes lymphoid follicles. *Nature* 406: 309-314.
210. Seth, S., L. Oberdorfer, R. Hyde, K. Hoff, V. Thies, T. Worbs, S. Schmitz, and R. Forster. 2011. CCR7 essentially contributes to the homing of plasmacytoid dendritic cells to lymph nodes under steady-state as well as inflammatory conditions. *J. Immunol.* 186: 3364-3372.

211. Liu, K., G. D. Victora, T. A. Schwickert, P. Guermonprez, M. M. Meredith, K. Yao, F. F. Chu, G. J. Randolph, A. Y. Rudensky, and M. Nussenzweig. 2009. In vivo analysis of dendritic cell development and homeostasis. *Science* 324: 392-397.
212. Tal, O., H. Y. Lim, I. Gurevich, I. Milo, Z. Shipony, L. G. Ng, V. Angeli, and G. Shakhar. 2011. DC mobilization from the skin requires docking to immobilized CCL21 on lymphatic endothelium and intralymphatic crawling. *J. Exp. Med.* 208: 2141-2153.
213. Bajenoff, M., J. G. Egen, H. Qi, A. Y. Huang, F. Castellino, and R. N. Germain. 2007. Highways, byways and breadcrumbs: directing lymphocyte traffic in the lymph node. *Trends Immunol.* 28: 346-352.
214. Cyster, J. G., and S. R. Schwab. 2012. Sphingosine-1-phosphate and lymphocyte egress from lymphoid organs. *Annu. Rev. Immunol.* 30: 69-94.
215. Mandala, S., R. Hajdu, J. Bergstrom, E. Quackenbush, J. Xie, J. Milligan, R. Thornton, G. J. Shei, D. Card, C. Keohane, M. Rosenbach, J. Hale, C. L. Lynch, K. Rupprecht, W. Parsons, and H. Rosen. 2002. Alteration of lymphocyte trafficking by sphingosine-1-phosphate receptor agonists. *Science* 296: 346-349.
216. Matloubian, M., C. G. Lo, G. Cinamon, M. J. Lesneski, Y. Xu, V. Brinkmann, M. L. Allende, R. L. Proia, and J. G. Cyster. 2004. Lymphocyte egress from thymus and peripheral lymphoid organs is dependent on S1P receptor 1. *Nature* 427: 355-360.
217. Grigorova, I. L., S. R. Schwab, T. G. Phan, T. H. Pham, T. Okada, and J. G. Cyster. 2009. Cortical sinus probing, S1P1-dependent entry and flow-based capture of egressing T cells. *Nat. Immunol.* 10: 58-65.
218. Sinha, R. K., C. Park, I. Y. Hwang, M. D. Davis, and J. H. Kehrl. 2009. B lymphocytes exit lymph nodes through cortical lymphatic sinusoids by a mechanism independent of sphingosine-1-phosphate-mediated chemotaxis. *Immunity* 30: 434-446.
219. Miller, M. J., A. S. Hejazi, S. H. Wei, M. D. Cahalan, and I. Parker. 2004. T cell repertoire scanning is promoted by dynamic dendritic cell behavior and random T cell motility in the lymph node. *Proc. Natl. Acad. Sci. U. S. A.* 101: 998-1003.
220. Wei, S. H., O. Safrina, Y. Yu, K. R. Garrod, M. D. Cahalan, and I. Parker. 2007. Ca2+ signals in CD4+ T cells during early contacts with antigen-bearing dendritic cells in lymph node. *J. Immunol.* 179: 1586-1594.
221. Friedman, R. S., J. Jacobelli, and M. F. Krummel. 2006. Surface-bound chemokines capture and prime T cells for synapse formation. *Nat. Immunol.* 7: 1101-1108.
222. Castellino, F., A. Y. Huang, G. Altan-Bonnet, S. Stoll, C. Scheinecker, and R. N. Germain. 2006. Chemokines enhance immunity by guiding naive CD8+ T cells to sites of CD4+ T cell-dendritic cell interaction. *Nature* 440: 890-895.
223. Hugues, S., A. Scholer, A. Boissonnas, A. Nussbaum, C. Combadiere, S. Amigorena, and L. Fetler. 2007. Dynamic imaging of chemokine-dependent CD8+ T cell help for CD8+ T cell responses. *Nat. Immunol.* 8: 921-930.
224. Shakhar, G., R. L. Lindquist, D. Skokos, D. Dudziak, J. H. Huang, M. C. Nussenzweig, and M. L. Dustin. 2005. Stable T cell-dendritic cell interactions precede the development of both tolerance and immunity in vivo. *Nat. Immunol.* 6: 707-714.
225. Scholer, A., S. Hugues, A. Boissonnas, L. Fetler, and S. Amigorena. 2008. Intercellular adhesion molecule-1-dependent stable interactions between T cells and dendritic cells determine CD8+ T cell memory. *Immunity* 28: 258-270.

226. Hugues, S., L. Fetler, L. Bonifaz, J. Helft, F. Amblard, and S. Amigorena. 2004. Distinct T cell dynamics in lymph nodes during the induction of tolerance and immunity. *Nat. Immunol.* 5: 1235-1242.
227. Hugues, S., A. Boissonnas, S. Amigorena, and L. Fetler. 2006. The dynamics of dendritic cell-T cell interactions in priming and tolerance. *Curr. Opin. Immunol.* 18: 491-495.
228. Henrickson, S. E., T. R. Mempel, I. B. Mazo, B. Liu, M. N. Artyomov, H. Zheng, A. Peixoto, M. P. Flynn, B. Senman, T. Junt, H. C. Wong, A. K. Chakraborty, and U. H. von Andrian. 2008. T cell sensing of antigen dose governs interactive behavior with dendritic cells and sets a threshold for T cell activation. *Nat. Immunol.* 9: 282-291.
229. Skokos, D., G. Shakhar, R. Varma, J. C. Waite, T. O. Cameron, R. L. Lindquist, T. Schwickert, M. C. Nussenzweig, and M. L. Dustin. 2007. Peptide-MHC potency governs dynamic interactions between T cells and dendritic cells in lymph nodes. *Nat. Immunol.* 8: 835-844.
230. Schneider, H., J. Downey, A. Smith, B. H. Zinselmeyer, C. Rush, J. M. Brewer, B. Wei, N. Hogg, P. Garside, and C. E. Rudd. 2006. Reversal of the TCR stop signal by CTLA-4. *Science* 313: 1972-1975.
231. Fife, B. T., K. E. Pauken, T. N. Eagar, T. Obu, J. Wu, Q. Tang, M. Azuma, M. F. Krummel, and J. A. Bluestone. 2009. Interactions between PD-1 and PD-L1 promote tolerance by blocking the TCR-induced stop signal. *Nat. Immunol.* 10: 1185-1192.
232. Kedl, R. M., B. C. Schaefer, J. W. Kappler, and P. Marrack. 2002. T cells down-modulate peptide-MHC complexes on APCs in vivo. *Nat. Immunol.* 3: 27-32.
233. Celli, S., F. Lemaitre, and P. Bousso. 2007. Real-time manipulation of T cell-dendritic cell interactions in vivo reveals the importance of prolonged contacts for CD4+ T cell activation. *Immunity* 27: 625-634.
234. Josefowicz, S. Z., L. F. Lu, and A. Y. Rudensky. 2012. Regulatory T cells: mechanisms of differentiation and function. *Annu. Rev. Immunol.* 30: 531-564.
235. Tadokoro, C. E., G. Shakhar, S. Shen, Y. Ding, A. C. Lino, A. Maraver, J. J. Lafaille, and M. L. Dustin. 2006. Regulatory T cells inhibit stable contacts between CD4+ T cells and dendritic cells in vivo. *J. Exp. Med.* 203: 505-511.
236. Tang, Q., J. Y. Adams, A. J. Tooley, M. Bi, B. T. Fife, P. Serra, P. Santamaria, R. M. Locksley, M. F. Krummel, and J. A. Bluestone. 2006. Visualizing regulatory T cell control of autoimmune responses in nonobese diabetic mice. *Nat. Immunol.* 7: 83-92.
237. Mempel, T. R., M. J. Pittet, K. Khazaie, W. Weninger, R. Weissleder, H. von Boehmer, and U. H. von Andrian. 2006. Regulatory T cells reversibly suppress cytotoxic T cell function independent of effector differentiation. *Immunity* 25: 129-141.
238. Boissonnas, A., A. Scholer-Dahirel, V. Simon-Blancal, L. Pace, F. Valet, A. Kissenpfennig, T. Sparwasser, B. Malissen, L. Fetler, and S. Amigorena. 2010. Foxp3+ T cells induce perforin-dependent dendritic cell death in tumor-draining lymph nodes. *Immunity* 32: 266-278.
239. Pace, L., A. Tempez, C. Arnold-Schrauf, F. Lemaitre, P. Bousso, L. Fetler, T. Sparwasser, and S. Amigorena. 2012. Regulatory T cells increase the avidity of primary CD8+ T cell responses and promote memory. *Science* 338: 532-536.
240. Bousso, P., N. R. Bhakta, R. S. Lewis, and E. Robey. 2002. Dynamics of thymocyte-stromal cell interactions visualized by two-photon microscopy. *Science* 296: 1876-1880.

241. Barral, P., M. D. Sanchez-Nino, N. van Rooijen, V. Cerundolo, and F. D. Batista. 2012. The location of splenic NKT cells favours their rapid activation by blood-borne antigen. *EMBO J.* 31: 2378-2390.
242. Odoardi, F., C. Sie, K. Streyl, V. K. Ulaganathan, C. Schlager, D. Lodygin, K. Heckelsmiller, W. Nietfeld, J. Ellwart, W. E. Klinkert, C. Lottaz, M. Nosov, V. Brinkmann, R. Spang, H. Lehrach, M. Vingron, H. Wekerle, C. Flugel-Koch, and A. Flugel. 2012. T cells become licensed in the lung to enter the central nervous system. *Nature* 488: 675-679.
243. Milo, I., A. Sapoznikov, V. Kalchenko, O. Tal, R. Krauthgamer, N. van Rooijen, D. Dudziak, S. Jung, and G. Shakhar. 2013. Dynamic imaging reveals promiscuous cross-presentation of blood-borne antigens to naive CD8+ T cells in the bone marrow. *Blood*.
244. Hickey, M. J., and P. Kubes. 2009. Intravascular immunity: the host-pathogen encounter in blood vessels. *Nat. Rev. Immunol.* 9: 364-375.
245. Peters, A., L. A. Pitcher, J. M. Sullivan, M. Mitsdoerffer, S. E. Acton, B. Franz, K. Wucherpfennig, S. Turley, M. C. Carroll, R. A. Sobel, E. Bettelli, and V. K. Kuchroo. 2011. Th17 cells induce ectopic lymphoid follicles in central nervous system tissue inflammation. *Immunity* 35: 986-996.
246. Beerling, E., L. Ritsma, N. Vrisekoop, P. W. Derksen, and J. van Rheenen. 2011. Intravital microscopy: new insights into metastasis of tumors. *J. Cell Sci.* 124: 299-310.
247. Cho, H. S., K. Mason, K. X. Ramyar, A. M. Stanley, S. B. Gabelli, D. W. Denney, Jr., and D. J. Leahy. 2003. Structure of the extracellular region of HER2 alone and in complex with the Herceptin Fab. *Nature* 421: 756-760.
248. Koeppen, H. K., B. D. Wright, A. D. Burt, P. Quirke, A. M. McNicol, N. O. Dybdal, M. X. Sliwkowski, and K. J. Hillan. 2001. Overexpression of HER2/neu in solid tumours: an immunohistochemical survey. *Histopathology* 38: 96-104.
249. Menard, S., S. M. Pupa, M. Campiglio, and E. Tagliabue. 2003. Biologic and therapeutic role of HER2 in cancer. *Oncogene* 22: 6570-6578.
250. Menard, S., S. Fortis, F. Castiglioni, R. Agresti, and A. Balsari. 2001. HER2 as a prognostic factor in breast cancer. *Oncology* 61 Suppl 2: 67-72.
251. Masood, S., and M. M. Bui. 2002. Prognostic and predictive value of HER2/neu oncogene in breast cancer. *Microsc. Res. Tech.* 59: 102-108.
252. Slamon, D. J., B. Leyland-Jones, S. Shak, H. Fuchs, V. Paton, A. Bajamonde, T. Fleming, W. Eiermann, J. Wolter, M. Pegram, J. Baselga, and L. Norton. 2001. Use of chemotherapy plus a monoclonal antibody against HER2 for metastatic breast cancer that overexpresses HER2. *N. Engl. J. Med.* 344: 783-792.
253. Molina, M. A., J. Codony-Servat, J. Albanell, F. Rojo, J. Arribas, and J. Baselga. 2001. Trastuzumab (herceptin), a humanized anti-Her2 receptor monoclonal antibody, inhibits basal and activated Her2 ectodomain cleavage in breast cancer cells. *Cancer Res.* 61: 4744-4749.
254. Baselga, J., J. Albanell, M. A. Molina, and J. Arribas. 2001. Mechanism of action of trastuzumab and scientific update. *Semin. Oncol.* 28: 4-11.
255. Spector, N. L., and K. L. Blackwell. 2009. Understanding the mechanisms behind trastuzumab therapy for human epidermal growth factor receptor 2-positive breast cancer. *J. Clin. Oncol.* 27: 5838-5847.
256. Nahta, R., and F. J. Esteva. 2006. Herceptin: mechanisms of action and resistance. *Cancer Lett.* 232: 123-138.

257. Berns, K., H. M. Horlings, B. T. Hennessy, M. Madiredjo, E. M. Hijmans, K. Beelen, S. C. Linn, A. M. Gonzalez-Angulo, K. Stemke-Hale, M. Hauptmann, R. L. Beijersbergen, G. B. Mills, M. J. van de Vijver, and R. Bernards. 2007. A functional genetic approach identifies the PI3K pathway as a major determinant of trastuzumab resistance in breast cancer. *Cancer cell* 12: 395-402.
258. Scaltriti, M., F. Rojo, A. Ocana, J. Anido, M. Guzman, J. Cortes, S. Di Cosimo, X. Matias-Guiu, S. Ramon y Cajal, J. Arribas, and J. Baselga. 2007. Expression of p95HER2, a truncated form of the HER2 receptor, and response to anti-HER2 therapies in breast cancer. *J. Natl. Cancer Inst.* 99: 628-638.
259. Vu, T., and F. X. Claret. 2012. Trastuzumab: updated mechanisms of action and resistance in breast cancer. *Front. Oncol.* 2: 62.
260. Wong, A. L., and S. C. Lee. 2012. Mechanisms of Resistance to Trastuzumab and Novel Therapeutic Strategies in HER2-Positive Breast Cancer. *Int. J. Breast Cancer* 2012: 415170.
261. Blackwell, K. L., H. J. Burstein, A. M. Storniolo, H. Rugo, G. Sledge, M. Koehler, C. Ellis, M. Casey, S. Vukelja, J. Bischoff, J. Baselga, and J. O'Shaughnessy. 2010. Randomized study of Lapatinib alone or in combination with trastuzumab in women with ErbB2-positive, trastuzumab-refractory metastatic breast cancer. *J. Clin. Oncol.* 28: 1124-1130.
262. Cortes, J., P. Fumoleau, G. V. Bianchi, T. M. Petrella, K. Gelmon, X. Pivot, S. Verma, J. Albanell, P. Conte, A. Lluch, S. Salvagni, V. Servent, L. Gianni, M. Scaltriti, G. A. Ross, J. Dixon, T. Szado, and J. Baselga. 2012. Pertuzumab monotherapy after trastuzumab-based treatment and subsequent reintroduction of trastuzumab: activity and tolerability in patients with advanced human epidermal growth factor receptor 2-positive breast cancer. *J. Clin. Oncol.* 30: 1594-1600.
263. Teicher, B. A., and J. H. Doroshow. 2012. The promise of antibody-drug conjugates. *N. Engl. J. Med.* 367: 1847-1848.
264. Lewis Phillips, G. D., G. Li, D. L. Dugger, L. M. Crocker, K. L. Parsons, E. Mai, W. A. Blattler, J. M. Lambert, R. V. Chari, R. J. Lutz, W. L. Wong, F. S. Jacobson, H. Koeppen, R. H. Schwall, S. R. Kenkare-Mitra, S. D. Spencer, and M. X. Sliwkowski. 2008. Targeting HER2-positive breast cancer with trastuzumab-DM1, an antibody-cytotoxic drug conjugate. *Cancer Res.* 68: 9280-9290.
265. Modi, S., A. Stopeck, H. Linden, D. Solit, S. Chandarlapaty, N. Rosen, G. D'Andrea, M. Dickler, M. E. Moynahan, S. Sugarman, W. Ma, S. Patil, L. Norton, A. L. Hannah, and C. Hudis. 2011. HSP90 inhibition is effective in breast cancer: a phase II trial of tanespimycin (17-AAG) plus trastuzumab in patients with HER2-positive metastatic breast cancer progressing on trastuzumab. *Clin. Cancer Res.* 17: 5132-5139.
266. Jager, M., A. Schoberth, P. Ruf, J. Hess, and H. Lindhofer. 2009. The trifunctional antibody ertumaxomab destroys tumor cells that express low levels of human epidermal growth factor receptor 2. *Cancer Res.* 69: 4270-4276.
267. Chow, L. W., B. Xu, S. Gupta, A. Freyman, Y. Zhao, R. Abbas, M. L. Vo Van, and I. Bondarenko. 2013. Combination neratinib (HKI-272) and paclitaxel therapy in patients with HER2-positive metastatic breast cancer. *Br. J. Cancer*.
268. Chakrabarty, A., N. E. Bhola, C. Sutton, R. Ghosh, M. G. Kuba, B. Dave, J. C. Chang, and C. L. Arteaga. 2013. Trastuzumab-resistant cells rely on a HER2-PI3K-FoxO-survivin axis and are sensitive to PI3K inhibitors. *Cancer Res.* 73: 1190-1200.

269. Zhang, B. 2008. Targeting the stroma by T cells to limit tumor growth. *Cancer Res.* 68: 9570-9573.
270. Khammari, A., N. Labarriere, V. Vignard, J. M. Nguyen, M. C. Pandolfino, A. C. Knol, G. Quereux, S. Saiagh, A. Brocard, F. Jotereau, and B. Dreno. 2009. Treatment of metastatic melanoma with autologous Melan-A/MART-1-specific cytotoxic T lymphocyte clones. *J. Invest. Dermatol.* 129: 2835-2842.
271. Bernhard, H., J. Neudorfer, K. Gebhard, H. Conrad, C. Hermann, J. Nahrig, F. Fend, W. Weber, D. H. Busch, and C. Peschel. 2008. Adoptive transfer of autologous, HER2-specific, cytotoxic T lymphocytes for the treatment of HER2-overexpressing breast cancer. *Cancer Immunol. Immunother.* 57: 271-280.
272. Knutson, K. L., Y. Dang, H. Lu, J. Lukas, B. Almand, E. Gad, E. Azeke, and M. L. Disis. 2006. IL-2 immunotoxin therapy modulates tumor-associated regulatory T cells and leads to lasting immune-mediated rejection of breast cancers in neu-transgenic mice. *J. Immunol.* 177: 84-91.
273. Kreitman, R. J. 2009. Recombinant immunotoxins for the treatment of chemoresistant hematologic malignancies. *Curr. Pharm. Des.* 15: 2652-2664.
274. Hodi, F. S., M. C. Mihm, R. J. Soiffer, F. G. Haluska, M. Butler, M. V. Seiden, T. Davis, R. Henry-Spires, S. MacRae, A. Willman, R. Padera, M. T. Jaklitsch, S. Shankar, T. C. Chen, A. Korman, J. P. Allison, and G. Dranoff. 2003. Biologic activity of cytotoxic T lymphocyte-associated antigen 4 antibody blockade in previously vaccinated metastatic melanoma and ovarian carcinoma patients. *Proc. Natl. Acad. Sci. U. S. A.* 100: 4712-4717.
275. Hodi, F. S., M. Butler, D. A. Oble, M. V. Seiden, F. G. Haluska, A. Kruse, S. Macrae, M. Nelson, C. Canning, I. Lowy, A. Korman, D. Lautz, S. Russell, M. T. Jaklitsch, N. Ramaiya, T. C. Chen, D. Neuberg, J. P. Allison, M. C. Mihm, and G. Dranoff. 2008. Immunologic and clinical effects of antibody blockade of cytotoxic T lymphocyte-associated antigen 4 in previously vaccinated cancer patients. *Proc. Natl. Acad. Sci. U. S. A.* 105: 3005-3010.
276. Disis, M. L., E. Calenoff, G. McLaughlin, A. E. Murphy, W. Chen, B. Groner, M. Jeschke, N. Lydon, E. McGlynn, R. B. Livingston, and et al. 1994. Existent T-cell and antibody immunity to HER-2/neu protein in patients with breast cancer. *Cancer Res.* 54: 16-20.
277. Peoples, G. E., P. S. Goedegebuure, R. Smith, D. C. Linehan, I. Yoshino, and T. J. Eberlein. 1995. Breast and ovarian cancer-specific cytotoxic T lymphocytes recognize the same HER2/neu-derived peptide. *Proc. Natl. Acad. Sci. U. S. A.* 92: 432-436.
278. Rongcun, Y., F. Salazar-Onfray, J. Charo, K. J. Malmberg, K. Evrin, H. Maes, K. Kono, C. Hising, M. Petersson, O. Larsson, L. Lan, E. Appella, A. Sette, E. Celis, and R. Kiessling. 1999. Identification of new HER2/neu-derived peptide epitopes that can elicit specific CTL against autologous and allogeneic carcinomas and melanomas. *J. Immunol.* 163: 1037-1044.
279. Fisk, B., T. L. Blevins, J. T. Wharton, and C. G. Ioannides. 1995. Identification of an immunodominant peptide of HER-2/neu protooncogene recognized by ovarian tumor-specific cytotoxic T lymphocyte lines. *J. Exp. Med.* 181: 2109-2117.
280. Peoples, G. E., J. P. Holmes, M. T. Hueman, E. A. Mittendorf, A. Amin, S. Khoo, Z. A. Dehqanzada, J. M. Gurney, M. M. Woll, G. B. Ryan, C. E. Storrer, D. Craig, C. G. Ioannides, and S. Ponniah. 2008. Combined clinical trial results of a HER2/neu (E75)

vaccine for the prevention of recurrence in high-risk breast cancer patients: U.S. Military Cancer Institute Clinical Trials Group Study I-01 and I-02. *Clin. Cancer Res.* 14: 797-803.

281. Benavides, L. C., J. D. Gates, M. G. Carmichael, R. Patil, J. P. Holmes, M. T. Hueman, E. A. Mittendorf, D. Craig, A. Stojadinovic, S. Ponniah, and G. E. Peoples. 2009. The impact of HER2/neu expression level on response to the E75 vaccine: from U.S. Military Cancer Institute Clinical Trials Group Study I-01 and I-02. *Clin. Cancer Res.* 15: 2895-2904.
282. Mittendorf, E. A., G. T. Clifton, J. P. Holmes, K. S. Clive, R. Patil, L. C. Benavides, J. D. Gates, A. K. Sears, A. Stojadinovic, S. Ponniah, and G. E. Peoples. 2012. Clinical trial results of the HER-2/neu (E75) vaccine to prevent breast cancer recurrence in high-risk patients: from US Military Cancer Institute Clinical Trials Group Study I-01 and I-02. *Cancer* 118: 2594-2602.
283. Mittendorf, E. A., C. E. Storrer, R. J. Foley, K. Harris, Y. Jama, C. D. Shriver, S. Ponniah, and G. E. Peoples. 2006. Evaluation of the HER2/neu-derived peptide GP2 for use in a peptide-based breast cancer vaccine trial. *Cancer* 106: 2309-2317.
284. Carmichael, M. G., L. C. Benavides, J. P. Holmes, J. D. Gates, E. A. Mittendorf, S. Ponniah, and G. E. Peoples. 2010. Results of the first phase 1 clinical trial of the HER-2/neu peptide (GP2) vaccine in disease-free breast cancer patients: United States Military Cancer Institute Clinical Trials Group Study I-04. *Cancer* 116: 292-301.
285. Disis, M. L., T. A. Gooley, K. Rinn, D. Davis, M. Piepkorn, M. A. Cheever, K. L. Knutson, and K. Schiffman. 2002. Generation of T-cell immunity to the HER-2/neu protein after active immunization with HER-2/neu peptide-based vaccines. *J. Clin. Oncol.* 20: 2624-2632.
286. Mittendorf, E. A., J. P. Holmes, J. L. Murray, E. von Hofe, and G. E. Peoples. 2009. CD4+ T cells in antitumor immunity: utility of an li-key HER2/neu hybrid peptide vaccine (AE37). *Expert Opin. Biol. Ther.* 9: 71-78.
287. Holmes, J. P., L. C. Benavides, J. D. Gates, M. G. Carmichael, M. T. Hueman, E. A. Mittendorf, J. L. Murray, A. Amin, D. Craig, E. von Hofe, S. Ponniah, and G. E. Peoples. 2008. Results of the first phase I clinical trial of the novel II-key hybrid preventive HER-2/neu peptide (AE37) vaccine. *J. Clin. Oncol.* 26: 3426-3433.
288. Salazar, L. G., V. Goodell, M. O'Meara, K. Knutson, Y. Dang, C. d. Rosa, K. A. Guthrie, and M. L. Disis. 2009. Persistent immunity and survival after immunization with a HER2/neu (HER2) vaccine. *ASCO Annual Meeting Proceedings* 27 (15_suppl): 3010.
289. Disis, M. L., K. Schiffman, K. Guthrie, L. G. Salazar, K. L. Knutson, V. Goodell, C. dela Rosa, and M. A. Cheever. 2004. Effect of dose on immune response in patients vaccinated with an her-2/neu intracellular domain protein--based vaccine. *J. Clin. Oncol.* 22: 1916-1925.
290. Limentani, S., T. Dorval, S. White, G. Curigliano, M. Campone, N. Disis, M. Piccart, M. Cheever, C. Gérard, and V. G. Brichard. 2005. Phase I dose-escalation trial of a recombinant HER2 vaccine in patients with Stage II/III HER2+ breast cancer. *ASCO Annual Meeting Proceedings* 23 (16_suppl): 2520.
291. Kitano, S., S. Kageyama, Y. Nagata, Y. Miyahara, A. Hiasa, H. Naota, S. Okumura, H. Imai, T. Shiraishi, M. Masuya, M. Nishikawa, J. Sunamoto, K. Akiyoshi, T. Kanematsu, A. M. Scott, R. Murphy, E. W. Hoffman, L. J. Old, and H. Shiku. 2006. HER2-specific

T-cell immune responses in patients vaccinated with truncated HER2 protein complexed with nanogels of cholesteryl pullulan. *Clin. Cancer Res.* 12: 7397-7405.

292. Kageyama, S., S. Kitano, M. Hirayama, Y. Nagata, H. Imai, T. Shiraishi, K. Akiyoshi, A. M. Scott, R. Murphy, E. W. Hoffman, L. J. Old, N. Katayama, and H. Shiku. 2008. Humoral immune responses in patients vaccinated with 1-146 HER2 protein complexed with cholesteryl pullulan nanogel. *Cancer Sci.* 99: 601-607.
293. Orlandi, F., F. M. Venanzi, A. Concetti, H. Yamauchi, S. Tiwari, L. Norton, J. D. Wolchok, A. N. Houghton, and P. D. Gregor. 2007. Antibody and CD8+ T cell responses against HER2/neu required for tumor eradication after DNA immunization with a Flt-3 ligand fusion vaccine. *Clin. Cancer Res.* 13: 6195-6203.
294. Yo, Y. T., K. F. Hsu, G. S. Shieh, C. W. Lo, C. C. Chang, C. L. Wu, and A. L. Shiau. 2007. Coexpression of Flt3 ligand and GM-CSF genes modulates immune responses induced by HER2/neu DNA vaccine. *Cancer Gene Ther.* 14: 904-917.
295. Renard, V., L. Sonderbye, K. Ebbehoj, P. B. Rasmussen, K. Gregorius, T. Gottschalk, S. Mouritsen, A. Gautam, and D. R. Leach. 2003. HER-2 DNA and protein vaccines containing potent Th cell epitopes induce distinct protective and therapeutic antitumor responses in HER-2 transgenic mice. *J. Immunol.* 171: 1588-1595.
296. Guardino, A., M. Cassidy, T. Pienkowski, S. Radulovic, F. Legrand, A. Nguyen, L. Fernandez, J. Coutts, N. Moore, O. Hwang, B. Trieger, L. Brand, L. Reiner, A. Delcayre, and W. Godfrey. 2009. Results of Two Phase I Clinical Trials of MVA-BN®-HER2 in HER-2 Overexpressing Metastatic Breast Cancer Patients. *Cancer Res.* 69(24 Suppl): 5089.
297. Park, J. W., M. E. Melisko, L. J. Esserman, L. A. Jones, J. B. Wollan, and R. Sims. 2007. Treatment with autologous antigen-presenting cells activated with the HER-2 based antigen Lapuleucel-T: results of a phase I study in immunologic and clinical activity in HER-2 overexpressing breast cancer. *J. Clin. Oncol.* 25: 3680-3687.
298. Emens, L. A., J. M. Asquith, J. M. Leatherman, B. J. Kobrin, S. Petrik, M. Laiko, J. Levi, M. M. Daphtary, B. Biedrzycki, A. C. Wolff, V. Stearns, M. L. Disis, X. Ye, S. Piantadosi, J. H. Fetting, N. E. Davidson, and E. M. Jaffee. 2009. Timed sequential treatment with cyclophosphamide, doxorubicin, and an allogeneic granulocyte-macrophage colony-stimulating factor-secreting breast tumor vaccine: a chemotherapy dose-ranging factorial study of safety and immune activation. *J. Clin. Oncol.* 27: 5911-5918.
299. Sakai, Y., B. J. Morrison, J. D. Burke, J. M. Park, M. Terabe, J. E. Janik, G. Forni, J. A. Berzofsky, and J. C. Morris. 2004. Vaccination by genetically modified dendritic cells expressing a truncated neu oncogene prevents development of breast cancer in transgenic mice. *Cancer Res.* 64: 8022-8028.
300. Chen, Y., P. Emtage, Q. Zhu, R. Foley, W. Muller, M. Hitt, J. Gauldie, and Y. Wan. 2001. Induction of ErbB-2/neu-specific protective and therapeutic antitumor immunity using genetically modified dendritic cells: enhanced efficacy by cotransduction of gene encoding IL-12. *Gene Ther.* 8: 316-323.
301. Chen, Z., H. Huang, T. Chang, S. Carlsen, A. Saxena, R. Marr, Z. Xing, and J. Xiang. 2002. Enhanced HER-2/neu-specific antitumor immunity by cotransduction of mouse dendritic cells with two genes encoding HER-2/neu and alpha tumor necrosis factor. *Cancer Gene Ther.* 9: 778-786.

302. Chan, T., A. Sami, A. El-Gayed, X. Guo, and J. Xiang. 2006. HER-2/neu-gene engineered dendritic cell vaccine stimulates stronger HER-2/neu-specific immune responses compared to DNA vaccination. *Gene Ther.* 13: 1391-1402.
303. Sas, S., T. Chan, A. Sami, A. El-Gayed, and J. Xiang. 2008. Vaccination of fiber-modified adenovirus-transfected dendritic cells to express HER-2/neu stimulates efficient HER-2/neu-specific humoral and CTL responses and reduces breast carcinogenesis in transgenic mice. *Cancer Gene Ther.* 15: 655-666.
304. Brossart, P., S. Wirths, G. Stuhler, V. L. Reichardt, L. Kanz, and W. Brugger. 2000. Induction of cytotoxic T-lymphocyte responses in vivo after vaccinations with peptide-pulsed dendritic cells. *Blood* 96: 3102-3108.
305. Czerniecki, B. J., G. K. Koski, U. Koldovsky, S. Xu, P. A. Cohen, R. Mick, H. Nisenbaum, T. Pasha, M. Xu, K. R. Fox, S. Weinstein, S. G. Orel, R. Vonderheide, G. Coukos, A. DeMichele, L. Araujo, F. R. Spitz, M. Rosen, B. L. Levine, C. June, and P. J. Zhang. 2007. Targeting HER-2/neu in early breast cancer development using dendritic cells with staged interleukin-12 burst secretion. *Cancer Res.* 67: 1842-1852.
306. Morse, M. A., A. Hobeika, T. Osada, D. Niedzwiecki, P. K. Marcom, K. L. Blackwell, C. Anders, G. R. Devi, H. K. Lyerly, and T. M. Clay. 2007. Long term disease-free survival and T cell and antibody responses in women with high-risk Her2+ breast cancer following vaccination against Her2. *J. Transl. Med.* 5: 42.
307. Peethambaram, P. P., M. E. Melisko, K. J. Rinn, S. R. Alberts, N. M. Provost, L. A. Jones, R. B. Sims, L. R. Lin, M. W. Frohlich, and J. W. Park. 2009. A phase I trial of immunotherapy with lapuleucel-T (APC8024) in patients with refractory metastatic tumors that express HER-2/neu. *Clin. Cancer Res.* 15: 5937-5944.
308. Disis, M. L., D. R. Wallace, T. A. Gooley, Y. Dang, M. Slota, H. Lu, A. L. Coveler, J. S. Childs, D. M. Higgins, P. A. Fintak, C. dela Rosa, K. Tietje, J. Link, J. Waisman, and L. G. Salazar. 2009. Concurrent trastuzumab and HER2/neu-specific vaccination in patients with metastatic breast cancer. *J. Clin. Oncol.* 27: 4685-4692.
309. Holmes, J. P., J. D. Gates, L. C. Benavides, M. T. Hueman, M. G. Carmichael, R. Patil, D. Craig, E. A. Mittendorf, A. Stojadinovic, S. Ponniah, and G. E. Peoples. 2008. Optimal dose and schedule of an HER-2/neu (E75) peptide vaccine to prevent breast cancer recurrence: from US Military Cancer Institute Clinical Trials Group Study I-01 and I-02. *Cancer* 113: 1666-1675.
310. Norell, H., I. Poschke, J. Charo, W. Z. Wei, C. Erskine, M. P. Piechocki, K. L. Knutson, J. Bergh, E. Lidbrink, and R. Kiessling. 2010. Vaccination with a plasmid DNA encoding HER-2/neu together with low doses of GM-CSF and IL-2 in patients with metastatic breast carcinoma: a pilot clinical trial. *J. Transl. Med.* 8: 53.
311. Emens, L. A., R. Gupta, S. Petrik, M. Laiko, J. M. Leatherman, J. Levi, J. M. Asquith, M. M. Daphtary, Garrett-Mayer , E., B. J. Kobrin, N. E. Davidson, T. Dauses, S. Atay-Rosenthal, X. Ye, A. C. Wolff, V. Stearns, and E. M. Jaffee. 2011. A feasibility study of combination therapy with trastuzumab (T), cyclophosphamide (CY), and an allogeneic GM-CSF-secreting breast tumor vaccine for the treatment of HER2+ metastatic breast cancer. *ASCO Annual Meeting Proceedings* 29 (15_suppl): 2535.
312. Hamilton, E., K. Blackwell, A. C. Hobeika, T. M. Clay, G. Broadwater, X. R. Ren, W. Chen, H. Castro, F. Lehmann, N. Spector, J. Wei, T. Osada, H. K. Lyerly, and M. A. Morse. 2012. Phase 1 clinical trial of HER2-specific immunotherapy with concomitant HER2 kinase inhibition [corrected]. *J. Transl. Med.* 10: 28.

313. Gershon, R. K., and K. Kondo. 1970. Cell interactions in the induction of tolerance: the role of thymic lymphocytes. *Immunology* 18: 723-737.
314. Cantor, H., J. Hugenberger, L. McVay-Boudreau, D. D. Eardley, J. Kemp, F. W. Shen, and R. K. Gershon. 1978. Immunoregulatory circuits among T-cell sets. Identification of a subpopulation of T-helper cells that induces feedback inhibition. *J. Exp. Med.* 148: 871-877.
315. Eardley, D. D., J. Hugenberger, L. McVay-Boudreau, F. W. Shen, R. K. Gershon, and H. Cantor. 1978. Immunoregulatory circuits among T-cell sets. I. T-helper cells induce other T-cell sets to exert feedback inhibition. *J. Exp. Med.* 147: 1106-1115.
316. Cantor, H., F. W. Shen, and E. A. Boyse. 1976. Separation of helper T cells from suppressor T cells expressing different Ly components. II. Activation by antigen: after immunization, antigen-specific suppressor and helper activities are mediated by distinct T-cell subclasses. *J. Exp. Med.* 143: 1391-1340.
317. Sakaguchi, S., N. Sakaguchi, M. Asano, M. Itoh, and M. Toda. 1995. Immunologic self-tolerance maintained by activated T cells expressing IL-2 receptor alpha-chains (CD25). Breakdown of a single mechanism of self-tolerance causes various autoimmune diseases. *J. Immunol.* 155: 1151-1164.
318. Bilate, A. M., and J. J. Lafaille. 2012. Induced CD4+Foxp3+ regulatory T cells in immune tolerance. *Annu. Rev. Immunol.* 30: 733-758.
319. Lahl, K., C. Loddenkemper, C. Drouin, J. Freyer, J. Arnason, G. Eberl, A. Hamann, H. Wagner, J. Huehn, and T. Sparwasser. 2007. Selective depletion of Foxp3+ regulatory T cells induces a scurfy-like disease. *J. Exp. Med.* 204: 57-63.
320. Wildin, R. S., F. Ramsdell, J. Peake, F. Faravelli, J. L. Casanova, N. Buist, E. Levy-Lahad, M. Mazzella, O. Goulet, L. Perroni, F. D. Bricarelli, G. Byrne, M. McEuen, S. Proll, M. Appleby, and M. E. Brunkow. 2001. X-linked neonatal diabetes mellitus, enteropathy and endocrinopathy syndrome is the human equivalent of mouse scurfy. *Nat. Genet.* 27: 18-20.
321. Bennett, C. L., J. Christie, F. Ramsdell, M. E. Brunkow, P. J. Ferguson, L. Whitesell, T. E. Kelly, F. T. Saulsbury, P. F. Chance, and H. D. Ochs. 2001. The immune dysregulation, polyendocrinopathy, enteropathy, X-linked syndrome (IPEX) is caused by mutations of FOXP3. *Nat. Genet.* 27: 20-21.
322. Wan, Y. Y., and R. A. Flavell. 2007. Regulatory T-cell functions are subverted and converted owing to attenuated Foxp3 expression. *Nature* 445: 766-770.
323. Bensinger, S. J., A. Bandeira, M. S. Jordan, A. J. Caton, and T. M. Laufer. 2001. Major histocompatibility complex class II-positive cortical epithelium mediates the selection of CD4(+)25(+) immunoregulatory T cells. *J. Exp. Med.* 194: 427-438.
324. Fontenot, J. D., J. P. Rasmussen, L. M. Williams, J. L. Dooley, A. G. Farr, and A. Y. Rudensky. 2005. Regulatory T cell lineage specification by the forkhead transcription factor foxp3. *Immunity* 22: 329-341.
325. Larkin, J., 3rd, A. L. Rankin, C. C. Picca, M. P. Riley, S. A. Jenks, A. J. Sant, and A. J. Caton. 2008. CD4+CD25+ regulatory T cell repertoire formation shaped by differential presentation of peptides from a self-antigen. *J. Immunol.* 180: 2149-2157.
326. Curotto de Lafaille, M. A., A. C. Lino, N. Kutchukhidze, and J. J. Lafaille. 2004. CD25- T cells generate CD25+Foxp3+ regulatory T cells by peripheral expansion. *J. Immunol.* 173: 7259-7268.

327. Cobbold, S. P., R. Castejon, E. Adams, D. Zelenika, L. Graca, S. Humm, and H. Waldmann. 2004. Induction of foxP3+ regulatory T cells in the periphery of T cell receptor transgenic mice tolerized to transplants. *J. Immunol.* 172: 6003-6010.
328. Mucida, D., N. Kutchukhidze, A. Erazo, M. Russo, J. J. Lafaille, and M. A. Curotto de Lafaille. 2005. Oral tolerance in the absence of naturally occurring Tregs. *J. Clin. Invest.* 115: 1923-1933.
329. Kretschmer, K., I. Apostolou, D. Hawiger, K. Khazaie, M. C. Nussenzweig, and H. von Boehmer. 2005. Inducing and expanding regulatory T cell populations by foreign antigen. *Nat. Immunol.* 6: 1219-1227.
330. Curotto de Lafaille, M. A., N. Kutchukhidze, S. Shen, Y. Ding, H. Yee, and J. J. Lafaille. 2008. Adaptive Foxp3+ regulatory T cell-dependent and -independent control of allergic inflammation. *Immunity* 29: 114-126.
331. Rodgers, J. R., and R. G. Cook. 2005. MHC class Ib molecules bridge innate and acquired immunity. *Nat. Rev. Immunol.* 5: 459-471.
332. Van Kaer, L. 2010. Comeback kids: CD8(+) suppressor T cells are back in the game. *J. Clin. Invest.* 120: 3432-3434.
333. Beeston, T., T. R. Smith, I. Maricic, X. Tang, and V. Kumar. 2010. Involvement of IFN-gamma and perforin, but not Fas/FasL interactions in regulatory T cell-mediated suppression of experimental autoimmune encephalomyelitis. *J. Neuroimmunol.* 229: 91-97.
334. Tang, X., I. Maricic, N. Purohit, B. Bakamjian, L. M. Reed-Loisel, T. Beeston, P. Jensen, and V. Kumar. 2006. Regulation of immunity by a novel population of Qa-1-restricted CD8alphaalpha+TCRalphabeta+ T cells. *J. Immunol.* 177: 7645-7655.
335. Sarantopoulos, S., L. Lu, and H. Cantor. 2004. Qa-1 restriction of CD8+ suppressor T cells. *J. Clin. Invest.* 114: 1218-1221.
336. Jiang, H., and L. Chess. 2004. An integrated view of suppressor T cell subsets in immunoregulation. *J. Clin. Invest.* 114: 1198-1208.
337. Jiang, H., H. Kashleva, L. X. Xu, J. Forman, L. Flaherty, B. Pernis, N. S. Braunstein, and L. Chess. 1998. T cell vaccination induces T cell receptor Vbeta-specific Qa-1-restricted regulatory CD8(+) T cells. *Proc. Natl. Acad. Sci. U. S. A.* 95: 4533-4537.
338. Tang, X., I. Maricic, and V. Kumar. 2007. Anti-TCR antibody treatment activates a novel population of nonintestinal CD8 alpha alpha+ TCR alpha beta+ regulatory T cells and prevents experimental autoimmune encephalomyelitis. *J. Immunol.* 178: 6043-6050.
339. Shmidt, T. E., T. D. Zhuchenko, and N. N. Iakhno. 2003. [Glatiramer acetate (Copaxone) influence on different stages of multiple sclerosis pathogenesis]. *Zhurnal nevrologii i psikhiatrii imeni S.S. Korsakova / Ministerstvo zdravookhraneniia i meditsinskoi promyshlennosti Rossiiskoi Federatsii, Vserossiiskoe obshchestvo nevrologov [i] Vserossiiskoe obshchestvo psikhiat*: 79-82.
340. Biegler, B. W., S. X. Yan, S. B. Ortega, D. K. Tennakoon, M. K. Racke, and N. J. Karandikar. 2006. Glatiramer acetate (GA) therapy induces a focused, oligoclonal CD8+ T-cell repertoire in multiple sclerosis. *J. Neuroimmunol.* 180: 159-171.
341. Tennakoon, D. K., R. S. Mehta, S. B. Ortega, V. Bhoj, M. K. Racke, and N. J. Karandikar. 2006. Therapeutic induction of regulatory, cytotoxic CD8+ T cells in multiple sclerosis. *J. Immunol.* 176: 7119-7129.

342. Yao, Y., W. Han, J. Liang, J. Ji, J. Wang, H. Cantor, and L. Lu. 2013. Glatiramer acetate ameliorates inflammatory bowel disease in mice through the induction of Qa-1-restricted CD8(+) regulatory cells. *Eur. J. Immunol.* 43: 125-136.
343. Panoutsakopoulou, V., K. M. Huster, N. McCarty, E. Feinberg, R. Wang, K. W. Wucherpfennig, and H. Cantor. 2004. Suppression of autoimmune disease after vaccination with autoreactive T cells that express Qa-1 peptide complexes. *J. Clin. Invest.* 113: 1218-1224.
344. Leavenworth, J. W., X. Tang, H. J. Kim, X. Wang, and H. Cantor. 2013. Amelioration of arthritis through mobilization of peptide-specific CD8+ regulatory T cells. *J. Clin. Invest.* 123: 1382-1389.
345. Kim, H. J., B. Verbinnen, X. Tang, L. Lu, and H. Cantor. 2010. Inhibition of follicular T-helper cells by CD8(+) regulatory T cells is essential for self tolerance. *Nature* 467: 328-332.
346. Cosmi, L., F. Liotta, E. Lazzeri, M. Francalanci, R. Angeli, B. Mazzinghi, V. Santarlasci, R. Manetti, V. Vanini, P. Romagnani, E. Maggi, S. Romagnani, and F. Annunziato. 2003. Human CD8+CD25+ thymocytes share phenotypic and functional features with CD4+CD25+ regulatory thymocytes. *Blood* 102: 4107-4114.
347. Prevosto, C., M. Zancolli, P. Canevali, M. R. Zocchi, and A. Poggi. 2007. Generation of CD4+ or CD8+ regulatory T cells upon mesenchymal stem cell-lymphocyte interaction. *Haematologica* 92: 881-888.
348. Joosten, S. A., K. E. van Meijgaarden, N. D. Savage, T. de Boer, F. Triebel, A. van der Wal, E. de Heer, M. R. Klein, A. Geluk, and T. H. Ottenhoff. 2007. Identification of a human CD8+ regulatory T cell subset that mediates suppression through the chemokine CC chemokine ligand 4. *Proc. Natl. Acad. Sci. U. S. A.* 104: 8029-8034.
349. Mahic, M., K. Henjum, S. Yaqub, B. A. Bjornbeth, K. M. Torgersen, K. Tasken, and E. M. Aandahl. 2008. Generation of highly suppressive adaptive CD8(+)CD25(+)FOXP3(+) regulatory T cells by continuous antigen stimulation. *Eur. J. Immunol.* 38: 640-646.
350. Jarvis, L. B., M. K. Matyszak, R. C. Duggleby, J. C. Goodall, F. C. Hall, and J. S. Gaston. 2005. Autoreactive human peripheral blood CD8+ T cells with a regulatory phenotype and function. *Eur. J. Immunol.* 35: 2896-2908.
351. Bienvenu, B., B. Martin, C. Auffray, C. Cordier, C. Becourt, and B. Lucas. 2005. Peripheral CD8+CD25+ T lymphocytes from MHC class II-deficient mice exhibit regulatory activity. *J. Immunol.* 175: 246-253.
352. Mayer, C. T., S. Floess, A. M. Baru, K. Lahl, J. Huehn, and T. Sparwasser. 2011. CD8+ Foxp3+ T cells share developmental and phenotypic features with classical CD4+ Foxp3+ regulatory T cells but lack potent suppressive activity. *Eur. J. Immunol.* 41: 716-725.
353. Bisikirska, B., J. Colgan, J. Luban, J. A. Bluestone, and K. C. Herold. 2005. TCR stimulation with modified anti-CD3 mAb expands CD8+ T cell population and induces CD8+CD25+ Tregs. *J. Clin. Invest.* 115: 2904-2913.
354. Wang, R., G. Han, L. Song, J. Wang, G. Chen, R. Xu, M. Yu, J. Qian, B. Shen, and Y. Li. 2009. CD8+ regulatory T cells are responsible for GAD-IgG gene-transferred tolerance induction in NOD mice. *Immunology* 126: 123-131.
355. Suzuki, H., T. M. Kundig, C. Furlonger, A. Wakeham, E. Timms, T. Matsuyama, R. Schmits, J. J. Simard, P. S. Ohashi, H. Griesser, and et al. 1995. Deregulated T cell

activation and autoimmunity in mice lacking interleukin-2 receptor beta. *Science* 268: 1472-1476.
356. Rifa'i, M., Y. Kawamoto, I. Nakashima, and H. Suzuki. 2004. Essential roles of CD8+CD122+ regulatory T cells in the maintenance of T cell homeostasis. *J. Exp. Med.* 200: 1123-1134.
357. Endharti, A. T., I. M. Rifa, Z. Shi, Y. Fukuoka, Y. Nakahara, Y. Kawamoto, K. Takeda, K. Isobe, and H. Suzuki. 2005. Cutting edge: CD8+CD122+ regulatory T cells produce IL-10 to suppress IFN-gamma production and proliferation of CD8+ T cells. *J. Immunol.* 175: 7093-7097.
358. Dai, H., N. Wan, S. Zhang, Y. Moore, F. Wan, and Z. Dai. 2010. Cutting edge: programmed death-1 defines CD8+CD122+ T cells as regulatory versus memory T cells. *J. Immunol.* 185: 803-807.
359. Saitoh, O., N. Abiru, M. Nakahara, and Y. Nagayama. 2007. CD8+CD122+ T cells, a newly identified regulatory T subset, negatively regulate Graves' hyperthyroidism in a murine model. *Endocrinology* 148: 6040-6046.
360. Lee, Y. H., Y. Ishida, M. Rifa'i, Z. Shi, K. Isobe, and H. Suzuki. 2008. Essential role of CD8+CD122+ regulatory T cells in the recovery from experimental autoimmune encephalomyelitis. *J. Immunol.* 180: 825-832.
361. Endharti, A. T., Y. Okuno, Z. Shi, N. Misawa, S. Toyokuni, M. Ito, K. Isobe, and H. Suzuki. 2011. CD8+CD122+ regulatory T cells (Tregs) and CD4+ Tregs cooperatively prevent and cure CD4+ cell-induced colitis. *J. Immunol.* 186: 41-52.
362. Shi, Z., Y. Okuno, M. Rifa'i, A. T. Endharti, K. Akane, K. Isobe, and H. Suzuki. 2009. Human CD8+CXCR3+ T cells have the same function as murine CD8+CD122+ Treg. *Eur. J. Immunol.* 39: 2106-2119.
363. Tsai, S., A. Shameli, J. Yamanouchi, X. Clemente-Casares, J. Wang, P. Serra, Y. Yang, Z. Medarova, A. Moore, and P. Santamaria. 2010. Reversal of autoimmunity by boosting memory-like autoregulatory T cells. *Immunity* 32: 568-580.
364. Liu, Z., S. Tugulea, R. Cortesini, and N. Suciu-Foca. 1998. Specific suppression of T helper alloreactivity by allo-MHC class I-restricted CD8+CD28- T cells. *Int. Immunol.* 10: 775-783.
365. Ciubotariu, R., A. I. Colovai, G. Pennesi, Z. Liu, D. Smith, P. Berlocco, R. Cortesini, and N. Suciu-Foca. 1998. Specific suppression of human CD4+ Th cell responses to pig MHC antigens by CD8+CD28- regulatory T cells. *J. Immunol.* 161: 5193-5202.
366. Colovai, A. I., Z. Liu, R. Ciubotariu, S. Lederman, R. Cortesini, and N. Suciu-Foca. 2000. Induction of xenoreactive CD4+ T-cell anergy by suppressor CD8+CD28- T cells. *Transplantation* 69: 1304-1310.
367. Jiang, S., S. Tugulea, G. Pennesi, Z. Liu, A. Mulder, S. Lederman, P. Harris, R. Cortesini, and N. Suciu-Foca. 1998. Induction of MHC-class I restricted human suppressor T cells by peptide priming in vitro. *Hum. Immunol.* 59: 690-699.
368. Suciu-Foca, N., J. S. Manavalan, L. Scotto, S. Kim-Schulze, S. Galluzzo, A. J. Naiyer, J. Fan, G. Vlad, and R. Cortesini. 2005. Molecular characterization of allospecific T suppressor and tolerogenic dendritic cells: review. *Int. Immunopharmacol.* 5: 7-11.
369. Scotto, L., A. J. Naiyer, S. Galluzzo, P. Rossi, J. S. Manavalan, S. Kim-Schulze, J. Fang, R. D. Favera, R. Cortesini, and N. Suciu-Foca. 2004. Overlap between molecular markers expressed by naturally occurring CD4+CD25+ regulatory T cells and antigen specific CD4+CD25+ and CD8+CD28- T suppressor cells. *Hum. Immunol.* 65: 1297-1306.

370. Chang, C. C., R. Ciubotariu, J. S. Manavalan, J. Yuan, A. I. Colovai, F. Piazza, S. Lederman, M. Colonna, R. Cortesini, R. Dalla-Favera, and N. Suciu-Foca. 2002. Tolerization of dendritic cells by T(S) cells: the crucial role of inhibitory receptors ILT3 and ILT4. *Nat. Immunol.* 3: 237-243.
371. Manavalan, J. S., S. Kim-Schulze, L. Scotto, A. J. Naiyer, G. Vlad, P. C. Colombo, C. Marboe, D. Mancini, R. Cortesini, and N. Suciu-Foca. 2004. Alloantigen specific CD8+CD28- FOXP3+ T suppressor cells induce ILT3+ ILT4+ tolerogenic endothelial cells, inhibiting alloreactivity. *Int. Immunol.* 16: 1055-1068.
372. Najafian, N., T. Chitnis, A. D. Salama, B. Zhu, C. Benou, X. Yuan, M. R. Clarkson, M. H. Sayegh, and S. J. Khoury. 2003. Regulatory functions of CD8+CD28- T cells in an autoimmune disease model. *J. Clin. Invest.* 112: 1037-1048.
373. Zhang, R., A. Huynh, G. Whitcher, J. Chang, J. S. Maltzman, and L. A. Turka. 2013. An obligate cell-intrinsic function for CD28 in Tregs. *J. Clin. Invest.* 123: 580-593.
374. Ben-David, H., A. Sharabi, M. Dayan, M. Sela, and E. Mozes. 2007. The role of CD8+CD28 regulatory cells in suppressing myasthenia gravis-associated responses by a dual altered peptide ligand. *Proc. Natl. Acad. Sci. U. S. A.* 104: 17459-17464.
375. Paas-Rozner, M., M. Dayan, Y. Paas, J. P. Changeux, I. Wirguin, M. Sela, and E. Mozes. 2000. Oral administration of a dual analog of two myasthenogenic T cell epitopes down-regulates experimental autoimmune myasthenia gravis in mice. *Proc. Natl. Acad. Sci. U. S. A.* 97: 2168-2173.
376. Davila, E., Y. M. Kang, Y. W. Park, H. Sawai, X. He, S. Pryshchep, J. J. Goronzy, and C. M. Weyand. 2005. Cell-based immunotherapy with suppressor CD8+ T cells in rheumatoid arthritis. *J. Immunol.* 174: 7292-7301.
377. Filaci, G., M. Rizzi, M. Setti, D. Fenoglio, M. Fravega, M. Basso, G. Ansaldo, P. Ceppa, G. Borgonovo, G. Murdaca, F. Ferrera, A. Picciotto, R. Fiocca, G. Torre, and F. Indiveri. 2005. Non-antigen-specific CD8(+) T suppressor lymphocytes in diseases characterized by chronic immune responses and inflammation. *Ann. N. Y. Acad. Sci.* 1050: 115-123.
378. Fenoglio, D., F. Battaglia, A. Parodi, S. Stringara, S. Negrini, N. Panico, M. Rizzi, F. Kalli, G. Conteduca, M. Ghio, R. De Palma, F. Indiveri, and G. Filaci. 2011. Alteration of Th17 and Treg cell subpopulations co-exist in patients affected with systemic sclerosis. *Clin. Immunol.* 139: 249-257.
379. Mikulkova, Z., P. Praksova, P. Stourac, J. Bednarik, L. Strajtova, R. Pacasova, J. Belobradkova, P. Dite, and J. Michalek. 2010. Numerical defects in CD8+CD28- T-suppressor lymphocyte population in patients with type 1 diabetes mellitus and multiple sclerosis. *Cell. Immunol.* 262: 75-79.
380. Balashov, K. E., S. J. Khoury, D. A. Hafler, and H. L. Weiner. 1995. Inhibition of T cell responses by activated human CD8+ T cells is mediated by interferon-gamma and is defective in chronic progressive multiple sclerosis. *J. Clin. Invest.* 95: 2711-2719.
381. Crucian, B., P. Dunne, H. Friedman, R. Ragsdale, S. Pross, and R. Widen. 1995. Alterations in levels of CD28-/CD8+ suppressor cell precursor and CD45RO+/CD4+ memory T lymphocytes in the peripheral blood of multiple sclerosis patients. *Clin. Diagn. Lab. Immunol.* 2: 249-252.
382. Filaci, G., S. Bacilieri, M. Fravega, M. Monetti, P. Contini, M. Ghio, M. Setti, F. Puppo, and F. Indiveri. 2001. Impairment of CD8+ T suppressor cell function in patients with active systemic lupus erythematosus. *J. Immunol.* 166: 6452-6457.

383. Vinay, D. S., C. H. Kim, B. K. Choi, and B. S. Kwon. 2009. Origins and functional basis of regulatory CD11c+CD8+ T cells. *Eur. J. Immunol.* 39: 1552-1563.
384. Choi, B. K., T. Asai, D. S. Vinay, Y. H. Kim, and B. S. Kwon. 2006. 4-1BB-mediated amelioration of experimental autoimmune uveoretinitis is caused by indoleamine 2,3-dioxygenase-dependent mechanisms. *Cytokine* 34: 233-242.
385. Seo, S. K., J. H. Choi, Y. H. Kim, W. J. Kang, H. Y. Park, J. H. Suh, B. K. Choi, D. S. Vinay, and B. S. Kwon. 2004. 4-1BB-mediated immunotherapy of rheumatoid arthritis. *Nat. Med.* 10: 1088-1094.
386. Beyer, M., H. Wang, N. Peters, S. Doths, C. Koerner-Rettberg, P. J. Openshaw, and J. Schwarze. 2005. The beta2 integrin CD11c distinguishes a subset of cytotoxic pulmonary T cells with potent antiviral effects in vitro and in vivo. *Respir. Res.* 6: 70.
387. Kim, Y. H., S. K. Seo, B. K. Choi, W. J. Kang, C. H. Kim, S. K. Lee, and B. S. Kwon. 2005. 4-1BB costimulation enhances HSV-1-specific CD8+ T cell responses by the induction of CD11c+CD8+ T cells. *Cell. Immunol.* 238: 76-86.
388. Fujiwara, D., L. Chen, B. Wei, and J. Braun. 2011. Small intestine CD11c+ CD8+ T cells suppress CD4+ T cell-induced immune colitis. *Am. J. Physiol. Gastrointest. Liver Physiol.* 300: G939-947.
389. Siegmund, K., M. Feuerer, C. Siewert, S. Ghani, U. Haubold, A. Dankof, V. Krenn, M. P. Schon, A. Scheffold, J. B. Lowe, A. Hamann, U. Syrbe, and J. Huehn. 2005. Migration matters: regulatory T-cell compartmentalization determines suppressive activity in vivo. *Blood* 106: 3097-3104.
390. Suffia, I., S. K. Reckling, G. Salay, and Y. Belkaid. 2005. A role for CD103 in the retention of CD4+CD25+ Treg and control of Leishmania major infection. *J. Immunol.* 174: 5444-5455.
391. Rotzschke, O., G. Borsellino, L. Battistini, K. Falk, and M. Kleinewietfeld. 2009. In vivo-activated CD103+ Foxp3+ Tregs: of men and mice. *Blood* 113: 2119-2120; author reply 2120.
392. El-Asady, R., R. Yuan, K. Liu, D. Wang, R. E. Gress, P. J. Lucas, C. B. Drachenberg, and G. A. Hadley. 2005. TGF-{beta}-dependent CD103 expression by CD8(+) T cells promotes selective destruction of the host intestinal epithelium during graft-versus-host disease. *J. Exp. Med.* 201: 1647-1657.
393. Gunnlaugsdottir, B., S. M. Maggadottir, I. Skaftadottir, and B. R. Ludviksson. 2013. The ex vivo induction of human CD103(+) CD25hi Foxp3(+) CD4(+) and CD8(+) Tregs is IL-2 and TGF-beta1 dependent. *Scand. J. Immunol.* 77: 125-134.
394. Uss, E., A. T. Rowshani, B. Hooibrink, N. M. Lardy, R. A. van Lier, and I. J. ten Berge. 2006. CD103 is a marker for alloantigen-induced regulatory CD8+ T cells. *J. Immunol.* 177: 2775-2783.
395. Myers, L., M. Croft, B. S. Kwon, R. S. Mittler, and A. T. Vella. 2005. Peptide-specific CD8 T regulatory cells use IFN-gamma to elaborate TGF-beta-based suppression. *J. Immunol.* 174: 7625-7632.
396. Ho, J., C. C. Kurtz, M. Naganuma, P. B. Ernst, F. Cominelli, and J. Rivera-Nieves. 2008. A CD8+/CD103high T cell subset regulates TNF-mediated chronic murine ileitis. *J. Immunol.* 180: 2573-2580.
397. Lu, L., Y. Yu, G. Li, L. Pu, F. Zhang, S. Zheng, and X. Wang. 2009. CD8(+)CD103(+) regulatory T cells in spontaneous tolerance of liver allografts. *Int. Immunopharmacol.* 9: 546-548.

398. Le Gal, F. A., B. Riteau, C. Sedlik, I. Khalil-Daher, C. Menier, J. Dausset, J. G. Guillet, E. D. Carosella, and N. Rouas-Freiss. 1999. HLA-G-mediated inhibition of antigen-specific cytotoxic T lymphocytes. *Int. Immunol.* 11: 1351-1356.
399. Lila, N., N. Rouas-Freiss, J. Dausset, A. Carpentier, and E. D. Carosella. 2001. Soluble HLA-G protein secreted by allo-specific CD4+ T cells suppresses the allo-proliferative response: a CD4+ T cell regulatory mechanism. *Proc. Natl. Acad. Sci. U. S. A.* 98: 12150-12155.
400. Li, C., I. Toth, J. Schulze Zur Wiesch, F. Pereyra, J. Rychert, E. S. Rosenberg, J. van Lunzen, M. Lichterfeld, and X. G. Yu. 2013. Functional characterization of HLA-G(+) regulatory T cells in HIV-1 infection. *PLoS Pathog.* 9: e1003140.
401. Huang, Y. H., A. L. Zozulya, C. Weidenfeller, I. Metz, D. Buck, K. V. Toyka, W. Bruck, and H. Wiendl. 2009. Specific central nervous system recruitment of HLA-G(+) regulatory T cells in multiple sclerosis. *Ann. Neurol.* 66: 171-183.
402. Feger, U., E. Tolosa, Y. H. Huang, A. Waschbisch, T. Biedermann, A. Melms, and H. Wiendl. 2007. HLA-G expression defines a novel regulatory T-cell subset present in human peripheral blood and sites of inflammation. *Blood* 110: 568-577.
403. Chen, M. L., B. S. Yan, D. Kozoriz, and H. L. Weiner. 2009. Novel CD8+ Treg suppress EAE by TGF-beta- and IFN-gamma-dependent mechanisms. *Eur. J. Immunol.* 39: 3423-3435.
404. Cai, J., J. Lee, E. Jankowska-Gan, R. Derks, J. Pool, T. Mutis, E. Goulmy, and W. J. Burlingham. 2004. Minor H antigen HA-1-specific regulator and effector CD8+ T cells, and HA-1 microchimerism, in allograft tolerance. *J. Exp. Med.* 199: 1017-1023.
405. Wei, S., I. Kryczek, L. Zou, B. Daniel, P. Cheng, P. Mottram, T. Curiel, A. Lange, and W. Zou. 2005. Plasmacytoid dendritic cells induce CD8+ regulatory T cells in human ovarian carcinoma. *Cancer Res.* 65: 5020-5026.
406. Kang, H. K., M. A. Michaels, B. R. Berner, and S. K. Datta. 2005. Very low-dose tolerance with nucleosomal peptides controls lupus and induces potent regulatory T cell subsets. *J. Immunol.* 174: 3247-3255.
407. Singh, R. P., A. La Cava, M. Wong, F. Ebling, and B. H. Hahn. 2007. CD8+ T cell-mediated suppression of autoimmunity in a murine lupus model of peptide-induced immune tolerance depends on Foxp3 expression. *J. Immunol.* 178: 7649-7657.
408. Skaggs, B. J., E. V. Lourenco, and B. H. Hahn. 2011. Oral administration of different forms of a tolerogenic peptide to define the preparations and doses that delay anti-DNA antibody production and nephritis and prolong survival in SLE-prone mice. *Lupus* 20: 912-920.
409. Yu, Y., Y. Liu, F. D. Shi, H. Zou, B. H. Hahn, and A. La Cava. 2012. Tolerance induced by anti-DNA Ig peptide in (NZBxNZW)F1 lupus mice impinges on the resistance of effector T cells to suppression by regulatory T cells. *Clin. Immunol.* 142: 291-295.
410. Singh, R. P., A. La Cava, and B. H. Hahn. 2008. pConsensus peptide induces tolerogenic CD8+ T cells in lupus-prone (NZB x NZW)F1 mice by differentially regulating Foxp3 and PD1 molecules. *J. Immunol.* 180: 2069-2080.
411. Mizumoto, N., T. Kumamoto, S. C. Robson, J. Sevigny, H. Matsue, K. Enjyoji, and A. Takashima. 2002. CD39 is the dominant Langerhans cell-associated ecto-NTPDase: modulatory roles in inflammation and immune responsiveness. *Nat. Med.* 8: 358-365.
412. Borsellino, G., M. Kleinewietfeld, D. Di Mitri, A. Sternjak, A. Diamantini, R. Giometto, S. Hopner, D. Centonze, G. Bernardi, M. L. Dell'Acqua, P. M. Rossini, L. Battistini, O.

Rotzschke, and K. Falk. 2007. Expression of ectonucleotidase CD39 by Foxp3+ Treg cells: hydrolysis of extracellular ATP and immune suppression. *Blood* 110: 1225-1232.
413. Deaglio, S., K. M. Dwyer, W. Gao, D. Friedman, A. Usheva, A. Erat, J. F. Chen, K. Enjyoji, J. Linden, M. Oukka, V. K. Kuchroo, T. B. Strom, and S. C. Robson. 2007. Adenosine generation catalyzed by CD39 and CD73 expressed on regulatory T cells mediates immune suppression. *J. Exp. Med.* 204: 1257-1265.
414. Parodi, A., F. Battaglia, F. Kalli, F. Ferrera, G. Conteduca, S. Tardito, S. Stringara, F. Ivaldi, S. Negrini, G. Borgonovo, A. Simonato, P. Traverso, G. Carmignani, D. Fenoglio, and G. Filaci. 2013. CD39 is highly involved in mediating the suppression activity of tumor-infiltrating CD8+ T regulatory lymphocytes. *Cancer Immunol. Immunother.* 62: 851-862.
415. Deaglio, S., and S. C. Robson. 2011. Ectonucleotidases as regulators of purinergic signaling in thrombosis, inflammation, and immunity. *Adv. Pharmacol.* 61: 301-332.
416. Chen, J., Y. G. Chen, P. C. Reifsnyder, W. H. Schott, C. H. Lee, M. Osborne, F. Scheuplein, F. Haag, F. Koch-Nolte, D. V. Serreze, and E. H. Leiter. 2006. Targeted disruption of CD38 accelerates autoimmune diabetes in NOD/Lt mice by enhancing autoimmunity in an ADP-ribosyltransferase 2-dependent fashion. *J. Immunol.* 176: 4590-4599.
417. Antonelli, A., P. Fallahi, C. Nesti, C. Pupilli, P. Marchetti, S. Takasawa, H. Okamoto, and E. Ferrannini. 2001. Anti-CD38 autoimmunity in patients with chronic autoimmune thyroiditis or Graves' disease. *Clin. Exp. Immunol.* 126: 426-431.
418. Pupilli, C., A. Antonelli, L. Iughetti, G. D'Annunzio, M. Cotellessa, M. Vanelli, H. Okamoto, R. Lorini, and E. Ferrannini. 2005. Anti-CD38 autoimmunity in children with newly diagnosed type 1 diabetes mellitus. *J. Pediatr. Endocrinol. Metab.* 18: 1417-1423.
419. Patton, D. T., M. D. Wilson, W. C. Rowan, D. R. Soond, and K. Okkenhaug. 2011. The PI3K p110delta regulates expression of CD38 on regulatory T cells. *PLoS One* 6: e17359.
420. Bahri, R., A. Bollinger, T. Bollinger, Z. Orinska, and S. Bulfone-Paus. 2012. Ectonucleotidase CD38 demarcates regulatory, memory-like CD8+ T cells with IFN-gamma-mediated suppressor activities. *PLoS One* 7: e45234.
421. Piechocki, M. P., Y. S. Ho, S. Pilon, and W. Z. Wei. 2003. Human ErbB-2 (Her-2) transgenic mice: a model system for testing Her-2 based vaccines. *J. Immunol.* 171: 5787-5794.
422. Sambrook, J., E. Fritsch, and T. Maniatis. 1989. *Molecular Cloning: a laboratory manual*. Cold Spring Harbor Laboratory Press, Cold Spring Harbor.
423. Sambrook, J., and D. Russell. 2001. *Molecular Cloning: A Laboratory Manual.* Cold Spring Harbor Laboratory Press, Cold Spring Harbor.
424. He, T. C., S. Zhou, L. T. da Costa, J. Yu, K. W. Kinzler, and B. Vogelstein. 1998. A simplified system for generating recombinant adenoviruses. *Proc. Natl. Acad. Sci. U. S. A.* 95: 2509-2514.
425. Liu, Y., T. Ye, D. Sun, J. Maynard, and A. Deisseroth. 2004. Conditionally replication-competent adenoviral vectors with enhanced infectivity for use in gene therapy of melanoma. *Hum. Gene Ther.* 15: 637-647.
426. Xiang, J., and J. Wu. 2003. Genetic engineering of dendritic cells by adenovirus-mediated TNF-alpha gene transfer. *Methods Mol. Biol.* 215: 213-225.

427. Qiao, M., A. M. Thornton, and E. M. Shevach. 2007. CD4+ CD25+ [corrected] regulatory T cells render naive CD4+ CD25- T cells anergic and suppressive. *Immunology* 120: 447-455.
428. Ye, Z., M. Shi, S. Xu, and J. Xiang. 2010. LFA-1 defect-induced effector/memory CD8+ T cell apoptosis is mediated via Bcl-2/Caspase pathways and associated with downregulation of CD27 and IL-15R. *Mol. Immunol.* 47: 2411-2421.
429. Abe, B. T., D. S. Shin, E. Mocholi, and F. Macian. 2012. NFAT1 supports tumor-induced anergy of CD4(+) T cells. *Cancer Res.* 72: 4642-4651.
430. Chen, Z., T. Moyana, A. Saxena, R. Warrington, Z. Jia, and J. Xiang. 2001. Efficient antitumor immunity derived from maturation of dendritic cells that had phagocytosed apoptotic/necrotic tumor cells. *Int. J. Cancer* 93: 539-548.
431. Hao, S., J. Yuan, and J. Xiang. 2007. Nonspecific CD4(+) T cells with uptake of antigen-specific dendritic cell-released exosomes stimulate antigen-specific CD8(+) CTL responses and long-term T cell memory. *J. Leukoc. Biol.* 82: 829-838.
432. Ye, Z., K. A. Ahmed, J. Huang, Y. Xie, M. A. Munegowda, and J. Xiang. 2008. T cell precursor frequency differentially affects CTL responses under different immune conditions. *Biochem. Biophys. Res. Commun.* 367: 427-434.
433. Ankathatti Munegowda, M., Y. Deng, R. Chibbar, Q. Xu, A. Freywald, S. J. Mulligan, S. van Drunen Littel-van den Hurk, D. Sun, S. Xiong, and J. Xiang. 2011. A distinct role of CD4+ Th17- and Th17-stimulated CD8+ CTL in the pathogenesis of type 1 diabetes and experimental autoimmune encephalomyelitis. *J. Clin. Immunol.* 31: 811-826.
434. Grakoui, A., S. K. Bromley, C. Sumen, M. M. Davis, A. S. Shaw, P. M. Allen, and M. L. Dustin. 1999. The immunological synapse: a molecular machine controlling T cell activation. *Science* 285: 221-227.
435. Monks, C. R., B. A. Freiberg, H. Kupfer, N. Sciaky, and A. Kupfer. 1998. Three-dimensional segregation of supramolecular activation clusters in T cells. *Nature* 395: 82-86.
436. O'Keefe, J. P., K. Blaine, M. L. Alegre, and T. F. Gajewski. 2004. Formation of a central supramolecular activation cluster is not required for activation of naive CD8+ T cells. *Proc. Natl. Acad. Sci. U. S. A.* 101: 9351-9356.
437. Probst, H. C., K. Tschannen, B. Odermatt, R. Schwendener, R. M. Zinkernagel, and M. Van Den Broek. 2005. Histological analysis of CD11c-DTR/GFP mice after in vivo depletion of dendritic cells. *Clin. Exp. Immunol.* 141: 398-404.
438. Mouries, J., G. Moron, G. Schlecht, N. Escriou, G. Dadaglio, and C. Leclerc. 2008. Plasmacytoid dendritic cells efficiently cross-prime naive T cells in vivo after TLR activation. *Blood* 112: 3713-3722.
439. Takahashi, T., Y. Kuniyasu, M. Toda, N. Sakaguchi, M. Itoh, M. Iwata, J. Shimizu, and S. Sakaguchi. 1998. Immunologic self-tolerance maintained by CD25+CD4+ naturally anergic and suppressive T cells: induction of autoimmune disease by breaking their anergic/suppressive state. *Int. Immunol.* 10: 1969-1980.
440. Ermann, J., V. Szanya, G. S. Ford, V. Paragas, C. G. Fathman, and K. Lejon. 2001. CD4(+)CD25(+) T cells facilitate the induction of T cell anergy. *J. Immunol.* 167: 4271-4275.
441. Cao, X., S. F. Cai, T. A. Fehniger, J. Song, L. I. Collins, D. R. Piwnica-Worms, and T. J. Ley. 2007. Granzyme B and perforin are important for regulatory T cell-mediated suppression of tumor clearance. *Immunity* 27: 635-646.

442. Goverman, J., A. Woods, L. Larson, L. P. Weiner, L. Hood, and D. M. Zaller. 1993. Transgenic mice that express a myelin basic protein-specific T cell receptor develop spontaneous autoimmunity. *Cell* 72: 551-560.
443. Pardoll, D. M. 2002. Spinning molecular immunology into successful immunotherapy. *Nat. Rev. Immunol.* 2: 227-238.
444. Isakov, N., and A. Altman. 2002. Protein kinase C(theta) in T cell activation. *Annu. Rev. Immunol.* 20: 761-794.
445. Curtsinger, J. M., and M. F. Mescher. 2010. Inflammatory cytokines as a third signal for T cell activation. *Curr. Opin. Immunol.* 22: 333-340.
446. Kapsenberg, M. L. 2003. Dendritic-cell control of pathogen-driven T-cell polarization. *Nat. Rev. Immunol.* 3: 984-993.
447. Pulendran, B. 2004. Modulating TH1/TH2 responses with microbes, dendritic cells, and pathogen recognition receptors. *Immunol. Res.* 29: 187-196.
448. Sumoza-Toledo, A., A. D. Eaton, and A. Sarukhan. 2006. Regulatory T cells inhibit protein kinase C theta recruitment to the immune synapse of naive T cells with the same antigen specificity. *J. Immunol.* 176: 5779-5787.
449. Schoenberger, S. P., R. E. Toes, E. I. van der Voort, R. Offringa, and C. J. Melief. 1998. T-cell help for cytotoxic T lymphocytes is mediated by CD40-CD40L interactions. *Nature* 393: 480-483.
450. Munroe, M. E., and G. A. Bishop. 2007. A costimulatory function for T cell CD40. *J. Immunol.* 178: 671-682.
451. Bevan, M. J. 2004. Helping the CD8(+) T-cell response. *Nat. Rev. Immunol.* 4: 595-602.
452. Behrens, G., M. Li, C. M. Smith, G. T. Belz, J. Mintern, F. R. Carbone, and W. R. Heath. 2004. Helper T cells, dendritic cells and CTL Immunity. *Immunol. Cell Biol.* 82: 84-90.
453. Beuneu, H., Z. Garcia, and P. Bousso. 2006. Cutting edge: cognate CD4 help promotes recruitment of antigen-specific CD8 T cells around dendritic cells. *J. Immunol.* 177: 1406-1410.
454. Yamamoto, T., S. Ikawa, T. Akiyama, K. Semba, N. Nomura, N. Miyajima, T. Saito, and K. Toyoshima. 1986. Similarity of protein encoded by the human c-erb-B-2 gene to epidermal growth factor receptor. *Nature* 319: 230-234.
455. Whittington, P. J., M. P. Piechocki, H. H. Heng, J. B. Jacob, R. F. Jones, J. B. Back, and W. Z. Wei. 2008. DNA vaccination controls Her-2+ tumors that are refractory to targeted therapies. *Cancer Res.* 68: 7502-7511.
456. Radkevich-Brown, O., J. Jacob, M. Kershaw, and W. Z. Wei. 2009. Genetic regulation of the response to Her-2 DNA vaccination in human Her-2 transgenic mice. *Cancer Res.* 69: 212-218.
457. Saha, A., S. K. Chatterjee, K. A. Foon, E. Celis, and M. Bhattacharya-Chatterjee. 2007. Therapy of established tumors in a novel murine model transgenic for human carcinoembryonic antigen and HLA-A2 with a combination of anti-idiotype vaccine and CTL peptides of carcinoembryonic antigen. *Cancer Res.* 67: 2881-2892.
458. Saha, A., M. Bhattacharya-Chatterjee, K. A. Foon, E. Celis, and S. K. Chatterjee. 2009. Stimulatory effects of CpG oligodeoxynucleotide on dendritic cell-based immunotherapy of colon cancer in CEA/HLA-A2 transgenic mice. *Int. J. Cancer* 124: 877-888.
459. Ward, R. L., N. J. Hawkins, D. Coomber, and M. L. Disis. 1999. Antibody immunity to the HER-2/neu oncogenic protein in patients with colorectal cancer. *Hum. Immunol.* 60: 510-515.

460. Kiessling, R., W. Z. Wei, F. Herrmann, J. A. Lindencrona, A. Choudhury, K. Kono, and B. Seliger. 2002. Cellular immunity to the Her-2/neu protooncogene. *Adv. Cancer Res.* 85: 101-144.
461. Baxevanis, C. N., P. A. Sotiropoulou, N. N. Sotiriadou, and M. Papamichail. 2004. Immunobiology of HER-2/neu oncoprotein and its potential application in cancer immunotherapy. *Cancer Immunol. Immunother.* 53: 166-175.
462. Baxevanis, C. N., I. F. Voutsas, A. D. Gritzapis, S. A. Perez, and M. Papamichail. 2010. HER-2/neu as a target for cancer vaccines. *Immunotherapy* 2: 213-226.
463. Baxevanis, C. N., N. N. Sotiriadou, A. D. Gritzapis, P. A. Sotiropoulou, S. A. Perez, N. T. Cacoullos, and M. Papamichail. 2006. Immunogenic HER-2/neu peptides as tumor vaccines. *Cancer Immunol. Immunother.* 55: 85-95.
464. Eck, S. C., and L. A. Turka. 2001. Adoptive transfer enables tumor rejection targeted against a self-antigen without the induction of autoimmunity. *Cancer Res.* 61: 3077-3083.
465. Garcia-Hernandez Mde, L., A. Gray, B. Hubby, O. J. Klinger, and W. M. Kast. 2008. Prostate stem cell antigen vaccination induces a long-term protective immune response against prostate cancer in the absence of autoimmunity. *Cancer Res.* 68: 861-869.
466. Lane, C., J. Leitch, X. Tan, J. Hadjati, J. L. Bramson, and Y. Wan. 2004. Vaccination-induced autoimmune vitiligo is a consequence of secondary trauma to the skin. *Cancer Res.* 64: 1509-1514.
467. Palmer, D. C., C. C. Chan, L. Gattinoni, C. Wrzesinski, C. M. Paulos, C. S. Hinrichs, D. J. Powell, Jr., C. A. Klebanoff, S. E. Finkelstein, R. N. Fariss, Z. Yu, R. B. Nussenblatt, S. A. Rosenberg, and N. P. Restifo. 2008. Effective tumor treatment targeting a melanoma/melanocyte-associated antigen triggers severe ocular autoimmunity. *Proc. Natl. Acad. Sci. U. S. A.* 105: 8061-8066.
468. Bos, R., S. van Duikeren, H. Morreau, K. Franken, T. N. Schumacher, J. B. Haanen, S. H. van der Burg, C. J. Melief, and R. Offringa. 2008. Balancing between antitumor efficacy and autoimmune pathology in T-cell-mediated targeting of carcinoembryonic antigen. *Cancer Res.* 68: 8446-8455.
469. Baxevanis, C. N., S. A. Perez, and M. Papamichail. 2009. Cancer immunotherapy. *Crit. Rev. Clin. Lab. Sci.* 46: 167-189.
470. Godfrey, W. R., Y. G. Ge, D. J. Spoden, B. L. Levine, C. H. June, B. R. Blazar, and S. B. Porter. 2004. In vitro-expanded human CD4(+)CD25(+) T-regulatory cells can markedly inhibit allogeneic dendritic cell-stimulated MLR cultures. *Blood* 104: 453-461.
471. Tang, Q., K. J. Henriksen, M. Bi, E. B. Finger, G. Szot, J. Ye, E. L. Masteller, H. McDevitt, M. Bonyhadi, and J. A. Bluestone. 2004. In vitro-expanded antigen-specific regulatory T cells suppress autoimmune diabetes. *J. Exp. Med.* 199: 1455-1465.
472. Pomie, C., I. Menager-Marcq, and J. P. van Meerwijk. 2008. Murine CD8+ regulatory T lymphocytes: the new era. *Hum. Immunol.* 69: 708-714.
473. Filaci, G., M. Fravega, D. Fenoglio, M. Rizzi, S. Negrini, R. Viggiani, and F. Indiveri. 2004. Non-antigen specific CD8+ T suppressor lymphocytes. *Clin. Exp. Med.* 4: 86-92.
474. Chen, M. L., M. J. Pittet, L. Gorelik, R. A. Flavell, R. Weissleder, H. von Boehmer, and K. Khazaie. 2005. Regulatory T cells suppress tumor-specific CD8 T cell cytotoxicity through TGF-beta signals in vivo. *Proc. Natl. Acad. Sci. U. S. A.* 102: 419-424.
475. Gondek, D. C., L. F. Lu, S. A. Quezada, S. Sakaguchi, and R. J. Noelle. 2005. Cutting edge: contact-mediated suppression by CD4+CD25+ regulatory cells involves a granzyme B-dependent, perforin-independent mechanism. *J. Immunol.* 174: 1783-1786.

476. Grossman, W. J., J. W. Verbsky, W. Barchet, M. Colonna, J. P. Atkinson, and T. J. Ley. 2004. Human T regulatory cells can use the perforin pathway to cause autologous target cell death. *Immunity* 21: 589-601.
477. Zhao, D. M., A. M. Thornton, R. J. DiPaolo, and E. M. Shevach. 2006. Activated CD4+CD25+ T cells selectively kill B lymphocytes. *Blood* 107: 3925-3932.
478. Huang, X., J. Zhu, and Y. Yang. 2005. Protection against autoimmunity in nonlymphopenic hosts by CD4+ CD25+ regulatory T cells is antigen-specific and requires IL-10 and TGF-beta. *J Immunol* 175: 4283-4291.
479. Doetze, A., J. Satoguina, G. Burchard, T. Rau, C. Loliger, B. Fleischer, and A. Hoerauf. 2000. Antigen-specific cellular hyporesponsiveness in a chronic human helminth infection is mediated by T(h)3/T(r)1-type cytokines IL-10 and transforming growth factor-beta but not by a T(h)1 to T(h)2 shift. *Int Immunol* 12: 623-630.
480. Wang, H. Y., D. A. Lee, G. Peng, Z. Guo, Y. Li, Y. Kiniwa, E. M. Shevach, and R. F. Wang. 2004. Tumor-specific human CD4+ regulatory T cells and their ligands: implications for immunotherapy. *Immunity* 20: 107-118.
481. Tarbell, K. V., S. Yamazaki, K. Olson, P. Toy, and R. M. Steinman. 2004. CD25+ CD4+ T cells, expanded with dendritic cells presenting a single autoantigenic peptide, suppress autoimmune diabetes. *J. Exp. Med.* 199: 1467-1477.
482. DiPaolo, R. J., C. Brinster, T. S. Davidson, J. Andersson, D. Glass, and E. M. Shevach. 2007. Autoantigen-specific TGFbeta-induced Foxp3+ regulatory T cells prevent autoimmunity by inhibiting dendritic cells from activating autoreactive T cells. *J. Immunol.* 179: 4685-4693.
483. Huter, E. N., G. H. Stummvoll, R. J. DiPaolo, D. D. Glass, and E. M. Shevach. 2008. Cutting edge: antigen-specific TGF beta-induced regulatory T cells suppress Th17-mediated autoimmune disease. *J. Immunol.* 181: 8209-8213.
484. Tsang, J. Y., Y. Tanriver, S. Jiang, S. A. Xue, K. Ratnasothy, D. Chen, H. J. Stauss, R. P. Bucy, G. Lombardi, and R. Lechler. 2008. Conferring indirect allospecificity on CD4+CD25+ Tregs by TCR gene transfer favors transplantation tolerance in mice. *J. Clin. Invest.* 118: 3619-3628.
485. Wright, G. P., C. A. Notley, S. A. Xue, G. M. Bendle, A. Holler, T. N. Schumacher, M. R. Ehrenstein, and H. J. Stauss. 2009. Adoptive therapy with redirected primary regulatory T cells results in antigen-specific suppression of arthritis. *Proc. Natl. Acad. Sci. U. S. A.* 106: 19078-19083.
486. Brusko, T. M., R. C. Koya, S. Zhu, M. R. Lee, A. L. Putnam, S. A. McClymont, M. I. Nishimura, S. Han, L. J. Chang, M. A. Atkinson, A. Ribas, and J. A. Bluestone. 2010. Human antigen-specific regulatory T cells generated by T cell receptor gene transfer. *PLoS One* 5: e11726.
487. Schmid, D. A., M. B. Irving, V. Posevitz, M. Hebeisen, A. Posevitz-Fejfar, J. C. Sarria, R. Gomez-Eerland, M. Thome, T. N. Schumacher, P. Romero, D. E. Speiser, V. Zoete, O. Michielin, and N. Rufer. 2010. Evidence for a TCR affinity threshold delimiting maximal CD8 T cell function. *J. Immunol.* 184: 4936-4946.
488. Weber, K. S., D. L. Donermeyer, P. M. Allen, and D. M. Kranz. 2005. Class II-restricted T cell receptor engineered in vitro for higher affinity retains peptide specificity and function. *Proc. Natl. Acad. Sci. U. S. A.* 102: 19033-19038.
489. Zhao, Y., A. D. Bennett, Z. Zheng, Q. J. Wang, P. F. Robbins, L. Y. Yu, Y. Li, P. E. Molloy, S. M. Dunn, B. K. Jakobsen, S. A. Rosenberg, and R. A. Morgan. 2007. High-

affinity TCRs generated by phage display provide CD4+ T cells with the ability to recognize and kill tumor cell lines. *J. Immunol.* 179: 5845-5854.
490. Robbins, P. F., Y. F. Li, M. El-Gamil, Y. Zhao, J. A. Wargo, Z. Zheng, H. Xu, R. A. Morgan, S. A. Feldman, L. A. Johnson, A. D. Bennett, S. M. Dunn, T. M. Mahon, B. K. Jakobsen, and S. A. Rosenberg. 2008. Single and dual amino acid substitutions in TCR CDRs can enhance antigen-specific T cell functions. *J. Immunol.* 180: 6116-6131.
491. LeGuern, C., Y. Akiyama, S. Germana, K. Tanaka, L. Fernandez, Y. Iwamoto, S. Houser, and G. Benichou. 2010. Intracellular MHC class II controls regulatory tolerance to allogeneic transplants. *J. Immunol.* 184: 2394-2400.
492. Qian, Z., K. A. Latham, K. B. Whittington, D. C. Miller, D. D. Brand, and E. F. Rosloniec. 2013. Engineered regulatory T cells coexpressing MHC class II:peptide complexes are efficient inhibitors of autoimmune T cell function and prevent the development of autoimmune arthritis. *J. Immunol.* 190: 5382-5391.
493. Nanjundappa, R. H., R. Wang, Y. Xie, C. S. Umeshappa, R. Chibbar, Y. Wei, Q. Liu, and J. Xiang. 2011. GP120-specific exosome-targeted T cell-based vaccine capable of stimulating DC- and CD4(+) T-independent CTL responses. *Vaccine* 29: 3538-3547.
494. Benoist, C., and D. Mathis. 1990. Regulation of major histocompatibility complex class-II genes: X, Y and other letters of the alphabet. *Annu. Rev. Immunol.* 8: 681-715.
495. Bettelli, E., M. Oukka, and V. K. Kuchroo. 2007. T(H)-17 cells in the circle of immunity and autoimmunity. *Nat. Immunol.* 8: 345-350.
496. Merrill, J. E., D. H. Kono, J. Clayton, D. G. Ando, D. R. Hinton, and F. M. Hofman. 1992. Inflammatory leukocytes and cytokines in the peptide-induced disease of experimental allergic encephalomyelitis in SJL and B10.PL mice. *Proc. Natl. Acad. Sci. U. S. A.* 89: 574-578.
497. Putnam, A. L., T. M. Brusko, M. R. Lee, W. Liu, G. L. Szot, T. Ghosh, M. A. Atkinson, and J. A. Bluestone. 2009. Expansion of human regulatory T-cells from patients with type 1 diabetes. *Diabetes* 58: 652-662.
498. Cao, T., A. Soto, W. Zhou, W. Wang, S. Eck, M. Walker, G. Harriman, and L. Li. 2009. Ex vivo expanded human CD4+CD25+Foxp3+ regulatory T cells prevent lethal xenogenic graft versus host disease (GVHD). *Cell. Immunol.* 258: 65-71.
499. Kohm, A. P., P. A. Carpentier, H. A. Anger, and S. D. Miller. 2002. Cutting edge: CD4+CD25+ regulatory T cells suppress antigen-specific autoreactive immune responses and central nervous system inflammation during active experimental autoimmune encephalomyelitis. *J. Immunol.* 169: 4712-4716.
500. Fransson, M., E. Piras, J. Burman, B. Nilsson, M. Essand, B. Lu, R. A. Harris, P. U. Magnusson, E. Brittebo, and A. S. Loskog. 2012. CAR/FoxP3-engineered T regulatory cells target the CNS and suppress EAE upon intranasal delivery. *J. Neuroinflammation* 9: 112.
501. Stephens, L. A., K. H. Malpass, and S. M. Anderton. 2009. Curing CNS autoimmune disease with myelin-reactive Foxp3+ Treg. *Eur. J. Immunol.* 39: 1108-1117.
502. Wright, G. P., M. R. Ehrenstein, and H. J. Stauss. 2011. Regulatory T-cell adoptive immunotherapy: potential for treatment of autoimmunity. *Expert Rev. Clin. Immunol.* 7: 213-225.

SUPPLEMENTARY MOVIE LEGENDS

sMovie 5.1 Migration of naive OTI CD8$^+$ T and OVA-T_{EXO} cells. C57BL/6 mouse was transferred with CFSE-labeled OVA-T_{EXO} (green) followed by CMTMR-labeled naive OTI CD8$^+$ T cells (red) 24 hrs later. Inguinal lymph nodes were immobilized in an imaging chamber and imaged in T-zone region by two-photon laser-scanning microscopy. OTI CD8$^+$ T cells form tight conjugates with both stationary (circle) and motile (arrow) OVA-T_{EXO}. Projection of a time-lapse series imaged in intact inguinal lymph nodes is shown. Dimensions: 83 μm × 83 μm × 21 μm × 30 min.

sMovie 5.2 Pathways of naive OTI CD8$^+$ T and OVA-T_{EXO} cells. Experiment was conducted in the same conditions as described in sMovie 5.1. Naive OTI CD8$^+$ T cells (red) move along behind OVA-T_{EXO} (green). The pathways of an OVA-T_{EXO} (green/grey line) and a CD8$^+$ T cell (red/grey line) are remaining bound to each other during the time of imaging. Dimensions: 106 μm × 106 μm × 18 μm × 30 min.

sMovie 5.3 Polygamous conjugate between naive OTI CD8$^+$ T and OVA-T_{EXO} cells. Experiment was conducted in the same conditions as described in sMovie 5.1. An OVA-T_{EXO} (green) simultaneously interacts with two naive OTI CD8$^+$ T cells (red). White points represent the central of cells. Images on the right panel show the pathways for each cell type. Dimensions: 47 μm × 43 μm × 21 μm × 30 min.

sMovie 5.4 Migration of naive OTI CD8$^+$ T cells in the presence of OVA-($K^{b-/-}$)T_{EXO} cells. C57BL/6 mouse was transferred with CFSE-labeled OVA-($K^{b-/-}$)T_{EXO} (green) followed by CMTMR-labeled naive OTI CD8$^+$ T cells (red) 24 hrs later. Inguinal lymph nodes were immobilized in an imaging chamber and imaged in T-zone region by two-photon laser-scanning microscopy. Projection of a time-lapse series imaged in intact inguinal lymph nodes is shown. Interactions between OVA-($K^{b-/-}$)T_{EXO} cells and naive OTI CD8$^+$ T cells are only intermittent. Dimensions: 106 μm × 106 μm × 27 μm × 30 min.

sMovie 5.5 Migration of naive OTI and polyclonal CD8$^+$ T cells in the presence of OVA-T_{EXO} cells. Unlabeled OVA-T_{EXO} cells were injected 24 hrs before co-transferring naive OTI (green) and polyclonal (red) CD8$^+$ T cells to the same recipient C57BL/6 mouse. OTI CD8$^+$ T cells (green tracks) show slower and much more confined movements than polyclonal CD8$^+$ T cells (red tracks). Dimensions: 121 μm × 67 μm × 28 μm × 40 min.

sMovie 5.6 Migration of naive OTI and polyclonal CD8$^+$ T cells in the presence of OVA-T_{EXO} and absence of host APCs. CD11c-DTR mouse was treated with DT, anti-CD20 and anti-pDC Abs to get rid of potential host APCs one day ahead. Unlabeled OVA-T_{EXO} cells were injected followed by co-transferring CFSE-labeled naive OTI (green) and CMTMR-labeled polyclonal (red) CD8$^+$ T cells to the same pre-treated recipient mouse. OTI CD8$^+$ T cells (green tracks) and polyclonal CD8$^+$ T cells (red tracks) show similar migration patterns as described in sMovie 5.5. Dimensions: 88 μm × 88 μm × 42 μm × 40 min.

sMovie 5.7 Migratory behavior of OTII CD4$^+$ T cells and sDC$_{OVA}$. DsRed-sDC$_{OVA}$ (red) were injected into the footpad of recipient C57BL/6 mouse. One day later, OTII CD4$^+$ T cells (green) were i.v. injected to the same recipient mouse. Popliteal lymph node imaging was performed 6 hrs subsequent to the adoptive transfer of OTII CD4$^+$ T cells. Dimensions: 200 μm × 200 μm × 21 μm × 40 min.

sMovie 5.8 Migratory behavior of OTII CD4$^+$ T cells and sDC$_{OVA}$ in the presence of OVAII-pulsed CD8$^+$CD25$^+$ Tregs. Unlabeled OVAII-pulsed CD8$^+$CD25$^+$ Tregs were i.v. injected one day before adoptive transfer of DsRed-sDC$_{OVA}$ (red). One day later, OTII CD4$^+$ T cells (green) were injected to the same recipient mouse. Popliteal lymph node imaging was performed 6 hrs subsequent to the adoptive transfer of OTII CD4$^+$ T cells. Dimensions: 200 μm × 200 μm × 30 μm × 40 min.